Studies on the geometry of Painlevé equations

Alexander Henry Stokes

A dissertation submitted in partial fulfillment

of the requirements for the degree of

Doctor of Philosophy

of

University College London.

Department of Mathematics

University College London

September 3, 2020

I, Alexander Henry Stokes, confirm that the work presented in this thesis is my own, except for the content of Section 2.3 and Chapter 3, which is based on collaborative work with Anton Dzhamay and Galina Filipuk [DFS19b]. Where information has been derived from other sources, I confirm that this has been indicated in the thesis.

Abstract

This thesis is a collection of work within the geometric framework for Painlevé equations. This approach was initiated by the Japanese school, and is based on studying Painlevé equations (differential or discrete) via certain rational surfaces associated with affine root systems. Our work is grouped into two main themes: on the one hand making use of tools and techniques from the geometric framework to study problems from applications where Painlevé equations appear, and on the other hand developing and extending the geometric framework itself.

Differential and discrete Painlevé equations arise in a wide range of areas of mathematics and physics, and we present a general procedure for solving the identification problem for Painlevé equations. That is, if a differential or discrete system is suspected to be equivalent to one of Painlevé type, we outline a method, based on constructing the associated surfaces explicitly, for identifying the system with a standard example, in which case known results can be used, and demonstrate it in the case of equations appearing in the theory of orthogonal polynomials.

Our results on the geometric framework itself begin with an observation of a new class of discrete equations that can described through the geometric theory, beyond those originally defined by Sakai in terms of translation symmetries of families of surfaces. To be precise, we build on previous studies of equations corresponding to non-translation symmetries of infinite order (so-called projective reductions, with fewer parameters than translations of the same surface type) and show that Sakai's theory allows for integrable discrete equations to be constructed from any element of infinite order in the symmetry group and still have the full parameter freedom for their surface type.

We then also make the first steps toward a geometric theory of delay-differential Painlevé equations by giving a description of singularity confinement in this setting in terms of mappings between jet spaces.

Impact Statement

The work in this thesis has implications for both the general theory of Painlevé equations and the applications in which they appear.

For the theory itself, the construction of equations from non-translation symmetries in Chapter 4 has been published [Sto18] and is likely to give a description of some discrete systems obtained recently independently of the geometric framework [GRT$^+$14, GRT$^+$16, RG17, GRWS20]. These are claimed to constitute some fifty new discrete Painlevé equations, and we hope that their geometric description in terms of non-translation symmetries will determine their relation to those originally defined by Sakai and how many are truly inequivalent. The work in Chapter 5 is the first time a geometric approach has been taken to the study of delay-differential Painlevé equations and will hopefully stimulate interest in this direction. It also develops new techniques which overcome one of the central difficulties in their study, namely the fact that they may admit infinite families of distinct singularity patterns. This has the potential to widen the range of applications of the theory of Painlevé equations, since delay-differential equations appear in areas such as mathematical biology and economics, which are different from those where discrete and differential Painlevé equations are known to commonly arise.

The method proposed in Chapter 3 for solving the identification problem represents a considerable improvement on the ways in which this was done previously, namely either by inspection or by brute force computation of the transformation to some choice of standard example one is aiming for. Using the geometric approach, this can be done without prior knowledge of which Painlevé equation the system is equivalent to, and is feasible regardless of how complicated the form of the system from applications is. This method has already been adopted by other researchers to study different examples from orthogonal polynomials [CDH19]. Further, the method has led to new results on the orthogonal polynomials side, which have the potential to be interpreted geometrically [DFS19a].

Acknowledgements

I would first like to thank my supervisor Rod Halburd for his mentorship, encouragement, wisdom and sense of humour over the last three years. I also thank Anton Dzhamay and Galina Filipuk for their ideas and insights, and for showing me how rewarding doing mathematics in a collaborative way can be.

I must also thank Nobutaka Nakazono, Yang Shi and Nalini Joshi for their mentorship and for introducing me to Painlevé equations while I was an undergraduate. I am very grateful also to Ralph Willox, Kenji Kajiwara, Masatoshi Noumi, Yasuhiko Yamada, Hidetaka Sakai, Tomoyuki Takenawa and Akane Nakamura for all they have taught me, both directly and indirectly.

I thank my family and friends in Sydney for their support, as well as newer friends in London who have enriched my time here beyond mathematics, in particular Brim, Akito, Samantha and the communities they have introduced me to, as well as everyone at Resonance FM.

I would also like to thank Nick, Viv, Emma and Emma for making our house a home, for allowing me to talk about mathematics and for their support during the final few months.

Finally, I would like to thank Emily for her boundless kindness and understanding, and for getting me through this.

Contents

List of Figures

List of Tables

Chapter 1

Introduction

Our main focus in this thesis is the geometric framework for the study of Painlevé equations, developed in particular by K. Okamoto in the differential case, and H. Sakai for discrete Painlevé equations. Before our treatment of this theory in Chapter 2, we begin by placing it in the context of previous developments with a historical overview of the Painlevé equations. In particular, we give a brief overview of the differential Painlevé equations and some reasons why they are considered in the context of integrable systems, namely their relation with integrable partial differential equations (PDEs), their associated linear problems from monodromy-preserving deformations, and their Bäcklund transformation symmetries. We then recall how ideas were developed regarding discrete analogues of them, pointing out the ways in which these inform Sakai's theory of discrete Painlevé equations.

1.1 The Painlevé differential equations

1.1.1 The Painlevé property

The differential Painlevé equations are six nonlinear second-order ordinary differential equations (ODEs) named after P. Painlevé, who originally studied them with a view to defining new special functions. Many classical special functions satisfy linear second-order ODEs, and can be defined in terms of their solutions. A natural idea, pursued by Painlevé, Gambier and R. Fuchs, was to define special functions in terms of the solutions of ODEs which are nonlinear. The main difficulty encountered when departing from the linear case is related to the locations of singularities of solutions of nonlinear ODEs in the complex plane. In the linear case, the equation dictates the only possible locations of singularities of the solutions. Take a linear second-order ODE

$$\frac{d^2y}{dz^2} + p_1(z)\frac{dy}{dz} + p_0(z)y = 0, \tag{1.1}$$

where $p_0(z), p_1(z)$ are meromorphic on $\mathbb{C}$. We extend the independent variable space to the Riemann sphere $\widetilde{\mathbb{C}} = \mathbb{C} \cup \{\infty\}$ in the natural way, by introducing $Z = 1/z$ so that the point at infinity is given by $Z = 0$ and the differential equation in this chart is

$$\frac{d^2y}{dZ^2} + \tilde{p}_1(Z)\frac{dy}{dZ} + \tilde{p}_0(Z)y = 0, \tag{1.2}$$

where

$$\tilde{p}_1(Z) = \frac{2Z^3 - Z^2 p_1(1/Z)}{Z^4}, \quad \tilde{p}_0(Z) = \frac{p_0(1/Z)}{Z^4}. \tag{1.3}$$

We say $z_0 \in \mathbb{C}$ is a singular point of the equation if it is a pole of either $p_1(z)$ or $p_0(z)$, and $z_0 = \infty$ is a singular point if $Z = 0$ is a pole of either $\tilde{p}_1(Z)$ or $\tilde{p}_0(Z)$. Importantly, if a solution fails to be analytic at some $z_0 \in \mathbb{C} \cup \{\infty\}$, then z_0 is a singular point of the equation. Thus for a linear second-order ODE with meromorphic coefficients we can obtain a Riemann surface on which the general solution defines an analytic function. We remove the singular points of the equation from the Riemann sphere and consider a covering space of this which allows for the branching about these singular points. Allowing *regular singular points*, where each p_{2-i} may have a pole of order at most i, the Frobenius method applied to the equation near such a point still gives two independent solutions, possibly with algebraic branching, so we again have a single Riemann surface on which the general solution is a well-defined function.

The problem with nonlinear ODEs is that different solutions may have different singularity structures. For example, if we take the first-order equation

$$\frac{dy}{dz} + y^2 = 0, \tag{1.4}$$

separation of variables allows us to obtain the general solution

$$y(z) = \frac{1}{z - C}, \tag{1.5}$$

where C is a constant of integration. From this, we see that solutions given by different values of C will have poles at different locations, and such singularities are called *movable*. A more illustrative example is the equation

$$\frac{dy}{dz} + \frac{1}{y} = 0. \tag{1.6}$$

Subject to the initial condition $y(0) = y_0 \in \mathbb{C}\backslash\{0\}$, near $z = 0$ we have a unique analytic solution

$$y(z) = \sqrt{2z - y_0^2}, \tag{1.7}$$

on the disc centred at the origin of radius $y_0^2/2$. However, we have an algebraic branch point at $z = y_0^2/2$, so altering the initial conditions gives particular solutions with branching at different points, and there is no single Riemann surface on which to place all solutions.
In the approach of Painlevé et. al., the way to avoid this problem is to require that second-order nonlinear ODEs have a simple singularity structure in the sense of the following condition, now known as the Painlevé property:

Definition 1.1.1. *An ODE is said to have the Painlevé property if all solutions are single-valued about all movable singularities.*

Painlevé, Gambier and R. Fuchs [Pai02, Fuc07, Fuc11, Gam10] considered a large class of second-order ODEs, namely those of the form

$$y'' = F(y, y', z), \tag{1.8}$$

where $' = \frac{d}{dz}$ and F is rational in y, y' and locally analytic in z, and isolated those for which the Painlevé property held. Up to equivalence by Möbius transformations of the dependent variable and analytic changes of independent variable, fifty classes of equations were obtained. Among these were six classes whose representatives are given by the Painlevé equations:

$$\begin{aligned}
\mathrm{P_I}:\ y'' &= 6y^2 + z\\
\mathrm{P_{II}}:\ y'' &= 2y^3 + zy + \alpha\\
\mathrm{P_{III}}:\ y'' &= \frac{(y')^2}{y} - \frac{y'}{z} + \alpha\frac{y^2}{z} + \frac{\beta}{z} + \gamma y^3 + \frac{\delta}{y}\\
\mathrm{P_{IV}}:\ y'' &= \frac{1}{2y}\left(y'\right)^2 + \frac{3}{2}y^3 + 4zy^2 + 2(z^2-\alpha)y + \frac{\beta}{y}\\
\mathrm{P_V}:\ y'' &= \left(\frac{1}{2y} + \frac{1}{y-1}\right)(y')^2 - \frac{y'}{z} + \frac{(y-1)^2}{z^2}\left(\alpha y + \frac{\beta}{y}\right) + \gamma\frac{y}{z} + \delta\frac{y(y+1)}{y-1}\\
\mathrm{P_{VI}}:\ y'' &= \frac{1}{2}\left(\frac{1}{y} + \frac{1}{y-1} + \frac{1}{y-z}\right)(y')^2 - \left(\frac{1}{z} + \frac{1}{z-1} + \frac{1}{y-z}\right)y'\\
&\quad + \frac{y(y-1)(y-z)}{z^2(z-1)^2}\left(\alpha + \beta\frac{z}{y^2} + \gamma\frac{z-1}{(y-1)^2} + \delta\frac{z(z-1)}{(y-z)^2}\right)
\end{aligned}$$

In each case $y = y(z)$, $' = \frac{d}{dz}$ and $\alpha, \beta, \gamma, \delta$ are complex parameters. These cannot be solved in general in terms of known functions, namely elliptic functions and classical special functions solving linear ODEs. Their solutions are known as the *Painlevé transcendents*, which together with known functions allow all fifty classes to be solved.

Removing the locations of fixed singularities of each equation P_J, we obtain a subset $B_J \subset \widetilde{\mathbb{C}}$, on whose covering space all solutions are meromorphic:

$$\begin{aligned} B_{\mathrm{I}} = \widetilde{\mathbb{C}}\backslash\{\infty\}, \quad B_{\mathrm{II}} = \widetilde{\mathbb{C}}\backslash\{\infty\}, \qquad B_{\mathrm{III}} = \widetilde{\mathbb{C}}\backslash\{0,\infty\}, \\ B_{\mathrm{IV}} = \widetilde{\mathbb{C}}\backslash\{\infty\}, \quad B_{\mathrm{V}} = \widetilde{\mathbb{C}}\backslash\{0,\infty\}, \quad B_{\mathrm{VI}} = \widetilde{\mathbb{C}}\backslash\{0,1,\infty\}, \end{aligned} \tag{1.9}$$

So we have each solution of P_J defining a single-valued function on a Riemann surface covering B_J, and in this sense the Painlevé transcendents are regarded as new special functions, which play a central role in modern nonlinear physics, see e.g. [GLS02, FIKN06, Cla06, Cla10] and numerous references within.

1.1.2 Integrability

We now briefly mention some of the reasons that the study of Painlevé equations is placed within the field of integrable systems. An important remark to make at this point is that there is a consensus that there is no one definition of integrability, even in a single class of equations, but rather a number of properties or features of systems that have come to be associated with it. The Painlevé equations exhibit many such hallmarks of integrability, which we outline now.

Firstly, we have a connection between Painlevé equations and integrable nonlinear partial differential equations (PDEs), which possess infinitely many conserved quantities and have a Lax representation as the compatibility condition for a pair of linear systems, which allows certain initial value problems to be solved exactly. Each of the Painlevé equations can be obtained as a kind of reduction of an integrable PDE, which means that they govern solutions of the PDE satsifying a kind of similarity constraint. We illustrate this, following [AC91], in the case of perhaps the most famous of all integrable PDEs, the Korteweg-de Vries equation:

$$u_t + 6uu_x + u_{xxx} = 0. \tag{1.10}$$

Here u is a function of x and t, with partial derivatives denoted by subscripts. If we take the following similarity reduction, i.e. assume a solution is of the form

$$u(x,t) = \frac{w(z)}{(3t)^{\frac{2}{3}}}, \qquad z = \frac{x}{(3t)^{\frac{1}{3}}},$$

then the equation (1.10) implies that $w(z)$ satisfies

$$w''' + 6w'w - zw' - 2w = 0. \tag{1.11}$$

If we take a solution $y(z)$ of $\mathrm{P_{II}}$ for arbitrary parameter α, it can be checked by direct calculation that

$$w(z) = -(y'(z) + y(z)^2) \tag{1.12}$$

satisfies (1.11). Altenatively, one may make this substitution in the third-order equation (1.11) and integrate once to obtain $\mathrm{P_{II}}$, with the parameter α appearing as the constant of integration. Other such reductions applied to other well-known integrable PDEs such as the sine-Gordon and Boussinesq equations have been shown to gives cases of the remaining Painlevé equations [AS77, ARS80a, ARS80b, AC91, BCH96].

Another parallel with integrable PDEs is in the fact that the Painlevé equations admit a kind of Lax representation, in that they arise as the compatibility condition for an associated pair of linear systems of differential equations. This comes from the theory of monodromy-preserving deformations of linear systems, the details of which are not important for the results of this thesis, but we will present the associated linear problem in the case of $\mathrm{P_{II}}$ following [AC91], which was originally obtained by Flaschka and Newell [FN80]. Consider the following coupled systems of linear differential equations for $\mathbf{w}(z,t) = (w_1(z,t), w_2(z,t))^T$:

$$\mathbf{w}_t = \begin{pmatrix} -\mathrm{i}(4t^2 + 2y^2 + z) & 4ty + 2\mathrm{i}y' + \alpha/t \\ 4ty - 2\mathrm{i}y' + \alpha/t & \mathrm{i}(4t^2 + 2y^2 + z) \end{pmatrix} \mathbf{w}, \tag{1.13a}$$

$$\mathbf{w}_z = \begin{pmatrix} -\mathrm{i}t & y \\ y & \mathrm{i}t \end{pmatrix} \mathbf{w}, \tag{1.13b}$$

where $y = y(z)$ and α is a free complex parameter. The compatibility condition of this pair of equations, i.e. $\mathbf{w}_{zt} = \mathbf{w}_{tz}$, is exactly that $y(z)$ satisfies $\mathrm{P_{II}}$ with parameter α. The connection with the theory of monodromy-preserving deformations is in the fact that if we consider the monodromy of the system (1.13a), the equation (1.13b) is precisely the condition on a deformation of the solution $\mathbf{w}$ in z to preserve the monodromy data for the singular points at $t = 0$ and $t = \infty$, see [AC91, FN80, FIKN06]. Each of the six differential Painlevé equations arises in such a way, and in particular $\mathrm{P_{VI}}$ was originally obtained by R. Fuchs as the condition for monodromy-preserving deformation of a Fuchsian system with four regular singular points [Fuc07, Fuc11]. This gives a powerful approach for studying the Painlevé equations in terms of Riemann-Hilbert problems (see e.g. [FIKN06] and references within), but beyond the conceptual link it provides with integrable PDEs it is not within the scope of this thesis.

1.1.3 Bäcklund transformation symmetries

A defining feature of the Painlevé equations, also associated with integrability in general, is the presence of symmetries. For each of the Painlevé equations involving one or more parameters (all but $\mathrm{P_I}$), there exist transformations that relate solutions for different parameter values. These are known as *Bäcklund transformations* and they are a key motivation for the geometric framework for both differential and discrete Painlevé equations. We will begin by illustrating this in the example of $\mathrm{P_{IV}}$, following [Nou04]. This makes use of the so-called symmetric form of $\mathrm{P_{IV}}$, which is a special case of a more general system first introduced by Veselov and Shabat as a dressing chain related to Schrödinger operators [VS93]. This more general system enjoys affine Weyl group symmetries generalising those from the $\mathrm{P_{IV}}$ case, which were first described geometrically by Adler [Adl93, Adl94], and was later studied by Noumi and Yamada [NY98b].

Consider the system of differential equations

$$\begin{aligned} \frac{df_0}{dt} &= f_0(f_1 - f_2) + a_0, \\ \frac{df_1}{dt} &= f_1(f_2 - f_0) + a_1, \qquad\qquad a_0 + a_1 + a_2 = 1, \\ \frac{df_2}{dt} &= f_2(f_0 - f_1) + a_2, \end{aligned} \tag{1.14}$$

where a_0, a_1, a_2 are parameters subject to the constraint given above. We note that this appears to be a third order autonomous system, but the condition on the parameters implies, by summing the three equations, that $f_0 + f_1 + f_2 = t + c$ for some consant of integration c. We can use freedom of translation in the independent variable to set it, without loss of generality, to be zero so we have the normalisation $f_0 + f_1 + f_2 = t$ and indeed two degrees of freedom.

This normalised system gives a second-order equation for f_1 which is then equivalent, via $y(z) = -\sqrt{2} f_1(t), t = \sqrt{2} z$, to the fourth Painlevé equation $\mathrm{P_{IV}}$ for $y(z)$, where the parameters are related by $\alpha = a_0 - a_2, \beta = -2a_1^2$. Now make the following change of variables:

$$\tilde{f}_0 = f_0, \quad \tilde{f}_1 = f_1 + \frac{a_0}{f_0}, \quad \tilde{f}_2 = f_2 - \frac{a_0}{f_0}.$$

This leads to the same system, but with different parameters:

$$\begin{aligned} \tilde{f}_0' &= \tilde{f}_0(\tilde{f}_1 - \tilde{f}_2) + \tilde{a}_0 \qquad & \tilde{a}_0 &= -a_0 \\ \tilde{f}_1' &= \tilde{f}_1(\tilde{f}_2 - \tilde{f}_0) + \tilde{a}_1 \qquad & \tilde{a}_1 &= a_1 + a_0 \\ \tilde{f}_2' &= \tilde{f}_2(\tilde{f}_0 - \tilde{f}_1) + \tilde{a}_2 \qquad & \tilde{a}_2 &= a_2 + a_0 \end{aligned} \tag{1.15}$$

Thus, if we have a solution of (1.14) for parameters a_0, a_1, a_2, then we obtain one for $\tilde{a}_0, \tilde{a}_1, \tilde{a}_2$ via this transformation, and the normalisation $\tilde{a}_0 + \tilde{a}_1 + \tilde{a}_2 = 1$ is preserved. There are other such transformations and they form an action of the *extended affine Weyl group* of type $A_2^{(1)}$ on the field of rational functions of the variables and parameters $\mathbb{C}(f_0, f_1, f_2; a_0, a_1, a_2)$. This group is defined by the presentation

$$\widetilde{W}(A_2^{(1)}) = \left\langle s_0, s_1, s_2, \pi \mid s_j^2 = \pi^3 = (s_j s_{j+1})^3 = 1,\ \pi s_j = s_{j+1}\pi \right\rangle, \tag{1.16}$$

where $j \in \mathbb{Z}/3\mathbb{Z}$, and the action of each generator is given by a map $(f_0, f_1, f_2; a_0, a_1, a_2) \mapsto (\tilde{f}_0, \tilde{f}_1, \tilde{f}_2; \tilde{a}_0, \tilde{a}_1, \tilde{a}_2)$, from the corresponding row of Table 1.1, with any composition of such transformations providing a symmetry of the differential system in the same sense.

	$\tilde{a}_0$	$\tilde{a}_1$	$\tilde{a}_2$	$\tilde{f}_0$	$\tilde{f}_1$	$\tilde{f}_2$
s_0	$-a_0$	$a_1 + a_0$	$a_2 + a_0$	f_0	$f_1 + \frac{a_0}{f_0}$	$f_2 - \frac{a_0}{f_0}$
s_1	$a_0 + a_1$	$-a_1$	$a_2 + a_1$	$f_0 - \frac{a_1}{f_1}$	f_1	$f_2 + \frac{a_1}{f_1}$
s_2	$a_0 + a_2$	$a_1 + a_2$	$-a_2$	$f_0 + \frac{a_2}{f_2}$	$f_1 - \frac{a_2}{f_2}$	f_2
π	a_1	a_2	a_0	f_1	f_2	f_0

Table 1.1: Action of $\widetilde{W}(A_2^{(1)})$ on variables and parameters in symmetric $\mathrm{P_{IV}}$

Extended affine Weyl groups will be treated in detail in Chapter 2, and each Painlevé equation that involves parameters admits an action of such a group by Bäcklund transformation symmetries, which we list in Table 1.2. We note that $\mathrm{P_{III}}$ is usually considered as three separate subcases corresponding to different constraints on the parameters, which lead to different symmetry groups, but here we list only the type corresponding to the most general case where no constraints are imposed on the parameters.

Equation	$\mathrm{P_I}$	$\mathrm{P_{II}}$	$\mathrm{P_{III}}$	$\mathrm{P_{IV}}$	$\mathrm{P_V}$	$\mathrm{P_{VI}}$
Symmetry	$-$	$A_1^{(1)}$	$(A_1 + A_1)^{(1)}$	$A_2^{(1)}$	$A_3^{(1)}$	$D_4^{(1)}$

Table 1.2: Bäcklund transformation symmetry types of differential Painlevé equations

Here the extended affine Weyl groups are labeled by their associated *Dynkin diagram* of affine type, sometimes called an *extended Dynkin diagram*. In Sakai's theory, each of these groups of Bäcklund transformations will be recast as an action on an associated family of rational surfaces, which we will outline in Chapter 2.

1.1.4 Okamoto's space

The connection between Painlevé equations and affine Weyl groups is deeper than their actions as Bäcklund transformation symmetries. This was observed by K. Okamoto, and forms one of the key ideas motivating Sakai's theory. The differential Painlevé equations admit a geometric description in terms of rational surfaces obtained by blowing up certain singularities, which leads to a space on which the equation is, in a sense, regularised. Discovered by Okamoto [Oka79], for each P_J this is a bundle over the independent variable space B_J, as given in (1.9), whose fibres are rational surfaces with certain curves removed. The bundle, known as Okamoto's space, admits a foliation by solution curves of the ODE system transverse to the fibres, and each fibre can be regarded as a space of initial conditions for the system. The connection with affine Weyl groups is hinted at by the fact that the curves removed from each fibre (the *inaccessible divisors*) have irreducible components whose intersection configuration is given by another Dynkin diagram of affine type. We will give a detailed treatment of the construction of Okamoto's space in Chapter 2 but for now we present the Dynkin diagrams associated with the symmetries and inaccessible divisors for each of the differential Painlevé equations in Table 1.3. Again $\mathrm{P_{III}}$ is usually considered according to three subcases because the intersection configuration can change depending on parameter constraints. Here we give the case where the parameters are generic, which corresponds to the symmetry type for $\mathrm{P_{III}}$ in Table 1.2.

Equation	$\mathrm{P_I}$	$\mathrm{P_{II}}$	$\mathrm{P_{III}}$	$\mathrm{P_{IV}}$	$\mathrm{P_V}$	$\mathrm{P_{VI}}$
Surface	$E_8^{(1)}$	$E_7^{(1)}$	$D_6^{(1)}$	$E_6^{(1)}$	$D_5^{(1)}$	$D_4^{(1)}$
Symmetry	–	$A_1^{(1)}$	$(A_1 + A_1)^{(1)}$	$A_2^{(1)}$	$A_3^{(1)}$	$D_4^{(1)}$

Table 1.3: Surface and symmetry types for the differential Painlevé equations

Note that as we move from $\mathrm{P_I}$ to $\mathrm{P_{VI}}$ the subscript for the surface type decreases, while that of the symmetry type increases. This is no coincidence, and there is a complementary relationship between the two, which was one of Okamoto's observations built on and formalised by Sakai, as we will illustrate in Chapter 2.

Studying Painlevé equations via Okamoto's space leads to many novel results inaccessible by working on the level of the equations themselves (see e.g. [JR19, JR18, DJ11, HJ14]), and can be used to explain many of their properties (see [KNY17] and references within). It was also shown that Okamoto's space essentially determines the differential equation in each case [ST97, MMT99, Mat97], so the study of Painlevé equations essentially reduces to the geometry of the associated space. This is a key idea behind Sakai's theory, where the focus is on using special geometric objects to define discrete systems with integrability properties.

1.2 Discrete Painlevé equations

The definitive framework for the study of discrete Painlevé equations was provided by H. Sakai in a seminal paper [Sak01]. This generalised the results of Okamoto, and provides the theoretical foundation for this thesis. Prior to this, equations had been proposed as discrete Painlevé from a variety of perspectives, including as those which give one of $\mathrm{P_I}$-$\mathrm{P_{VI}}$ in a continuum limit [RGH91], via discrete versions of isomonodromy deformation [JS96], from birational representations of affine Weyl groups [NY98a], as reductions of discrete analogues of integrable PDEs [NP91, Hof99], to name a few. Our discussion here will focus on the ideas that most directly inform Sakai's theory, namely the singularity confinement property for discrete equations, and deautonomisations of Quispel-Roberts-Thompson (QRT) mappings based on this. Among the most significant positive reflections on Sakai's work is that it has been consistently observed to cover examples proposed by other means to be discrete Painlevé, examples of which we will see in later chapters.

1.2.1 Singularity confinement

In the 1990s, important steps were made towards defining and understanding discrete analogues of the Painlevé equations through the proposal by Ramani and Grammaticos, together with Papageorgiou, of singularity confinement [GRP91] as the discrete counterpart to the Painlevé property. This analogy comes from the idea of isolating nonlinear equations with simple singularity structures. We will illustrate this in the example of the second-order difference equation

$$f_{n+1} = \frac{(f_n - k)(f_n + k)f_{n-1}}{k^2 - f_n^2 + 2t f_n f_{n-1}}, \tag{1.17}$$

with parameters $k \neq 0, \pm 1$ and $t \neq 0$. The initial value problem for this equation requires two values of the solution, say f_0, f_1, which in almost all cases will allow the values f_2, f_3 and so on to be determined recursively. The system (1.17) has singular values $f_n = \pm k$, in the sense that if while iterating the solution takes one of these values, f_{n+1} is zero independent of the value of f_{n-1} (provided $f_{n-1} \neq 0$). This is usually referred to as a loss of a degree of freedom occurring while iterating the system. For generic (non-integrable) discrete systems, the singularity will propagate, in the sense that the subsequent values $f_{n+2}, f_{n+3}, \ldots$ will all be determined independently of f_{n-1} and the lost degree of freedom will never be recovered. In the case of equation (1.17), we may compute the next iterate $f_{n+2} = \mp k$, but then, importantly, arrive at an indeterminacy of the rational function giving f_{n+3}, namely at $(f_{n+1}, f_{n+2}) = (0, \mp k)$. If, however, we consider a perturbation of the singular value $f_n = \pm k$ by introducing a small parameter ε, we may compute the following in the small ε limit:

$$\begin{aligned} f_{n-1} &\neq 0, \\ f_n &= \pm k + \mathcal{O}(\varepsilon), \\ f_{n+1} &= \mathcal{O}(\varepsilon), \\ f_{n+2} &= \mp k + \mathcal{O}(\varepsilon), \\ f_{n+3} &= f_{n-1} + \mathcal{O}(\varepsilon). \end{aligned} \tag{1.18}$$

If we define the values of the iterates as the limits of the above sequence as $\varepsilon \to 0$, the lost degree of freedom is 'recovered' in the value of f_{n+3}, and the singularity at $f_n = \pm k$ is said to be confined.

1.2.2 QRT mappings and rational elliptic surfaces

The singularity confinement property for second-order discrete systems can be understood as the existence of a space of initial conditions for the system: a family of rational surfaces to which the birational iteration mappings lift to isomorphisms, which we illustrate now. The example (1.17) in fact belongs to the family of QRT mappings [QRT88, QRT89], the definition of which ensures they have a space of initial conditions given by a rational elliptic surface (see [Tsu04, Dui10, Ves91]). The equation (1.17) can be considered as a birational mapping on $\mathbb{P}^1 \times \mathbb{P}^1$, where $\mathbb{P}^1 = \mathbb{P}^1(\mathbb{C})$. Letting $f_{n-1} = y$, $f_n = x = \bar{y}$, $f_{n+1} = \bar{x}$, the iteration $(f_n, f_{n-1}) \mapsto (f_{n+1}, f_n)$ gives a birational map $(x, y) \mapsto (\bar{x}, \bar{y})$. At this point we emphasise that the bar notation used here should not be confused with complex conjugation, and will continue to be employed for iterates of discrete systems for the remainder of the thesis. We consider this on $\mathbb{P}^1 \times \mathbb{P}^1$ by regarding x, y as affine coordinates in the $\mathbb{P}^1$ factors, and introduce $X = 1/x, Y = 1/y$, so $\mathbb{P}^1 \times \mathbb{P}^1$ is covered by the four charts $(x, y), (X, y), (x, Y), (X, Y)$, and we have a mapping defined by

$$\begin{aligned} \varphi : \mathbb{P}^1 \times \mathbb{P}^1 &\to \mathbb{P}^1 \times \mathbb{P}^1 \\ (x, y) &\mapsto (\bar{x}, \bar{y}) = \left(\frac{(x-k)(x+k)y}{k^2 - x^2 + 2txy}, x \right), \end{aligned} \tag{1.19}$$

where we have used The mapping (1.19) preserves each member of a pencil of elliptic curves on $\mathbb{P}^1 \times \mathbb{P}^1$, and the space of initial conditions is obtained from $\mathbb{P}^1 \times \mathbb{P}^1$ by resolving its basepoints through a number of blow-ups. This is ensured by the definition of the QRT map in terms of this pencil, which we outline now. Consider the matrices

$$\mathbf{A} = \begin{pmatrix} 0 & 0 & \frac{-1}{2t} \\ 0 & 1 & 0 \\ \frac{-1}{2t} & 0 & \frac{k^2}{2t} \end{pmatrix}, \qquad \mathbf{B} = \begin{pmatrix} 1 & 0 & 0 \\ 0 & 0 & 0 \\ 0 & 0 & 0 \end{pmatrix}, \tag{1.20}$$

where again $k \neq 0, \pm 1$ and $t \neq 0$, which define a pencil of biquadratic curves $\left\{ \Gamma_{[\alpha:\beta]} \mid [\alpha : \beta] \in \mathbb{P}^1 \right\}$ on $\mathbb{P}^1 \times \mathbb{P}^1$, written in the affine coordinates (x, y) as

$$\Gamma_{[\alpha:\beta]} : \quad \alpha \mathbf{x}^T \mathbf{A} \mathbf{y} + \beta \mathbf{x}^T \mathbf{B} \mathbf{y} = \frac{\alpha}{2t}(k^2 - x^2 - y^2 + 2txy) + \beta x^2 y^2 = 0, \tag{1.21}$$

where $\mathbf{x}^T = \begin{pmatrix} x^2 & x & 1 \end{pmatrix}, \mathbf{y}^T = \begin{pmatrix} y^2 & y & 1 \end{pmatrix}$. The QRT mapping is defined as follows. A generic point, say given by (x, y), lies on exactly one curve $\Gamma_{[\alpha:\beta]}$ in the pencil.

There is then exactly one other point $(\bar{x}, y)$ on $\Gamma_{[\alpha:\beta]}$ with the same y-coordinate, from which we can define the involution $r_x : (x, y) \mapsto (\bar{x}, y)$. Similarly we have another involution $r_y : (x, y) \mapsto (x, \bar{y})$, and their composition $r_x \circ r_y$ is the QRT mapping.

Following [CDT17] we introduce the involution $\sigma_{xy} : (x, y) \mapsto (y, x)$ and work with the map $\varphi = \sigma_{xy} \cdot r_y$, which for the pencil (1.21) is precisely (1.19), and can be thought of as a 'half QRT mapping' due to the fact that $\varphi^2 = r_x \circ r_y$. The pencil (1.21) has four double basepoints, given in coordinates by

$$\begin{aligned} p_1 : (x, y) &= (k, 0), \qquad & p_2 : (x, y) &= (-k, 0), \\ p_3 : (x, y) &= (0, k), \qquad & p_4 : (x, y) &= (0, -k). \end{aligned} \tag{1.22}$$

Blowing these up, we denote the blow-up projection by

$$\pi_1 : \mathrm{Bl}_{p_1,p_2,p_3,p_4}(\mathbb{P}^1 \times \mathbb{P}^1) \to \mathbb{P}^1 \times \mathbb{P}^1, \tag{1.23}$$

and denote the exceptional curves by $\pi_1^{-1}(p_i) = E_i$ for $i = 1, 2, 3, 4$. The proper transform of the pencil under π_1 still has four basepoints $p_5 \in E_1$, $p_6 \in E_2$, $p_7 \in E_3$, $p_8 \in E_4$. After the blow-ups of these, the proper transform of the pencil is basepoint-free and we obtain a rational elliptic surface $\mathcal{X}$. Denote the projection under the second four blow-ups by

$$\pi_2 : \mathcal{X} \to \mathrm{Bl}_{p_1,p_2,p_3,p_4}(\mathbb{P}^1 \times \mathbb{P}^1), \tag{1.24}$$

and the exceptional curves by $\pi_2^{-1}(p_i) = E_i$ for $i = 5, 6, 7, 8$. Composing the projections we obtain

$$\pi = \pi_1 \circ \pi_2 : \mathcal{X} \to \mathbb{P}^1 \times \mathbb{P}^1, \tag{1.25}$$

and $\mathcal{X}$ is a rational surface fibred by the proper transform of the pencil. Under π, we have the preimage of each basepoint $p_1, \ldots, p_4$ given by the union of two irreducible curves:

$$\begin{aligned} \pi^{-1}(p_1) &= (E_1 - E_5) \cup E_5, \qquad & \pi^{-1}(p_2) &= (E_2 - E_6) \cup E_6, \\ \pi^{-1}(p_1) &= (E_3 - E_7) \cup E_7, \qquad & \pi^{-1}(p_4) &= (E_4 - E_8) \cup E_8, \end{aligned} \tag{1.26}$$

where we have used the usual notation for divisors to denote by $E_1 - E_5$ the proper transform of E_1 under π_2, and so on, which we illustrate in Figure 1.1.

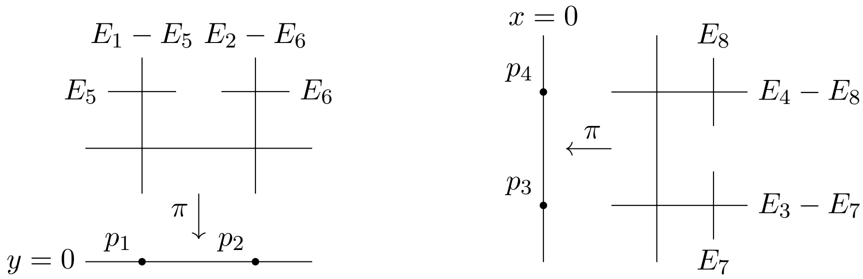

Figure 1.1: Configuration of curves in the space of initial conditions for the QRT mapping (1.19)

The iteration mapping (1.19) lifts uniquely under the blow-ups to give a birational map

$$\tilde{\varphi} : \mathcal{X} \to \mathcal{X}, \tag{1.27}$$

which is in fact a true isomorphism. At this point we omit the calculations necessary to establish this, as methods for lifting mappings under blow-ups explicitly will be outlined in detail in later chapters. The singularity confinement behaviour observed earlier can be understood in terms of this space of initial conditions as follows. Lifted under the blow-ups, the initial data $f_{n-1} \neq 0, f_n = k$ correspond to a point on the proper transform of the line $\{x = k\}$ on $\mathbb{P}^1 \times \mathbb{P}^1$, while the pairs $(f_n, f_{n+1}) = (k, 0)$, $(f_{n+1}, f_{n+2}) = (0, -k)$ correspond to the basepoints p_3, p_2 respectively. Further, the recovery of the degree of freedom $(f_{n+2}, f_{n+3}) = (-k, f_{n-1})$ corresponds to a one-to-one correspondence between the proper transforms of the lines $\{x = k\}$ and $\{y = -k\}$ under the iterated mapping $\tilde{\varphi}^3$, as we illustrate in Figure 1.2.

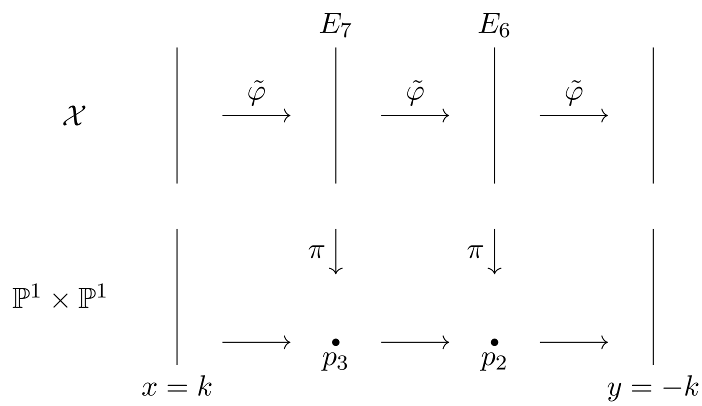

Figure 1.2: Confinement of a singularity as an isomorphism between exceptional curves

The loss of a degree of freedom when $f_n = \pm k$ can now be understood in terms of curves in $\mathbb{P}^1 \times \mathbb{P}^1$ being blown down to points under the mapping φ. The recovery of the lost degree of freedom occurs precisely when, while iterating after a blow-down, we arrive at an indeterminacy of the forward iteration map φ (in the case of the singularity $f_n = k$, this is p_2), so the point is blown back up to a curve. For generic (non-integrable) systems, after a blow-down we will not arrive at an indeterminacy of the forward mapping and the lost degree of freedom will never be recovered. In other words, we cannot lift the mapping to an isomorphism through a finite number of blow-ups.

1.2.3 Deautonomisation by singularity confinement

Ramani, Grammaticos and Hietarinta [RGH91] obtained a plethora of discrete Painlevé equations via the process of 'deautonomisation by singularity confinement' applied to members of the QRT family. This involves considering nonautonomous generalisations of a given QRT map by introducing n-dependence into the coefficients of the mapping, then isolating examples for which the singularity confinement behaviour persists. We will illustrate this in the example of the QRT mapping (1.17), by considering a nonautonomous generalisation

$$f_{n+1} = \frac{(f_n - k_n)(f_n + k_n) f_{n-1}}{k_n^2 - f_n^2 + 2 t_n f_n f_{n-1}}, \tag{1.28}$$

where for now k_n, t_n are arbitrary sequences of complex numbers again with $k_n \neq 0, \pm 1, t_n \neq 0$ for all n. Calculating as before, initial data given by a small perturbation about the singular values $f_n = \pm k_n$ leads to the following:

$$\begin{aligned}
f_{n-1} &\neq 0, \\
f_n &= \pm k_n + \mathcal{O}(\varepsilon), \\
f_{n+1} &= \mathcal{O}(\varepsilon), \\
f_{n+2} &= \mp k_n + \mathcal{O}(\varepsilon), \\
f_{n+3} &= \pm \frac{W}{f_{n-1}^5 k_n^5 k_{n+1}^2 t_n^4 \left(k_{n+1}^2 t_n - 2 k_n^2 t_{n+1} + k_{n+1}^2 t_{n+2}\right)} \varepsilon + \mathcal{O}(\varepsilon^2),
\end{aligned} \tag{1.29}$$

where we assume that the denominator of the leading term in f_{n+3} is nonzero. Here W is a known polynomial function of f_{n-1} and the parameter sequences, which we omit for conciseness as it plays no role in what follows. Under this assumption, the values of iterates will continue to cycle through the pattern $(\pm k_n, 0, \mp k_n, 0, \pm k_n)$, and the lost degree of freedom will never be recovered. Deautonomisation by singularity confinement in this case means imposing conditions such that this behaviour is avoided, and the degree of freedom is recovered. Here the denominator of the term in ε from f_{n+3} being nonzero causes the singularity to propagate indefinitely, so to avoid this we require the following condition for all $n \in \mathbb{Z}$:

$$k_{n+1}^2 t_n - 2k_n^2 t_{n+1} + k_{n+1}^2 t_{n+2} = 0, \tag{1.30}$$

so that if f_n takes the singular values $\pm k$ then f_{n+3} might avoid a zero. For simplicity, we assume k_n is a constant sequence with value k, so it suffices to solve the linear recurrence

$$t_{n+2} - 2t_{n+1} + t_n = 0. \tag{1.31}$$

Indeed, the general solution is $t_n = \alpha n + \beta$, so we have a nonautonomous generalisation of equation (1.17), which we hope shows the same kind of singularity confinement behaviour:

$$f_{n+1} = \frac{(f_n - k)(f_n + k)f_{n-1}}{k^2 - f_n^2 + 2(\alpha n + \beta)f_n f_{n-1}}, \tag{1.32}$$

Indeed, computing as before we find the following:

$$\begin{aligned}
f_{n-1} &\neq 0, \\
f_n &= \pm k + \mathcal{O}(\varepsilon), \\
f_{n+1} &= \mathcal{O}(\varepsilon), \\
f_{n+2} &= \mp k + \mathcal{O}(\varepsilon), \\
f_{n+3} &= \frac{k\left((n+2)\alpha + \beta\right) f_{n-1}}{2\alpha\left((n+1)\alpha + \beta\right) f_{n-1} \pm k(\alpha n + \beta)} + \mathcal{O}(\varepsilon),
\end{aligned} \tag{1.33}$$

and we have avoided f_{n+3} developing a zero if f_n takes one of the singular values. Further, the lost degree of freedom is recovered in the appearance of f_{n-1} in f_{n+3}. Similarly to the QRT mapping it generalises, the equation (1.32) admits a space of conditions, but this will be given by a family of surfaces indexed by n, as opposed to the single elliptic surface $\mathcal{X}$. To be precise, we recast the equation as a family of mappings $\{\varphi_n : n \in \mathbb{Z}\}$, by letting $(x_n, y_n) = (f_n, f_{n-1})$ or each n, and using these to define mappings on $\mathbb{P}^1 \times \mathbb{P}^1$ via the same charts$(x, y), (X, Y)$ etc. via $(x_n, y_n) = (x, y)$ for the domain copy of $\mathbb{P}^1 \times \mathbb{P}^1$, and

$(\bar{x},\ \bar{y})$ etc. for the target, via $(x_{n+1}, y_{n+1}) = (\bar{x}, \bar{y})$:

$$\begin{aligned} \varphi_n :\ \mathbb{P}^1 \times \mathbb{P}^1 &\to \mathbb{P}^1 \times \mathbb{P}^1 \\ (x, y) &\mapsto (\bar{x}, \bar{y}) = \left(\frac{(x-k)(x+k)y}{k^2 - x^2 + 2(\alpha n + \beta)xy}, x \right). \end{aligned} \tag{1.34}$$

Again, we can lift these mappings to isomorphisms under eight blow-ups, but in this cases the locations of the basepoints depend on n, so instead of a single surface we obtain a family of rational surfaces $\mathcal{X}_n$, between which the mappings lift to isomorphisms. This deatunomisation procedure can be understood geometrically; the surfaces belong to the family defined by Sakai and the resulting equations can be placed in Sakai's framework for discrete Painlevé equations, following [CDT17].

1.2.4 Integrability

We now make some remarks about some notions of integrability of discrete Painlevé equations and their relation to the geometric framework. Firstly, we will see in Chapter 2 that Sakai's definition of discrete Painlevé equations ensures that any example involving one or more parameters will admit Bäcklund transformation symmetries. For the most general form of a given discrete Painlevé equation, i.e. one arising from the most general form of a family of surfaces of its type, these symmetries will correspond to an action of an extended affine Weyl group in the same way as was observed for the differential Painlevé equations.
Secondly, many examples admit Lax representations as compatibility conditions of associated linear systems. One of the most famous discrete Painlevé equations, usually referred to as q-P_{VI} due to it being a q-difference equation with a continuum limit to P_{VI}, was obtained by Jimbo and Sakai as a kind of connection-preserving deformation of a linear q-difference equation [JS96]. A method for obtaining Lax representations for Sakai's discrete Painlevé equations from the associated surfaces is outlined in [KNY17], which built on earlier results, e.g. [Yam09, Yam11].
Sakai's discrete Painlevé equations also satisfy the most accepted definition of integrability in discrete systems corresponding to birational mappings, namely that they have vanishing algebraic entropy. This property was proposed by Bellon and Viallet [BV99], and continues the paradigm in which integrability is characterised by a kind of slow growth in complexity under the dynamics, which goes back to the ideas of topological entropy of Arnol'd [Arn90a, Arn90b] and growth of complexity in discrete systems of Veselov [Ves92]. We

remark that algebraic entropy is closely related to the notions of entropy considered by Friedland [Fri91] following from his work with Milnor [FM89], which have led to a range of studies which should be of interest to researchers working on discrete integrable systems (see [Fri07] and references within). We recall the definition of algebraic entropy in the case of second-order equations. Consider a system of two first-order discrete equations

$$f_{n+1} = P(f_n, g_n), \tag{1.35a}$$

$$g_{n+1} = Q(f_n, g_n), \tag{1.35b}$$

where P, Q are rational functions in their arguments (with coefficients possibly depending on n), and there exists a rational inverse giving (f_n, g_n) in terms of (f_{n+1}, g_{n+1}). We then have a birational map defined, as outlined in our treatment of the QRT mappings, in inhomogeneous coordinates $(f, g) = (f_n, g_n)$ for $\mathbb{P}^1 \times \mathbb{P}^1$ by

$$\begin{aligned} \eta:\ \mathbb{P}^1 \times \mathbb{P}^1 &\to \mathbb{P}^1 \times \mathbb{P}^1, \\ (f,g) &\mapsto (P(f,g), Q(f,g)), \end{aligned} \tag{1.36}$$

and define its degree to be

$$\deg(\eta) = \max\left\{\deg P(f,g), \deg Q(f,g)\right\}, \tag{1.37}$$

where the degree of a rational function $P(f, g)$ is defined as the maximum of the degrees of its numerator and denominator as bivariate polynomials, after any cancellations. Letting the maps induced by iteration of the system (1.35) be $\eta_n : (f_n, g_n) \mapsto (f_{n+1}, g_{n+1})$, we write the map giving the n-th iterate as a function of arbitrary initial conditions $(f_0, g_0) = (f, g)$ as

$$\begin{aligned} \eta^{(n)}:\ \ &\mathbb{P}^1 \times \mathbb{P}^1 \to \mathbb{P}^1 \times \mathbb{P}^1, \\ \eta^{(n)} = \eta_{n-1} \circ \cdots \circ \eta_1 \circ \eta_0:\ \ &(f,g) \mapsto (P_n(f,g), Q_n(f,g)), \end{aligned} \tag{1.38}$$

where P_n, Q_n are rational functions obtained by composing the ones in (1.35). The sequence of degrees of iterates of the system is then given by $d_n = \deg \eta^{(n)}$, and its algebraic entropy is defined as

$$\varepsilon = \lim_{n\to\infty} \frac{1}{n} \log d_n, \tag{1.39}$$

in the cases where the limit exists. If the system is nonlinear, generically no cancellations will occur in the computation of P_n, Q_n, and the degrees will grow exponentially. However, the system is said to be integrable in the sense of vanishing algebraic entropy if $\varepsilon = 0$, or in other words if sufficient cancellations occur and the growth of the degrees is polynomial.
In [Tak01a], T. Takenawa gave a method for computing the sequence of degrees explicitly in the case when the system admits a space of initial conditions, and showed that Sakai's definition of discrete Painlevé equations ensured that they are integrable in the sense of vanishing algebraic entropy. Sakai's construction recovers many of the examples obtained by singularity confinement methods, but we make an important remark here that lifting to isomorphisms under a finite number of blow-ups is not sufficient for integrability, and the geometry of the space of initial conditions plays a defining role. In particular, an example given by Hietarinta and Viallet [HV98] admits a space of initial conditions but exhibits chaotic behaviour in the sense of exponential degree growth, which was explained in terms of its geometry by Takenawa [Tak01b]. It has since been shown by Mase [Mas18] that if a second-order discrete system with the singularity confinement property (in the sense that it admits a space of initial conditions) is nontrivially integrable (in the sense of quadratic degree growth), then it must arise from the surfaces defined by Sakai.

Chapter 2

Geometric framework for differential and discrete Painlevé equations

Sakai's theory formalises and builds on Okamoto's observations of complementary affine Weyl group structures associated with the Bäcklund transformation symmetries and the intersection configuration of inaccessible divisors for each of the differential Painlevé equations. The central idea of our presentation of this theory is the construction of rational surfaces associated with affine Weyl groups and their associated root systems. We remark that Sakai's work is not the only one to pursue generalisations of Okamoto's space. The inaccessible divisors in each fibre were observed to give a decomposition into irreducible components of an anticanonical divisor of the surface, which led to the idea of classifying rational surfaces with such a configuration of curves via the notion of an *Okamoto-Painlevé pair* [ST02,STT02]. This is a pair (S, D) of a smooth rational surface S and a representative D of its anticanonical divisor class which is of *canonical type*, which is a notion considered by Sakai and which we will define in the coming sections.

Sakai's theory employs a similar approach, but additionally focuses on the construction of discrete equations for which the surfaces provide spaces of initial conditions, and the way in which symmetries of these equations come from the geometry of the surfaces. This chapter establishes this theory as the foundation for the thesis, following both Sakai's original paper [Sak01] and the important survey of Kajiwara, Noumi and Yamada [KNY17]. It both equips us with a suite of tools for the study of Painlevé equations appearing in applications, as in Chapter 3, and is our starting point for extensions of the geometric approach to wider classes of equations, as in Chapter 4 and Chapter 5.

We first review background material on the affine root systems and Weyl groups relevant to Painlevé equations, following Kac [Kac90], before presenting Sakai's theory in generality. We then finish this chapter by illustrating this theory in detail with a family of surfaces associated with both the sixth differential Painlevé equation and a discrete analogue of $\mathrm{P_V}$, which will be relevant to our work in later chapters.

2.1 Preliminaries on affine Weyl groups

The root systems and Weyl groups we are interested in arise in the theory of certain infinite-dimensional Lie algebras. We follow [Kac90], by first making the following definition:

Definition 2.1.1. *A* generalised Cartan matrix *is an $n \times n$ matrix $A = (A_{ij})_{i,j=1}^{n}$ with:*

- $A_{ii} = 2, \quad$ *for* $\quad i = 1, \dots n$*;*
- A_{ij} *nonpositive integers for* $i \neq j$*;*
- $A_{ij} = 0 \quad \iff \quad A_{ji} = 0.$

Generalised Cartan matrices can be used to define a class of Lie algebras generalising the classical finite-dimensional semi-simple ones, and much of what follows is motivated by the study of these Kac-Moody algebras, including the associated Weyl groups. We first introduce the Weyl group associated with a generalised Cartan matrix purely as an abstract Coxeter group defined by the following presentation:

Definition 2.1.2. *The* Weyl group *of a generalised Cartan matrix A, denoted $W(A)$ is generated by r_i, $i = 1, \dots, n$, subject to the relations*

- $r_i^2 = e \quad$ *for* $\quad i = 1, \dots, n.$
- $(r_i r_j)^{m_{ij}} = e \quad \textit{for } i \neq j, \quad \textit{where } m_{ij} = \begin{cases} 2 & \textit{if } A_{ij}A_{ji} = 0, \\ 3 & \textit{if } A_{ij}A_{ji} = 1, \\ 4 & \textit{if } A_{ij}A_{ji} = 2, \\ 6 & \textit{if } A_{ij}A_{ji} = 3, \\ \infty & \textit{if } A_{ij}A_{ji} \geq 4. \end{cases}$

The generators r_i are called simple reflections and here, following [Kac90]*, we use the convention that $x^{\infty} = e$ for any x, so in particular when $A_{ij}A_{ji} \geq 4$ there are no relations between r_i and r_j.*

This group $W(A)$ arises naturally in the study of the Kac-Moody algebra associated to A, but for our purposes it will be sufficient to understand it in terms of reflections about hyperplanes in a complex vector space, which can be established without introducing the algebra itself. Make the following definition:

Definition 2.1.3. *A* realisation *of A is a triple $(\mathfrak{h}, \Pi, \Pi^\vee)$, where*

- *$\mathfrak{h}$ is a vector space over $\mathbb{C}$,*
- *$\Pi = \{\alpha_1, \ldots, \alpha_n\} \subset \mathfrak{h}^* = \mathrm{Hom}_{\mathbb{C}}(\mathfrak{h}, \mathbb{C})$ is a linearly independent set of* simple roots.
- *$\Pi^\vee = \{\alpha_1^\vee, \ldots, \alpha_n^\vee\} \subset \mathfrak{h}$ is a linearly independent set of* simple coroots,

subject to the conditions

- *$\langle \alpha_i^\vee, \alpha_j \rangle = A_{ij}, \quad for \quad i, j = 1, \ldots n,$*
- *$n - \mathrm{rank}\, A = \dim \mathfrak{h} - n,$*

where $\langle\ ,\ \rangle : \mathfrak{h} \times \mathfrak{h}^* \to \mathbb{C}$ is the evaluation pairing.

For a realisation $(\mathfrak{h}, \Pi, \Pi^\vee)$ of A, define the *simple reflection* $r_i \in \mathbf{GL}(\mathfrak{h}^*)$ corresponding to α_i by

$$r_i(\lambda) = \lambda - \langle \alpha_i^\vee, \lambda \rangle \alpha_i. \tag{2.1}$$

It can be quickly checked this gives a faithful representation of the Weyl group $W(A)$ introduced in Definition 2.1.2.

If we have two matrices A_1, A_2 with realisations $(\mathfrak{h}_1, \Pi_1, \Pi_1^\vee), (\mathfrak{h}_2, \Pi_2, \Pi_2^\vee)$ respectively, we obtain a realisation of the direct sum of the two matrices

$$\begin{pmatrix} A_1 & 0 \\ 0 & A_2 \end{pmatrix}, \tag{2.2}$$

given by

$$\left(\mathfrak{h}_1 \oplus \mathfrak{h}_2, (\Pi_1 \times \{0\}) \cup (\{0\} \times \Pi_2), (\Pi_1^\vee \times \{0\}) \cup (\{0\} \times \Pi_2^\vee)\right). \tag{2.3}$$

If a generalised Cartan matrix and its realisation can be written as a nontrivial direct sum as above after a reordering of indices, then it is called *decomposable*. Kac showed that any indecomposable generalised Cartan matrix A belongs to one of three classes, which we quote here from [Kac90]. These are defined as follows, where the matrix A is of size $n \times n$ and we use notation to refer to the signs of vectors according to those of their entries, for example $\mathbf{u} > 0$ to indicate that a vector $\mathbf{u} \in \mathbb{R}^n$ has all entries positive.

(Fin) $\det A \neq 0$; there exists $\mathbf{u} > 0$ such that $A\mathbf{u} > 0$; $A\mathbf{v} \geq 0$ implies $\mathbf{v} > 0$ or $\mathbf{v} = 0$.

(Aff) $\operatorname{corank} A = 1$; there exists $\mathbf{u} > 0$ such that $A\mathbf{u} = 0$; $A\mathbf{v} \geq 0$ implies $A\mathbf{v} = 0$.

(Ind) there exists $\mathbf{u} > 0$ such that $A\mathbf{u} < 0$; $A\mathbf{v} \geq 0$, $v \geq 0$ imply $A\mathbf{v} = 0$.

Generalised Cartan matrices from these classes are referred to as of Finite, Affine and Indefinite type respectively. The indecomposable matrices from the class (Fin) account for all Cartan matrices associated with finite-dimensional simple complex Lie algebras. Each of these matrices can be encoded in a Dynkin diagram, which consists of a node for each index $i \in \{1, \dots, n\}$, with nodes corresponding to i and j connected by $|A_{ij}A_{ji}|$ edges, with an arrow pointing towards i if $|A_{ij}| > |A_{ji}|$. The Dynkin diagrams for the class (Fin) are given in Figure 2.1.

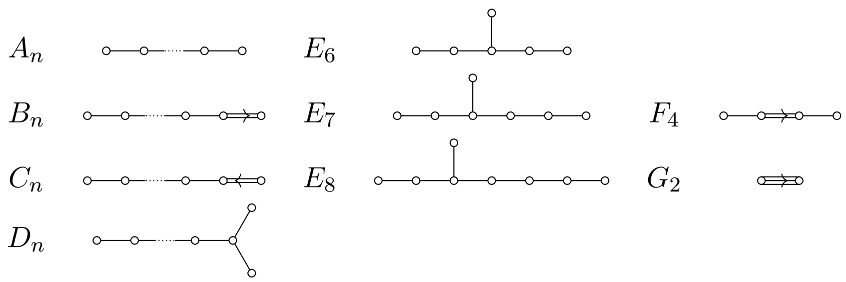

Figure 2.1: Dynkin diagrams for indecomposable generalised Cartan matrices of finite type

In the theory of Painevé equations, we will be interested in the matrices of affine type, and in particular those which are symmetric and whose affine Dynkin diagrams (sometimes known as extended Dynkin diagrams) are *simply laced* (meaning they only have single edges), which we present in Figure 2.2.

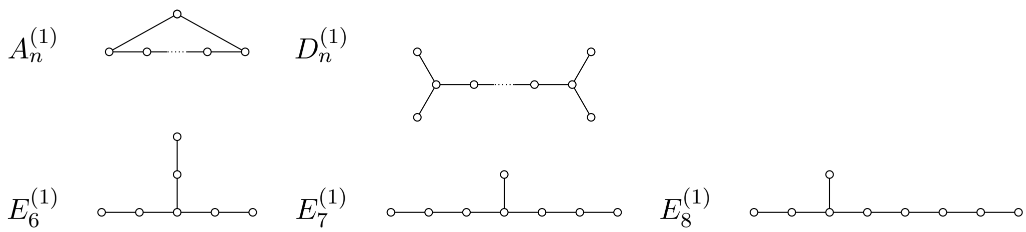

Figure 2.2: Dynkin diagrams for symmetric generalised Cartan matrices of affine type

We now describe in detail the properties of a realisation of a generalised Cartan matrix A, which in what follows will be assumed to be symmetric and of affine type, with simply laced Dynkin diagram. We take A to be of size $n+1$ with enumeration $A = (A_{ij})_{i,j=0}^{n}$, $\Pi = \{\alpha_0, \dots, \alpha_n\}, \Pi^\vee = \{\alpha_0^\vee, \dots, \alpha_n^\vee\}$. Firstly, as A is of affine type, the matrix is of corank 1, so we have the *null root* in $\mathfrak{h}^*$

$$\delta = \sum_{i=0}^{n} m_i \alpha_i, \quad m_0 = 1, \tag{2.4}$$

such that $\langle \alpha_i^\vee, \delta \rangle = 0$ for $i = 0, \dots, n$, which is determined uniquely by imposing $m_0 = 1$. The values of m_i for all symmetric A of affine type can be computed directly using its null space and are listed in [Kac90]. Similarly we have a unique element $K \in \mathfrak{h}$ given by a positive integer combination of simple coroots

$$K = \sum_{i=0}^{n} m_i^\vee \alpha_i^\vee, \quad m_0^\vee = 1 \tag{2.5}$$

such that $\langle K, \alpha_i \rangle = 0$ for $i = 0, \dots, n$. This is called the *canonical central element*, because when $\mathfrak{h}$ is considered as part of the Kac-Moody algebra associated with A it spans the centre. As we are considering symmetric matrices, we have $m_i^\vee = m_i$ for all i.
To describe the spaces $\mathfrak{h}, \mathfrak{h}^*$, we recall that the condition from the realisation with our enumeration determines the dimension of $\mathfrak{h}$ to be $n+2$, so we extend $\Pi, \Pi^\vee$ to bases as follows. Fix a *scaling element* $d \in \mathfrak{h}$ satisfying

$$\langle d, \alpha_i \rangle = \delta_{i0} \quad \text{for } i = 0, \dots, n, \tag{2.6}$$

where δ_{ij} is the Kronecker delta. Such an element is determined up to addition of a constant multiple of K, and is linearly independent from $\Pi^\vee$, so we have a basis $\{d, \alpha_0^\vee, \dots, \alpha_n^\vee\}$ for $\mathfrak{h}$. Similarly, we define an element $\Lambda_0 \in \mathfrak{h}^*$ uniquely by the conditions

$$\left\langle \alpha_i^\vee, \Lambda_0 \right\rangle = \delta_{i0} \quad \text{for } i = 0, \dots, n, \quad \langle d, \Lambda_0 \rangle = 0, \tag{2.7}$$

and we have a basis $\{\Lambda_0, \alpha_0, \dots, \alpha_n\}$ for $\mathfrak{h}^*$. We may now define a symmetric bilinear form $(\,|\,)$ on $\mathfrak{h}^*$, in terms of which we can describe the reflections and Weyl group. For the symmetric matrices this can be introduced directly on $\mathfrak{h}^*$ by the formulae

$$\begin{aligned} &(\alpha_i|\alpha_j) = A_{ij}, && \text{for } i, j, = 0, \dots, n, \\ &(\alpha_i|\Lambda_0) = 0, && \text{for } i = 1, \dots, n, \\ &(\alpha_0|\Lambda_0) = 1, && (\Lambda_0|\Lambda_0) = 0, \end{aligned} \tag{2.8}$$

so in particular we have

$$(\delta|\delta) = 0. \tag{2.9}$$

The action of the Weyl group $W = W(A)$ on $\mathfrak{h}^*$ can now be written in terms of this symmetric bilinear form, with the simple reflection r_i acting on $\lambda \in \mathfrak{h}^*$ by

$$r_i(\lambda) = \lambda - (\lambda|\alpha_i)\alpha_i. \tag{2.10}$$

In particular, we have that the null root δ is fixed by all $w \in W$, as $(\alpha_i|\delta) = 0$ for all i, and it can be verified by direct calculation that the bilinear form is W-invariant: $(w(\lambda_1)|w(\lambda_2)) = (\lambda_1|\lambda_2)$ for all $w \in W$, $\lambda_1, \lambda_2 \in \mathfrak{h}^*$. The symmetric bilinear form (2.8) defines an isomorphism $\nu : \mathfrak{h} \to \mathfrak{h}^*$ via $\langle h_1, \nu(h_2)\rangle = (h_1|h_2)$, which is given by

$$\nu(\alpha_i^\vee) = \alpha_i, \quad \nu(K) = \delta, \quad \nu(d) = \Lambda_0, \tag{2.11}$$

so we have a symmetric bilinear form on $\mathfrak{h}$ induced by ν, which we also denote $(\,|\,)$, i.e. $(h_1|h_2) = (\nu(h_1)|\nu(h_2))$ for $h_1, h_2 \in \mathfrak{h}$, so

$$\begin{aligned} &(\alpha_i^\vee|\alpha_j^\vee) = A_{ij}, && \text{for } i, j, = 0, \dots, n, \\ &(\alpha_i^\vee|d) = 0, && \text{for } i = 1, \dots, n, \\ &(\alpha_0^\vee|d) = 1, && (d|d) = 0. \end{aligned} \tag{2.12}$$

We introduce the *root lattice*

$$Q = \sum_{i=0}^{n} \mathbb{Z}\alpha_i \subset \mathfrak{h}^*, \tag{2.13}$$

and the *coroot lattice*

$$Q^\vee = \sum_{i=0}^{n} \mathbb{Z}\alpha_i^\vee \subset \mathfrak{h}. \tag{2.14}$$

These are true lattices: free $\mathbb{Z}$-modules with symmetric bilinear form, and are isomorphic since we are considering symmetric matrices.

In the thesis, the property of most interest to us of the Weyl groups associated with matrices of affine type is that they are of infinite order and each contains a subgroup of translations, which corresponds to a sublattice associated with an underlying finite root system. This allows Kac's theory to recover the classical definition of an affine Weyl group as an extension of that of a finite root system to include reflections about affine hyperplanes in a Euclidean space [Hum90], which we now explain. Taking A as above, the matrix $\mathring{A} = (A_{ij})_{i,j=1}^{l}$ obtained by deleting the 0-th row and column is a generalised Cartan matrix of finite type. From the realisation of A, we obtain one for the finite type matrix $\mathring{A}$, denoted by $\left(\mathring{\mathfrak{h}}, \mathring{\Pi}, \mathring{\Pi}^\vee\right)$, where

$$\begin{aligned} \mathring{\Pi} &= \{\alpha_1, \ldots, \alpha_n\}, & \mathring{\mathfrak{h}}^* &= \operatorname{span}_{\mathbb{C}} \{\alpha_1, \ldots, \alpha_n\} \\ \mathring{\Pi}^\vee &= \left\{\alpha_1^\vee, \ldots, \alpha_n^\vee\right\}, & \mathring{\mathfrak{h}} &= \operatorname{span}_{\mathbb{C}} \left\{\alpha_1^\vee, \ldots, \alpha_n^\vee\right\}. \end{aligned} \tag{2.15}$$

We denote the root and coroot lattices associated with this realisation by $\mathring{Q} = \sum_{i=1}^n \mathbb{Z}\alpha_i$ and $\mathring{Q}^\vee = \sum_{i=1}^n \mathbb{Z}\alpha_i^\vee$ respecively. The subgroup $\mathring{W} = W(\mathring{A}) \subset W$ generated by the simple reflections $r_1, \ldots, r_n$ is the *underlying finite Weyl group*, the action of which on $\mathfrak{h}^*$ restricts to a faithful action on $\mathring{\mathfrak{h}}^*$. All nontrivial elements of $\mathring{W}$ correspond to reflections associated with roots in the finite root system, which here it is sufficient to define as the orbit of the set of simple roots $\mathring{\Phi} = \mathring{W}(\mathring{\Pi})$. For $\alpha \in \mathring{\Phi}$, we have an element $r_\alpha \in \mathring{W}$, which acts on $\mathfrak{h}^*$ by the formula

$$r_\alpha(\lambda) = \lambda - (\lambda|\alpha)\alpha, \tag{2.16}$$

so in particular $r_i = r_{\alpha_i}$. Consider the element

$$\theta = \delta - \alpha_0 = \sum_{i=1}^{l} m_i \alpha_i, \tag{2.17}$$

where m_i are the same as in the expression (2.4) for the null root. This element θ is the unique *highest root* in the finite root system with respect to the partial order induced by writing roots as $\mathbb{Z}$-linear combinations of simple roots. Composing reflections associated with θ and α_0, by direct calculation we obtain

$$r_0 r_\theta(\lambda) = \lambda + (\lambda|\delta)\theta - [(\lambda|\theta) + (\lambda|\delta)]\,\delta, \tag{2.18}$$

where we have used the fact that for symmetric matrices we have $(\theta|\theta) = 2$.
Motivated by this formula, Kac introduces for $v \in \mathring{\mathfrak{h}}^*$ the element $T_v \in \mathbf{GL}(\mathfrak{h}^*)$ according to

$$T_v(\lambda) = \lambda + (\lambda|\delta)v - \left[(\lambda|v) + (\lambda|\delta)\frac{(v|v)}{2}\right]\delta. \tag{2.19}$$

We refer to this as the *Kac translation formula*, and the *Kac translation* T_v has the following properties:

$$T_uT_v = T_{u+v}, \qquad T_{w(v)} = wT_vw^{-1} \quad \text{for all } u, v \in \mathring{\mathfrak{h}}^*, \quad w \in \mathring{W}. \tag{2.20}$$

For $\beta \in \mathfrak{h}^*$ such that $(\beta|\delta) = 0$, we have

$$T_v(\beta) = \beta - (\beta|v)\delta, \tag{2.21}$$

so the properties (2.20) can be deduced on this part of $\mathfrak{h}^*$ using the W-invariance of the bilinear form and the fact that δ is fixed by all $w \in W$. The extra terms in the formula (2.19) ensure these properties hold on the rest of $\mathfrak{h}^*$, which is spanned by Λ_0. Indeed, for $v \in \mathring{\mathfrak{h}}^*$ we may compute the following, using the formula (2.19):

$$T_v(\Lambda_0) = \Lambda_0 + v - \frac{(v|v)}{2}\delta, \tag{2.22}$$

where we have used $(v|\Lambda_0) = 0$ as $v \in \mathring{\mathfrak{h}}^*$, and $(\Lambda_0|\delta) = 1$. The properties (2.20) can be verified by direct calculation.
Recall the root lattice $\mathring{Q} \subset \mathfrak{h}^*$ associated with the underlying finite root system, which because of the properties (2.20) defines a normal subgroup

$$T_{\mathring{Q}} = \{T_v \mid v \in \mathring{Q}\}. \tag{2.23}$$

The Kac translation formula then gives the following isomorphism:

$$\begin{aligned} W &\cong \mathring{W} \ltimes T_{\mathring{Q}}, \\ r_0 &\mapsto r_\theta T_{-\theta}, \end{aligned} \tag{2.24}$$

The group W can be identified with the usual affine Weyl group associated with the finite root system $\mathring{\Phi}$ by considering an action of W induced on

$$\mathfrak{h}_1^* \bmod \mathbb{R}\delta, \quad \text{where} \quad \mathfrak{h}_1^* := \{\lambda \in \operatorname{span}_{\mathbb{R}}\{\alpha_0, \ldots, \alpha_n\} \mid (\lambda|\delta) = 1\}, \tag{2.25}$$

but we will continue to work with the action of the Weyl group on $\mathfrak{h}^*$, and in particular on the root lattice Q.

From the fact that Q is orthogonal to δ, the action of $T_{\mathring{Q}}$ on Q is given by the formula (2.21), and we can deduce that the action preserves the root lattice. However, for Q to be preserved, we may choose a lattice finer than $\mathring{Q}$ to act by Kac translation. Let $\omega_1, \ldots, \omega_n \in \mathring{\mathfrak{h}}^*$ be the basis of *fundamental weights* dual to $\mathring{\Pi}^\vee$, so $\left\langle \omega_i, \alpha_j^\vee \right\rangle = \delta_{ij}$ for $i, j = 1, \ldots n$ and we have the weight lattice of the underlying finite root system given by

$$\mathring{P} = \sum_{i=1}^{n} \mathbb{Z}\omega_i. \tag{2.26}$$

The weight lattice is the maximal set of elements v in the span of $\mathring{\Pi}$ with integer pairing $(\beta|v) \in \mathbb{Z}$ for all $\beta \in Q$, so the subgroup

$$T_{\mathring{P}} = \{T_v \mid v \in \mathring{P}\}, \tag{2.27}$$

preserves the root lattice. The *extended affine Weyl group* associated with a symmetric generalised Cartan matrix of affine type is defined as

$$\widetilde{W} = \mathring{W} \ltimes T_{\mathring{P}}. \tag{2.28}$$

This is an extension of the regular affine Weyl group in the sense that we have

$$\widetilde{W} \cong W \rtimes \Sigma, \tag{2.29}$$

where $\Sigma \cong \mathring{P}/\mathring{Q}$ is a finite group which acts by special automorphisms of the affine Dynkin diagram. We list the group Σ for the cases we are interested in in Figure 2.3.

	$A_n^{(1)}$	$D_{2n}^{(1)}$	$D_{2n+1}^{(1)}$	$E_6^{(1)}$	$E_7^{(1)}$	$E_8^{(1)}$
Σ	$\mathbb{Z}_{n+1}$	$\mathbb{Z}_2 \times \mathbb{Z}_2$	$\mathbb{Z}_4$	$\mathbb{Z}_3$	$\mathbb{Z}_2$	–

Figure 2.3: Special automorphism groups for symmetric generalised Cartan matrices of affine type.

The group of Bäcklund transformation symmetries for $\mathrm{P_{IV}}$ defined in Subsection 1.1.3 by the presentation (1.16) is precisely the extended affine Weyl group associated with the generalised Cartan matrix

$$A = \begin{pmatrix} 2 & -1 & -1 \\ -1 & 2 & -1 \\ -1 & -1 & 2 \end{pmatrix} \tag{2.30}$$

with Dynkin diagram $A_2^{(1)}$. The generators s_0, s_1, s_2 are the simple reflections and the Dynkin diagram automorphism π generates the group $\Sigma \cong \mathbb{Z}_3$.

2.2 Sakai theory and generalised Halphen surfaces

We now follow Sakai's construction of rational surfaces associated with the affine root system structures reviewed in the previous section. We will begin by identifying a natural way for a root lattice of type $E_8^{(1)}$ to appear in the Picard group of a smooth rational surface.

2.2.1 Root lattice of type $E_8^{(1)}$ in the Picard group

Consider a smooth projective rational surface $\mathcal{X}$ obtained from $\mathbb{P}^1 \times \mathbb{P}^1$ by eight successive blow-ups. We denote by $\mathrm{Pic}(\mathcal{X})$ the Picard group, whose elements are line bundles on $\mathcal{X}$, with the group operation being the tensor product. As $\mathcal{X}$ is smooth, $\mathrm{Pic}(\mathcal{X})$ is isomorphic to the divisor class group, which is the quotient of the group $\mathrm{Div}(\mathcal{X})$ of Weil divisors (formal $\mathbb{Z}$-linear combinations of closed codimension one subvarieties) by the subgroup of principal divisors (those which are divisors of rational functions on $\mathcal{X}$). Thus $\mathrm{Pic}(\mathcal{X})$ can be identified with the group of divisors up to linear equivalance, which we denote $\sim$ so divisors $D_1, D_2 \in \mathrm{Div}(\mathcal{X})$ are linearly equivalent $D_1 \sim D_2$ if $D_1 - D_2 = \mathrm{div}(f)$ for some rational function f on $\mathcal{X}$.

Writing operations additively, $\mathrm{Pic}(\mathcal{X})$ is a free $\mathbb{Z}$-module of rank 10 given by the direct sum

$$\mathrm{Pic}(\mathcal{X}) = \mathbb{Z}\mathcal{H}_1 \oplus \mathbb{Z}\mathcal{H}_2 \oplus \mathbb{Z}\mathcal{E}_1 \oplus \cdots \oplus \mathbb{Z}\mathcal{E}_8, \tag{2.31}$$

where $\mathcal{H}_1$ and $\mathcal{H}_2$ are the total transforms (or pullbacks) of divisor classes of hyperplanes in each $\mathbb{P}^1$ factor, while $\mathcal{E}_i,\ i = 1,\dots,8$ are the exceptional classes arising from the eight blow-ups. In particular, if f, g are inhomogenous coordinates for each of the $\mathbb{P}^1$ factors, $\mathcal{H}_1, \mathcal{H}_2$ are classes of total transforms of curves on $\mathbb{P}^1 \times \mathbb{P}^1$ of constant f, g respectively. The intersection product on $\mathrm{Pic}(\mathcal{X})$ is the symmetric bilinear pairing defined by

$$\mathcal{H}_1 \cdot \mathcal{H}_1 = \mathcal{H}_2 \cdot \mathcal{H}_2 = \mathcal{H}_1 \cdot \mathcal{E}_i = \mathcal{H}_2 \cdot \mathcal{E}_j = 0, \quad \mathcal{H}_1 \cdot \mathcal{H}_2 = 1, \quad \mathcal{E}_i \cdot \mathcal{E}_j = -\delta_{ij}, \tag{2.32}$$

where $i, j \in \{1,\dots,8\}$ and δ_{ij} is the Kronecker delta. The top wedge product of the (holomorphic) cotangent bundle on $\mathcal{X}$ is the canonical bundle, which here is given by $\mathcal{K}_{\mathcal{X}} = -2\mathcal{H}_1 - 2\mathcal{H}_2 + \mathcal{E}_1 + \dots + \mathcal{E}_8 \in \mathrm{Pic}(\mathcal{X})$. The dual of this is the anticanonical bundle

$$-\mathcal{K}_{\mathcal{X}} = 2\mathcal{H}_1 + 2\mathcal{H}_2 - \mathcal{E}_1 - \mathcal{E}_2 - \mathcal{E}_3 - \mathcal{E}_4 - \mathcal{E}_5 - \mathcal{E}_6 - \mathcal{E}_7 - \mathcal{E}_8, \tag{2.33}$$

which corresponds to the equivalence class of pole divisors of rational 2-forms on $\mathcal{X}$. We quote the following observation of Sakai [Sak01]:

Proposition 2.2.1. *For $\mathcal{X}$ as above,* $\mathrm{Pic}(\mathcal{X})$ *equipped with the negative of the intersection pairing is isomorphic, as a free $\mathbb{Z}$-module with symmetric bilinear product, to the rank 10 Lorentzian lattice given as an orthogonal direct sum by $\Lambda_{10} = \mathbb{Z}v_0 \oplus \mathbb{Z}v_1 \oplus \dots \oplus \mathbb{Z}v_9$ with the symmetric bilinear form $(\cdot \mid \cdot)$ given by*

$$\left| \sum_{i=0}^{9} a_i v_i \right|^2 = -a_0^2 + a_1^2 + \dots + a_9^2, \tag{2.34}$$

where $|v|^2 = (v|v)$. Further, the orthogonal complement in $\mathrm{Pic}(\mathcal{X})$ *of the canonical class $\mathcal{K}_{\mathcal{X}}$ is isomorphic to the root lattice $Q(E_8^{(1)})$, with the null root $\delta \in Q(E_8^{(1)})$ identified with the anticanonical class $-\mathcal{K}_{\mathcal{X}}$.*

2.2.2 Generalised Halphen surfaces

Sakai defined a class of complex projective surfaces generalising both the surfaces associated with Okamoto's space and the rational elliptic surfaces associated with QRT maps. This generalisation is based not just on the $E_8^{(1)}$ root lattice in the Picard group outlined above, but the existence of two complementary sublattices associated with affine root systems, which captures the observations made by Okamoto of surface and symmetry types of differential Painlevé equations.

Sakai defined a *generalised Halphen surface* to be a smooth projective rational surface whose anticanonical class is effective, with any representative $D \in |-\mathcal{K}_{\mathcal{X}}|$ being of canonical type. That is, its decomposition into irreducible components

$$D = \sum_i m_i D_i, \tag{2.35}$$

is such that $-\mathcal{K}_{\mathcal{X}} \cdot \delta_i = 0$ for all i, where $\delta_i = [D_i] \in \mathrm{Pic}(\mathcal{X})$ are the divisor classes of the irreducible components. Such a surface then has $\dim |-\mathcal{K}_{\mathcal{X}}|$ being either zero or one. If a generalised Halphen surface has $\dim |-\mathcal{K}_{\mathcal{X}}| = 1$, then it is a Halphen surface of index one, which is the kind of rational elliptic surface associated with QRT mappings. Sakai classified generalised Halphen surfaces with $\dim |-\mathcal{K}_{\mathcal{X}}| = 0$, i.e. those that have a unique anticanonical divisor, which we call Sakai surfaces:

Definition 2.2.2. *A Sakai surface is a smooth projective rational surface with unique anticanonical divisor of canonical type.*

This definition leads to two important complementary root sublattices of $Q(E_8^{(1)}) \subset \mathrm{Pic}(\mathcal{X})$, as shown by the following result of Sakai [Sak01].

Proposition 2.2.3. *For a Sakai surface $\mathcal{X}$, the classes of irreducible components of the anticanonical divisor define a basis of simple roots δ_i for an indecomposable root system in* $\mathrm{Pic}(\mathcal{X})$*, with generalised Cartan matrix $A = (A_{ij})$ given by*

$$A_{ij} = -\delta_i \cdot \delta_j. \tag{2.36}$$

This root system is of affine type, with null root identified with the anticanonical class:

$$\delta = -\mathcal{K}_{\mathcal{X}} = \sum_i m_i \delta_i. \tag{2.37}$$

Further, if we denote the associated root lattice by $Q(R) = \sum_i \mathbb{Z}\delta_i \subset Q(E_8^{(1)})$, the orthogonal complement in $Q(E_8^{(1)})$ is another root lattice $Q(R^{\perp})$, which is also of affine type. The possible pairs of complementary root systems $R, R^{\perp}$ are classified according to root sublattices of the $E_8^{(1)}$ lattice.

The possible surface root system types R are shown in Figure 2.4, where arrows indicate inclusion of root lattices as in [Rai13]. We use, following Sakai, $A_7^{(1)}$ and $A_7^{(1)'}$ to differentiate between two different emdeddings of the $A_7^{(1)}$ root lattice into $Q(E_8^{(1)})$. We also use $A_0^{(1)}$ to indicate when the anticanonical divisor is irreducible, so $Q(A_0^{(1)}) = \mathbb{Z}\mathcal{K}_{\mathcal{X}}$.

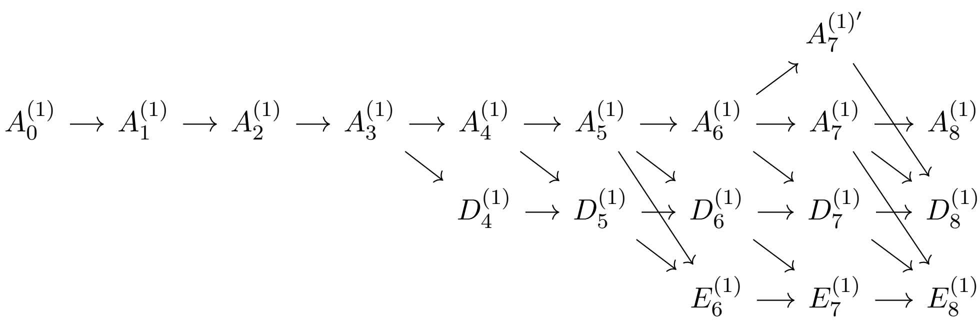

Figure 2.4: Surface root system type R for Sakai surfaces

The classification given in Sakai's paper [Sak01] is finer than the type R of the root system defined by the components of D. By further classifying $\mathcal{X}$ with unique anticanonical divisor $D = \sum_i m_i D_i$ according to $\operatorname{rank} H_1\left(D_{\text{red}}; \mathbb{Z}\right)$, where $D_{\text{red}} = \bigcup_i D_i$, we differentiate between families of surfaces from which the discrete Painlevé equations constructed are of elliptic, multiplicative and additive type. By this, we mean those where the independent variable appearing in the coefficients of the mapping in either an affine-linear way (additive type), as exponents of a parameter q (multiplicative type) or in an affine-linear way in the arguments of elliptic functions (elliptic type). This is essentially due to how the root variables (to be introduced in the following subsection) are related to the locations of basepoints giving the surfaces. We will see this explicitly when we construct a discrete Painlevé equation from a family of additive surfaces in Subsection 2.3.4, and when we consider equations associated with multiplicative surfaces in Section 4.1, but we refer the reader to [Sak01] for more details. The 22 possible surface types are shown in Table 1, and we refer to them by type as $\mathcal{R}$-surfaces.

Elliptic type	*ell*-$A_0^{(1)}$
Multiplicative type	q-$A_0^{(1)}, q$-$A_1^{(1)}, q$-$A_2^{(1)}, A_3^{(1)}, \ldots, A_7^{(1)}, A_7^{(1)'}, A_8^{(1)}$
Additive type	d-$A_0^{(1)}, d$-$A_1^{(1)}, d$-$A_2^{(1)}, D_4^{(1)}, \ldots, D_8^{(1)}$ $E_6^{(1)}, E_7^{(1)}, E_8^{(1)}$

Table 2.1: Classification of Sakai surfaces by surface type $\mathcal{R}$

In the cases where multiple surface types $\mathcal{R}$ share the root system type R, we differentiate between them according to whether they are elliptic, multiplicative or additive, e.g. *ell*-$A_0^{(1)}$, *q*-$A_0^{(1)}$, *d*-$A_0^{(1)}$ correspond to surfaces with irreducible anticanonical divisor and for which $\operatorname{rank} H_1(D_{\text{red}};\mathbb{Z}) = 2, 1, 0$ respectively. When there is only one surface type associated with a root system we omit such notation, e.g. $\mathcal{R} = D_4^{(1)}$ corresponds to the only surface type with root system type $R = D_4^{(1)}$, which is of additive type.

2.2.3 Families of surfaces and root variable parametrisation

Surface types can be described in terms of configurations of eight (possibly infinitely near) points in $\mathbb{P}^1 \times \mathbb{P}^1$, the blow-ups of which will lead to an anticanonical divisor with the required decomposition. We remark at this point that in order to obtain Sakai surfaces of each type directly through blowups we should consider configurations of nine points in $\mathbb{P}^2$, but all the surfaces that give rise to discrete Painlevé equations can be obtained directly from $\mathbb{P}^1 \times \mathbb{P}^1$ through a sequence of eight blowups, and this approach is more suited to the kind of calculations performed in this thesis. The surface type $\mathcal{R} = E_8^{(1)}$ is the only one which cannot be obtained from $\mathbb{P}^1 \times \mathbb{P}^1$ directly through blowups, and in fact requires nine blowups of $\mathbb{P}^1 \times \mathbb{P}^1$ followed by one blowdown.
Sakai gave a parametrisation of the set of isomorphism classes of surfaces of each type, and in particular isolated the number of free parameters from a basepoint configuration that can be varied while preserving the surface type. The set of isomorphism classes of surfaces of each type can be parametrised in a way that naturally corresponds to the symmetry root system $R^{\perp}$. This is done by making use of a kind of *period mapping*, which we outline now.

Definition 2.2.4. *Consider a Sakai surface $\mathcal{X}$ with anticanonical divisor $D = \sum_i m_i D_i$, $D_{\text{red}} = \bigcup_i D_i$, and with surface and symmetry root systems of type R and $R^{\perp}$ respectively. Let ω be a rational 2-form on $\mathcal{X}$ such that $\operatorname{div}(\omega) = -D$. Then from relative homology of the pair $(X, X - D_{\text{red}})$ and Poincaré duality on D_{red} we have a short exact sequence:*

$$0 \longrightarrow H_1(D_{\text{red}};\mathbb{Z}) \longrightarrow H_2(X - D_{\text{red}};\mathbb{Z}) \longrightarrow Q(R^{\perp}) \longrightarrow 0. \qquad (2.38)$$

The isomorphism given by this sequence, together with the map

$$\begin{aligned} \hat{\chi} : H_2(X - D_{\text{red}}; \mathbb{Z}) &\to \mathbb{C}, \\ \Gamma &\mapsto \int_\Gamma \omega, \end{aligned} \tag{2.39}$$

defines the period mapping

$$\chi : Q(R^\perp) \to \mathbb{C} \mod \hat{\chi}(H_1(D_{\text{red}}; \mathbb{Z})). \tag{2.40}$$

This mapping depends on the choice of the rational 2-form ω, and in practice we may choose this according to a normalisation such that the period mapping defines a $\mathbb{C}$-valued function. The kind of normalisation required depends on the rank of $H_1(D_{\text{red}}; \mathbb{Z})$, and therefore whether the $\mathcal{R}$-surface is of elliptic, multiplicative or additive type. We will see this normalisation in practice when we present the standard model of surfaces of type $D_4^{(1)}$ later in this chapter. If a family of $\mathcal{R}$-surfaces gives the whole set of isomorphism classes we call it a family of *generic* $\mathcal{R}$-surfaces.

The period mapping allows us to construct the *root variable parametrisation* of a family of generic $\mathcal{R}$-surfaces. Pick a basis of simple roots $\{\alpha_0, \dots, \alpha_n\}$ for $Q(R^\perp)$ and define the associated *root variables* as

$$a_j = \chi(\alpha_j). \tag{2.41}$$

Together with the 'extra parameter' corresponding to the independent variable of the continuous Painlevé equation in the (additive) cases $\mathcal{R} = D_4^{(1)}, D_5^{(1)}, D_6^{(1)}, D_7^{(1)}, D_8^{(1)}, E_6^{(1)}, E_7^{(1)}$ and $E_8^{(1)}$, the root variables allow us to parametrise the family of generic $\mathcal{R}$-surfaces. The extra parameter ζ for the case corresponding to the Painlevé equation P_J takes values precisely in the independent variable space B_J introduced in Section 1.1, which we recall in Table 2.2

P_J	P_{I}	P_{II}	$\mathrm{P}_{\mathrm{III}}$	P_{IV}	P_{V}	P_{VI}
$\mathcal{R}$	$E_8^{(1)}$	$E_7^{(1)}$	$D_8^{(1)}/D_7^{(1)}/D_6^{(1)}$	$E_6^{(1)}$	$D_5^{(1)}$	$D_4^{(1)}$
B_J	$\mathbb{C}$	$\mathbb{C}$	$\mathbb{C}\backslash\{0\}$	$\mathbb{C}\backslash\{0\}$	$\mathbb{C}\backslash\{0\}$	$\mathbb{C}\backslash\{0,1\}$

Table 2.2: Extra parameter for surface types associated with differential Painlevé equations

In particular, a family of $\mathcal{R}$-surfaces gives the whole set of isomorphism classes if it has the same number of free parameters as the rank of the generalised Cartan matrix for its symmetry type $R^\perp$, as well as the extra parameter in the types noted above. This is ensured by Theorem 25 of [Sak01], which we do not recall explicitly, but for our purposes is sufficient to understand as follows. If $\mathcal{X}$ and $\tilde{\mathcal{X}}$ are two $\mathcal{R}$-surfaces for which we have an isometry $\phi : \mathrm{Pic}(\mathcal{X}) \to \mathrm{Pic}(\tilde{\mathcal{X}})$ that identifies the classes of components of the anticanonical divisors on $\mathcal{X}$, $\tilde{\mathcal{X}}$, the rational 2-forms and the period mappings, the bases of symmetry roots and the extra parameter when $\mathcal{R}$ is a type associated with a differential Painlevé equation, then ϕ is realised by a unique isomorphism between $\mathcal{X}$ and $\tilde{\mathcal{X}}$.

For a family $\mathcal{X}_{\mathcal{A}} = \{\mathcal{X}_{\mathbf{a}} : \mathbf{a} \in \mathcal{A}\}$ of $\mathcal{R}$-surfaces indexed by some list $\mathbf{a} \in \mathcal{A}$ of parameters, we may naturally identify their Picard groups to form a single $\mathbb{Z}$-module, which we also denote $\mathrm{Pic}(\mathcal{X})$. Special automorphisms [Dol83, Loo81] of this $\mathbb{Z}$-module will correspond to symmetries of the family of surfaces, which we now describe.

Definition 2.2.5. *Let $\mathcal{X}_{\mathcal{A}}$ be a family of $\mathcal{R}$-surfaces, and let $\mathrm{Pic}(\mathcal{X})$ be the identification of the Picard groups $\mathrm{Pic}(\mathcal{X}_{\mathbf{a}})$ as above. A $\mathbb{Z}$-module automorphism of $\mathrm{Pic}(\mathcal{X})$ is called a* Cremona isometry *of the family of $\mathcal{R}$-surfaces if it:*

1. *preserves the intersection form on $\mathrm{Pic}(\mathcal{X})$,*
2. *leaves the canonical class $\mathcal{K}_{\mathcal{X}}$ fixed,*
3. *preserves effectiveness of divisor classes.*

For each surface type $\mathcal{R}$, Sakai described the group $\mathrm{Cr}(\mathcal{X}(\mathcal{R}))$ of Cremona isometries of a family of $\mathcal{R}$-surfaces. We quote the result most relevant to this thesis, but the results for the other types $\mathcal{R}$ can be found in [Sak01], where the Cremona isometries are described in terms of the Weyl group of the root system of type $R^\perp$.

Theorem 2.2.6. *For $\mathcal{R} \neq A_6^{(1)}, A_7^{(1)}, A_7^{(1)'}, A_8^{(1)}, D_7^{(1)}$ or $D_8^{(1)}$, the group of Dynkin diagram automorphisms Aut$(R^\perp)$ acts on $\mathrm{Pic}(\mathcal{X})$, and*

$$\mathrm{Cr}(\mathcal{X}(\mathcal{R})) \cong \left(W(R^\perp) \rtimes \mathrm{Aut}(R^\perp)\right)_{\Delta^{\mathrm{nod}}}. \tag{2.42}$$

Here the right-hand side is the part of the extension by Dynkin diagram automorphisms of the affine Weyl group of $R^\perp$ which stabilises the set $\Delta^{\mathrm{nod}} \subset \mathrm{Pic}(\mathcal{X})$ of classes of nodal curves (i.e. effective classes of self-intersection -2) disjoint from the irreducible components of the anticanonical divisor. For a family of generic $\mathcal{R}$-surfaces the set Δ^{nod} will be empty.

Thus we have an action of $\widetilde{W}(R^\perp) = W(R^\perp) \rtimes \mathrm{Aut}(R^\perp)$ on $\mathrm{Pic}(\mathcal{X})$ defined as the extension of the usual one on the root lattice $Q(R^\perp)$, where the reflection associated to the simple root α_i is given by

$$r_{\alpha_i}(\lambda) = \lambda + (\lambda \cdot \alpha_i)\alpha_i, \tag{2.43}$$

where $\lambda \in \mathrm{Pic}(\mathcal{X})$, and we have actions on $\mathrm{Pic}(\mathcal{X})$ of the Dynkin diagram automorphisms that induce the natural actions on $Q(R^\perp), Q(R)$ according to the permutation of simple roots. We note here that this group $\widetilde{W}(R^\perp)$ is larger than the extended affine Weyl group defined in Section 2.1, because it includes all Dynkin diagram automorphisms and not just those associated to the finite group Σ obtained as the quotient of the weight lattice by the root lattice, but still includes the translation part.

2.2.4 Cremona action

In Sakai's theory, discrete Painlevé equations are constructed through the *Cremona action* of the symmetry group, which realises the Cremona isometries as an action on a family of generic $\mathcal{R}$-surfaces by birational maps. This action of $\mathrm{Cr}(\mathcal{X}_\mathcal{A})$ on the family $\mathcal{X}_\mathcal{A}$ is most easily described by two actions: one on the parameter space $\mathcal{A}$ via maps $\mathbf{a} \mapsto w \cdot \mathbf{a}$ and another on the surfaces by birational mappings $\mathcal{X}_\mathbf{a} \to \mathcal{X}_{w\cdot\mathbf{a}}$. The fact that the action permutes the family in a non-trivial way leads to the equations being nonautonomous, as opposed to those associated with QRT mappings, which are given by automorphisms of rational elliptic surfaces.

The Cremona action is known for standard models of each surface type [Sak01, KNY17], and the action on parameters is most conveniently described in terms of the root variables. This is because the birational maps are constructed from changes of blowing-down structures, which naturally induce changes in the root variables. Take a parametrisation of a family of generic $\mathcal{R}$-surfaces by a tuple of root variables $\mathbf{a} = (a_0, \dots, a_n)^T \in \mathcal{A}$ associated with a choice of simple roots $\{\alpha_0, \dots, \alpha_n\}$ for the symmetry root system $R^\perp$, where we also include in $\mathbf{a}$ the extra parameter ζ if $\mathcal{R} = D_l^{(1)}, E_l^{(1)}$. Consider the action of $w \in \mathrm{Cr}(\mathcal{X}_\mathcal{A})$ as a birational map

$$\begin{aligned} \phi_w :\ \mathcal{X}_\mathbf{a} &\to \mathcal{X}_{w\cdot\mathbf{a}}, \\ (f,g) &\mapsto (w\cdot f, w\cdot g), \end{aligned} \tag{2.44}$$

such that $\phi_w^* : \mathrm{Pic}(\mathcal{X}_{w\cdot\mathbf{a}}) \to \mathrm{Pic}(\mathcal{X}_\mathbf{a})$ induces w via the natural identification of the Picard groups of the members of the family $\mathcal{X}_\mathcal{A}$. That is, if we take $\boldsymbol{\alpha} = (\alpha_0, \dots, \alpha_n)^T$ and $\bar{\boldsymbol{\alpha}} =$

$(\bar{\alpha}_0, \ldots, \bar{\alpha}_n)^T$ as the tuples of elements in $\mathrm{Pic}(\mathcal{X}_{\mathbf{a}}), \mathrm{Pic}(\mathcal{X}_{w\cdot\mathbf{a}})$ respectively corresponding to our choice of symmetry roots, we have the Cremona isometry induced by the linear map

$$\phi_w^* : \bar{\boldsymbol{\alpha}} \mapsto M\boldsymbol{\alpha}, \tag{2.45}$$

where M is some matrix with integer entries. In particular, ϕ_w^* identifies the rational 2-forms defining the period mappings $\chi, \bar{\chi}$ on $\mathcal{X}_{\mathbf{a}}, \mathcal{X}_{w\cdot\mathbf{a}}$ respectively, and the definition of the period mapping ensures we have the following correspondence between actions on $\mathcal{A}$ and $\mathrm{Pic}(\mathcal{X})$:

$$w \cdot \mathbf{a} = \chi_{\bar{\mathcal{X}}}(\bar{\boldsymbol{\alpha}}) = \chi_{\mathcal{X}}(\phi_w^*(\boldsymbol{\alpha})) = M\mathbf{a}. \tag{2.46}$$

This will be illustrated in practice in Section 2.3 when we outline the methods for computing root variables using the period mapping explicitly. In later chapters, we will often compute actions on $\mathrm{Pic}(\mathcal{X})$ induced by isomorphisms as their pushforwards, but it is important to keep in mind that this is inverse to the action on parameters.

2.2.5 Discrete Painlevé equations from translation symmetries

We are now ready to formally define Sakai's discrete Painlevé equations associated with a family of $\mathcal{R}$-surfaces, which arise from translation elements of $\mathrm{Cr}(\mathcal{X}(\mathcal{R}))$ and correspond to a weight lattice via the Kac translation formula. As the symmetry type $R^{\perp}$ is affine, denote the type of the underlying finite root system by $\mathring{R}^{\perp}$. The group of Cremona isometries includes the translations associated with the weight lattice $P(\mathring{R}^{\perp})$, and we have the following definition:

Definition 2.2.7. *A discrete Painlevé equation of surface type $\mathcal{R}$ is a second-order difference equation whose iteration mapping is given by the Cremona action of a translation element of* $\mathrm{Cr}(\mathcal{X}(\mathcal{R})$ *on a family of $\mathcal{R}$-surfaces.*

In other words, we call a second-order difference equation a discrete Painlevé equation if its birational iteration mappings lift to a family of isomorphisms between $\mathcal{R}$-surfaces, inducing a translational Cremona isometry. The Cremona action provides Bäcklund transformation symmetries for any discrete Painlevé equation arising from the family of surfaces. While discrete Painlevé equations are classified according to their surface type $\mathcal{R}$ in Sakai's scheme, we make the important remark that there are still infinitely many inequivalent discrete Painlevé equations for each surface type. This is because equivalence on the level of equations corresponds to conjugacy of translations in the symmetry group, and in general the weight lattice corresponds to infinitely many non-conjugate translations. Further describing or classifying the discrete Painlevé equations associated with each surface type remains an open problem, and will not be discussed in this thesis.

At this point, it will be illustrative to present the list of some pairs of root system types R and $R^{\perp}$, which represent the surfaces associated with some standard and well-studied examples of discrete Painlevé equations [KNY17], as well as $\mathrm{P_I}$-$\mathrm{P_{VI}}$. In Table 2.3, R is the surface root system and $R^{\perp}$ is the symmetry type, in terms of which the Cremona isometries of a generic family of surfaces can be described.

2.3 Standard model of $D_4^{(1)}$-surfaces

In this section we demonstrate the theory from this chapter in practice, by reviewing the standard model of surfaces of type $D_4^{(1)}$, and in particular a well-known example of a discrete Painlevé equation of this type. These surfaces also provide Okamoto's space for $\mathrm{P_{VI}}$, and the Cremona action gives Bäcklund transformation symmetries for both of these equations. This section is adapted from the appendix of [DFS19b], and we follow the standard reference [KNY17] for the choice of root bases and the forms of the equations. We make the important remark at this point that the construction of spaces of initial conditions for Painlevé equations usually involve calculations that are not feasible to be performed by hand, and a computer algebra system becomes essential. For the calculations in this thesis we have used **Mathematica**®.

2.3.1 The point configuration

Here we will work, as before, with $\mathbb{P}^1 \times \mathbb{P}^1$ with affine charts $(f,g),(F,g),(f,G),(F,G)$ where $F = 1/f, G = 1/g$, and present a configuration of eight points $p_1,\ldots,p_8$ to be blown-up to arrive at a generic family of $D_4^{(1)}$-surfaces. We start with the basis of simple roots for the surface root lattice $Q(D_4^{(1)})$, which will be given by the classes $\delta_i = [D_i]$ of the irreducible components of the anti-canonical divisor. The expressions of these in terms of generators of the Picard group and the associated Dynkin diagram of type $D_4^{(1)}$ are given in Figure 2.5, where we have used $\mathcal{H}_f, \mathcal{H}_g$ to denote pullbacks of divisor classes of hyperplanes of constant f,g respectively, and $\mathcal{E}_1,\ldots,\mathcal{E}_8$ to denote the exceptional classes arising from the eight blow-ups.

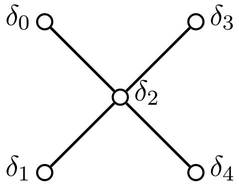

$$\begin{aligned} \delta_0 &= \mathcal{E}_3 - \mathcal{E}_4, & \delta_3 &= \mathcal{E}_7 - \mathcal{E}_8, \\ \delta_1 &= \mathcal{H}_f - \mathcal{E}_1 - \mathcal{E}_2, & \delta_4 &= \mathcal{H}_f - \mathcal{E}_5 - \mathcal{E}_6. \\ \delta_2 &= \mathcal{H}_g - \mathcal{E}_3 - \mathcal{E}_7, \end{aligned}$$

$$\delta = \delta_0 + \delta_1 + 2\delta_2 + \delta_3 + \delta_4.$$

Figure 2.5: The surface root basis for the standard model of $D_4^{(1)}$-surfaces

To realise these as classes of irreducible curves and obtain a unique anticanonical divisor with them as components, we will impose conditions on the configuration of points, for example that p_1, p_2 are such that there exists a unique representative of the class $\delta_1 = \mathcal{H}_f - \mathcal{E}_1 - \mathcal{E}_2$, given by the proper transform of a line of constant f passing through p_1 and p_2. The decomposition of the anticanonical class that we will arrive at is

$$\delta = -\mathcal{K}_{\mathcal{X}} = \delta_0 + \delta_1 + 2\delta_2 + \delta_3 + \delta_4. \tag{2.47}$$

To obtain the point configuration explicitly, we first use the action of $\mathbf{PGL}_2(\mathbb{C}) \times \mathbf{PGL}_2(\mathbb{C})$ on $\mathbb{P}^1 \times \mathbb{P}^1$ (i.e., the action of a Möbius group on each of the $\mathbb{P}^1$ factors), to put without loss of generality D_i, with $\delta_i = [D_i]$ as follows:

$$D_1 = \{F = 0\}', \quad D_2 = \{G = 0\}' \quad D_4 = \{f = 0\}', \tag{2.48}$$

where we have used $\mathcal{C}'$ to denote the proper transform on $\mathcal{X}$ of the curve $\mathcal{C}$ on $\mathbb{P}^1 \times \mathbb{P}^1$ under the eight blow-ups. We then still have a gauge group action of a three-parameter subgroup, $(f, g) \mapsto (\lambda f, \mu g + \nu)$. The point configuration giving the $D_4^{(1)}$ surface type can then be parameterised by $b_1, \ldots, b_8$ as follows: First take the following six points in $\mathbb{P}^1 \times \mathbb{P}^1$, which we define in coordinates by

$$\begin{aligned} &p_1 : (F, g) = (0, b_1), && p_2 : (F, g) = (0, b_2), && p_3 : (f, G) = (b_3, 0), \\ &p_5 : (f, g) = (0, b_5), && p_6 : (f, g) = (0, b_6), && p_7 : (f, G) = (b_7, 0). \end{aligned} \tag{2.49}$$

We blow up each of these points, introducing affine coordinates to cover the exceptional divisor E_i replacing p_i in the following way, which we will maintain for the rest of the thesis. For a point in an algebraic surface given in some local affine coordinates (x, y) by $p_i : (x, y) = (x_i, y_i)$, we introduce the two affine coordinate charts $(u_i, v_i), (U_i, V_i)$ for the blown-up surface given by

$$(u_iv_i, v_i) = (V_i, U_iV_i) = (x - x_i, y - y_i), \tag{2.50}$$

in which the part of the exceptional divisor E_i visible in the charts $(u_i, v_i), (U_i, V_i)$ is given by $v_i = 0, V_i = 0$, parametrised by u_i, U_i respectively. We then consider two points $p_4 \in E_3, p_8 \in E_7$, given in coordinates by

$$\begin{aligned} p_4 : (u_3, v_3) &= \left(\frac{f - b_3}{G}, G \right) = (b_4, 0), \\ p_8 : (u_7, v_7) &= \left(\frac{f - b_7}{G}, G \right) = (b_8, 0), \end{aligned} \tag{2.51}$$

and blow them up to arrive at a family of surfaces $\mathcal{X}_\mathcal{B}$ parametrised by $\mathbf{b} = (b_1, \dots, b_8) \in \mathcal{B}$, which we give a schematic representation of in Figure 2.6.

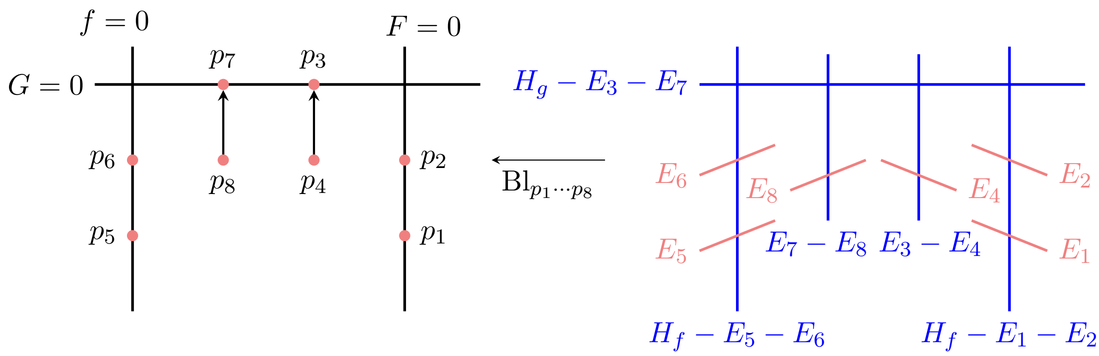

Figure 2.6: Point configuration for standard model of Sakai surfaces of type $D_4^{(1)}$

Here we have indicated the curves D_i giving irreducible components of the anticanonical divisor in blue, with certain exceptional curves in red. We use the usual notation for proper transforms of curves passing through points which are blown up, so for example $D_2 = H_g - E_3 - E_7$ is the proper transform of the line $\{G = 0\}$ under the blow-ups, since here everything is smooth and it passes through p_3 and p_7 each with multiplicity one. The three-parameter gauge group above acts on this configuration of points via

$$\begin{pmatrix} b_1 & b_2 & b_3 & b_4 & f \\ b_5 & b_6 & b_7 & b_8 & g \end{pmatrix} \sim \begin{pmatrix} \mu b_1 + \nu & \mu b_2 + \nu & \lambda b_3 & \lambda\mu b_4 & \lambda f \\ \mu b_5 + \nu & \mu b_6 + \nu & \lambda b_7 & \lambda\mu b_8 & \mu g + \nu \end{pmatrix}, \ \lambda, \mu \neq 0, \tag{2.52}$$

and so the true number of parameters is five, which corresponds exactly to the parametrisation of the set of isomorphism classes of $D_4^{(1)}$-surfaces by root variables, which we now describe explicitly.

2.3.2 The period map and the root variables

To obtain the root variables we begin by choosing a basis of simple roots for the symmetry root lattice $Q(R^\perp) = Q(D_4^{(1)}) \subset \mathrm{Pic}(\mathcal{X})$ and a rational 2-form ω whose pole divisor is the anticanonical divisor, decomposed into the -2-curves shown on Figure 2.6. We make the same choice as in [KNY17], which we present in Figure 2.7.

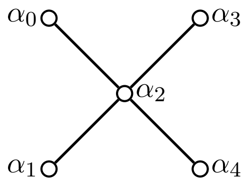

$$
\begin{aligned}
&\alpha_0 = \mathcal{H}_f - \mathcal{E}_3 - \mathcal{E}_4, \qquad && \alpha_3 = \mathcal{H}_f - \mathcal{E}_7 - \mathcal{E}_8,\\
&\alpha_1 = \mathcal{E}_1 - \mathcal{E}_2, && \alpha_4 = \mathcal{E}_5 - \mathcal{E}_6.\\
&\alpha_2 = \mathcal{H}_g - \mathcal{E}_1 - \mathcal{E}_5, &&\\
&\delta = \alpha_0 + \alpha_1 + 2\alpha_2 + \alpha_3 + \alpha_4. &&
\end{aligned}
$$

Figure 2.7: The symmetry root basis for the standard model of $D_4^{(1)}$-surfaces

Any such rational 2-form ω is given in charts by

$$
\begin{aligned}
\omega &= k\frac{df \wedge dg}{f} = -k\frac{dF \wedge dg}{F} = -k\frac{df \wedge dG}{fG^2} = k\frac{dF \wedge dG}{FG^2}\\
&= -k\frac{du_3 \wedge dv_3}{(b_3 + u_3 v_3)v_3} = -k\frac{du_7 \wedge dv_7}{(b_7 + u_7 v_7)v_7},
\end{aligned}
\tag{2.53}
$$

where k is a non-zero constant that we will normalise later . We outline in the following Lemma the standard method for computing root variables, which was given by Sakai in [Sak01]. For further exposition of these calculation methods we refer the reader to [DT18].

Lemma 2.3.1.

(a) The residues of ω along the irreducible components of the anticanonical divisor are given in charts by

$$
\begin{aligned}
&\mathrm{res}_{D_0}\,\omega = k\frac{du_3}{b_3}, \qquad && \mathrm{res}_{D_1}\,\omega = -kdg, \qquad && \mathrm{res}_{D_2}\,\omega = 0,\\
&\mathrm{res}_{D_3}\,\omega = k\frac{du_7}{b_7}, && \mathrm{res}_{D_4}\,\omega = kdf. &&
\end{aligned}
\tag{2.54}
$$

(b) The period mapping $\chi : Q(R^\perp) \to \mathbb{C}$ defined by ω with k fixed gives the root variables

$a_i = \chi(\alpha_i)$ *as*

$$
\begin{aligned}
a_0 &= -k\frac{b_4}{b_3}, \qquad a_1 = k(b_2 - b_1), \qquad a_2 = k(b_1 - b_5), \\
a_3 &= -k\frac{b_8}{b_7}, \qquad a_4 = k(b_5 - b_6).
\end{aligned}
\tag{2.55}
$$

It is convenient to take our normalisation such that $k = -1$*. We can then use the gauge action* (2.52) *to normalize* $b_5 = 0$, $b_7 = 1$, *and* $\chi(\delta) = a_0 + a_1 + 2a_2 + a_3 + a_4 = 1$*. After this normalisation, in this model the role of the extra parameter (the independent variable for* P_{VI}*) will be played by* b_3*, so we denote it by* t*. We then have the parameters* b_i*, after imposing the normalisation above, given in terms of root variables for the surface* $\mathcal{X}_{\mathbf{b}}$ *as follows:*

$$
\begin{aligned}
b_1 &= -a_2, \qquad b_2 = -a_1 - a_2, \qquad b_3 = t, \qquad b_4 = ta_0, \\
b_5 &= 0, \qquad b_6 = a_4, \qquad b_7 = 1, \qquad b_8 = a_3.
\end{aligned}
\tag{2.56}
$$

Proof. Part (a) is a standard computation in local charts. For example, we have $D_0 = E_3 - E_4$ being given in the chart (u_3, v_3) by $v_3 = 0$, so we obtain

$$
\operatorname{res}_{D_0} \omega = \operatorname{res}_{v_3=0} \left(-k\frac{du_3 \wedge dv_3}{(b_3 + u_3v_3)v_3} \right) = k\frac{du_3}{b_3}. \tag{2.57}
$$

Other computations in part (a) are similar. For part (b), we recall from [Sak01] the following method for computing the root variables $a_i = \chi(\alpha_i)$:

First, represent α_i as a difference of two effective divisor classes, $\alpha_i = [C_i^1] - [C_1^0]$, where C_i^1, C_i^0 are curves on $\mathcal{X}_{\mathbf{b}}$. Second, note that there exists a unique component D_k of the anticanonical divisor such that $D_k \cdot C_i^1 = D_k \cdot C_i^0 = 1$, and denote the points of intersection by $P_i = D_k \cap C_i^0$ and $Q_i = D_k \cap C_i^1$. Then we have

$$
\chi(\alpha_i) = \chi\left([C_i^1] - [C_i^0]\right) = \int_{P_i}^{Q_i} \frac{1}{2\pi \mathrm{i}} \oint_{D_k} \omega = \int_{P_i}^{Q_i} \operatorname{res}_{D_k} \omega, \tag{2.58}
$$

so the computation reduces to an integration along a contour in D_k.

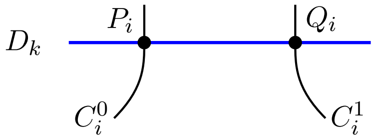

Figure 2.8: Configuration of curves in root variable computation

We illustrate this procedure by computing the root variable a_0. First represent

$$\alpha_0 = \mathcal{H}_f - \mathcal{E}_3 - \mathcal{E}_4 = [H_f - E_3] - [E_4], \tag{2.59}$$

where $H_f - E_3 = \{f = b_3\}'$ is the proper transform of the line of constant f passing through p_3, and E_4 is the exceptional curve arising from the blow-up of p_4. The unique component of the anticanonical divisor which these curves intersect is D_0, and we show the coordinate systems relevant to the computation in Figure 2.9.

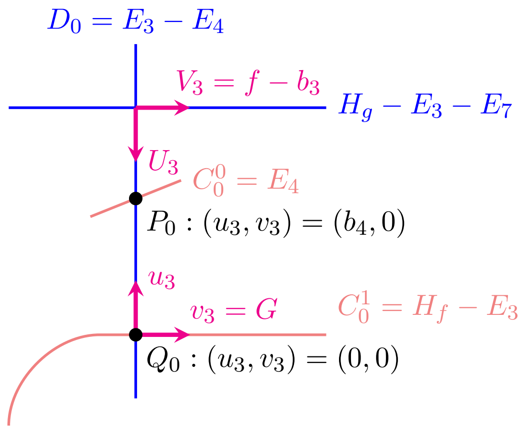

Figure 2.9: Coordinate systems for computation of a_0

We evaluate the integral to obtain

$$a_0 = \chi(\alpha_0) = \int_{P_0}^{Q_0} \mathrm{res}_{D_0}\, \omega = k \int_{b_4}^{0} \frac{dU_3}{b_3} = -k \frac{b_4}{b_3}, \tag{2.60}$$

and the computations of the remaining root variables are similar. □

2.3.3 Cremona action

We now give the Cremona action of the extended affine Weyl symmetry group $\widetilde{W}\left(D_4^{(1)}\right) = \mathrm{Aut}\left(D_4^{(1)}\right) \ltimes W\left(D_4^{(1)}\right)$. We recall the presentation of the affine Weyl group $W\left(D_4^{(1)}\right)$ is in terms of generators $r_i = r_{\alpha_i}$ and relations that can be read off the affine Dynkin diagram for the symmetry roots in Figure 2.7,

$$W\left(D_4^{(1)}\right) = \left\langle w_0, \dots, w_4 \;\middle|\; \begin{array}{ll} r_i^2 = e, \quad r_i r_j = r_j r_i & \text{when } \overset{\circ}{\alpha_i}\ \overset{\circ}{\alpha_j} \\ r_i r_j r_i = r_j r_i r_j & \text{when } \overset{\circ\!-\!\circ}{\alpha_i\ \alpha_j} \end{array} \right\rangle. \tag{2.61}$$

Reflections r_i on $\operatorname{Pic}(\mathcal{X})$ are induced by induced by isomorphisms

$$\begin{aligned} \phi_{r_i} : \mathcal{X}_{\mathbf{b}} &\to \mathcal{X}_{\bar{\mathbf{b}}}, \\ (f,g) &\mapsto (\bar{f},\bar{g}), \end{aligned} \tag{2.62}$$

where $\bar{\mathbf{b}} = r_i \cdot \mathbf{b}$, and the maps ϕ_{r_i} are the birational maps $(f,g) \mapsto (\bar{f},\bar{g})$ extended to $\mathbb{P}^1 \times \mathbb{P}^1$ as before and then lifted under the blow-ups. Though it is sufficient to consider the parametrisation of the family by root variables, we can also maintain the gauge freedom and work with point configuration in terms of b_i by requiring that each map preserves our normalisation

$$\begin{pmatrix} b_1 & b_2 & b_3 & b_4 \\ b_5 & b_6 & b_7 & b_8 \end{pmatrix} = \begin{pmatrix} b_1 & b_2 & t & b_4 \\ 0 & b_6 & 1 & b_8 \end{pmatrix} = \begin{pmatrix} -a_2 & -a_1 - a_2 & t & ta_0 \\ 0 & a_4 & 1 & a_3 \end{pmatrix}. \tag{2.63}$$

Therefore we give the action of the mappings on parameters b_i parametrising point configurations as well as on the root variables, together with the extra parameter t. We take the surface $\mathcal{X}_{\mathbf{b}}$ with parameters and coordinates

$$\begin{pmatrix} b_1 & b_2 & t & b_4 & f \\ & & & ; & \\ 0 & b_6 & 1 & b_8 & g \end{pmatrix} \sim \begin{pmatrix} a_0 & a_1 & a_2 & f \\ & & ; & \\ a_3 & a_4 & t & g \end{pmatrix}, \tag{2.64}$$

and for each r_i, we give the Cremona action as in (2.62) by specifying the parameters $\bar{\mathbf{b}} = r_i \cdot \mathbf{b}$ as well $\bar{f}, \bar{g}$ defining the map ϕ_{r_i}. In the following we write this in terms of the parameters $\bar{b}_i$ subject to our normalisation as well as in terms of the root variables $\bar{a}_i$, in the format

$$r_i : \begin{pmatrix} \bar{b}_1 & \bar{b}_2 & \bar{t} & \bar{b}_4 & \bar{f} \\ & & & ; & \\ 0 & \bar{b}_6 & 1 & \bar{b}_8 & \bar{g} \end{pmatrix} \sim \begin{pmatrix} \bar{a}_0 & \bar{a}_1 & \bar{a}_2 & \bar{f} \\ & & ; & \\ \bar{a}_3 & \bar{a}_4 & \bar{t} & \bar{g} \end{pmatrix}, \tag{2.65}$$

so for each r_i we have a row of the following array in which we give the values of $\bar{b}_i, \bar{a}_i, \bar{f}, \bar{g}$ required to define the Cremona action (2.62) in the same format as (2.65):

$$r_0 : \begin{pmatrix} b_1 - \frac{b_4}{t} & b_2 - \frac{b_4}{t} & t & -b_4 & ; & f \\ 0 & b_6 & 1 & b_8 & & g - \frac{b_4 f}{t(f-t)} \end{pmatrix} \sim \begin{pmatrix} -a_0 & a_1 & a_0 + a_2 & ; & f \\ a_3 & a_4 & t & & g - \frac{a_0 f}{f-t} \end{pmatrix},$$

$$r_1 : \begin{pmatrix} b_2 & b_1 & t & b_4 & ; & f \\ 0 & b_6 & 1 & b_8 & & g \end{pmatrix} \sim \begin{pmatrix} a_0 & -a_1 & a_1 + a_2 & ; & f \\ a_3 & a_4 & t & & g \end{pmatrix},$$

$$r_2 : \begin{pmatrix} -b_1 & b_2 - b_1 & t & b_4 - tb_1 & ; & f - \frac{b_1 f}{g} \\ 0 & b_6 - b_1 & 1 & b_8 - b_1 & & g - b_1 \end{pmatrix} \sim \begin{pmatrix} a_0 + a_2 & a_1 + a_2 & -a_2 & ; & f + \frac{a_2 f}{g} \\ a_2 + a_3 & a_2 + a_4 & t & & g + a_2 \end{pmatrix},$$

$$r_3 : \begin{pmatrix} b_1 - b_8 & b_2 - b_8 & t & b_4 & ; & f \\ 0 & b_6 & 1 & -b_8 & & g - \frac{b_8 f}{f-1} \end{pmatrix} \sim \begin{pmatrix} a_0 & a_1 & a_2 + a_3 & ; & f \\ -a_3 & a_4 & t & & g - \frac{a_3 f}{f-1} \end{pmatrix},$$

$$r_4 : \begin{pmatrix} b_1 - b_6 & b_2 - b_6 & t & b_4 & ; & f \\ 0 & -b_6 & 1 & b_8 & & g - b_6 \end{pmatrix} \sim \begin{pmatrix} a_0 & a_1 & a_2 + a_4 & ; & f \\ a_3 & -a_4 & t & & g - a_4 \end{pmatrix}.$$

Verifying that each of these defines an isomorphism is done according to standard methods of calculation in charts, which we will give detailed expositions of in later chapters.

We now turn to the Dynkin diagram automorphisms. It is clear that $\operatorname{Aut}\left(D_4^{(1)}\right) \simeq \mathcal{S}_4$, so we only describe three transpositions that generate the whole group. Consider the following generators $\sigma_1, \sigma_2, \sigma_3$ of $\operatorname{Aut}\left(D_4^{(1)}\right)$ that act on the symmetry and the surface root bases as follows (here we use the standard cycle notations for permutations):

$$\sigma_1 = (\alpha_3\alpha_4) = (\delta_3\delta_4), \qquad \sigma_2 = (\alpha_0\alpha_3) = (\delta_0\delta_3), \qquad \sigma_3 = (\alpha_1\alpha_4) = (\delta_1\delta_4). \quad (2.66)$$

These σ_i correspond to the following Cremona isometries of $\operatorname{Pic}(\mathcal{X})$:

$$\sigma_1 = (\mathcal{E}_6\mathcal{E}_8)w_\rho, \qquad \sigma_2 = (\mathcal{E}_3\mathcal{E}_7)(\mathcal{E}_4\mathcal{E}_8), \qquad \sigma_3 = (\mathcal{E}_1\mathcal{E}_5)(\mathcal{E}_2\mathcal{E}_6), \qquad (2.67)$$

where w_ρ is a reflection in the root $\rho = \mathcal{H}_f - \mathcal{E}_5 - \mathcal{E}_7$ (note also that a transposition $(\mathcal{E}_i\mathcal{E}_j)$ is induced by a reflection in the root $\mathcal{E}_i - \mathcal{E}_j$). The semi-direct product structure is defined by the action of $\sigma \in \operatorname{Aut}\left(D_4^{(1)}\right)$ on $W\left(D_4^{(1)}\right)$ via $r_{\sigma(\alpha_i)} = \sigma r_{\alpha_i} \sigma^{-1}$.

We now give the birational maps and actions on parameter realising these in the same format as we did for the reflections:

$$\sigma_1 : \begin{pmatrix} b_1 & b_2 & 1-t & \frac{(1-t)b_4}{t} \\ 0 & b_8 & 1 & b_6 \end{pmatrix}; \begin{matrix} 1-f \\ \frac{(f-1)g}{f} \end{pmatrix} = \begin{pmatrix} a_0 & a_1 & a_2 \\ a_4 & a_3 & 1-t \end{pmatrix}; \begin{matrix} 1-f \\ \frac{(f-1)g}{f} \end{pmatrix},$$

$$\sigma_2 : \begin{pmatrix} b_1 & b_2 & \frac{1}{t} & \frac{b_8}{t} \\ 0 & b_6 & 1 & \frac{b_4}{t} \end{pmatrix}; \begin{matrix} \frac{f}{t} \\ g \end{pmatrix} = \begin{pmatrix} a_3 & a_1 & a_2 \\ a_0 & a_4 & \frac{1}{t} \end{pmatrix}; \begin{matrix} \frac{f}{t} \\ g \end{pmatrix},$$

$$\sigma_3 : \begin{pmatrix} b_1 & b_1-b_6 & \frac{1}{t} & \frac{b_4}{t^2} \\ 0 & b_1-b_2 & 1 & b_8 \end{pmatrix}; \begin{matrix} \frac{1}{f} \\ b_1-g \end{pmatrix} = \begin{pmatrix} a_0 & a_4 & a_2 \\ a_3 & a_1 & \frac{1}{t} \end{pmatrix}; \begin{matrix} \frac{1}{f} \\ -g-a_2 \end{pmatrix}.$$

2.3.4 The standard discrete d-$\mathrm{P_V}$ Painlevé equation

As mentioned previously, there are infinitely many different discrete Painlevé equations of the same surface type, but some of these equations provide model examples since they either appear in applications, have a particularly nice form, or have degenerations to other known equations. In the family of equations with surface type $D_4^{(1)}$, one such equation is known as a d-$\mathrm{P_V}$ equation, since it has a continuous limit to the fifth differential Painlevé equation. In [KNY17] this equation is given in the following form,

$$\bar{f}f = \frac{tg(g-a_4)}{(g+a_2)(g+a_1+a_2)}, \qquad g + \underline{g} = a_0 + a_3 + a_4 + \frac{a_3}{f-1} + \frac{ta_0}{f-t}, \tag{2.68}$$

with the root variable evolution and normalization given by

$$\begin{gathered} \bar{a}_0 = a_0 - 1, \quad \bar{a}_1 = a_1, \quad \bar{a}_2 = a_2 + 1, \quad \bar{a}_3 = a_3 - 1, \quad \bar{a}_4 = a_4, \\ a_0 + a_1 + 2a_2 + a_3 + a_4 = 1. \end{gathered} \tag{2.69}$$

Though writing the nonautonomous nature of discrete Painlevé equations via evolution of parameters is the norm in much of the literature [Sak01, KNY17] we should show at this point how we may rewrite them as system of difference equations with the independent variable appearing explicitly. We note that the evolution of the root variables (2.69) can be used to deduce that

$$a_0 = \hat{a}_0 - n, \quad a_1 = \hat{a}_1, \quad a_2 = \hat{a}_2 + n, \quad a_3 = \hat{a}_3 - n, \quad a_4 = \hat{a}_4, \tag{2.70}$$

where $\hat{a}_i$ are now arbitrary parameters independent of n, so we can let $f = f_n, g = g_n, \bar{f} = f_{n+1}, \underline{g} = g_{n-1}$ and rewrite (2.68) as

$$\begin{aligned} f_{n+1}f_n &= \frac{tg_n(g_n - a_4)}{(g_n + a_2 + n)(g_n + a_1 + a_2 + n)}, \\ g_n + g_{n-1} &= a_0 + a_3 + a_4 - 2n + \frac{a_3 - n}{f_n - 1} + \frac{t(a_0 - n)}{f_n - t}, \end{aligned} \tag{2.71}$$

where we have omitted the hats and a_i play the role of parameters.
Returning to the form of this equation with parameter evolution, we have a map

$$\begin{aligned} \varphi : \mathcal{X}_{\mathbf{b}} &\to \mathcal{X}_{\bar{\mathbf{b}}}, \\ (f, g) &\mapsto (\bar{f}, \bar{g}), \end{aligned} \tag{2.72}$$

which is in fact an isomorphism, with $\bar{\mathbf{b}}$ being the root variables after evolution according to (2.69). To compute the induced Cremona isometry, we consider the identification of the Picard groups of the family of surfaces to form the single $\mathbb{Z}$-module $\operatorname{Pic}(\mathcal{X})$. To be precise, consider two surfaces $\mathcal{X}_{\mathbf{b}}$ and $\mathcal{X}_{\bar{\mathbf{b}}}$ in the family, and take $\mathcal{H}_f, \mathcal{H}_g, \mathcal{E}_i$ to be the generators of $\operatorname{Pic}(\mathcal{X}_{\mathbf{b}})$, with $\mathcal{E}_i$ arising from the blow-up of the point p_i given in coordinates in terms of $\mathbf{b}$. Similarly take $\bar{\mathcal{H}}_f, \bar{\mathcal{H}}_g, \bar{\mathcal{E}}_i$ to be the generators of $\operatorname{Pic}(\mathcal{X}_{\bar{\mathbf{b}}})$, with $\bar{\mathcal{E}}_i$ arising from the blow-up of the point $\bar{p}_i$ given in coordinates in terms of $\bar{\mathbf{b}}$. Then we identify $\mathcal{E}_i$ with $\bar{\mathcal{E}}_i$, $\mathcal{H}_f$ with $\bar{\mathcal{H}}_f$ and so on, and denote the resulting $\mathbb{Z}$-module by

$$\operatorname{Pic}(\mathcal{X}) = \mathbb{Z}\mathcal{H}_f \oplus \mathbb{Z}\mathcal{H}_g \oplus \mathbb{Z}\mathcal{E}_1 \oplus \cdots \oplus \mathbb{Z}\mathcal{E}_8. \tag{2.73}$$

The isomorphism (2.72) induces a Cremona isometry w via its pullback, which acts on the symmetry roots according to

$$w : \boldsymbol{\alpha} = \langle \alpha_0, \alpha_1, \alpha_2, \alpha_3, \alpha_4 \rangle \mapsto \boldsymbol{\alpha} + \langle -1, 0, 1, -1, 0 \rangle \delta, \tag{2.74}$$

and indeed corresponds to a translation element of $\widetilde{W}(D_4^{(1)})$ in the sense of Kac. Using standard techniques for obtaining expressions for Weyl group elements in terms of generators, which are based on results of [Kac90] and can be seen applied to discrete Painlevé equations e.g. in [DT18], we obtain the following decomposition of $w \in \widetilde{W}(D_4^{(1)})$:

$$w = r_2 r_1 r_4 r_2 r_0 r_3 \sigma_2 \sigma_3 = \sigma_2 \sigma_3 r_2 r_4 r_1 r_2 r_3 r_0. \tag{2.75}$$

Indeed, composing the actions on surfaces and parameters using the data from Subsection 2.3.3 we obtain precisely the equation (2.68) with parameter evolution (2.69). Further, we may identify the element w as the translation T_v for a weight $v \in \mathring{P} = P(D_4)$ as follows, working purely on the level of the symmetry root lattice without reference to the embedding into $\operatorname{Pic}(\mathcal{X})$. The fundamental weights $\omega_1, \dots, \omega_4$ dual to $\alpha_1, \dots, \alpha_4$, so $\alpha_i \cdot \omega_j = -\delta_{ij}$, are given by

$$\begin{aligned} \omega_1 &= \alpha_1 + \alpha_2 + \frac{1}{2}\alpha_3 + \frac{1}{2}\alpha_4, \qquad & \omega_2 &= \alpha_1 + 2\alpha_2 + \alpha_3 + \alpha_4, \\ \omega_3 &= \frac{1}{2}\alpha_1 + \alpha_2 + \alpha_3 + \frac{1}{2}\alpha_4, \qquad & \omega_4 &= \frac{1}{2}\alpha_1 + \alpha_2 + \frac{1}{2}\alpha_3 + \alpha_4. \end{aligned} \tag{2.76}$$

The Kac translation formula for an element $v \in \operatorname{span}_{\mathbb{C}}\{\alpha_1, \dots, \alpha_4\}$ gives the action of T_v on the symmetry roots as

$$T_v(\alpha_i) = \alpha_i + (v \cdot \alpha_i)\delta, \tag{2.77}$$

so to find $v = \sum_{i=1}^{4} c_i \omega_i$ such that T_v gives the action (2.74) on the symmetry roots, we must have

$$\begin{aligned} v \cdot \alpha_1 &= -c_1 = 0, \qquad & v \cdot \alpha_2 &= -c_2 = 1, \\ v \cdot \alpha_3 &= -c_3 = -1, \qquad & v \cdot \alpha_4 &= -c_4 = 0, \end{aligned} \tag{2.78}$$

so the element w in (2.75) is indeed a translation element of $\widetilde{W}(D_4^{(1)})$, associated to the weight

$$v = \omega_3 - \omega_2 = -\frac{1}{2}\alpha_1 - \alpha_2 - \frac{1}{2}\alpha_4. \tag{2.79}$$

2.4 Okamoto's space

As we are now equipped with the theory of Sakai surfaces, we can illustrate how this framework recovers Okamoto's space. For each differential Painlevé equation P_J, this will be a bundle over the independent variable space B_J (given in (1.9)), obtained from the product $\mathbb{C}^2 \times B_{\mathrm{VI}}$ by first compactifying the $\mathbb{C}^2$-fibres to $\mathbb{P}^1 \times \mathbb{P}^1$ then blowing up each fibre at points whose locations depend on $t \in B_{\mathrm{VI}}$, then removing inaccessible divisors. This will give Okamoto's space with fibre being a Sakai surface with the support D_{red} of the anticanonical divisor removed.

2.4.1 Construction for P_{VI}

We will first demonstrate how the family of $D_4^{(1)}$-surfaces outlined in this section can be used to construct Okamoto's space for the sixth differential Painlevé equation. We begin by rewriting P_{VI} for $y(t)$ with parameters $\alpha, \beta, \gamma, \delta$ as a (nonautonomous) Hamiltonian system for $q(t), p(t)$ as

$$\begin{gathered} q' = \frac{\partial H}{\partial p}, \quad p' = -\frac{\partial H}{\partial q}, \\ H = \frac{q(q-1)(q-t)}{t(t-1)} \left\{ p^2 - p\left(\frac{a_0 - 1}{q-t} + \frac{a_3}{q-1} + \frac{a_4}{q} \right) + \frac{a_2(a_1+a_2)}{q(q-1)} \right\}. \end{gathered} \tag{2.80}$$

The equivalence to P_{VI} is via $q(t) = y(t)$, where the root variables (which in this situation do not have any discrete evolution) are related to the parameters from P_{VI} by

$$\begin{gathered} \alpha = \frac{a_1^2}{2}, \quad \beta = -\frac{a_4^2}{2}, \quad \gamma = \frac{\alpha_3^2}{2}, \quad \delta = \frac{1-a_0^2}{2}, \\ a_0 + a_1 + 2a_2 + a_3 + a_4 = 1. \end{gathered} \tag{2.81}$$

Make the change of variables $(f, g) = (q, qp)$ so we have the following system of differential equations equivalent to P_{VI}:

$$\begin{aligned} f' &= \frac{f(f-1)(f-t)}{t(t-1)} \left(\frac{2g}{f} - \frac{a_0 - 1}{f-t} - \frac{a_3}{f-1} - \frac{a_4}{f} \right), \\ g' &= \frac{tg(g-a_4) - f^2(g+a_2)(g+a_1+a_2)}{t(t-1)f}. \end{aligned} \tag{2.82}$$

We consider this system (2.82) on the product bundle $(\mathbb{P}^1 \times \mathbb{P}^1) \times B_{VI} \to B_{VI} = \mathbb{C}\backslash\{0, 1\}$ with fibre over t being $\mathbb{P}^1 \times \mathbb{P}^1$. We do this in the same way as in the discrete case, with the differential equation being interpreted as the flow of a vector field on a part of the bundle visible in a $\mathbb{C}^2$-chart (f, g), extended to $\mathbb{P}^1 \times \mathbb{P}^1$ via $F = 1/f, G = 1/g$. We first note, from (2.82), that the vector field is regular on the part of the bundle visible in the (f, g)-chart where $f \neq 0$. Extended to $\mathbb{P}^1 \times \mathbb{P}^1$, the vector field in the (F, g)-chart is computed directly from (2.82) to be

$$\begin{aligned} F' &= \frac{a_0(1-F) + a_3(1-tF) + (1-F)\left[a_4(1-tF) - 1 + 2g(1-tF)\right]}{t(t-1)}, \\ g' &= \frac{g^2(tF^2-1) - (a_1 + 2a_2 + ta_4F^2)g - a_2(a_1+a_2)}{t(t-1)F}. \end{aligned} \tag{2.83}$$

Like the discrete case, we encounter singularities in the form of indeterminacies of rational functions, in this case those giving the components of the vector field. We note that in (2.82), the rational function g' has indeterminacies at p_1, p_2 (as in previous section), but F'

stays finite. These are given in the root variable parametrisation by

$$p_1 : (F, g) = (0, -a_2), \qquad p_2 : (F, g) = (0, -a_1 - a_2), \tag{2.84}$$

and represent the only indeterminacies of the vector field in this chart. Further, we see that the vector field on the part of the bundle given by $F = 0$ away from p_1, p_2 diverges, with the denominators of both components vanishing while the numerators remain non-zero.
On the level of solutions to the differential system, these observations correspond to the fact that there are infinite families of solution curves passing through each of the points p_1, p_2, while there are none passing through any other points with $F = 0$. This can be seen via classical Painlevé analysis, which involves considering Laurent series expansions of solutions about movable poles. Suppose a solution to the system (2.83) is given locally about some $t_0 \in B_J$ by the series expansions

$$\begin{aligned} f &= F_1(t - t_0) + F_2(t - t_0)^2 + \dots \\ G &= g_0 + g_1(t - t_0) + g_2(t - t_0)^2 + \dots \end{aligned} \tag{2.85}$$

so $(F(t_0), g(t_0)) = (0, g_0)$, and the corresponding solution $y = q = f$ of $\mathrm{P_{VI}}$ has a pole. Substituting these into the differential equation, we obtain asymptotic identities which must hold as $t \to t_0$. We let $\tau = t - t_0$, and in particular the equation for g' gives

$$0 = (a_2 + g_0)(a_1 + a_2 + g_0) + g_1 \left(a_1 + 2a_2 + F_1 t_0^2 - F_1 t_0 + 2g_0\right) \tau + \mathcal{O}(\tau^2), \tag{2.86}$$

in the limit as $\tau \to 0$, where for now we have only kept track of the first two terms. From this, we see that g_0 must take one of the values $-a_2, -a_1 - a_2$, so indeed any solution given by (2.85) must pass through either p_1 or p_2 when $t = t_0$, which corresponds to the fact that the vector field has indeterminacies there but diverges on the rest of the part of the bundle where $F = 0$.
Considering the case $g_0 = -a_2$, with the solution passing through p_1, the asymptotic identities become

$$\begin{aligned} 0 &= (a_1 + (t_0 - 1)t_0 F_1) + \mathcal{O}(\tau), \\ 0 &= g_1(a_1 + (t_0 - 1)t_0 F_1)\tau + \mathcal{O}(\tau^2), \end{aligned} \tag{2.87}$$

where we have again only kept track of the minimal number of coefficients necessary at this stage, so we must have

$$F_1 = \frac{a_1}{t_0(1-t_0)}. \tag{2.88}$$

Again refining the expansions (2.85) and inserting them into the differential equations we have from the equation for F' the following:

$$\begin{aligned} 0 = &\left[a_1\left(1+a_1+a_3+t_0(a_0+a_1-3)\right)+2g_1(t_0-1)t_0+2F_2(t_0-1)^2t_0^2\right]\tau \\ &+\mathcal{O}(\tau^2), \end{aligned} \tag{2.89}$$

from which we deduce the following expression for F_2 in terms of g_1:

$$F_2 = -\frac{a_1\left(a_0t_0+a_1(t_0+1)+a_3-3t_0+1\right)+2g_1(t_0-1)t_0}{2(t_0-1)^2t_0^2}. \tag{2.90}$$

After this, we find from the equation for g' that

$$g_2 = \frac{g_1(t_0-1)\left(2a_2t_0+a_4t_0+a_3(t_0-1)-a_1-2t_0+1\right)-2a_1a_2\left(a_2+a_4\right)}{2(t_0-1)^2t_0}, \tag{2.91}$$

in which g_1 is still arbitrary. In fact, proceeding in this way all coefficients in (2.85) are determined recursively in terms of g_1, in addition to the location t_0 of the pole and the parameters a_i, so we have a one-parameter family of solutions passing through p_1 for any given value of $t_0 \in B_J$, parametrised by the free coefficient g_1.

This can be understood in terms of the differential system lifted under the blow-ups as follows. Blowing up p_1, we introduce the standard pairs of coordinate charts according to (2.50), namely $(u_1, v_1), (U_1, V_1)$ for the neighbourhood of the exceptional divisor E_1 given by

$$(u_1v_1, v_1) = (V_1, U_1V_1) = (F, g+a_2). \tag{2.92}$$

The differential system in the chart (u_1, v_1) then becomes

$$\begin{aligned} u_1' &= \frac{-1+Au_1+Bu_1^2+2(t+1)u_1v_1+Cu_1^2v_1-3tu_1^2v_1^2}{t(t-1)}, \\ v_1' &= \frac{v_1\left(tu_1^2\left(a_2-v_1\right)\left(a_2+a_4-v_1\right)-1\right)-a_1}{(t-1)tu_1}, \end{aligned} \tag{2.93}$$

$$A = a_1-2ta_2+(1-t)a_3-ta_4, \quad B = -ta_2(a_2+a_4), \quad C = 2t(2a_2+a_4),$$

and the vector field is regular on the part of the exceptional line given by $v_1 = 0, u_1 \neq 0$, and we can obtain it explicitly as

$$\begin{aligned} u_1' &= \frac{-1 + (a_1 + a_3 - t(1 - a_0 - a_1))\, u_1 - a_2(a_2 + a_4)u_1^2}{t(t-1)}, \\ v_1' &= \frac{a_1}{(1-t)tu_1}, \end{aligned} \tag{2.94}$$

and from calculation of the differential system in the other chart (U_1, V_1) we see that the vector field is regular everywhere on the exceptional divisor except for at the point given by $(u_1, v_1) = (0, 0)$ where it diverges, which corresponds to the intersection of E_1 with the proper transform of the line defined by $F = 0$. The family of series solutions passing through p_1 lifts under the blow-ups to a family of disjoint solution curves parametrised by where they cross the exceptional divisor E_1. Indeed, if we take the series solutions with coefficients determined in terms of g_1, t_0 and the parameters a_i and compute the expressions for these lifted under the blow-up of p_1, we find in the (U_1, V_1)-chart that

$$\begin{aligned} U_1(t) &= \frac{t_0(1-t_0)g_1}{a_1} + \mathcal{O}(\tau), \\ V_1(t) &= \frac{a_1}{t_0(1-t_0)}\tau + \mathcal{O}(\tau^2), \end{aligned} \tag{2.95}$$

where again $\tau = t - t_0$. We see from this that parametrisation of the family of solutions by $g_1 \in \mathbb{C}$ corresponds exactly to where on the part of the exceptional line visible in the (U_1, V_1)-chart (all but $(u_1, v_1) = (0, 0)$) they cross, namely

$$(U_1(t_0), V_1(t_0)) = \left(\frac{t_0(1-t_0)g_1}{a_1}, 0 \right). \tag{2.96}$$

Calculations in the pairs of charts for the neighbourhoods of E_2, E_5, E_6 show that the singularities p_2, p_5, p_6 are resolved similarly, with each family of solutions passing through the point separated after being lifted under a single blow-up, parametetrised by where they cross the exceptional divisor. Through these calculations in charts we see that the vector field diverges on the proper transforms $H_f - E_1 - E_2$ and $H_f - E_5 - E_6$ of the lines $\{F = 0\}$ and $\{f = 0\}$ respectively, and these inaccessible divisors will be removed from each fibre when we construct Okamoto's space.

After this, it remains only to consider the part of the bundle where $G = 0$. The system in the chart (f, G) is given by

$$f' = \frac{\begin{pmatrix} 2(f-1)(t-f) \\ \quad - G\left(ta_4 - f(a_0 + a_4 + t(a_3 + a_4) - 1) - (a_1 + 2a_2)f^2\right) \end{pmatrix}}{t(t-1)G}, \qquad (2.97)$$
$$G' = \frac{f^2(1 + a_2 G)(1 + (a_1 + a_2)G) + t(a_4 G - 1)}{t(t-1)f}.$$

and we find three points where components are indeterminate, one of which is just p_6 given in this chart, namely by $(f, G) = (0, a_4^{-1})$. The other two are precisely p_3, p_7 from our point configuration, given with our normalisation by

$$p_3 : (f, G) = (t, 0), \quad p_7 : (f, G) = (1, 0). \qquad (2.98)$$

At both p_3 and p_7, the component f' is indeterminate, while G' is regular. The vector field diverges on $\{G = 0\}$ away from these two points, and we have no solution curves passing through this part of the bundle. After the blow-ups of p_3, p_7, we lift the system using the usual charts, for example in the chart $(u_3, v_3) = ((f-t)/G, G)$ obtaining

$$u_3' = \frac{t(t-1)(a_0 t - u_3) + v_3 P(u_3, v_3)}{t(1-t)(t + u_3 v_3)v_3}, \qquad (2.99)$$
$$v_3' = \frac{t(t-1) + v_3 Q(u_3, v_3)}{t(1-t)(t + u_3 v_3)},$$

where P, Q are polynomial in their arguments, which we omit for conciseness. In contrast to the singularities at p_1, p_2, p_5, p_6, the vector field (or more precisely u_3') diverges everywhere on the exceptional divisor except for at $p_4 : (u_3, v_3) = (a_0 t, 0)$, where u_3' is indeterminate while v_4' is regular. After blowing this up, we have the system in the chart (u_4, v_4), which is regular on the exceptional line where $v_4 = 0$, given by

$$u_4' = \frac{ta_0\left(a_0^2 - ta_1 a_2 - ta_2^2 + a_0 a_4\right) - (1 - t + 2a_0 + ta_1 + 2ta_2 + a_4)\, u_4}{t(1-t)}, \qquad (2.100)$$
$$v_4' = \frac{1}{t}.$$

Together with a similar calculation in the (U_4, V_4)-chart, this allows us to deduce that the vector field is regular on the part of E_4 away from its intersection with the proper transform $E_3 - E_4$. Again, the regularity of the vector field on this part of the exceptional divisor ensures we have separated the infinite family of solution curves passing through p_3 according to where they cross E_4, and the proper transform $E_3 - E_4$ is an inaccessible divisor.

We may again see this separation of the family of solution curves by lifting the series expansions under the blow-ups, and these methods can in fact be used to identify the points to be blown up to regularise the vector field as an alternative to rewriting the differential equations in charts. This method can often bypass tedious calculations of the differential system in different charts, and we will demonstrate it applied to the singularity at p_7. Consider a series expansion giving a solution to (2.97) locally about some $t_0 \in B_J$:

$$\begin{aligned} f &= f_0 + f_1(t-t_0) + f_2(t-t_0)^2 + \dots \\ G &= G_1(t-t_0) + G_2(t-t_0)^2 + \dots \end{aligned} \tag{2.101}$$

so $(f(t_0), G(t_0)) = (f_0, 0)$. Inserting this into the equation we obtain

$$\begin{aligned} 0 &= 2(1-f_0)(f_0-t_0) + \mathcal{O}(\tau), \\ 0 &= \big(t_0 - f_0^2 + t_0(t_0-1)f_0G_1\big) + \mathcal{O}(\tau), \end{aligned} \tag{2.102}$$

so again we see that f_0 is forced to take one of two values, corresponding to p_3 and p_7. Considering p_7, we take $f_0 = 1$, and see immediately from the leading term in the second line of (2.102) that must have $G_1 = -t_0^{-1}$. Proceeding as before, we arrive at the following family of solutions passing through p_7 parametrised by the free coefficient f_2:

$$\begin{aligned} f &= 1 - \frac{a_3}{t_0}\tau + f_2\tau^2 + \mathcal{O}(\tau^3), \\ G &= -\frac{1}{t_0}\tau + \left(\frac{a_0 + a_4 + t_0 - 2 - (a_3 + a_4)\, t_0}{2(t_0-1)t_0^2}\right)\tau^2 \\ &\qquad + \left(\frac{P}{6t_0^3(1-t_0)^2} + \frac{t_0+1}{3t_0(t_0-1)}f_2\right)\tau^3 + \mathcal{O}(\tau^4). \end{aligned} \tag{2.103}$$

Here P is a polynomial in t_0, a_i, which we omit for conciseness, $\tau = t - t_0$ as before, and the rest of the coefficients are determined recursively in terms of f_2, but we only keep track of the ones necessary for what follows.

We now use the expansions (2.103) to identify the sequence of blow-ups required to resolve the singularity at p_7, without rewriting the differential system. As $t \to t_0$, all solutions from this family pass through p_7, so we lift them under the blow-up of p_7, after which they are written in coordinates as

$$u_7(t) = a_3 + \mathcal{O}(\tau), \qquad v_7(t) = \mathcal{O}(\tau), \tag{2.104}$$

and the whole family passes through $(u_7(t_0), v_7(t_0)) = (a_3, 0)$, which is precisely p_8 in the fibre over t_0, so we must blow this up. Again lifting the solution curves under the blow-ups via the usual charts, we find

$$\begin{aligned} u_8(t) &= t_0^2 f_2 + \frac{a_3}{2(t_0-1)}\left(2 - a_0 - a_4 + t_0(a_3 - a_4 - 1)\right) + \mathcal{O}(\tau), \\ v_8(t) &= \mathcal{O}(\tau), \end{aligned} \tag{2.105}$$

and the family of solution curves are separated, with the free coefficient f_2 controlling where they cross the affine part of the exceptional line visible in the (u_8, v_8)-chart. In particular, there are no solution curves passing through the proper transform $E_7 - E_8$ in the fibre over t_0, so this represents another inaccessible divisor.

So, after all of the blow-ups, we have in each fibre a number of inaccessible divisors, which are precisely the components D_i of the anticanonical divisor of $\mathcal{X}_{\mathbf{b}}$ as given in the previous section. We remove their support $D_{\mathrm{red}} = \cup_i D_i$ and obtain a bundle

$$\begin{aligned} E &\to B_J \\ \mathcal{X}_{\mathbf{b}} \backslash D_{\mathrm{red}} &\mapsto t \end{aligned} \tag{2.106}$$

where $\mathbf{b}$ includes t varying over B_J, but the rest of the root variables a_i are fixed. Our calculations above (with the assumption of the Painlevé property, so the only solutions passing through anywhere over $\{f = 0\}, \{F = 0\}$ or $\{G = 0\}$ are given by series expansions as considered above) allow us to deduce that the vector field is regular on E, and that E is foliated by solution curves transverse to the fibres.

2.4.2 Hamiltonian structure and uniqueness

We now outline the sense in which Painlevé equations are determined uniquely by Okamoto's space, as shown in a series of papers by Takano, Shioda, Matumiya and Matano [MMT99, Mat97, ST97]. Okamoto's construction of the spaces of initial conditions for the Painlevé equations was done via equivalent nonautonomous Hamiltonian systems. For P_J, the system is of the form

$$q' = \frac{\partial H_J}{\partial p}, \qquad p' = -\frac{\partial H_J}{\partial q}, \tag{2.107}$$

where H_J are Okamoto's Hamiltonians, which we present now, where the parameters a_i in different Hamiltonians are unrelated, and arise as root variables for each associated family of Sakai surfaces:

$$\begin{aligned}
H_{\mathrm{I}} &= \frac{p^2}{2} - 2q^3 - tq, \\
H_{\mathrm{II}} &= \frac{p^2}{2} - \left(q^2 + \frac{t}{2}\right) p - a_1 q, \\
H_{\mathrm{III}} &= \frac{1}{t}\left\{p(p-1)q^2 + (a_1 + a_2)qp + tp - a_2 q\right\}, \\
H_{\mathrm{IV}} &= pq(p - q - t) - a_1 p - a_2 q, \\
H_{\mathrm{V}} &= \frac{1}{t}\left\{q(q-1)p(p+t) - (a_1 + a_3)qp + a_1 p + a_2 tq\right\}, \\
H_{\mathrm{VI}} &= \frac{q(q-1)(q-t)}{t(t-1)}\left\{p^2 - p\left(\frac{a_0 - 1}{q-t} + \frac{a_3}{q-1} + \frac{a_4}{q}\right) + \frac{a_2(a_1 + a_2)}{q(q-1)}\right\}.
\end{aligned} \tag{2.108}$$

We consider each system firstly on the trivial bundle $\mathbb{C}^2 \times B_J \to B_J$, where the system is Hamiltonian with respect to the usual symplectic form $dq \wedge dp$ on the fibre, and the Hamiltonian H_J is holomorphic on $\mathbb{C}^2 \times B_J$, as can be seen from the fact that each listed in (2.108) is polynomial in q, p and holomorphic in t on the corresponding B_J.

Okamoto's space is a bundle $E_J \to B_J$ which includes the product $\mathbb{C}^2 \times B_J$ in such a way that the $\mathbb{C}^2$ fibre over $t \in B_J$ is emdedded into that of E_J. The fibre of E_J over t is $\mathcal{X}_t \backslash D_{\mathrm{red}}$, where $\mathcal{X}_t$ is a Sakai surface of one of the types with extra parameter t, and we include only t in the subscript as the rest of the root variables are fixed. The symplectic form on the $\mathbb{C}^2$ fibre over t extends uniquely to a rational 2-form on $\mathcal{X}_t$, whose pole divisor is D_{red}. The differential system on the bundle $\mathbb{C}^2 \times B_J \to B_J$ extends to one on E_J, which is Hamiltonian with respect to the symplectic form extended to $\mathcal{X}_t \backslash D_{\mathrm{red}}$ in the following sense:

Suppose we have the Hamiltonian $H_J(q,p)$ defined in the (q,p)-chart, where the 2-form is given by $dq \wedge dp$. Suppose we have another chart (x,y) in which the 2-form is written as $R(x,y,t)dx \wedge dy$ for R rational in x, y and t. Then the Hamiltonian system (2.107) is transformed into a Hamiltonian system in the (x,y)-chart with respect to this 2-form:

$$R(x,y,t)x' = \frac{\partial K}{\partial y}, \qquad R(x,y,t)y' = -\frac{\partial K}{\partial x}, \tag{2.109}$$

where on the overlap of the two coordinate patches the Hamiltonian K satisfies

$$dq \wedge dp - dH_J \wedge dt = R(x, y, t) dx \wedge dy - dK \wedge dt. \tag{2.110}$$

Here we note that the Hamiltonian K is determined by H modulo functions of the independent variable t. We say that the system on E_J is Hamiltonian if it is given in charts by a collection $\{K_i\}$ of such Hamiltonians, with

$$\begin{aligned} K_i : \mathbb{C}^2 \times B_J &\to \mathbb{C}, \\ (x_i, y_i, t) &\mapsto K_i(x_i, y_i, t), \end{aligned} \tag{2.111}$$

on a collection of charts $\{(x_i, y_i, t)\}$ covering E_J. The Hamiltonians $\{K_i\}$ are equivalent under the transition functions modulo functions of t. If each K_i is holomorphic on the corresponding coordinate patch of E_J, then we say that the Hamiltonian system is holomorphic on E_J. We say that the system extends meromorphically to the bundle $\overline{E}_J$ of Sakai surfaces (without D_{red} removed) if the Hamiltonians extend to the closures of their $\mathbb{C}^2$-coordinate patches corresponding to the extension of E_J to $\overline{E}_J$.

We have the following result, which was shown for P_{VI} by Shioda and Takano in [ST97] then for P_{II}-P_{V} by Matumiya in [Mat97], using the results of Matano, Matumiya and Takano [MMT99].

Theorem 2.4.1. *Any Hamiltonian system holomorphic on E_J and extending meromorphically to the associated bundle of Sakai surfaces is equivalent to the Okamoto Hamiltonian form of P_J.*

This result is important for studying differential Painlevé equations appearing in applications for the following reason. If a system of differential equations can be regularised on a bundle isomorphic to Okamoto's space (in the sense that it is realised by an isomorphism between the associated Sakai surfaces which identifies their anticanonical divisors), then if we can show that the system is Hamiltonian with respect to the symplectic form corresponding to the anticanonical divisor and that the Hamiltonians are holomorphic on the complement of D_{red}, then it must coincide with the Okamoto Hamiltonian form of the relevant Painlevé equation.

	R	$R^{\perp}$	
Elliptic	$A_0^{(1)}$	$E_8^{(1)}$	
Multiplicative	$A_0^{(1)}$	$E_8^{(1)}$	
	$A_1^{(1)}$	$E_7^{(1)}$	
	$A_2^{(1)}$	$E_6^{(1)}$	
	$A_3^{(1)}$	$D_5^{(1)}$	
	$A_4^{(1)}$	$A_4^{(1)}$	
	$A_7^{(1)}$	$A_1^{(1)}$	
Additive	$A_0^{(1)}$	$E_8^{(1)}$	
	$A_1^{(1)}$	$E_7^{(1)}$	
	$A_2^{(1)}$	$E_6^{(1)}$	
	$D_4^{(1)}$	$D_4^{(1)}$	$\mathrm{P_{VI}}$
	$D_5^{(1)}$	$A_3^{(1)}$	$\mathrm{P_{V}}$
	$D_6^{(1)}$	$2A_1^{(1)}$	$\mathrm{P}_{\mathrm{III}}^{D_6^{(1)}}$
	$E_6^{(1)}$	$A_2^{(1)}$	$\mathrm{P_{IV}}$
	$D_7^{(1)}$	$A_1^{(1)}$ $\lvert\alpha\rvert^2=14$	$\mathrm{P}_{\mathrm{III}}^{D_7^{(1)}}$
	$E_7^{(1)}$	$A_1^{(1)}$	$\mathrm{P_{II}}$
	$D_8^{(1)}$	$A_0^{(1)}$	$\mathrm{P}_{\mathrm{III}}^{D_8^{(1)}}$
	$E_8^{(1)}$	$A_0^{(1)}$	$\mathrm{P_{I}}$

Table 2.3: Root system types for some families of Sakai surfaces

Chapter 3

Painlevé equations in applications - the identification problem

We now turn to applications of the geometric framework outlined in Chapter 2, and further illustrate how it works in practice. Over the last decade it has become clear that discrete Painlevé equations, like their differential counterparts, appear in a wide range of important mathematical and physical problems. These include the computations of gap probabilities [Bor03] of various ensembles in the emerging field of *integrable probability* [BG16], as well as describing recurrence coefficients of semi-classical orthogonal polynomials [VA18]. Thus, the ability to recognise a given nonautonomous recurrence as a discrete Painlevé equation is crucial to the application of the wealth of knowledge of their properties to problems arising in other areas. In particular, a method for determining the type of a discrete Painlevé equation according to Sakai's classification scheme, understanding whether it is equivalent to some well-studied example, and especially finding an explicit change of variables transforming it to such an example becomes desirable. Fortunately, Sakai's geometric theory provides an almost algorithmic procedure for identifying a given recurrence as a discrete Painlevé equation. In this chapter, adapted from [DFS19b], we illustrate this procedure by studying an example coming from the theory of discrete orthogonal polynomials. There are many connections between orthogonal polynomials and Painlevé equations, both differential and discrete. In particular, often the coefficients of three-term recurrence relations for orthogonal polynomials can be expressed in terms of solutions of discrete and differential Painlevé equations. In this work we study the so-called discrete orthogonal polynomials with hypergeometric weight and show that the difference equations satisfied by their recurrence coefficients are equivalent to the standard d-P_{V} equation from Chapter 2. The equivalence is obtained by first constructing a space of initial conditions for the given system and identifying it as a family of $D_4^{(1)}$-surfaces, with the discrete dynamics corresponding to a translational Cremona isometry. The change of variables is given by an isomorphism between this family of surfaces and the standard model from Chapter 2, which identifies the translation with that corresponding to d-P_{V}.

The purpose of this chapter is to illustrate this procedure for solving the identification problem in detail using one concrete example, which can be easily adapted to other cases. We also consider a second-order ODE satisfied by the same recurrence coefficients, and outline a similar method which identifies it with P_{VI}, by constructing a space of initial conditions explicitly and a transformation from this to the standard model of Okamoto's space for P_{VI}.

3.1 Painlevé equations from orthogonal polynomials

The problem that we consider comes from the theory of orthogonal polynomials. In fact, the relationship between discrete Painlevé equations and orthogonal polynomials is much older than the actual definition of a discrete Painlevé equation — the first example of a discrete analogue of P_{I} originally appeared in the work of Shohat [Sho39]. There are many connections between recurrence coefficients of orthogonal polynomials and solutions of Painlevé equations, both discrete and differential (see, for instance, [VA18] and numerous references therein).

We are interested in the difference equations themselves, but at this point we give a brief outline of how they are obtained in this case. Let $\{p_n(x) = \gamma_n x^n + \cdots\}$ be the collection of polynomials that are orthonormal on the set $\mathbb{N} = \{0, 1, 2, \ldots\}$ of non-negative integers with respect to the *hypergeometric weight* w_k, so

$$\sum_{k=0}^{\infty} p_n(k)p_m(k)w_k = \delta_{mn}, \qquad w_k = \frac{(\alpha)_k(\beta)_k}{(\gamma)_k k!}c^k, \quad \alpha, \beta, \gamma > 0,\ 0 < c < 1, \tag{3.1}$$

where $(\,\cdot\,)_k$ is the usual Pochhammer symbol and δ_{mn} is the Kronecker delta. This collection is known as the discrete orthogonal polynomials with hypergeometric weights, since the moments of this weight function are given in terms of the Gauss hypergeometric function ${}_2F_1(\alpha, \beta; \gamma; c)$ and its derivatives; it has been studied in [FVA18]. These polynomials satisfy a three-term recurrence relation

$$xp_n(x) = a_{n+1}p_{n+1}(x) + b_n p_n(x) + a_n p_{n-1}(x), \tag{3.2}$$

where $a_0 = 0$. The coefficients a_n and b_n are called the recurrence coefficients [Chi78, Ism05, Sze75]. Note that the corresponding monic orthogonal polynomials $P_n = p_n/\gamma_n$ satisfy a similar three-term recurrence relation

$$xP_n(x) = P_{n+1}(x) + b_n P_n(x) + a_n^2 P_{n-1}(x). \tag{3.3}$$

In [FVA18] it was shown that as functions of the discrete variable n these recurrence coefficients $\{a_n, b_n\}$ satisfy, after some change of variables, a system of nonlinear difference equations. As functions of the continuous parameter c of the hypergeometric weight, they satisfy a system of differential-difference equations which are equivalent to the Toda lattice. From these two systems one can obtain a differential equation, which we study in Section 3.3. In [HFC19], using a direct computation, it was shown that the discrete system is a composition of Bäcklund transformations of the sixth Painlevé equation. In this chapter we give a geometric explanation of this result, show that the discrete system is in fact equivalent to the standard d-$\mathrm{P_V}$ equation, and provide an explicit change of variables realising this.

To give the discrete system explicitly, let us introduce two new variables x_n and y_n parametrising the recurrence coefficients a_n^2 and b_n via

$$\begin{aligned} a_n^2 \frac{1-c}{c} &= y_n + \sum_{k=0}^{n-1} x_k + \frac{n(n+\alpha+\beta-\gamma-1)}{1-c}, \\ b_n &= x_n + \frac{n + (n+\alpha+\beta)c - \gamma}{1-c}. \end{aligned} \tag{3.4}$$

It was shown in [FVA18, Theorem 3.1] that x_n, y_n, $n \in \mathbb{N}$, satisfy the first-order system of nonlinear nonautonomous difference equations

$$\begin{aligned} (y_n - \alpha\beta + (\alpha+\beta+n)x_n - x_n^2)(y_{n+1} - \alpha\beta + (\alpha+\beta+n+1)x_n - x_n^2) \\ = \frac{1}{c}(x_n - 1)(x_n - \alpha)(x_n - \beta)(x_n - \gamma), \end{aligned} \tag{3.5a}$$

$$\begin{aligned} (x_n + \mathfrak{Y}_n)(x_{n-1} + \mathfrak{Y}_n) \\ = \frac{(y_n + n\alpha)(y_n + n\beta)\left[y_n + n\gamma - (\gamma-\alpha)(\gamma-\beta)\right]\left[y_n + n - (1-\alpha)(1-\beta)\right]}{\left[y_n(2n+\alpha+\beta-\gamma-1) + n((n+\alpha+\beta)(n+\alpha+\beta-\gamma-1) - \alpha\beta + \gamma)\right]^2}, \end{aligned} \tag{3.5b}$$

where α, β, γ, c are the parameters of the hypergeometric weight w_k in (3.1) and

$$\mathfrak{Y}_n = \frac{y_n^2 + y_n(n(n+\alpha+\beta-\gamma-1) - \alpha\beta+\gamma) - \alpha\beta n(n+\alpha+\beta-\gamma-1)}{y_n(2n+\alpha+\beta-\gamma-1) + n((n+\alpha+\beta)(n+\alpha+\beta-\gamma-1) - \alpha\beta+\gamma)}.$$

We call this discrete system (3.5a-3.5b) the *hypergeometric weight recurrence*, and its initial conditions are given by

$$x_0 = \frac{\alpha\beta c}{\gamma} \frac{{}_2F_1(\alpha+1,\beta+1;\gamma+1;c)}{{}_2F_1(\alpha,\beta;\gamma;c)} + \frac{(\alpha+\beta)c-\gamma}{c-1}, \quad y_0 = 0. \tag{3.6}$$

For the hypergeometric weights the connection with a certain form of the sixth Painlevé equation (with independent variable c) is known (see [FVA18, Theorem 5.1]). The essential role is played by the Toda differential-difference system for the recurrence coefficients (see, e.g., [Ism05, §2.8] or [VA18, §3.2.2]). For the hypergeometric weight, it is given by

$$\begin{aligned} c\frac{d}{dc}a_n^2 &= a_n^2(b_n - b_{n-1}), \qquad && n \geq 1, \\ c\frac{d}{dc}b_n &= a_{n+1}^2 - a_n^2, && n \geq 0. \end{aligned} \tag{3.7}$$

It is proved in [FVA18, Theorem 5.1] that a simple linear change of variables transforms $S_n = \sum_{k=0}^{n-1} x_k$ into the solutions of the so-called σ-form of $\mathrm{P_{VI}}$ [JMU81, JM81a, JM81b]. Knowing S_n one can find x_n, y_n and, hence, the recurrence coefficients a_n^2, b_n in terms of S_n and its derivatives. Moreover, it is shown in [HFC19] that the differential equation for x_n can be directly reduced to the sixth Painlevé equation, which we give a geometric explanation of in Section 3.3.

3.2 The identification procedure for discrete equations

The main objective of this chapter is to illustrate a general procedure for identifying a given discrete system as a discrete Painlevé equation and explicitly rewriting it in some standard form, using the system (3.5a–3.5b) as an example. This process consists of the following steps, where we assume that we indeed have some discrete Painevé equation, otherwise the process will terminate before the final result.

(Step 1) **Lift the given system to a family of isomorphisms.** For that, if necessary, rewrite the recurrence as a system of two first-order recurrences, $(x_{n+1}, y_{n+1}) = \psi^{(n)}(x_n, y_n)$. The mapping $\psi^{(n)} : \mathbb{C}^2 \to \mathbb{C}^2$ should be a birational mapping that may depend on various parameters, including the iteration step n that we consider to be generic. Then extend $\psi^{(n)}$ to $\mathbb{P}^1 \times \mathbb{P}^1$ in the same way as in previous chapters. Find the indeterminacies of the mapping and its inverse, and resolve them using the blow-up procedure (for discrete Painlevé equations this will require finitely many blow-ups) until the mapping lifts to an isomorphism of rational surfaces $\psi^{(n)} : \mathcal{X}_n \xrightarrow{\sim} \mathcal{X}_{n+1}$.

(Step 2) **Find the induced mapping on $\mathrm{Pic}(\mathcal{X})$.** With the natural identification of Picard groups of the family $\{\mathcal{X}_n\}$ of surfaces, compute the induced Cremona isometry.

(Step 3) **Determine the surface type.** Determine whether the family $\{\mathcal{X}_n\}$ are Sakai surfaces and, if so, their type. If the resolution of indeterminacies performed in Step 1 led directly to a family of Sakai surfaces, there would have been eight blow-ups performed, but it is also possible that this initial procedure leads to more. In this case, if we can find sufficiently many (-1)-curves that are fixed by the dynamics, we can blow them down to arrive at a family of Sakai surfaces between which the system still gives isomorphisms. In the case of the hypergeometric weight recurrence we arrive directly at a family of Sakai surfaces, but see [DST13] and [DK19] for examples requiring blow-downs.

(Step 4) **Find a preliminary identification of $\mathrm{Pic}(\mathcal{X})$ with the standard model.** The aim is to find a transformation from the given system to the standard example via isomorphisms identifying the families of Sakai surfaces. This will be most efficiently obtained by first finding an identification of the Picard lattices associated with the two families. At this step, we only need to ensure that this identifies the surface roots with the standard example.

(Step 5) **Find the translational Cremona isometry and compare it with that of the standard discrete Painlevé equation.** Using this preliminary change of basis we can choose symmetry roots for our family of surfaces that match the standard example. We can then examine the induced action of the mapping on the symmetry root lattice and whether this corresponds to a translation. If so, we compare this with the translation giving the standard example, and if they are the same we do not need to adjust our identification on the level of $\mathrm{Pic}(\mathcal{X})$. If the translations are different, the equations will still be equivalent if the translations are conjugate in the group of Cremona isometries. To find out whether this is the case, we may either represent each translation as a word in the generators of the extended affine Weyl group and solve the conjugacy problem for words in groups, or determine whether the weights associated with the translations are in the same orbit. If they are conjugate, the conjugation element is the necessary adjustment to our preliminary change of basis, so we arrive at a final identification on the level of Picard groups which matches the translations, and which we will use to construct the transformation between discrete systems.

(Step 6) **Find the change of variables reducing the given system to the standard example.** We now obtain an isomorphism between the family of Sakai surfaces from the given system and that of the standard model, which induces the final identification we obtained on the level of Picard groups. An important part of this computation is the identification of the parameters from the given system with the root variables for the standard model of surfaces. This can be done by computing the root variables for $\mathcal{X}_n$ with our choice of symmetry roots using the period mapping. Once we have this isomorphism between the families of surfaces that matches the translations, we verify that this gives a change of variables reducing the given system to the standard example.

In what follows, we will illustrate the calculations at each step of this procedure using equations (3.5a–3.5b) as an example of a given system. Our main result is the following Theorem.

Theorem 3.2.1. *Recurrences (3.5a–3.5b) are equivalent to the standard d-P_{V} equation* (2.68). *This equivalence is achieved via the following change of variables:*

$$\begin{aligned} f(x,y) &= \frac{t(x-\beta)(x-\gamma)}{((x-\alpha)(x-\beta)-nx-y)}, \\ g(x,y) &= -\frac{(x-\gamma)(((x-\alpha)(x-\beta)-nx-y)-t(x-\beta)(x-\gamma+\beta+n))}{((x-\alpha)(x-\beta)-nx-y)-t(x-\beta)(x-\gamma)}, \end{aligned} \tag{3.8}$$

where we have written $x = x_n, y = y_n$ for conciseness. Note that the parameters c and t are related by $ct = 1$, and the root variable parameters in d-P_{V} are related to those from *the system (3.5a–3.5b) by*

$$\begin{aligned} a_0 &= \gamma - n - \alpha, \qquad a_1 = \alpha - 1, \quad a_2 = 1 + n + \beta - \gamma, \\ a_3 &= -n - \beta, \qquad\quad a_4 = \gamma - \beta. \end{aligned} \tag{3.9}$$

3.2.1 Lifting the system to isomorphisms

For the hypergeometric weight recurrence, we have the iteration mapping $\psi^{(n)} : (x_n, y_n) \mapsto (x_{n+1}, y_{n+1})$ expressed in terms of a *forward mapping* $\psi_1^{(n)} : (x_n, y_n) \mapsto (x_n, y_{n+1})$ defined by equation (3.5a) and a *backward mapping* $\psi_2^{(n)} : (x_n, y_n) \mapsto (x_{n-1}, y_n)$ defined by equation (3.5b). From this we have a decomposition $\psi^{(n)} = \psi_1^{(n)} \circ (\psi_2^{(n+1)})^{-1}$, which this is fairly typical of discrete Painlevé equations obtained as deautonomisations of QRT mappings, see [CDT17].

First, we extend the mappings from $\mathbb{C}^2$ to $\mathbb{P}^1 \times \mathbb{P}^1$ in the same way as throughout the thesis by introducing homogeneous coordinates $[x^0 : x^1]$ and $[y^0 : y^1]$ with $x = x^0/x^1$ in the affine chart $x_1 \neq 0$, $X = 1/x = x^1/x^0$ in the affine chart $x_0 \neq 0$, and $y, Y = 1/y$ defined similarly. The fact that we have the decomposition in terms of forward and backward mappings means that to lift the system to isomorphisms it will be sufficient to resolve the indeterminacies of the birational maps $\psi_1^{(n)}$ and $\psi_2^{(n)}$ on $\mathbb{P}^1 \times \mathbb{P}^1$.

3.2.1.1 The Forward Mapping

We begin by considering the forward mapping. We put $\bar{x} = x := x_n$, $y := y_n$, $\bar{y} := y_{n+1}$ and omit the index n in the mapping notation. The map $\psi_1 : (x, y) \mapsto (\bar{x}, \bar{y})$ then becomes

$$(\bar{x}, \bar{y}) = \left(x, \frac{(x-1)(x-\alpha)(x-\beta)(x-\gamma)}{c(y - (x-\alpha)(x-\beta) + nx)} + (x-\alpha)(x-\beta) - (n+1)x \right), \tag{3.10}$$

and we immediately see the following indeterminacies in the (x, y)-chart

$$\begin{aligned} &q_1 : (x, y) = (1, (1-\alpha)(1-\beta) - n), \quad q_2 : (x, y) = (\alpha, -n\alpha), \\ &q_3 : (x, y) = (\beta, -n\beta), \quad q_4 : (x, y) = (\gamma, (\gamma-\alpha)(\gamma-\beta) - n\gamma), \end{aligned} \tag{3.11}$$

which we sometimes refer to as basepoints in analogy with the case of linear systems of divisors. Rewriting the rational function giving $\bar{y}$ in the (X, Y)-chart, we get

$$\bar{y} = \frac{\left(\begin{aligned} &Y(1-X)(1-\alpha X)(1-\beta X)(1-\gamma X) \\ &\quad + c\Big(X^2 - Y\left((1-\alpha X)(1-\beta X) - nX\right)\Big)\Big((1-\alpha X)(1-\beta X) - (n+1)X\Big)\end{aligned}\right)}{cX^2\Big(X^2 - Y\left((1-\alpha X)(1-\beta X) - nX\right)\Big)},$$

and we see that we have a new basepoint $q_5 : (X, Y) = (0, 0)$. By calculation in the other two charts we see that these points are the only indeterminacies in $\mathbb{P}^1 \times \mathbb{P}^1$ for the forward mapping.

We now illustrate some methods of calculation for resolving singularities of discrete systems, which are best performed using a computer algebra software. Here we use **Mathematica**®. We introduce coordinates for the neighbourhoods of the exceptional divisors F_i arising from the blow-ups of q_i, $i = 1, \ldots, 4$ according to the convention established in Section 2.3. For example, for q_1 we have two affine charts (u_1, v_1), (U_1, V_1) defined by

$$\begin{aligned} x &= 1 + u_1 v_1 = 1 + V_1, \\ y &= (1-\alpha)(1-\beta) - n + v_1 = (1-\alpha)(1-\beta) - n + U_1 V_1. \end{aligned} \tag{3.12}$$

In the coordinates (U_1, V_1) we have

$$\begin{aligned} \bar{x} &= 1 + V_1, \\ \bar{y} &= \frac{(1-\alpha+V_1)(1-\beta+V_1)(1-\gamma+V_1)}{c(U_1 - (2-\alpha-\beta+V_1) + n)} \\ &\qquad + (1-\alpha+V_1)(1-\beta+V_1) - (n+1)(1+V_1), \end{aligned} \tag{3.13}$$

where the cancellation of V_1 in the rational function $\bar{y}$ has resolved the indeterminacy, so the mapping lifts to the exceptional divisor F_1, which is given in this chart by $V_1 = 0$. Rewriting the mapping in the (u_1, v_1)-chart does not reveal any other basepoints.

The computation is similar for the points $q_2, \ldots, q_4$, and these indeterminacies are each resolved through a single blow-up, with the mapping lifting to be well-defined on the exceptional divisors F_i, $i = 1, \ldots, 4$.

The situation at the point $q_5 : (X, Y) = (0, 0)$ is less trivial. Introducing blow-up coordinates at this point via

$$X = V_5 = u_5 v_5, \qquad Y = U_5 V_5 = v_5, \tag{3.14}$$

and considering the mapping in the (u_5, v_5)-chart, we get, after cancelling the factor of V_5 in the numerator and denominator,

$$\bar{y} = \frac{\begin{pmatrix} U_5(1-V_5)(1-\alpha V_5)(1-\beta V_5)(1-\gamma V_5) \\ \quad + c\Big(V_5 - U_5\left((1-\alpha V_5)(1-\beta V_5) - nV_5\right)\Big)\Big((1-\alpha V_5)(1-\beta V_5) - (n+1)V_5\Big) \end{pmatrix}}{cV_5^2\Big(V_5 - U_5\left((1-\alpha V_5)(1-\beta V_5) - nV_5\right)\Big)}.$$

We see that this mapping has a new indeterminacy at $q_6 : (U_5, V_5) = (Y/X, X) = (0,0)$ (note that this point is not visible in the (u_5, v_5)-chart). Continuing in this way, we get the following sequence of "infinitely near" basepoints for the forward mapping:

$$\begin{aligned}
&q_5 : (X, Y) = (0,0) \\
&q_6 : (U_5, V_5) = (Y/X, X) = (0,0) \\
&q_7 : (u_6, v_6) = \left(\frac{U_5}{V_5}, V_5\right) = \left(\frac{c}{c-1}, 0\right) \\
&q_8 : (u_7, v_7) = \left(\frac{(c-1)u_6 - c}{(c-1)v_6}, v_6\right) = \left(\frac{c\Big(c(\alpha+\beta+n) + n - \gamma\Big)}{(c-1)^2}, 0\right).
\end{aligned} \tag{3.15}$$

Writing the lifted map in both charts (u_8, v_8) and (U_8, V_8), we see that we have no more basepoints on the exceptional line F_8, so all indeterminacies of the forward mapping are resolved.

3.2.1.2 The Backward Mapping

Consider now the backward mapping. We put $x := x_n$, $\underline{x} = x_{n-1}$, $\underline{y} = y := y_n$, so the backward mapping $\psi_2 : (x, y) \mapsto (\underline{x}, \underline{y})$ is given by

$$\begin{aligned}
&\underline{x} = \frac{(y+n\alpha)(y+n\beta)(y+n\gamma-(\gamma-\alpha)(\gamma-\beta))(y-n-(1-\alpha)(1-\beta))}{(x+\mathfrak{Y})\mathfrak{Z}^2} - \mathfrak{Y}, \\
&\underline{y} = y,
\end{aligned} \tag{3.16}$$

where $\mathfrak{Y}$ is given by (3.1) (we omit the index n) and

$$\mathfrak{Z} = y(2n+\alpha+\beta-\gamma-1) + n\left((n+\alpha+\beta)(n+\alpha+\beta-\gamma-1) - \alpha\beta + \gamma\right). \quad (3.17)$$

The same standard computation shows that the only indeterminacies of the backward mapping are the same points $q_1, \ldots, q_4$ as for the forward one, but q_5 is not present. Calculations in the same coordinates (u_i, v_i) and (U_i, V_i) for $i = 1, \ldots, 4$ shows that these indeterminacies are all resolved after a single blow-up, as was the case for the forward mapping.
We now have a family of surfaces to which the iteration mappings $\psi^{(n)}$ lift to isomorphisms. Take the points $q_1, \ldots, q_8$ in the surface with coordinates $(x, y) = (x_n, y_n)$, and denote by $\mathcal{X}_n := \mathrm{Bl}_{q_1 \cdots q_8}(\mathbb{P}^1 \times \mathbb{P}^1)$ the surface obtained after the blow-ups of these, with projection $\eta_n : \mathcal{X}_n \to \mathbb{P}^1 \times \mathbb{P}^1$. For each n, we have an isomorphism

$$\psi^{(n)} : \mathcal{X}_n \to \mathcal{X}_{n+1}. \quad (3.18)$$

3.2.2 The mapping on $\mathrm{Pic}(\mathcal{X})$

We now compute the Cremona isometry induced by the iteration mapping $\psi^{(n)}$. We do this by considering those induced by isomorphisms ψ_1 and ψ_2 between $\underline{\mathcal{X}}, \mathcal{X}$ and $\bar{\mathcal{X}}$ obtained from $\mathbb{P}^1 \times \mathbb{P}^1$ with coordinates $(\underline{x}, \underline{y}) = (x_{n-1}, y_n), (x, y) = (x_n, y_n)$ and $(\bar{x}, \bar{y}) = (x_n, y_{n+1})$ respectively, as in the previous section. The basepoints $\underline{q}_i$ and $\bar{q}_i$, to be blown up to arrive at the surfaces $\underline{\mathcal{X}}$ and $\bar{\mathcal{X}}$ will be given in what follows, and we will use $\bar{F}_i$ to denote the exceptional divisor arising from the blow-up of the point $\bar{q}_i$, $\bar{H}_x$ to denote the class of the total transform of a line of constant $\bar{x}$, etc., and similarly for divisor classes. We will also use $(\bar{u}_i, \bar{v}_i), (\bar{U}_i, \bar{V}_i)$ for the charts introduced for the blow-up of $\bar{q}_i$ according to the convention established in Section 2.3. Notations for divisors on $\underline{\mathcal{X}}$ and their classes are similar. The result for the forward and backward mappings is given by the following Lemma, where we use the notation $\mathcal{F}_{ij} = \mathcal{F}_i + \mathcal{F}_j$ and so on.

Lemma 3.2.2.

(a) The forward mapping gives an isomorphism $\psi_1 : \mathcal{X} \to \bar{\mathcal{X}}$ with pushforward action

$(\psi_1)_* : \mathrm{Pic}(\mathcal{X}) \to \mathrm{Pic}(\bar{\mathcal{X}})$ *given by*

$$\begin{aligned} &\mathcal{H}_x \mapsto \bar{\mathcal{H}}_x, && \mathcal{H}_y \mapsto 4\bar{\mathcal{H}}_x + \bar{\mathcal{H}}_y - \bar{\mathcal{F}}_{12345678}, \\ &\mathcal{F}_1 \mapsto \bar{\mathcal{H}}_x - \bar{\mathcal{F}}_1, && \mathcal{F}_2 \mapsto \bar{\mathcal{H}}_x - \bar{\mathcal{F}}_2, \\ &\mathcal{F}_3 \mapsto \bar{\mathcal{H}}_x - \bar{\mathcal{F}}_3, && \mathcal{F}_4 \mapsto \bar{\mathcal{H}}_x - \bar{\mathcal{F}}_4, \\ &\mathcal{F}_5 \mapsto \bar{\mathcal{H}}_x - \bar{\mathcal{F}}_8, && \mathcal{F}_6 \mapsto \bar{\mathcal{H}}_x - \bar{\mathcal{F}}_7, \\ &\mathcal{F}_7 \mapsto \bar{\mathcal{H}}_x - \bar{\mathcal{F}}_6, && \mathcal{F}_8 \mapsto \bar{\mathcal{H}}_x - \bar{\mathcal{F}}_5. \end{aligned} \tag{3.19}$$

The base points $\bar{q}_i$ for the $(\bar{x}, \bar{y})$-surface $\bar{\mathcal{X}}$ are given by

$$\begin{aligned} &\bar{q}_1 : (\bar{x}, \bar{y}) = (1, (1-\alpha)(1-\beta) - (n+1)), \\ &\bar{q}_2 : (\bar{x}, \bar{y}) = (\alpha, -(n+1)\alpha), \\ &\bar{q}_3 : (\bar{x}, \bar{y}) = (\beta, -(n+1)\beta), \\ &\bar{q}_4 : (\bar{x}, \bar{y}) = (\gamma, (\gamma-\alpha)(\gamma-\beta) - (n+1)\gamma), \end{aligned} \tag{3.20}$$

for the first four, and for the infinitely near points by

$$\begin{aligned} &\bar{q}_5 : && (\bar{X}, \bar{Y}) = (0,0), \\ &\bar{q}_6 : && (\bar{U}_5, \bar{V}_5) = (\bar{Y}/\bar{X}, \bar{X}) = (0,0), \\ &\bar{q}_7 : && (\bar{u}_6, \bar{v}_6) = \left(\frac{\bar{U}_5}{\bar{V}_5}, \bar{V}_5\right) = \left(\frac{c}{c-1}, 0\right), \\ &\bar{q}_8 : && (\bar{u}_7, \bar{v}_7) = \left(\frac{(c-1)\bar{u}_6 - c}{(c-1)\bar{v}_6}, \bar{v}_6\right) \\ & && = \left(\frac{c\Big(c(\alpha+\beta+n+1) + n - \gamma - 1\Big)}{(c-1)^2}, 0\right). \end{aligned} \tag{3.21}$$

(b) The backward mapping gives an isomorphism $\psi_2 : \mathcal{X} \to \underline{\mathcal{X}}$ with pushforward action $(\psi_2)_* : \mathrm{Pic}(\mathcal{X}) \to \mathrm{Pic}(\underline{\mathcal{X}})$ given by

$$\begin{aligned} &\mathcal{H}_x \mapsto \underline{\mathcal{H}}_x + 2\underline{\mathcal{H}}_y - \underline{\mathcal{F}}_{1234}, && \mathcal{H}_y \mapsto \underline{\mathcal{H}}_y, \\ &\mathcal{F}_1 \mapsto \underline{\mathcal{H}}_y - \underline{\mathcal{F}}_1, && \mathcal{F}_2 \mapsto \underline{\mathcal{H}}_y - \underline{\mathcal{F}}_2, \\ &\mathcal{F}_3 \mapsto \underline{\mathcal{H}}_y - \underline{\mathcal{F}}_3, && \mathcal{F}_4 \mapsto \underline{\mathcal{H}}_y - \underline{\mathcal{F}}_4, \\ &\mathcal{F}_5 \mapsto \underline{\mathcal{F}}_5, && \mathcal{F}_6 \mapsto \underline{\mathcal{F}}_6, \\ &\mathcal{F}_7 \mapsto \underline{\mathcal{F}}_7, && \mathcal{F}_8 \mapsto \underline{\mathcal{F}}_8. \end{aligned} \tag{3.22}$$

The basepoints $\underline{q}_i$ are given by

$$
\begin{aligned}
\underline{q}_1 &: (\underline{x}, \underline{y}) = (1, (1-\alpha)(1-\beta) - n),\\
\underline{q}_2 &: (\underline{x}, \underline{y}) = (\alpha, -n\alpha),\\
\underline{q}_3 &: (\underline{x}, \underline{y}) = (\beta, -n\beta),\\
\underline{q}_4 &: (\underline{x}, \underline{y}) = (\gamma, (\gamma-\alpha)(\gamma-\beta) - n\gamma),
\end{aligned}
\tag{3.23}
$$

as well as

$$
\begin{aligned}
\underline{q}_5 :&\quad (\underline{X}, \underline{Y}) = (0,0),\\
\underline{q}_6 :&\quad (\underline{U}_5, \underline{V}_5) = (\underline{Y}/\underline{X}, \underline{X}) = (0,0),\\
\underline{q}_7 :&\quad (\underline{u}_6, \underline{v}_6) = \left(\frac{\underline{U}_5}{\underline{V}_5}, \underline{V}_5\right) = \left(\frac{c}{c-1}, 0\right),\\
\underline{q}_8 :&\quad (\underline{u}_7, \underline{v}_7) = \left(\frac{(c-1)\underline{u}_6 - c}{(c-1)\underline{v}_6}, \underline{v}_6\right)\\
&\quad = \left(\frac{c\Big(c(\alpha+\beta+n) + n - \gamma - 2\Big)}{(c-1)^2}, 0\right).
\end{aligned}
\tag{3.24}
$$

Proof. This is a standard computation in charts that we illustrate through a few examples for the forward mapping ψ_1. First, since $\bar{x} = x$, we see that $(\psi_1)_*(\mathcal{H}_x) = \bar{\mathcal{H}}_x$. To find $(\psi_1)_*(\mathcal{F}_1)$ we take the mapping (3.13) and restrict to the part of the exceptional divisor given by $V_1 = 0$ to obtain

$$
(\bar{x}, \bar{y}) = \left(1, \frac{(1-\alpha)(1-\beta)(1-\gamma)}{c(U_1 + \alpha + \beta + n - 2)} + (1-\alpha)(1-\beta) - (n+1)\right), \tag{3.25}
$$

so $\bar{y}$ is just a fractional linear transformation of the coordinate U_1 parametrising the affine part of the exceptional divisor, and thus F_1 maps bijectively to the proper transform $\bar{H}_x - \bar{F}_1$ of the line $\bar{x} = 1$. After passing to divisor classes, this gives $(\psi_1)_*(\mathcal{F}_1) = \bar{\mathcal{H}}_x - \mathcal{F}_1$ as required. The computations for $F_2, \ldots, F_4$ are similar.

The computation gets slightly more complicated over the point q_5. For example, to find $(\psi_1)_*(F_5)$ we compute ψ_1 in the chart (U_5, V_5) and restrict to $V_5 = 0$. However, since there is a single base point q_6 on F_5, writing the mapping in the chart and setting $V_5 = 0$ gives the mapping from the proper transform $F_5 - F_6$ of F_5 on $\mathcal{X}$. Writing the mapping in the charts (U_5, V_5) for the domain and $(\bar{X}, \bar{Y})$ for the target, we find that when $V_5 = 0$ we have

$(\bar{X},\bar{Y})=(0,0)$, so F_5-F_6 maps somewhere over the point $\bar{q}_5$. Switching to coordinates $(\bar{U}_5,\bar{V}_5)$ in the range, we set $V_5=0$ and find $(\bar{U}_5,\bar{V}_5)=(0,0)$. Thus, F_5-F_6 is still mapped somewhere over $\bar{q}_6$, and we need to compute in the chart $(\bar{u}_6,\bar{v}_6)$. We see similarly that F_5-F_6 is sent somewhere over $\bar{q}_7$, but setting $V_5=0$ in the mapping written in the chart $(\bar{u}_7,\bar{v}_7)$ gives

$$(\bar{u}_7,\bar{v}_7)=\left(\frac{c+c(-1+n+c(1+n+\alpha+\beta)-\gamma)U_5}{(c-1)^2U_5},0\right), \tag{3.26}$$

and so $(\psi_1)_*(F_5-F_6)=\bar{F}_7-\bar{F}_8$. Other computations for curves over q_5 are similar and result in

$$\begin{aligned}(\psi_1)_*(F_6-F_7)&=\bar{F}_6-\bar{F}_7,\\(\psi_1)_*(F_7-F_8)&=\bar{F}_5-\bar{F}_6,\\(\psi_1)_*(F_8)&=\bar{H}_x-\bar{F}_5.\end{aligned} \tag{3.27}$$

Passing to classes, these allow us to deduce by linearity that

$$\begin{aligned}(\psi_1)_*(\mathcal{F}_7)&=(\psi_1)_*(\mathcal{F}_7-\mathcal{F}_8)+(\psi_1)_*(\mathcal{F}_8)\\&=(\bar{\mathcal{F}}_5-\bar{\mathcal{F}}_6)+(\bar{\mathcal{H}}_x-\bar{\mathcal{F}}_5)\\&=\bar{\mathcal{H}}_x-\bar{\mathcal{F}}_6,\end{aligned} \tag{3.28}$$

and similarly for $\mathcal{F}_5$ and $\mathcal{F}_6$. For the forward mapping it remains only to find $(\psi_1)_*(\mathcal{H}_y)$, and for this calculation it is convenient to compute the mapping on the proper transform of some line of constant y or Y passing through one or more basepoints. For example $H_y-F_5-F_6$ is the proper transform of the line $\{Y=0\}$, and we can set $Y=0$ in the mapping to obtain

$$(\bar{x},\bar{y})=(x,x^2+\alpha\beta-x(n+1+\alpha+\beta)), \tag{3.29}$$

so $H_y-F_5-F_6$ is mapped to the proper transform of the bi-degree $(2,1)$-curve in the range given by the equation

$$\bar{x}^2+\alpha\beta-\bar{x}(n+1+\alpha+\beta)-\bar{y}=0. \tag{3.30}$$

To compute the class in $\mathrm{Pic}(\bar{\mathcal{X}})$ of the proper transform, we can check by calculation in charts that it passes through $\bar{q}_1,\ldots,\bar{q}_6$, each with multiplicity one. For example, substituting

$$(\bar{x}, \bar{y}) = (\bar{u}_2\bar{v}_2 + \alpha, \bar{v}_2 - (n+1)\alpha) \tag{3.31}$$

into the equation (3.30) we obtain

$$\bar{v}_2\left(\bar{u}_2^2\bar{v}_2 - (n+1-\alpha+\beta)\bar{u}_2 - 1\right) = 0, \tag{3.32}$$

so the total transform of the curve defined by (3.30) has F_2 as a component. Through similar calculations using charts covering the other exceptional divisors we obtain

$$(\psi_1)_*(H_y - F_5 - F_6) = 2\bar{H}_x + \bar{H}_y - \bar{F}_{123456}, \tag{3.33}$$

and deduce

$$\begin{aligned} (\psi_1)_*(\mathcal{H}_y) &= (\psi_1)_*(\mathcal{H}_y - \mathcal{F}_5 - \mathcal{F}_6) + (\psi_1)_*(\mathcal{F}_5) + (\psi_1)_*(\mathcal{F}_6) \\ &= (2\bar{\mathcal{H}}_x + \bar{\mathcal{H}}_y - \bar{F}_{123456}) + (\bar{\mathcal{H}}_x - \bar{\mathcal{F}}_8) + (\bar{\mathcal{H}}_x - \bar{F}_7) \\ &= 4\bar{\mathcal{H}}_x + \bar{\mathcal{H}}_y - \bar{\mathcal{F}}_{12345678}. \end{aligned} \tag{3.34}$$

This completes the computation for the forward mapping ψ_1, and the backward mapping ψ_2 follows along the same lines. □

We now deduce the Cremona isometry induced by $\psi^{(n)}$ through its pushforward $\psi_*^{(n)} = (\psi_2)_*^{-1} \circ (\psi_1)_* : \mathrm{Pic}(\mathcal{X}_n) \to \mathrm{Pic}(\mathcal{X}_{n+1})$, where $\mathcal{X}_n$ is obtained through the blow-ups of q_i as given in Subsection 3.2.1, and $\mathcal{X}_{n+1}$ is obtained through the blow-ups of the same points with n replaced with $n+1$, which we denote $\bar{\bar{q}}_i$. The Cremona isometry is induced by this pushforward under the natural identification of the Picard groups, where we identify the class of the exceptional divisor arising from the blow-up of q_i in $\mathcal{X}_n$ with that on $\mathcal{X}_{n+1}$ corresponding to $\bar{\bar{q}}_i$, and similarly the class of the total transform of a curve of constant x_n on $\mathcal{X}_n$ with that of constant x_{n+1} on $\mathcal{X}_{n+1}$, etc. The Cremona isometry induced by $\psi_*^{(n)}$ is computed by composing $(\psi_1)_*$ and $(\psi_2)_*^{-1}$ then imposing the identification, so we arrive at

$$\begin{aligned}
&\mathcal{H}_x \mapsto \mathcal{H}_x + 2\mathcal{H}_y - \mathcal{F}_{1234}, && \mathcal{H}_y \mapsto 4\mathcal{H}_x + 5\mathcal{H}_y - 3\mathcal{F}_{1234} - \mathcal{F}_{5678},\\
&\mathcal{F}_1 \mapsto \mathcal{H}_x + \mathcal{H}_y - \mathcal{F}_{234}, && \mathcal{F}_5 \mapsto \mathcal{H}_x + 2\mathcal{H}_y - \mathcal{F}_{12348}\\
&\mathcal{F}_2 \mapsto \mathcal{H}_x + \mathcal{H}_y - \mathcal{F}_{134}, && \mathcal{F}_6 \mapsto \mathcal{H}_x + 2\mathcal{H}_y - \mathcal{F}_{12347},\\
&\mathcal{F}_3 \mapsto \mathcal{H}_x + \mathcal{H}_y - \mathcal{F}_{124}, && \mathcal{F}_7 \mapsto \mathcal{H}_x + 2\mathcal{H}_y - \mathcal{F}_{12346},\\
&\mathcal{F}_4 \mapsto \mathcal{H}_x + \mathcal{H}_y - \mathcal{F}_{123}, && \mathcal{F}_8 \mapsto \mathcal{H}_x + 2\mathcal{H}_y - \mathcal{F}_{12345}.
\end{aligned} \tag{3.35}$$

We remark briefly that this is in line with what we expect, in particular that it preserves the intersection product on $\operatorname{Pic}(\mathcal{X})$ as well as the canonical class. This is of course guaranteed by the fact that it is induced by an isomorphism, which means that it also preserves effectiveness of divisor classes.

3.2.3 The surface type

We now confirm that each $\mathcal{X}_n$ is a Sakai surface, and determine their type. In order to do this, we must identify the unique anticanonical divisor, which for a surface obtained as in this case through eight blow-ups of $\mathbb{P}^1 \times \mathbb{P}^1$ can be done by identifying a unique biquadratic curve passing through the eight points $q_1, \ldots, q_8$.
Consider such a curve Γ on $\mathbb{P}^1 \times \mathbb{P}^1$ defined in the (X, Y)-chart by

$$(a_{22}X^2+a_{12}X+a_{02})Y^2+(a_{21}X^2+a_{11}X+a_{01})Y+(a_{20}X^2+a_{10}X+a_{00}) = 0. \tag{3.36}$$

From the condition $q_5 \in \Gamma$ we see that $a_{00} = 0$. To impose the condition that the first infinitely near point q_6 lies on the proper transform of Γ under the blow-up of q_5, we rewrite this equation in the (U_5, V_5)-chart (we should also include the (u_5, v_5)-chart, but unless it gives any new information, we omit those computations) via the substitution $X = V_5$, $Y = U_5V_5$. The resulting equation factorises,

$$V_5\Big((a_{22}V_5^2+a_{12}V_5+a_{02})V_5U_5^2+(a_{21}V_5^2+a_{11}V_5+a_{01})U_5+a_{20}V_5+a_{10}\Big) = 0. \tag{3.37}$$

This factorisation corresponds, like we saw in the previous section, to the decomposition of the total transform of Γ under the blow-up of q_5 $\operatorname{Bl}_{q_5} : \mathcal{X}_{q_5} \to \mathbb{P}^1 \times \mathbb{P}^1$ into the irreducible components

$$\operatorname{Bl}_{q_5}^{-1}(\Gamma) = F_5 + (\Gamma - F_5), \tag{3.38}$$

where F_5 is the exceptional divisor arising from the blow-up, and $\Gamma - F_5$ is the proper transform. We note that on the right-hand side of equation (3.38), Γ refers to the total transform of Γ, which is a divisor on $\mathcal{X}_{q_5}$, and we will continue to use such notation in cases when the meaning is clear from the context. We then see that the condition $q_6 \in \Gamma - F_5$ implies $a_{10} = 0$. Continuing in this way for the rest of the points over q_5, as well as imposing the conditions $q_i \in \Gamma$ for $i = 1, \dots, 4$, we get the following equation for Γ in the (X, Y)-chart, which is sufficient to define it on the whole of $\mathbb{P}^1 \times \mathbb{P}^!$:

$$\begin{gathered} \Gamma \quad : \quad Y s(X,Y) = 0, \\ s(X,Y) = X^2 - \alpha\beta X^2 Y + (n + \alpha + \beta) XY - Y. \end{gathered} \tag{3.39}$$

The proper transform Γ' of Γ has the following decomposition into irreducible components:

$$\Gamma' = D_0 + D_1 + 2D_2 + D_3 + D_4, \tag{3.40}$$

where

$$\begin{gathered} D_0 = F_5 - F_6, \quad D_1 = 2H_x - H_y - F_{123456}, \quad D_2 = F_6 - F_7, \\ D_3 = F_7 - F_8, \quad D_4 = H_y - F_{56}. \end{gathered} \tag{3.41}$$

The proper transform Γ' is in fact the pole divisor of a rational 2-form ω on $\mathcal{X} = \mathcal{X}_n$, and is therefore a representative of the anticanonical class $-\mathcal{K}_{\mathcal{X}}$. This 2-form ω in the affine (X, Y)-chart is given uniquely up to some nonzero constant k by

$$\omega = k \frac{dX \wedge dY}{s(X,Y)\, Y} = k \frac{dX \wedge ds}{s(s - X^2)}, \tag{3.42}$$

since

$$ds = (2X - 2\alpha\beta XY + (n + \alpha + \beta) Y)\, dX - (\alpha\beta X^2 - (n + \alpha + \beta) X + 1)\, dY, \tag{3.43}$$

and

$$\frac{X^2 - s(X,Y)}{Y} = \alpha\beta X^2 - (n + \alpha + \beta) X + 1. \tag{3.44}$$

The fact that the pole divisor of ω gives a unique representative of the anticanonical class follows from the fact that Γ is the unique biquadratic curve passing through $q_1, \dots, q_8$, and it can be seen to be of canonical type by calculating the intersection product of the class of each component with $\mathcal{K}_{\mathcal{X}}$. A schematic representation of the point configuration, the blow-ups, and the components of the anticanonical divisor are shown on Figure 3.1.

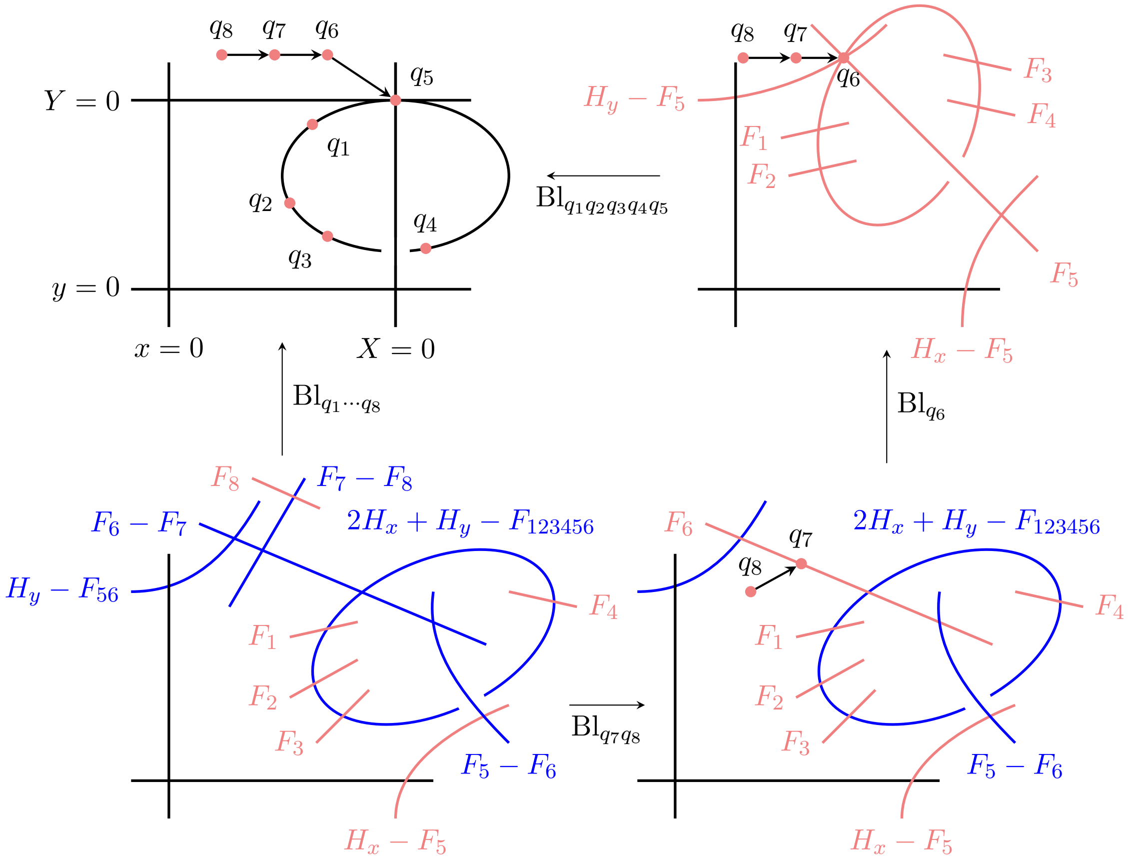

Figure 3.1: The Sakai surface for the hypergeometric weight recurrence

Thus, we see that the anticanonical divisor class $-\mathcal{K}_{\mathcal{X}}$ can be written as

$$-\mathcal{K}_{\mathcal{X}} = \delta_0 + \delta_1 + 2\delta_2 + \delta_3 + \delta_4, \tag{3.45}$$

where $\delta_i = [D_i]$ are classes of the irreducible components, whose intersection configuration is given by the $D_4^{(1)}$ affine Dynkin diagram shown in Figure 3.2.

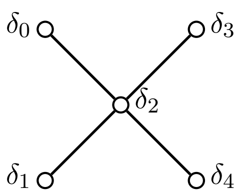

$$\delta_0 = \mathcal{F}_5 - \mathcal{F}_6, \qquad \delta_3 = \mathcal{F}_7 - \mathcal{F}_8,$$
$$\delta_1 = 2\mathcal{H}_x + \mathcal{H}_y - \mathcal{F}_{123456}, \qquad \delta_4 = \mathcal{H}_y - \mathcal{F}_{56}.$$
$$\delta_2 = \mathcal{F}_6 - \mathcal{F}_7,$$

Figure 3.2: The surface root basis for the hypergeometric weight recurrence

Therefore we have $\mathcal{X}_n$ being a Sakai surface of type $D_4^{(1)}$, and to see whether our recurrence is equivalent to d-$\mathrm{P_V}$ we need to determine whether the Cremona isometry (3.35) is a translation, and if so compare it with that corresponding to d-$\mathrm{P_V}$.

3.2.4 Initial identification on the level of Picard lattices

To compare the Cremona isometries, we need to find a choice of symmetry roots in $\mathrm{Pic}(\mathcal{X})$ that matches the one in terms of which d-$\mathrm{P_V}$ is described. Thus, we begin by finding some identification of $\mathrm{Pic}(\mathcal{X})$ with that from the standard model that will identify the surface roots between our recurrence and the standard example, and then use this to choose symmetry roots and compare the translations. Recall that the Picard lattice for the standard model in Section 2.3 is generated by $\mathcal{H}_f, \mathcal{H}_g, \mathcal{E}_1, \ldots, \mathcal{E}_8$; we now denote it by $\mathrm{Pic}(\mathcal{X}^{\mathrm{KNY}})$ with reference to the survey by Kajiwara, Noumi and Yamada [KNY17] in which this standard model is given.

Lemma 3.2.3. *The following identification of* $\mathrm{Pic}(\mathcal{X})$ *with* $\mathrm{Pic}(\mathcal{X}^{\mathrm{KNY}})$ *identifies our surface root basis with that from the standard model of* $D_4^{(1)}$*-surfaces:*

$$
\begin{aligned}
\mathcal{H}_x &= \mathcal{H}_g, & \mathcal{H}_f &= 2\mathcal{H}_x + \mathcal{H}_y - \mathcal{F}_3 - \mathcal{F}_4 - \mathcal{F}_5 - \mathcal{F}_6,\\
\mathcal{H}_y &= \mathcal{H}_f + 2\mathcal{H}_g - \mathcal{E}_3 - \mathcal{E}_4 - \mathcal{E}_5 - \mathcal{E}_6, & \mathcal{H}_g &= \mathcal{H}_x,\\
\mathcal{F}_1 &= \mathcal{E}_1, & \mathcal{E}_1 &= \mathcal{F}_1,\\
\mathcal{F}_2 &= \mathcal{E}_2, & \mathcal{E}_2 &= \mathcal{F}_2,\\
\mathcal{F}_3 &= \mathcal{H}_g - \mathcal{E}_6, & \mathcal{E}_3 &= \mathcal{H}_x - \mathcal{F}_6,\\
\mathcal{F}_4 &= \mathcal{H}_g - \mathcal{E}_5, & \mathcal{E}_4 &= \mathcal{H}_x - \mathcal{F}_5,\\
\mathcal{F}_5 &= \mathcal{H}_g - \mathcal{E}_4, & \mathcal{E}_5 &= \mathcal{H}_x - \mathcal{F}_4,\\
\mathcal{F}_6 &= \mathcal{H}_g - \mathcal{E}_3, & \mathcal{E}_6 &= \mathcal{H}_x - \mathcal{F}_3,\\
\mathcal{F}_7 &= \mathcal{E}_7, & \mathcal{E}_7 &= \mathcal{F}_7,\\
\mathcal{F}_8 &= \mathcal{E}_8, & \mathcal{E}_8 &= \mathcal{F}_8.
\end{aligned}
$$

Proof. Consider the surface root basis in Figure 3.2 and compare it with the standard one in Figure 2.5. Since the $D_4^{(1)}$ affine Dynkin diagram has the distinguished node δ_2, we must have

$$\delta_2 = \mathcal{F}_6 - \mathcal{F}_7 = \mathcal{H}_g - \mathcal{E}_3 - \mathcal{E}_7.$$

Thus, we can put $\mathcal{F}_6 = \mathcal{H}_g - \mathcal{E}_3$ and $\mathcal{F}_7 = \mathcal{E}_7$, and then, matching $\mathcal{F}_7 - \mathcal{F}_8 = \mathcal{E}_7 - \mathcal{E}_8$, we see that we can put $\mathcal{F}_8 = \mathcal{E}_8$. Next, matching $\mathcal{F}_5 - \mathcal{F}_6 = \mathcal{E}_3 - \mathcal{E}_4$, we see that $\mathcal{F}_5 = \mathcal{H}_g - \mathcal{E}_4$. Matching $\mathcal{H}_y - \mathcal{F}_5 - \mathcal{F}_6 = \mathcal{H}_f - \mathcal{E}_5 - \mathcal{E}_6$ we get $\mathcal{H}_y$. The final node matching gives us the equation $2\mathcal{H}_x - \mathcal{F}_{1234} = \mathcal{E}_5 + \mathcal{E}_6 - \mathcal{E}_1 - \mathcal{E}_2$. Thus, we can put (again, at this point we do not worry about making the right choice) $\mathcal{F}_1 = \mathcal{E}_1$, $\mathcal{F}_2 = \mathcal{E}_2$, $\mathcal{E}_5 = \mathcal{H}_x - \mathcal{F}_4$ and $\mathcal{E}_6 = \mathcal{H}_x - \mathcal{F}_3$, so that $\mathcal{H}_x = \mathcal{E}_6 + \mathcal{F}_3 = \mathcal{H}_g$. □

3.2.5 The symmetry roots and the translations

We are now in a position to compare the dynamics. We choose a symmetry root basis in $\mathrm{Pic}(\mathcal{X})$ by mapping the standard choice in Figure 2.7 under the identification in Lemma 3.2.3. This leads to the choice given in Figure 3.3.

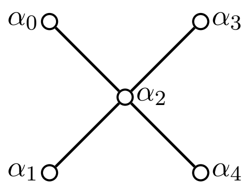

$$\alpha_0 = \mathcal{H}_y - \mathcal{F}_{34}, \qquad \alpha_3 = 2\mathcal{H}_x + \mathcal{H}_y - \mathcal{F}_{345678},$$
$$\alpha_1 = \mathcal{F}_1 - \mathcal{F}_2, \qquad \alpha_4 = \mathcal{F}_3 - \mathcal{F}_4.$$
$$\alpha_2 = \mathcal{F}_4 - \mathcal{F}_1,$$

Figure 3.3: The symmetry root basis for the hypergeometric weight recurrence (preliminary choice)

From the formulae given in Lemma 3.2.2 we immediately see that the Cremona isometry induced by $\psi^{(n)}$ through pushforwards, which we denote by ψ_*, acts by translation on the symmetry root lattice:

$$\psi_* : \boldsymbol{\alpha} = \langle \alpha_0, \alpha_1, \alpha_2, \alpha_3, \alpha_4 \rangle \mapsto \psi_*(\boldsymbol{\alpha}) = \boldsymbol{\alpha} + \langle 1, 0, 0, -1, 0 \rangle \delta. \tag{3.46}$$

Recall that in (2.69) we considered the d-$\mathrm{P_V}$ mapping φ and the Cremona isometry induced by its pullback, here it will be convenient to consider the one induced by its pushforward, which here we denote by φ_*:

$$\varphi_* : \boldsymbol{\alpha} \mapsto \boldsymbol{\alpha} + \langle 1, 0, -1, 1, 0 \rangle \delta, \tag{3.47}$$

We see immediately that ψ_* and φ^* are different, but decomposing both in terms of generators of the extended affine Weyl symmetry group (as in Subsection 2.3.3), we obtain

$$\psi_* = \sigma_3 \sigma_2 r_3 r_2 r_4 r_1 r_2 r_3, \qquad \varphi_* = \sigma_3 \sigma_2 r_3 r_0 r_2 r_4 r_1 r_2, \tag{3.48}$$

and we immediately see that $\psi_* = r_3 \circ \varphi_* \circ r_3^{-1}$ (recall that $r_3\sigma_3\sigma_2 = \sigma_3\sigma_2 r_0$ and that r_3 is an involution, $r_3^{-1} = r_3$). Thus if we adjust the identification in Lemma 3.2.3 by acting by r_3, the Cremona isometry for the hypergeometric weight recurrence will be identified with that corresponding to the standard d-$\mathrm{P_V}$ equation.

3.2.6 Final identification on the level of Picard lattices

We will now adjust our identification of $\mathrm{Pic}(\mathcal{X})$ and $\mathrm{Pic}(\mathcal{X}^{\mathrm{KNY}})$ such that the translations corresponding to our recurrence and d-$\mathrm{P_V}$ are matched. We will realise this as an isomorphism between the families of surfaces themselves, under which the Cremona actions giving the systems coincide, so will provide an explicit change of variables relating the equations.

Lemma 3.2.4. *The identification of* $\mathrm{Pic}(\mathcal{X})$ *and* $\mathrm{Pic}(\mathcal{X}^{\mathrm{KNY}})$ *given by*

$$
\begin{aligned}
&\mathcal{H}_x = \mathcal{H}_f + \mathcal{H}_g - \mathcal{E}_7 - \mathcal{E}_8,\\
&\mathcal{H}_y = 3\mathcal{H}_f + 2\mathcal{H}_g - \mathcal{E}_3 - \mathcal{E}_4 - \mathcal{E}_5 - \mathcal{E}_6 - 2\mathcal{E}_7 - 2\mathcal{E}_8,\\
&\mathcal{F}_1 = \mathcal{E}_1, \qquad \mathcal{F}_2 = \mathcal{E}_2,\\
&\mathcal{F}_3 = \mathcal{H}_f + \mathcal{H}_g - \mathcal{E}_6 - \mathcal{E}_7 - \mathcal{E}_8,\\
&\mathcal{F}_4 = \mathcal{H}_f + \mathcal{H}_g - \mathcal{E}_5 - \mathcal{E}_7 - \mathcal{E}_8,\\
&\mathcal{F}_5 = \mathcal{H}_f + \mathcal{H}_g - \mathcal{E}_4 - \mathcal{E}_7 - \mathcal{E}_8,\\
&\mathcal{F}_6 = \mathcal{H}_f + \mathcal{H}_g - \mathcal{E}_3 - \mathcal{E}_7 - \mathcal{E}_8,\\
&\mathcal{F}_7 = \mathcal{H}_f - \mathcal{E}_8, \qquad \mathcal{F}_8 = \mathcal{H}_f - \mathcal{E}_7,
\end{aligned}
$$

or equivalently

$$
\begin{aligned}
&\mathcal{H}_f = 2\mathcal{H}_x + \mathcal{H}_y - \mathcal{F}_3 - \mathcal{F}_4 - \mathcal{F}_5 - \mathcal{F}_6,\\
&\mathcal{H}_g = 3\mathcal{H}_x + \mathcal{H}_y - \mathcal{F}_3 - \mathcal{F}_4 - \mathcal{F}_5 - \mathcal{F}_6 - \mathcal{F}_7 - \mathcal{F}_8,\\
&\mathcal{E}_1 = \mathcal{F}_1, \qquad \mathcal{E}_2 = \mathcal{F}_2,\\
&\mathcal{E}_3 = \mathcal{H}_x - \mathcal{F}_6, \qquad \mathcal{E}_4 = \mathcal{H}_x - \mathcal{F}_5,\\
&\mathcal{E}_5 = \mathcal{H}_x - \mathcal{F}_4, \qquad \mathcal{E}_6 = \mathcal{H}_x - \mathcal{F}_3,\\
&\mathcal{E}_7 = 2\mathcal{H}_x + \mathcal{H}_y - \mathcal{F}_3 - \mathcal{F}_4 - \mathcal{F}_5 - \mathcal{F}_6 - \mathcal{F}_8,\\
&\mathcal{E}_8 = 2\mathcal{H}_x + \mathcal{H}_y - \mathcal{F}_3 - \mathcal{F}_4 - \mathcal{F}_5 - \mathcal{F}_6 - \mathcal{F}_7,
\end{aligned}
$$

leads to the identification of the symmetry root bases shown in Figure 3.4. With this identi-

fication we have a map from the group of of Cremona isometries for the family $\mathcal{X}$ we have constructed from the hypergeometric weight recurrence to that of the standard model, via reflections r_i being identified according to that of the associated roots α_i. Further, this map identifies the Cremona isometries ψ_* and φ_*

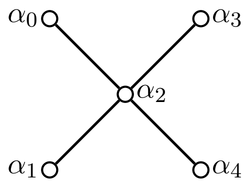

$$\alpha_0 = \mathcal{H}_y - \mathcal{F}_{34}, \qquad \alpha_3 = -2\mathcal{H}_x - \mathcal{H}_y + \mathcal{F}_{345678},$$
$$\alpha_1 = \mathcal{F}_1 - \mathcal{F}_2, \qquad \alpha_4 = \mathcal{F}_3 - \mathcal{F}_4.$$
$$\alpha_2 = 2\mathcal{H}_x + \mathcal{H}_y - \mathcal{F}_{135678},$$

Figure 3.4: The symmetry root basis for the hypergeometric weight recurrence (final choice)

In order to find an isomorphism realising this identification, we will need to find a correspondence of parameters between the application family of surfaces and the standard one, which will be done using the period map.

3.2.7 The period map and the identification of parameters

The computation is similar to that performed for the standard model in Subsection 2.3.2, where the residues of the symplectic form along components of the anticanonical divisor are used to evaluate integrals defining the root variables. Thus, we only state the results.

Lemma 3.2.5.

(i) The residue of the symplectic form $\omega = k\frac{dX \wedge dY}{s(X,Y)\,Y} = k\frac{dX\wedge ds}{s(s-X^2)}$ defined in (3.42) *along the irreducible components D_i of the anticanonical divisor is given by*

$$\begin{aligned} &\operatorname{res}_{D_0}\omega = -k\frac{dU_5}{U_5^2}, && \operatorname{res}_{D_1}\omega = k\frac{dX}{X^2}, \\ &\operatorname{res}_{D_2}\omega = -k\frac{(n+\alpha+\beta)du_6}{(u_6-1)^2}, && \operatorname{res}_{D_3}\omega = -k\frac{(c-1)^2 du_7}{c}, \\ &\operatorname{res}_{D_4}\omega = -k\frac{dX}{X^2}. \end{aligned} \tag{3.49}$$

(ii) The root variables for the surface $\mathcal{X}_n$ for our final choice of symmetry roots are given by

$$\begin{aligned} &a_0 = k(\gamma - n - \alpha), && a_1 = k(\alpha - 1), \quad a_2 = k(1 + n + \beta - \gamma), \\ &a_3 = -k(n+\beta), && a_4 = k(\gamma - \beta). \end{aligned} \tag{3.50}$$

We require the same normalisation $a_0 + a_1 + 2a_2 + a_3 + a_4 = 1$ as for the standard model, so we set $k = 1$ and obtain the following relations between our parameters for the surface $\mathcal{X}_n$ and the root variables for a $D_4^{(1)}$-surface in the standard form:

$$\alpha = a_1 + 1, \quad \beta = a_0 + a_1 + a_2, \quad \gamma = 1 - a_2 - a_3, \quad n = a_2 + a_4 - 1. \tag{3.51}$$

Note that if we consider the evolution of the root variables under the d-$\mathrm{P_V}$ dynamic as given in (2.69), this corresponds to the evolution of parameters from $\mathcal{X}_n$ to $\mathcal{X}_{n+1}$ under our dynamics: α, β, γ staying constant while $n \mapsto n+1$, which is ensured by our final identification matching the translations. Also observe that we can not yet see the relationship between parameters t and c in this identification. This is because they each play the role of the 'extra parameter' for $D_4^{(1)}$-surfaces, and we will see when we construct the isomorphism that they must be related by $ct = 1$.

3.2.8 The change of variables

We are now ready to prove Theorem 3.2.1. The idea is to find an isomorphism $\iota : \mathcal{X}_n \to \mathcal{X}_{\mathbf{b}}$ from our surface to the one in Section 2.3 which realises our final identification on the level of Picard lattices in Lemma 3.2.4. Here the parameters in the surfaces are matched according to the results of the previous section, so the evolution of the parameters $\mathbf{b} \mapsto \bar{\mathbf{b}}$ for d-$\mathrm{P_V}$ corresponds to shifting $n \mapsto n+1$ in the point configuration giving $\mathcal{X}_n$, and ι also provides an isomorphism from $\mathcal{X}_{n+1}$ to $\mathcal{X}_{\bar{\mathbf{b}}}$. If ι induces the identification of $\mathrm{Pic}(\mathcal{X})$ and $\mathrm{Pic}(\mathcal{X}^{\mathrm{KNY}})$ through its pushforward, then we have the following commutative diagram:

$$\begin{array}{ccc} \mathrm{Pic}(\mathcal{X}) & \xrightarrow{\psi_*} & \mathrm{Pic}(\mathcal{X}) \\ \downarrow{\scriptstyle \iota_*} & & \downarrow{\scriptstyle \iota_*} \\ \mathrm{Pic}(\mathcal{X}^{\mathrm{KNY}}) & \xrightarrow{\varphi_*} & \mathrm{Pic}(\mathcal{X}^{\mathrm{KNY}}) \end{array} \tag{3.52}$$

This descends to the Cremona action, so we have the following commutative diagram of isomorphisms between $D_4^{(1)}$-surfaces:

$$\begin{array}{ccc} \mathcal{X}_n & \xrightarrow{\psi^{(n)}} & \mathcal{X}_{n+1} \\ \downarrow{\scriptstyle \iota} & & \downarrow{\scriptstyle \iota} \\ \mathcal{X}_{\mathbf{b}} & \xrightarrow{\varphi} & \mathcal{X}_{\bar{\mathbf{b}}} \end{array} \tag{3.53}$$

Therefore the iteration mappings of the two discrete Painlevé equations are conjugate under ι, so this isomorphism provides a change of variables under which the equations are equivalent with our parameter identification.

Proof. (**Theorem 3.2.1**)

We will form an ansatz for the map in terms of coordinates for $\mathcal{X}_n$ and $\mathcal{X}_{\mathbf{b}}$, then successively refine it by imposing conditions such that the pushforward induces the identification until we have determined the birational map, then verify it gives the required isomorphism. First, we require

$$\begin{aligned} \mathcal{H}_f &= 2\mathcal{H}_x + \mathcal{H}_y - \mathcal{F}_3 - \mathcal{F}_4 - \mathcal{F}_5 - \mathcal{F}_6, \\ \mathcal{H}_g &= 3\mathcal{H}_x + \mathcal{H}_y - \mathcal{F}_3 - \mathcal{F}_4 - \mathcal{F}_5 - \mathcal{F}_6 - \mathcal{F}_7 - \mathcal{F}_8, \end{aligned} \tag{3.54}$$

so we form an ansatz in coordinates (here for convenience we use $(X,Y),(f,g)$) of the form

$$\iota : (X,Y) \mapsto (f(X,Y), g(X,Y)),$$

$$f(X,Y) = \frac{a_{00} + a_{10}X + a_{20}X^2 + a_{01}Y + a_{11}XY + a_{21}X^2Y}{b_{00} + b_{10}X + b_{20}X^2 + b_{01}Y + b_{11}XY + b_{21}X^2Y},$$

$$g(X,Y) = \frac{c_{00} + c_{10}X + c_{20}X^2 + c_{30}X^2 + c_{01}Y + c_{11}XY + c_{21}X^2Y + c_{31}X^3Y}{d_{00} + d_{10}X + d_{20}X^2 + d_{30}X^2 + d_{01}Y + d_{11}XY + d_{21}X^2Y + d_{31}X^3Y},$$

so the class of a line of constant f corresponds to a curve of bi-degree $(2,1)$ in (x,y), and one of constant g corresponds to a curve of bi-degree $(3,1)$.

We require f taking any constant value to give a curve in (X,Y) coordinates passing through $q_5 : (X,Y) = (0,0)$, so $a_{00} = b_{00} = 0$. This can also be thought of as f providing a coordinate for a pencil of bi-degree $(2,1)$-curves which all pass through q_5. Similarly, we may pass to coordinates (U_5, V_5) and impose the condition that the proper transform of any curve in the pencil passes through q_6, which leads to $a_{10} = b_{10} = 0$. Proceeding similarly for q_3, q_4 we determine more coefficients, and we arrive at the following form of the coordinate f on the pencil when written in the (x,y)-chart:

$$f(x,y) = \frac{A(x-\beta)(x-\gamma) + B\Big(x^2(n+\alpha-\gamma) + y(\beta+\gamma) - \beta(\alpha\beta - \beta\gamma - n\gamma)\Big)}{C(x-\beta)(x-\gamma) + D\Big(x^2(n+\alpha-\gamma) + y(\beta+\gamma) - \beta(\alpha\beta - \beta\gamma - n\gamma)\Big)},$$

where the coefficients A, B, C, D are still to be determined. To do that, we use the information about the correspondence between exceptional divisors in Lemma 3.2.4. For example, the condition $\mathcal{E}_2 = \mathcal{F}_2$ means that q_2 should be mapped to p_2, and in particular inserting the coordinates of $q_2 : (x, y) = (\alpha, -n\alpha)$ into our refined ansatz for f (or rewritten for F in this case) should give the F-coordinate for p_2, namely $F = 0$. Indeed, we compute

$$F(\alpha, -n\alpha) = \frac{C + D(n + \alpha + \beta)}{A + B(n + \alpha + \beta)} = 0, \qquad \text{and so} \quad C = -D(n + \alpha + \beta).$$

The condition $\mathcal{E}_6 = \mathcal{H}_x - \mathcal{F}_3$ means that $f(\beta, y) = B/D = 0$, and so $B = 0$. As a result, after some simplifications, we get

$$f(x, y) = \frac{\tilde{A}(x - \beta)(x - \gamma)}{(x - \alpha)(x - \beta) - nx - y}, \tag{3.55}$$

where $\tilde{A}$ is some non-zero constant. To find $\tilde{A}$, we use the condition $\mathcal{E}_3 - \mathcal{E}_4 = \mathcal{F}_5 - \mathcal{F}_6$, which means that, after doing a sequence of substitutions to express f in the (u_5, v_5)-chart and then restricting to $v_5 = 0$, the image of the proper transform $F_5 - F_6$ of the exceptional divisor F_5 should be sent to the point $p_3 : (f, G) = (t, 0)$. This results in $\tilde{A} = 1$. Similarly, the condition $\mathcal{E}_7 - \mathcal{E}_8 = \mathcal{F}_7 - \mathcal{F}_8$ results in the relationship between c and t, $ct = 1$, which is to be expected given that we are dealing with surfaces which are of a type with extra parameter, so even after matching root variables, rational 2-forms and period mappings an isomorphism between them will require a relation between the extra parameters, as in Sakai's theorem [Sak01, Theorem 25] explained in Subsection 2.2.3. Computing $g(x, y)$ is done exactly along the same lines but the calculation is longer since the basis curves in the $\mathcal{H}_g$ pencil are of higher degree. It does not illustrate anything beyond what was seen for the $\mathcal{H}_f$ pencil so this computation is omitted. The final step is to verify that this map between the surfaces is indeed an isomorphism, which is done using similar techniques as when we lift iteration mappings, but in this case we rewrite the mapping in charts for $\mathcal{X}_n$ as introduced in this chapter and $\mathcal{X}_{\mathrm{b}}$ as provided in Section 2.3. □

3.3 The identification procedure for differential equations

The procedure outlined above can be adapted to provide a method for determining whether a given second-order nonlinear nonautonomous differential equation is equivalent to one of the Painlevé equations. Again this involves constructing Sakai surfaces which provide a space of initial conditions for the system, but this time it is in the sense of Okamoto, as a bundle over the independent variable space foliated by solution curves. After the construction of this bundle, whose fibres are Sakai surfaces with anticanonical divisor removed, the method then mimics the discrete case, where an isomorphism between Sakai surfaces is obtained from an identification on the level of their Picard groups. However, the differential case is in a sense more straightforward since there are no translations to match, and we can use the initial identification which is only required to identify the surface roots. At this point we repeat our remark from Chapter 2 that in order to allow for all surface types associated with differential Painlevé equations we should be considering $\mathbb{P}^2$ blown up nine times. To be consistent with the rest of the chapter we will outline the procedure as follows using $\mathbb{P}^1 \times \mathbb{P}^1$, which is sufficient to describe all but $\mathrm{P_I}$, and is sufficient for discrete Painlevé equations of any type.

(Step 1) **Construct a space of initial conditions.** Begin by considering the system on a trivial bundle over the independent variable space with fibre $\mathbb{P}^1 \times \mathbb{P}^1$ by introducing charts in the usual way. Consider the differential equation as the flow of a rational vector field on this bundle, and find the points in each fibre where its components have indeterminacies. Here we run into a subtle point that is specific to the differential case, namely that we must determine whether these indeterminacies correspond to singular points which are accessible (in the sense that they can be reached by solutions with initial data where the vector field is regular). Resolve all such accessible singular points using the blow-up procedure, until we have a bundle on which the vector field has no more accessible singularities (we will address the question of when an indeterminacy of the vector field represents an accessible singularity in what follows). Identify the inaccessible divisors where the vector field diverges and remove them from each fibre so we have a foliation of the resulting bundle by solution curves transverse to the fibres.

(Step 2) **Determine the surface type.** The fibres should be Sakai surfaces with anticanonical divisor removed. Determine their type, which will be one of those associated with differential Painlevé equations involving an 'extra parameter'. Again there is the possibility that the procedure in Step 1 results in (-1)-curves that must be blown down, but we will not see this in our example.

(Step 3) **Find an identification of $\mathrm{Pic}(\mathcal{X})$ with the standard model.** This step is the same as the preliminary identification in the discrete case, and we only require that the surface roots are identified.

(Step 4) **Find the change of variables to the standard form.** Since we do not need to match translations, we proceed directly to find the isomorphism of Sakai surfaces realising the identification of Picard groups obtained in the previous step. The parameter correspondence is again computed using the period mapping and in the process of finding this isomorphism we obtain a relation between the independent variables. From this, we have an isomorphism between the bundles providing the two spaces of initial conditions. If the applied system can be shown to be Hamiltonian in the sense required by the uniqueness results of Subsection 2.4.2, then the isomorphism provides a change of variables identifying the applied system with the Painlevé equation in standard form.

We will illustrate this procedure for a system of differential equations satisfied by the same recurrence coefficients as considered earlier in the chapter, namely those of the discrete orthogonal polynomials with hypergeometric weight. The system of differential equations for $x_n(c)$ and $y_n(c)$ follows from the discrete system (3.5a-3.5b) and the Toda differential-difference system (3.7). Essentially, we rewrite the Toda system for a_n^2, b_n in terms of the quantities x_n, y_n according to the relation (3.4), then use the discrete system to replace y_{n+1} and x_{n-1} in the resulting equations with x_n, y_n and their derivatives with respect to c. This gives us a system of two first-order differential equations for $x(c) = x_n(c)$ and $y(c) = y_n(c)$ of the following form, where we write x, y without subscripts because n in this case plays the role of a parameter:

$$\begin{aligned} x'(c) &= \frac{P_1(x(c), y(c), c)}{c(c-1)S(x(c), y(c))}, \\ y'(c) &= \frac{P_2(x(c), y(c), c)}{c(c-1)S(x(c), y(c))}, \end{aligned} \tag{3.56}$$

where $S(x,y)=\alpha\beta-(n+\alpha+\beta)x+x^2-y$, and P_1, P_2 are polynomials in their arguments, which can be written explicitly, with $x=x(c)$, $y=y(c)$, as

$$\begin{aligned}
P_1(x,y,c) &= (1-c)x^4+(-\alpha-\beta+2c(\alpha+\beta+n)-\gamma-1)x^3 \\
&\quad + \left(\alpha(\beta+\gamma+1)+\beta\gamma+\beta-c\left(\beta^2+2\beta(2\alpha+n)+(\alpha+n)^2\right)+\gamma\right)x^2 \\
&\quad + \left(\alpha\beta(2c(\alpha+\beta+n)-1)-\gamma(\alpha\beta+\alpha+\beta)\right)x+\alpha\beta(\gamma-\alpha\beta c) \\
&\quad + 2cy\left[x^2-(\alpha+\beta+n)x+\alpha\beta\right]-cy^2, \\
P_2(x,y,c) &= n\left(\alpha^2+\alpha\beta-\alpha+\beta^2-\beta+\gamma+n^2-\gamma(\alpha+\beta+n)+2\alpha n+2\beta n-n\right)x^2 \\
&\quad - 2\alpha\beta n\left(\alpha+\beta-\gamma+n-1\right)x+n\alpha\beta(\alpha\beta-\gamma) \\
&\quad + y\Big[\left(\alpha+\beta-\gamma+2n-1\right)x^2+2\left(-\alpha\beta+\gamma+n^2+n(\alpha+\beta-\gamma-1)\right)x \\
&\quad - \alpha\gamma-\beta\gamma+\alpha\beta(\gamma-2n+1)\Big]+y^2\left[2x-\gamma+n-1\right].
\end{aligned}$$

Similarly to in Subsection 2.4.1, we first consider this system on the trivial bundle over $B:=\mathbb{C}\backslash\{0,1\}$ with fibre over c being $\mathbb{P}^1\times\mathbb{P}^1$, for which we use the same charts as in the previous sections with $X=1/x, Y=1/y$. Our choice of the independent variable space B here comes from the fact that both $x'(c), y'(c)$ have singularities at $c=0,1$, so if this system is to be identified with one of the Painlevé equations these will play the role of fixed singularities and are removed from the base space.

3.3.1 Space of initial conditions and inaccessible singularities

The construction of the space of initial conditions for the differential system (3.56) is done mostly according to the same methods as were illustrated in Subsection 2.4.1 for $\mathrm{P_{VI}}$. However with this system we run into a subtle point that sets this step of the procedure apart from the discrete version, namely the necessity to distinguish between indeterminacies of the vector field that require blow-ups and those that do not.

In the (x,y)-chart we find the following points at which one or both of x', y' have indeterminacies:

$$\begin{aligned}
q_1 &:(x,y)=(1,(1-\alpha)(1-\beta)-n), \\
q_2 &:(x,y)=(\alpha,-n\alpha), \\
q_3 &:(x,y)=(\beta,-n\beta), \\
q_4 &:(x,y)=(\gamma,(\gamma-\alpha)(\gamma-\beta)-n\gamma), \\
\hat{q}_1 &:(x,y)=\left(\frac{1}{2}(\alpha+\beta+n),\alpha\beta-\frac{1}{4}(\alpha+\beta+n)^2\right).
\end{aligned} \tag{3.57}$$

We note that $q_1, \ldots, q_4$ are the same as those identified for the discrete case, but we have the extra point $\hat{q}_1$ giving an indeterminacy of y'. Inspecting the vector field at each of these points we find that at $q_1, \ldots, q_4$, both components x' and y' are indeterminate, whereas at $\hat{q}_1$, we have an indeterminacy of y' while x' diverges, with its denominator vanishing but numerator non-zero. This corresponds to the fact that we have infinite families of solution curves passing through each of $q_1, \ldots q_4$, but none through $\hat{q}_1$.

This can be seen by looking for solutions given by Taylor series expansions about some $c_0 \in B$ passing through a point on the curve γ in the $\mathbb{P}^1 \times \mathbb{P}^1$-fibre over c_0 defined in the (x, y)-chart by

$$\gamma : \quad S(x, y) = x^2 - (\alpha + \beta + n)x - y + \alpha\beta = 0. \tag{3.58}$$

We note that this curve is the same as the one defined in the (X, Y)-chart by $s(X, Y) = 0$ in Subsection 3.2.3 and whose proper transform formed one of the components of the anticanonical divisor. From the system (3.56) we see that the denominators of both x' and y' in the (x, y)-chart vanish on γ, and so the points $q_1, \ldots, q_4, \hat{q}_1$ lie on this curve. Similarly to in Subsection 2.4.1, consider a solution given as an expansion about c_0 by

$$\begin{aligned} x(c) &= x_0 + x_1(c - c_0) + x_2(c - c_0)^2 + \ldots, \\ y(c) &= y_0 + y_1(c - c_0) + y_2(c - c_0)^2 + \ldots, \end{aligned} \tag{3.59}$$

and assume that this passes through γ in the fibre over c_0, so

$$S(x_0, y_0) = x_0^2 - (\alpha + \beta + n)x_0 - y_0 + \alpha\beta = 0. \tag{3.60}$$

Assuming that this system is equivalent by some birational transformation to a Painlevé equation (whose only movable singularities are poles) then these are the only solutions that could take a value on this curve at c_0. Substituting (3.59) subject to (3.60) into the differential equations, we obtain the asymptotic identities from the equations for x', y' respectively, which must hold as $c \to c_0$:

$$\begin{aligned} 0 &= (x_0 - 1)(x_0 - \alpha)(x_0 - \beta)(x_0 - \gamma) + \mathcal{O}(c - c_0), \\ 0 &= (x_0 - 1)(x_0 - \alpha)(x_0 - \beta)(x_0 - \gamma)(2x_0 - \alpha - \beta - n) + \mathcal{O}(c - c_0). \end{aligned} \tag{3.61}$$

From this, we see that x_0 must take one of the values $1, \alpha, \beta, \gamma$, so the solution must pass through one of $q_1, \dots, q_4$. In particular we see that while the value of x_0 corresponding to the extra point $\hat{q}_1$ would be compatible with the second line of (3.61), the other equation would fail to balance, which corresponds to $\hat{q}_1$ being a root of the denominator but not numerator of x'. Thus we see that even though $\hat{q}_1$ was identified as an indeterminacy of one of the rational functions giving the vector field, there are no solution curves passing through it. We say $\hat{q}_1$ is an *inaccessible* singular point, and we do not need to blow it up to achieve a foliation by solution curves.

Blowing up each of $q_1, \dots, q_4$ and calculating the lifted vector field as in Subsection 2.4.1 we see that it is regular on each of $F_1, \dots, F_4$, away from their intersections with the proper transform of the curve γ. Carrying out the standard procedure in the rest of the charts we find q_5 to be a singular point, with an infinite family of solution curves passing through it. Lifting under the blow-up of q_5 we see q_6 as the only indeterminacy on F_5, but then when we lift under the blow-up of q_6 we see the following points where one or both components of the vector field are indeterminate:

$$q_7 : (u_6, v_6) = \left(\frac{c}{c-1}, 0 \right), \qquad , \hat{q}_2 : (u_6, v_6) = (1, 0). \tag{3.62}$$

Again the vector field at $\hat{q}_2$ has one component indeterminate but the other divergent. We can confirm through calculating series representations of solutions through q_5 in the same way as above that this extra point $\hat{q}_2$ is another inaccessible singularity, so we do not blow it up. After lifting under the blow-up of q_7, we find the only singularity on F_7 to be q_8, after the blow-up of which we confirm by calculation that the vector field is regular on F_8 away from the proper transform of F_7. Thus through this process we have arrived at the same Sakai surface as in the discrete case, which form the fibres of a bundle as c varies while n is constant so we denote them $\mathcal{X}_c$. In the process of the calculations above we have seen that the part of each fibre where the vector field diverges and so no solution curves pass through is precisely the support $D_{\text{red}} = \cup_i D_i$ of the anticanonical divisor, so we remove this from each fibre $\mathcal{X}_c$ to arrive at a space of initial conditions. We remark here that the inaccessible singularities $\hat{q}_1, \hat{q}_2$ lie on D_{red} and are removed as part of the inaccessible divisors.

3.3.2 Change of variables from initial identification

We now find an isomorphism between the Sakai surfaces which will provide a change of variables to the standard form of P_{VI}. In this case we can use our initial geometry identification, because if the system is indeed equivalent to the Okamoto Hamiltonian form of P_{VI}, then different choices of identification with the correct matching of surface roots will only differ by a Cremona isometry, and the isomorphisms will be conjugate under its Cremona action. This means that if we map the original system to the standard model of $D_4^{(1)}$-surfaces using two different identifications, then the resulting differential equations will be equivalent under some Bäcklund transformation.

Recall our initial identification of Picard groups between the surface $\mathcal{X}_n$ from the given system and $\mathcal{X}_{\mathbf{b}}$ from the standard model of $D_4^{(1)}$-surfaces in Lemma 3.2.3. This gives the choice of symmetry roots in Figure 3.3, and proceeding along the same lines as in Lemma 3.2.5, we compute the root variables for this choice of symmetry roots to be as follows:

$$\begin{aligned} &a_0 = -\alpha + \gamma - n, \qquad a_1 = \alpha - 1, \qquad a_2 = 1 - \gamma, \\ &a_3 = \beta + n, \qquad\qquad\ \ a_4 = \gamma - \beta, \end{aligned} \tag{3.63}$$

We obtain the isomorphism realising the initial identification explicitly by the same techniques as in Subsection 3.2.8, arriving at the following result, which can be checked by direct computation:

Theorem 3.3.1. *The system of differential equations* (3.56) *is equivalent to the Okamoto Hamiltonian form* (2.82) *of P_{VI} for $(f, g) = (f(t), g(t))$. This equivalence is achieved via the following change of variables:*

$$\begin{aligned} f &= \frac{t(x-\beta)(x-\gamma)}{\alpha\beta - (n+\alpha+\beta)x + x^2 - y}, \\ g &= \gamma - x, \end{aligned} \tag{3.64}$$

where the independent variables are related by $ct = 1$, and the root variable parameters a_i from the standard form (2.82) *are related to α, β, γ, n by* (3.63).

3.3.3 Hamiltonian structure and justification of equivalence

While the change of variables in Theorem 3.3.1 can be checked by direct calculation, we make some remarks about why the isomorphism of Sakai surfaces should provide an identification of the two differential systems. In the discrete case, such an isomorphism is guaranteed to identify the discrete systems because by design it provides a conjugation of the Cremona actions giving their iterations as in the definition of discrete Painlevé equations. However in the differential case, it is natural to ask why the systems should be equivalent under an isomorphism that identifies their spaces of initial conditions, and in particular whether there could be two inequivalent systems associated with the same Okamoto's space. A partial answer to this question is provided by the uniqueness results explained in Subsection 2.4.2, because if we can demonstrate that the given system is Hamiltonian with respect to the symplectic form ω associated with the anticanonical divisor, and the Hamiltonians have the appropriate holomorphicity properties, then the given system mapped to the standard model under the isomorphism of bundles must coincide with the Okamoto Hamiltonian system.

Denote the bundle obtained as a space of initial conditions for the system (3.56) by

$$\begin{aligned} E &\to B, \\ \mathcal{X}_c \backslash D_{\mathrm{red}} &\mapsto c, \end{aligned} \tag{3.65}$$

and the one for the standard model in terms of the surfaces $\mathcal{X}_{\mathbf{b}}$ (where $\mathbf{b}$ includes the extra parameter t) by

$$\begin{aligned} E_{\mathrm{VI}} &\to B_{\mathrm{VI}}, \\ \mathcal{X}_{\mathbf{b}} \backslash D_{\mathrm{red}}^{\mathrm{KNY}} &\mapsto t, \end{aligned} \tag{3.66}$$

where we have used $D_{\mathrm{red}}^{\mathrm{KNY}}$ to distinguish support of the anticanonical divisor of the surface $\mathcal{X}_{\mathbf{b}}$ from that of $\mathcal{X}_c$. The isomorphism of Sakai surfaces $\iota : \mathcal{X}_c \to \mathcal{X}_{\mathbf{b}}$ defined by (3.64) with parameters identified according to (3.63) together with $ct = 1$ provides an isomorphism of bundles, as it maps D_{red} to $D_{\mathrm{red}}^{\mathrm{KNY}}$ and the correspondence $c \mapsto t = 1/c$ maps B to B_{VI} bijectively. The system (2.82) is Hamiltonian with respect to the symplectic form

$$\eta = \frac{df \wedge dg}{f} \tag{3.67}$$

on each fibre $\mathcal{X}_{\mathbf{b}}$, obtained by the pull back of the standard one $dq \wedge dp$ for the Okamoto Hamiltonian form of $\mathrm{P_{VI}}$ via $(q, p) = (f, g/f)$. The Hamiltonian is

$$\begin{aligned} H_{\mathrm{VI}} = &\frac{a_2(a_1+a_2)(f-t)}{t(t-1)} \\ &+ \frac{f(f-1)(f-t)}{t(t-1)} \left\{ \frac{g^2}{f} - \left(\frac{a_4}{f} + \frac{a_3}{f-1} + \frac{a_0-1}{f-t} \right) \right\} \end{aligned} \tag{3.68}$$

and the system (2.82) can be rewritten in the form

$$\frac{f'}{f} = \frac{\partial H_{\mathrm{VI}}}{\partial g}, \quad \frac{g'}{f} = -\frac{\partial H_{\mathrm{VI}}}{\partial f}. \tag{3.69}$$

The symplectic form $\omega = \iota^* \eta$ on $\mathcal{X}_c$ has the anticanonical divisor on $\mathcal{X}_c$ as its pole divisor, and our aim is to show that the system (3.56) is Hamiltonian with respect to this. In the (x, y)-chart, this symplectic form is given by

$$\omega = \frac{dx \wedge dy}{S(x,y)} = \frac{dx \wedge dy}{\alpha\beta - (n+\alpha+\beta)x + x^2 - y}, \tag{3.70}$$

so we aim to find a function $K(x, y, c)$ such that the system of differential equations (3.56) is of the form

$$\frac{x'}{S} = \frac{\partial K}{\partial y}, \quad \frac{y'}{S} = -\frac{\partial K}{\partial x}. \tag{3.71}$$

Theorem 3.3.2. *The system* (3.56) *can be written as the following nonautonomous Hamiltonian system with respect to the symplectic form ω given in* (3.70)*, with the Hamiltonian*

$$K(x, y, c) = \frac{P(x,y,c)}{c(c-1)\left(\alpha\beta - (n+\alpha+\beta)x + x^2 - y\right)}, \tag{3.72}$$

where

$$\begin{aligned} P(x,y,c) = {} & x^2 \left(n(\alpha+\beta-\gamma+n-1) - (c-1)y\right) \\ & + x\left(y(c(\alpha+\beta) + (c+1)n - \gamma - 1\right) \\ & + n(\gamma - \alpha\beta) + y(cy - c\alpha\beta + \gamma). \end{aligned} \tag{3.73}$$

The Hamiltonian K in the (x, y)-chart is unique modulo functions of c independent of x, y. Moreover, we have

$$\eta + dH_{\mathrm{VI}} \wedge dt = \omega + dK \wedge dc \tag{3.74}$$

with parameters identified according to (3.63)*, and $t = 1/c$.*

We immediately see that K is holomorphic on the part of the bundle E visible in the (x, y)-chart, away from the curve $\gamma : S(x, y) = 0$. We can verify that via our charts for the rest of the surface $\mathcal{X}_c$ we can extend K to a collection of Hamiltonians holomorphic on E, adding functions of c when necessary. This is done by direct calculation in charts. For example, in the (u_1, v_1)-chart covering F_1, we can substitute directly and obtain the Hamiltonian $K_1(u_1, v_1, c)$ in this chart, which does not require functions of c to be added.

When restricted to F_1 this is given by an expression of the form

$$K_1(u_1, v_1 = 0, c) = \frac{A + Bu_1}{c(c-1)\left(1 + (\alpha + \beta + n - 2)u_1\right)}, \tag{3.75}$$

where A, B are polynomials in α, β, γ, n and c. From this we see that K_1 is holomorphic in this chart except for at $(u_1, v_1) = (1/(\alpha + \beta + n - 2), 0)$, which is the intersection of F_1 with the proper transform of the curve γ, so corresponds to part of D_{red}. Proceeding in this way, we can extend K to a collection of Hamiltonians holomorphic on E and extending meromorphically to the bundle of surfaces $\bar{E}$. Therefore Theorem 2.4.1 (which for $\mathrm{P_{VI}}$ was given by Shioda and Takano [ST97]) ensures that the differential system mapped to the bundle E_{VI} must coincide with the standard form of $\mathrm{P_{VI}}$ (2.82) for f, g. This provides a justification of the result of Theorem 3.3.1.

Chapter 4

Full-parameter discrete Painlevé systems from non-translational Cremona isometries

It is now widely appreciated among researchers studying discrete Painlevé equations that Sakai's scheme classifies surfaces into a finite number of types, but does not further classify the equations belonging to each. Recently, much research has sought to understand the range of inequivalent discrete systems which can arise from each of the surface types in Sakai's list. In particular, systems proposed to be of discrete Painlevé type independently of Sakai's scheme being studied via the geometric framework has shed much light on the infinite number of discrete integrable systems associated with each surface type. Examples include equations which share the same space of initial conditions but correspond to non-conjugate translations, such as those associated with surfaces of elliptic type $\mathcal{R} = ell\text{-}A_0^{(1)}$ identified and studied in [JN17, RG09]. There are also examples of symmetries of infinite order, though not translations, giving rise to difference equations with finer time evolution and fewer free parameters than those associated with translations, known in the literature as projective reductions [AHJN16, HHNS15, KNT11, Tak03, KN15], which we explain in Section 4.1.

Our work in this chapter continues along these lines, in that we begin with a difference equation previously proposed as a discrete analogue of a special case of the third Painlevé equation, and by placing it within the geometric framework reveal more features of Sakai's scheme.

The equation we consider was constructed by T. Hoffmann in [Hof99], through a discrete version of the process by which Amsler surfaces (surfaces of constant negative Gaussian curvature with two straight asymptotic lines, studied by Bianchi [Bia10] then Amsler

[Ams55]) are controlled by a reduction of the sine-Gordon equation to a special case of P_{III}, similar to the example of P_{II} coming from the KdV equation in Subsection 1.1.2. The discrete analogues of this class are known as discrete Amsler surfaces [Hof99, BP96], and are related to solutions of the discrete sine-Gordon equation [Hir77]

$$Q_{l+1,m+1}Q_{l,m} = F(Q_{l+1,m})F(Q_{l,m+1}), \tag{4.1}$$

which is a partial difference equation for $Q_{l,m}$ with two discrete independent variables $l, m \in \mathbb{Z}$, where $F(x) = \frac{1-kx}{k-x}$, with free complex parameter $k \notin \{0, \pm 1\}$. Solutions of equation (4.1) corresponding to discrete Amsler surfaces satisfy an additional condition, which may be interpreted as invariance under Lorentz rotations of the frame (see [Hof99, BP96] for details, but these are not important for our analysis of the difference equations). The way in which an ordinary difference is obtained from (4.1) is analogous to the continuous case, which involves considering solutions of the PDE in terms of some function z of the independent variables x and t. Equation (4.1), after imposing the additional condition, gives a system which may be iterated along a zigzag path in the (l, m)-lattice parametrised by an integer n, which leads to the following system of ordinary difference equations:

$$Q_{2n+1} = \frac{\frac{1}{F(Q_{2n})} - \frac{Q_{2n-1}}{2n+1}}{Q_{2n-1}F(Q_{2n}) - \frac{1}{2n+1}}, \tag{4.2a}$$

$$Q_{2n+2} = \frac{1}{Q_{2n}(F(Q_{2n+1}))^2}. \tag{4.2b}$$

We rewrite this in terms of the variables $(x_n, y_n) = (Q_{2n}, Q_{2n-1})$ (of no relation to the variables for the hypergeometric weight recurrence in Chapter 3), which gives

$$\bar{x} = \frac{(k-\bar{y})^2}{f(k\bar{y}-1)^2}, \tag{4.3a}$$

$$\bar{y} = \frac{(k-x)\,(kxy-(2n+1)x-y+k(2n+1))}{(kx-1)\,(k(2n+1)xy-x-(2n+1)y+k)}, \tag{4.3b}$$

where $(x, y) = (x_n, y_n)$ and $(\bar{x}, \bar{y}) = (x_{n+1}, y_{n+1})$.

In what follows, we construct the space of initial values for the system (4.3), which is a family of $D_4^{(1)}$-surfaces with one free parameter, rather than five in the generic case in Section 2.3. The Cremona isometry induced by the iteration maps of the system is a ‘twisted translation': the composition of a translation with a Dynkin diagram automorphism which preserves the translation direction. The parameter specialisation causes the action on parameter space to coincide with that of the untwisted translation, so the system is in a sense similar to the projective reductions we define in Section 4.1, and we compare it to previously studied examples [KNT11, HHNS15, AHJN16, Tak03, JN17]. This prompts us to construct a generic version of the equation from the Cremona action of the same twisted translation on a generic family of $D_4^{(1)}$-surfaces, for which the action on parameter space is translational except for a permutation of parameters. We express this explicitly, and show that it is integrable in the sense of vanishing algebraic entropy [BV99] as in Subsection 1.2.4. We then show how full-parameter discrete integrable systems can be obtained in this way from the Cremona action of elements of infinite order on a family of generic surfaces, though they will not necessarily be difference equations of purely additive, multiplicative or elliptic type.

4.1 Background: projective reductions

In the years since the publication of Sakai's paper [Sak01], many known discrete analogues of the Painlevé equations have been found to fit naturally into the geometric framework even if they do not fit Sakai's definition of a discrete Painlevé equation as arising from a translational Cremona isometry. For example, the degeneration from a q-discrete analogue of $\mathrm{P_{III}}$ [KTGR00] to a q-discrete $\mathrm{P_{II}}$ [RG96] was formulated as the process of *projective reduction* [KNT11], which in the geometric framework corresponds to difference equations being obtained from elements of infinite order which are not translations in the affine Weyl group sense, by projecting onto an appropriate parameter subspace.

Here we will briefly recount this important example, following [KNT11], as it will give context for the results of the rest of this chapter. Consider the extended affine Weyl group

$$\begin{aligned}\widetilde{W}\left((A_2+A_1)^{(1)}\right) &= W\left((A_2+A_1)^{(1)}\right) \rtimes \mathrm{Aut}\left((A_2+A_1)^{(1)}\right) \\ &= \langle s_0, s_1, s_2, \pi, w_0, w_1, r \rangle ,\end{aligned} \tag{4.4}$$

defined as in [KNY01, KNT11] by the fundamental relations

$$\begin{gathered} s_i^2 = (s_i s_{i+1})^3 = \pi^3 = 1, \quad w_0^2 = w_1^2 = r^2 = 1, \quad (s_i w_j)^2 = 1, \\ \pi s_i = s_{i+1}\pi, \qquad w_0 r = r w_1, \end{gathered} \tag{4.5}$$

where $i \in \mathbb{Z}/3\mathbb{Z}$, $j \in \mathbb{Z}/2\mathbb{Z}$. Here s_i, w_i are simple reflections, while π, r generate $\mathrm{Aut}\left((A_2+A_1)^{(1)}\right)$. In [KNT11], Kajiwara, Nakazono and Tsuda considered an action of this group on the field of rational functions of parameters a_0, a_1, a_2, c, and variables f_0, f_1, f_2 subject to the constraint

$$f_0 f_1 f_2 = a_0 a_1 a_2 c^2, \tag{4.6}$$

which corresponds to the Cremona action of the symmetry group $\widetilde{W}\left((A_2+A_1)^{(1)}\right)$ on a family of generic $A_5^{(1)}$-surfaces. Letting $q = a_0 a_1 a_2$, the action of the element $T_1 = \pi s_2 s_1$ on the parameters is given by

$$T_1 \cdot (a_0, a_1, a_2, c) = \left(q a_0, q^{-1} a_1, a_2, c\right). \tag{4.7}$$

The element T_1 is a translation by a weight of the root system (A_2+A_1), and its action on the variables leads to a system of first-order q-difference equations since this is a multiplicative surface type. To be precise, this is given by repeated iteration of its action

$$T_1 : \begin{pmatrix} a_0, a_1, a_2 & \\ & ; f_0, f_1, f_2 \\ c & \end{pmatrix} \mapsto \begin{pmatrix} q a_0, q^{-1} a_1, a_2 & \\ & ; T \cdot f_0\,,\ T \cdot f_1\,,\ T \cdot f_2 \\ c & \end{pmatrix}, \tag{4.8}$$

where by letting $F_n = T_1^n \cdot f_0$ and $G_n = T_1^n \cdot f_1$, we obtain

$$G_{n+1} G_n = \frac{q c^2}{F_n} \frac{1 + q^n a_0 F_n}{q^n a_0 + F_n}, \qquad F_{n+1} F_n = \frac{q c^2}{G_{n+1}} \frac{1 + q^n a_0 a_2 G_{n+1}}{q^n a_0 a_2 + G_{n+1}}, \tag{4.9}$$

which is a previously known q-discrete analogue of $\mathrm{P_{III}}$ [KTGR00], in the sense that it gives $\mathrm{P_{III}}$ in a continuous limit. We note that this equation fits Sakai's definition of a discrete Painlevé equation associated with a family of generic $A_5^{(1)}$-surfaces (which are of multiplicative type), and indeed this is a system of 'multiplicative' difference equations in the sense mentioned in Chapter 2. We recall that by this we mean that, when written explicitly as a nonautonomous system, the independent variable n enters into the coefficients of the rational functions as the exponent of a parameter q. The reason such examples are sometimes referred to as q-Painlevé is that they may be naturally written as q-difference equations in a way which we now illustrate. While we have written the system (4.9) with dependent variables F_n, G_n depending on n so the nonautonomous nature manifests in the explicit appearance of n in the equation, we could alternatively take these as functions of a continuous independent variable t, and have the action of T_1 define a relation between values of the solution at t, qt, with the parameter evolution reflected in the way in which t appears in the equations:

$$G(qt)G(t) = \frac{qc^2}{F(t)} \frac{1 + a_0 t F(t)}{a_0 t + F(t)}, \qquad F(qt)F(t) = \frac{qc^2}{G(qt)} \frac{1 + a_0 a_2 t G(qt)}{a_0 a_2 t + G(qt)}. \tag{4.10}$$

Returning to this system written as in (4.9), a related equation, obtained as a q-discrete analogue of $\mathrm{P_{II}}$ [RG96], is given by

$$X_{k+1}X_{k-1} = \frac{p^2c^2}{X_k} \frac{1 + p^k a_0 X_k}{p^k a_0 + X_k}, \tag{4.11}$$

where a_0, c are free parameters and p is not a root of unity. The equation (4.9) can be obtained from (4.11) by introducing $X_k, k \in \mathbb{Z}$ according to

$$F_n = X_{2n}, \quad G_n = X_{2n-1}, \tag{4.12}$$

and imposing the parameter constraint $a_2 = q^{1/2}$, after which from (4.9) we obtain

$$\begin{aligned} X_{2n+1}X_{2n-1} &= \frac{qc^2}{X_{2n}} \frac{1 + q^n a_0 X_{2n}}{q^n a_0 + X_{2n}}, \\ X_{2n+2}X_{2n} &= \frac{qc^2}{X_{2n+1}} \frac{1 + q^{n-1/2} a_0 X_{2n+1}}{q^{n-1/2} a_0 + X_{2n+1}}. \end{aligned} \tag{4.13}$$

With the parameter constraint, the forms of the two equations are such that we can set $p = q^{1/2}$ and write this as a single difference equation for the sequence X_k, which is precisely (4.11).

This relationship between equations (4.9) and (4.11) was found to correspond in the geometric setting to features of the affine Weyl group and its birational representation [KNT11], in a way which we now recall. With the same birational representation of $\widetilde{W}\left((A_2 + A_1)^{(1)}\right)$, consider the element $R = \pi^2 s_1$, which is regarded as a half-translation because of the identity

$$R^2 = T_1. \tag{4.14}$$

The action of R on the parameters is given by

$$R \cdot (a_0, a_1, a_2, c) = (a_2 a_0, q^{-1} a_2 a_1, q a_2^{-1}, c), \tag{4.15}$$

which is not translational, meaning that the action on variables does not directly give a q-difference equation as in the case of T_1. However, restricting to the parameter subspace on which $a_2 = q^{1/2}$, the action becomes

$$R \cdot (a_0, a_1, c) = (q^{1/2} a_0, q^{-1/2} a_1, c). \tag{4.16}$$

With the parameter specialisation, the action of R on the variables f_0, f_1 is given by

$$R \cdot f_1 = f_0, \qquad R \cdot f_0 = \frac{qc^2}{f_0 f_1} \frac{1 + a_0 f_0}{a_0 + f_0}, \tag{4.17}$$

which, because of the translational motion in parameter space, induces the q-difference equation (4.11), where $X_k = R^k \cdot f_0$, which is said to be a *projective reduction* of equation (4.9).

We now make some remarks about the equations (4.9) and equation (4.11), as well as the restriction to the parameter subspace. In the language of Sakai's theory established in Chapter 2, the birational representation of $\widetilde{W}\left((A_2 + A_1)^{(1)}\right)$ is the Cremona action on a family $\{X_{\mathbf{a}} \mid \mathbf{a} \in \mathcal{A}\}$ of generic $A_5^{(1)}$-surfaces, where the parameters $\mathbf{a} = (a_0, a_1, a_2, c)$ are the root variables associated with a basis of the symmetry root lattice of the family. In particular, this means that the action of the symmetry group $\widetilde{W}\left((A_2 + A_1)^{(1)}\right)$ on the parameters will correspond in a natural way to its action by Cremona isometries on the basis of simple roots for the symmetry lattice $Q((A_2 + A_1)^{(1)})$. This guarantees that a translation element of the symmetry group will give a translational motion in parameter space with root variables as coordinates, and its action on the variables will give a q-difference equation, as in the case of T_1 giving equation (4.9).

The system (4.11), on the other hand, was constructed from the non-translation element R acting on the subfamily of surfaces with $a_2 = q^{1/2}$. In the geometric framework, projective reduction refers to the process by which a difference equation is obtained from the Cremona action of a non-translation element on a proper subfamily of a family of generic surfaces of one of the types in Sakai's list, with the subfamily corresponding to a parameter subspace on which the non-translation element in question acts by translation. In keeping with the literature [KNT11, JNS1608, JN17, AHJN16], we use the term projective reduction to refer to both this process, and the resulting equations. Further, as in the case above, when some power of the non-translation element φ is a translation, say $\varphi^m = T$, we say the equation given by φ with the parameter restriction is a projective reduction of the full-parameter discrete Painlevé equation associated to T.

We note that without the restriction to the parameter subspace, the birational action of R on parameters and variables still defines a discrete dynamical system which is non-trivial in the sense that R is of infinite order. The fact that the motion in parameter space is not translational for general $\mathbf{a}$ means that without the parameter constraint the system will not be given directly by a difference equation of purely multiplicative type using these parameters, as we will illustrate when we construct it explicitly in Section 4.4. Here we mean 'multiplicative type' in the same sense as in Chapter 2, related to the fact that translation symmetries of surfaces of multiplicative type lead to nonautonomous discrete equations in which the independent variable appears in the exponents of a parameter q.

The fact that the Cremona actions of non-translation elements of infinite order still give discrete integrable systems with the full number of parameters for their surface type is the central idea of this chapter.

4.1.1 Outline of the chapter

The chapter is structured as follows. In Section 4.2 we proceed along similar lines to in Chapter 2, first constructing the space of initial values for the system (4.3), finding bases for the surface and symmetry root lattices and computing the induced Cremona isometry. We then express this Cremona isometry in terms of generators of the extended affine Weyl group, and show that it is the composition of a Kac translation and a Dynkin diagram automorphism. The main result of Section 4.3 is the construction of a generic (5-parameter) version of equation (4.3). To do this, we first introduce a 5-parameter family of $D_4^{(1)}$-surfaces generalising the space of initial values for equation (4.3), and obtain the Cremona action of the extended affine Weyl group $\widetilde{W}(D_4^{(1)})$ on this family, from which we recover (4.3) as a special case of a projective reduction. Next we obtain the parametrisation of this family by root variables, through a transformation to the standard form of $D_4^{(1)}$-surfaces as in Section 2.3. With the root variable parametrisation, we use the Cremona action to construct a generic version of equation (4.3), and demonstrate that it has vanishing algebraic entropy. In Section 4.4, we construct more examples of difference equations with the maximal number of free parameters for their surface type from non-translation elements of infinite order in the symmetry group, which are shown to be integrable but not directly of additive, multiplicative or elliptic type. We then discuss examples from the literature which have been obtained via deautonomisation by singularity confinement, which are likely to belong to the class of full-parameter discrete Painlevé systems from non-translational Cremona isometries.

4.2 Geometry of Hoffmann's discrete P_{III}

We now give a geometric treatment of equation (4.3), beginning with the construction of its space of initial values.

4.2.1 Space of initial conditions

As usual, we consider the system (4.3) on $\mathbb{P}^1 \times \mathbb{P}^1$ via the charts $(x, y), (X, y), (x, Y)$ and (X, Y) for the domain space, where $X = 1/x, Y = 1/y$, and the same charts with the overline notation for the target space.

Proposition 4.2.1. *The birational iteration mapping $(x, y) \mapsto (\bar{x}, \bar{y})$ of the system* (4.3) *lifts to a family of isomorphisms*

$$\psi_n : \mathcal{X}_{k,n} \longrightarrow \mathcal{X}_{k,n+1}, \tag{4.18}$$

where for each $n \in \mathbb{Z}$ the surface $\mathcal{X}_{k,n}$ is obtained from $\mathbb{P}^1 \times \mathbb{P}^1$ by blowing up the points $q_1, \ldots, q_8$ given in coordinates by

$$q_1 : (x, y) = (k, 0), \qquad p_5 : (u_1, v_1) = \left(\frac{x-k}{y}, y\right) = \left((k^2-1)(2n+1), 0\right), \tag{4.19a}$$

$$q_2 : (X, Y) = (k, 0), \qquad p_6 : (u_2, v_2) = \left(\frac{X-k}{Y}, Y\right) = \left((k^2-1)(2n+1), 0\right), \tag{4.19b}$$

$$q_3 : (x, y) = (0, k), \qquad p_7 : (u_3, v_3) = \left(\frac{x}{y-k}, y-k\right) = (0, 0), \tag{4.19c}$$

$$q_4 : (X, Y) = (0, k), \qquad p_8 : (u_4, v_4) = \left(\frac{X}{Y-k}, Y-k\right) = (0, 0). \tag{4.19d}$$

Again the points q_i, mapping ψ_n and, in what follows, the charts (u_i, v_i) are of no relation to those in Chapter 2, and we have recycled them purely for economy of notation.

Proof. This is a standard computation in charts, much like that in Subsection 3.2.1, but here we illustrate a slightly different approach as we deal with the iteration $(x, y) \mapsto (\bar{x}, \bar{y})$ directly rather than a decomposition into forward and backward half-mappings.

Recall that in the (x, y)-chart, we have the forward iteration of the system given by $(x, y) \mapsto (\bar{x}, \bar{y})$, which here we call the *forward mapping*:

$$\bar{x} = \frac{(k - \bar{y})^2}{f(k\bar{y} - 1)^2}, \qquad \bar{y} = \frac{(k - x)\,(kxy - (2n+1)x - y + k(2n+1))}{(kx - 1)\,(k(2n+1)xy - x - (2n+1)y + k)}. \tag{4.20}$$

We also have its inverse, which we call the *backward mapping*, given by

$$f = \frac{(k - \bar{y})^2}{\bar{s}(k\bar{y} - 1)^2}, \qquad y = \frac{(x - k)\,(kx\bar{y} + (2n+1)x - \bar{y} - k(2n+1))}{(kx - 1)\,(k(2n+1)x\bar{y} + x - (2n+1)\bar{y} - k)}. \tag{4.21}$$

Direct calculation shows that the only indeterminacies of the forward mapping are

$$q_1 : (x, y) = (k, 0), \qquad q_2 : (X, Y) = (k, 0), \tag{4.22}$$

while the indeterminacies of the backward mapping are given in coordinates by

$$\bar{q}_3 : (\bar{x}, \bar{y}) = (0, k), \qquad \bar{q}_4 : (\bar{X}, \bar{Y}) = (0, k). \tag{4.23}$$

We blow up these points in both the domain and target copies of $\mathbb{P}^1 \times \mathbb{P}^1$ using the same convention as throughout the thesis, namely that for each $j = 1, \ldots, 4$, the exceptional divisor F_j replacing q_j in the domain space is covered by the pair of local affine coordinate charts (u_j, v_j) and (U_j, V_j), with the part of the line visible in the first chart parametrised by u_j when $v_j = 0$, and similarly in the second chart by U_j when $V_j = 0$. After the blow-ups of the points $\bar{q}_i$ in the target space we use the same charts with overline notation to cover the exceptional divisors $\bar{F}_i$.

In order to examine the image of F_1 under the forward mapping after these blow-ups, we rewrite (4.20) using the chart (u_1, v_1) for the domain, and $(\bar{x}, \bar{y})$ for the target. Direct calculation reveals another basepoint on the exceptional line F_1, with the lifted forward mapping becoming indeterminate at

$$q_5 : (u_1, v_1) = \left(\frac{x - k}{y}, y\right) = \left((k^2 - 1)(2n+1), 0\right). \tag{4.24}$$

The corresponding point $\bar{q}_5$ in the target space is also an indeterminacy of the backward iteration, which is evidenced by the following. Writing the mapping (4.20) in charts (x, y) and $(\bar{u}_1, \bar{v}_1)$, we see that $x = k, y \neq 0$ implies

$$\bar{u}_1 = (k^2 - 1)(2n + 3), \qquad \bar{v}_1 = 0, \tag{4.25}$$

so the forward mapping sends the line $x = k$ (excluding p_1) to the single point $\bar{p}_5$ on $\bar{E}_1$. We blow up this point in both the domain and target spaces too, covering the exceptional line F_5 with the affine charts (u_5, v_5) and (U_5, V_5) defined by

$$\begin{aligned} u_5 &= \frac{u_1 - (k^2-1)(2n+1)}{v_1}, \quad v_5 = v_1, \\ U_5 &= \frac{v_1}{u_1 - (k^2-1)(2n+1)}, \quad V_5 = u_1 - (k^2-1)(2n+1), \end{aligned} \tag{4.26}$$

and similar for $\bar{F}_5$. Writing (4.20) in charts (x, y) and $(\bar{u}_5, \bar{v}_5)$, we see that $x = k$ with $y \neq 0$ implies that

$$\bar{u}_5 = \frac{(k^2-1)\big((k^2(4n+5) - 4(n+1)^2)y - 4n(2n^2+3n+1)k\big)}{ky}, \quad \bar{v}_5 = 0, \tag{4.27}$$

and as $\bar{u}_5$ here is a fractional-linear function of y we have a one-to-one correspondence under the forward mapping between the proper transform of the line $x = k$ in the domain surface and the exceptional line $\bar{F}_5$ in the target surface.

Since we have now blown up q_5 on F_1 we next compute the image of the proper transform $F_1 - F_5$ under the forward mapping. Using the charts (u_1, v_1) and $(\bar{u}_1, \bar{v}_1)$ we see that when $v_1 = 0$ and $u_1 \neq (k^2 - 1)(2n + 1)$, we have

$$\bar{u}_1 = \frac{(k^2-1)\big((k^2-1)(2n+3) - (4n+3)u_1\big)}{k^2 - 1 - (2n+1)u_1}, \quad \bar{v}_1 = 0. \tag{4.28}$$

With similar results in the charts (U_1, V_1), we see that the forward mapping injects F_1 (excluding q_5) into $\bar{F}_1$. We now examine the image of the exceptional line F_5 under the forward mapping, writing (4.20) in charts (u_5, v_5) and $(\bar{x}, \bar{y})$ then setting $v_5 = 0$, we see that the exceptional line F_5 is mapped bijectively to the proper transform of the curve defined in the $(\bar{x}, \bar{y})$-chart by

$$k\bar{x}(k\bar{y} - 1)^2 - (k - \bar{y})^2 = 0. \tag{4.29}$$

We also deduce from (4.28) that the proper transforms $F_1 - F_5$ and $\bar{F}_1 - \bar{F}_5$ of the exceptional lines arising from $q_1, \bar{q}_1$ are in bijective correspondence under the mapping. Further, (4.27) shows that the exceptional line $\bar{F}_5$ is in bijective correspondence with the proper transform $H_x - F_1$ of the line $x = k$, so we have lifted the mapping to an isomorphism in the neighbourhood of q_1. Calculations in the neighbourhoods of the exceptional lines F_2, F_3 and F_4 are similar, for example with $H_x - F_2$ being blown down by the forward mapping to the single point $q_6 \in F_2$, while under the backward mapping $H_{\bar{y}} - \bar{F}_3$ and $H_{\bar{y}} - \bar{F}_4$ are blown down to $q_7 \in F_3$ and $q_8 \in F_4$ respectively. After blowing up these points q_6, q_7 and q_8 in both domain and target surfaces, calculations in local coordinates similar to those above show that we have the isomorphism ψ_n as claimed. □

4.2.2 Surface type

We next show that the surfaces $\mathcal{X}_{k,n}$ are a family of Sakai surfaces and determine their type.

Proposition 4.2.2. *Each surface $\mathcal{X}_{k,n}$ has a unique representative of its anticanonical class, given by*

$$D = D_0 + D_1 + 2D_2 + D_3 + D_4, \tag{4.30}$$

where

$$D_0 = F_1 - F_5 \qquad D_1 = F_2 - F_6 \qquad D_3 = F_3 - F_7, \qquad D_4 = F_4 - F_8, \tag{4.31}$$

are the proper transforms of the exceptional divisors F_1, F_2, F_3, F_4 under the blow-ups of q_5, q_6, q_7, q_8 respectively, and D_2 is the proper transform of the unique curve of bi-degree $(1, 1)$ passing through q_1, q_2, q_3, q_4, which is defined in the (x, y)-chart by

$$kxy - x - y - k = 0. \tag{4.32}$$

The divisor D is of canonical type, and $\mathcal{X}_{k,n}$ form a family of $\mathcal{R}$-surfaces with $\mathcal{R} = D_4^{(1)}$. A schematic representation of the point configuration and the curves D_i is given in Figure 4.1. The surface roots $\delta_j = [D_j]$ and our choice of symmetry roots $\alpha_0, \ldots, \alpha_4$ are given in Figure 4.2.

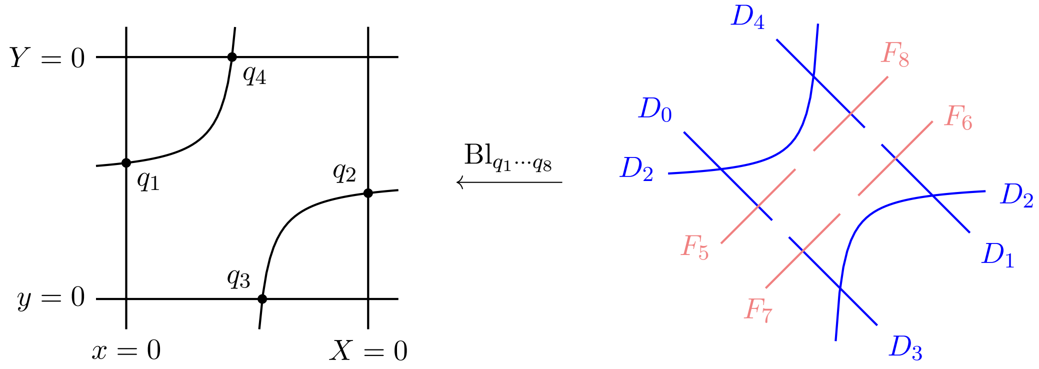

Figure 4.1: Point configuration for $D_4^{(1)}$-surfaces from Hoffmann's d-P_{III}

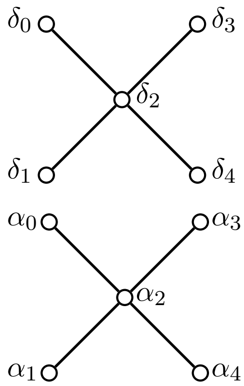

$$\delta_0 = \mathcal{F}_1 - \mathcal{F}_5, \qquad \delta_3 = \mathcal{F}_3 - \mathcal{F}_7$$
$$\delta_1 = \mathcal{F}_2 - \mathcal{F}_6, \qquad \delta_4 = \mathcal{F}_4 - \mathcal{F}_8.$$
$$\delta_2 = \mathcal{H}_x + \mathcal{H}_y - \mathcal{F}_1 - \mathcal{F}_2 - \mathcal{F}_3 - \mathcal{F}_4,$$

$$\alpha_0 = \mathcal{H}_y - \mathcal{F}_1 - \mathcal{F}_5, \qquad \alpha_3 = \mathcal{H}_y - \mathcal{F}_3 - \mathcal{F}_7,$$
$$\alpha_1 = \mathcal{H}_y - \mathcal{F}_2 - \mathcal{F}_6, \qquad \alpha_4 = \mathcal{H}_y - \mathcal{F}_4 - \mathcal{F}_8.$$
$$\alpha_2 = \mathcal{H}_x - \mathcal{H}_y,$$

Figure 4.2: Root data for $D_4^{(1)}$-surfaces from Hoffmann's d-P_{III}

Proof. The divisors D_0, D_1, D_3, D_4 in (4.31) all have self-intersection -2 and are irreducible. The proper transform of the curve defined in the (x, y)-chart by

$$kxy - x - y - k = 0, \tag{4.33}$$

gives a representative of the divisor class $\mathcal{H}_x + \mathcal{H}_y - \mathcal{E}_1 - \mathcal{E}_2 - \mathcal{E}_3 - \mathcal{E}_4$. This can be verified by noting that the polynomial defining the curve is of bi-degree $(1, 1)$ in (x, y), and the curve passes through the points $q_1, \ldots, q_4$ with multiplicity 1, but its proper transform under their blow-ups does not intersect $q_5, \ldots, q_8$, which can be checked by direct calculation. We immediately see that $D = D_0 + D_1 + 2D_2 + D_3 + D_4$ is a representative of the anticanonical class of $\mathcal{X}_{k,n}$, as

$$[D] = [D_0] + [D_1] + 2[D_2] + [D_3] + [D_4] = 2\mathcal{H}_x + 2\mathcal{H}_y - \mathcal{F}_1 - \cdots - \mathcal{F}_8. \tag{4.34}$$

With regards to D being a unique anticanonical divisor, we note that each of the divisors D_0, D_1, D_3 and D_4 defined as proper transforms of exceptional lines give unique representatives of their classes in $\mathrm{Pic}(\mathcal{X}_{k,n})$. Further, it can be shown by direct calculation that (4.33) defines the unique curve of bi-degree $(1,1)$ passing through $q_1, \ldots, q_4$, which means the divisor D_2 is also a unique representative of its class. Direct computation shows that $[D_i] \cdot \mathcal{K}_{\mathcal{X}_{k,n}} = 0$ for $i = 0, \ldots, 4$, so D is of canonical type.

Computing the pairwise intersections of the classes $\delta_i = [D_i]$, for $i = 0, \ldots, 4$, we obtain

$$-\left(\delta_i \cdot \delta_j\right) = \begin{pmatrix} 2 & 0 & -1 & 0 & 0 \\ 0 & 2 & -1 & 0 & 0 \\ -1 & -1 & 2 & -1 & -1 \\ 0 & 0 & -1 & 2 & 0 \\ 0 & 0 & -1 & 0 & 2 \end{pmatrix}, \tag{4.35}$$

which is the generalised Cartan matrix of type $D_4^{(1)}$, meaning that each $\mathcal{X}_{k,n}$ is a $D_4^{(1)}$-surface as claimed, with surface root lattice $Q(R) =_{\mathbb{Z}} \{\delta_0, \ldots, \delta_4\}$, $R = D_4^{(1)}$. The root lattice given by the orthogonal complement $Q(R)^{\perp} \subset \delta^{\perp} \subset \mathrm{Pic}(X)$ is by Sakai's results of type $R^{\perp} = D_4^{(1)}$. We find a basis of simple roots for $Q(R^{\perp})$ by looking for a set of five linearly independent elements $\alpha_0, \ldots, \alpha_4$ orthogonal to all δ_i, with the required $D_4^{(1)}$ intersection matrix $-(\alpha_i \cdot \alpha_j)$. This yields a system of linear equations for the coefficients of the generators $\mathcal{H}_x, \mathcal{H}_y, \mathcal{F}_i$ in each of the simple roots, from which we obtain the choice of basis in Figure 4.2. □

4.2.3 Cremona isometry

We now identify the Cremona isometry induced by the isomorphism ψ_n, which determines whether the system is a discrete Painlevé equation according to Definition 2.2.7.

Proposition 4.2.3. *The family of isomorphisms ψ_n lifted from the birational iteration map-*

ping of system (4.3) *have pullbacks* $(\psi_n)^* : \mathrm{Pic}(\mathcal{X}_{k,n+1}) \to \mathrm{Pic}(\mathcal{X}_{k,n})$ *given by*

$$\begin{aligned}
\bar{\mathcal{H}}_x &\mapsto 5\mathcal{H}_x + 2\mathcal{H}_y - 2\mathcal{F}_1 - 2\mathcal{F}_2 - \mathcal{F}_3 - \mathcal{F}_4 - 2\mathcal{F}_5 - 2\mathcal{F}_6 - \mathcal{F}_7 - \mathcal{F}_8,\\
\bar{\mathcal{H}}_y &\mapsto 2\mathcal{H}_x + \mathcal{H}_y - \mathcal{F}_1 - \mathcal{F}_2 - \mathcal{F}_5 - \mathcal{F}_6,\\
\bar{\mathcal{F}}_1 &\mapsto \mathcal{H}_x - \mathcal{F}_5,\\
\bar{\mathcal{F}}_2 &\mapsto \mathcal{H}_x - \mathcal{F}_6,\\
\bar{\mathcal{F}}_3 &\mapsto 2\mathcal{H}_x + \mathcal{H}_y - \mathcal{F}_1 - \mathcal{F}_2 - \mathcal{F}_5 - \mathcal{F}_6 - \mathcal{F}_7,\\
\bar{\mathcal{F}}_4 &\mapsto 2\mathcal{H}_x + \mathcal{H}_y - \mathcal{F}_1 - \mathcal{F}_2 - \mathcal{F}_5 - \mathcal{F}_6 - \mathcal{F}_8,\\
\bar{\mathcal{F}}_5 &\mapsto \mathcal{H}_x - \mathcal{F}_1,\\
\bar{\mathcal{F}}_6 &\mapsto \mathcal{H}_x - \mathcal{F}_2,\\
\bar{\mathcal{F}}_7 &\mapsto 2\mathcal{H}_x + \mathcal{H}_y - \mathcal{F}_1 - \mathcal{F}_2 - \mathcal{F}_3 - \mathcal{F}_5 - \mathcal{F}_6,\\
\bar{\mathcal{F}}_8 &\mapsto 2\mathcal{H}_x + \mathcal{H}_y - \mathcal{F}_1 - \mathcal{F}_2 - \mathcal{F}_4 - \mathcal{F}_5 - \mathcal{F}_6.
\end{aligned} \tag{4.36}$$

Proof. This is a standard computation, most of which we have already performed in our lifting of the maps to isomorphisms. We note that there are many equivalent sequences of calculations by which the map (4.36) may be deduced, but the basic idea is to choose effective classes in $\mathrm{Pic}(\mathcal{X}_{k,n})$ such that computing the images of their representatives under the mapping ψ_n is as simple as possible, and gives enough conditions to deduce $(\psi_n)^*$ (or equivalently the pushforward $(\psi_n)_*$) on divisor classes. The calculations we outline here are based on those from the proof of Proposition 4.2.1.

First recall that by considering the forward mapping in charts (u_1, v_1) and $(\bar{u}_1, \bar{v}_1)$, we obtained (4.28), from which we deduce that on divisors we have $(\psi_n)_*(F_1 - F_5) = \bar{F}_1 - \bar{F}_5$, so passing to divisor classes where we also denote the pushforward by $(\psi_n)_*$ we have

$$(\psi_n)_*(\mathcal{F}_1 - \mathcal{F}_5) = \bar{\mathcal{F}}_1 - \bar{\mathcal{F}}_5 \tag{4.37}$$

Similarly, our calculation of the image under ψ_n of the line $f = k$ led to (4.27), which shows that (on divisors) $(\psi_n)_*(H_x - F_1) = \bar{F}_5$ and therefore on classes we have

$$(\psi_n)_*(\mathcal{H}_x - \mathcal{F}_1) = \bar{\mathcal{F}}_5. \tag{4.38}$$

By linearity of the map $(\psi_n)_*$ on $\mathrm{Pic}(\mathcal{X}_{k,n})$, if we obtain $(\psi_n)_*(\mathcal{F}_5)$, we may deduce $(\psi_n)_*(\mathcal{H}_x)$ and $(\psi_n)_*(\mathcal{F}_1)$ from (4.37) and (4.38). In order to do this, we consider the mapping in charts (u_5, v_5) and $(\bar{x}, \bar{y})$ and obtain the image of E_5 to be the proper transform of the curve defined by (4.29). To determine its class in $\mathrm{Pic}(\mathcal{X}_{k,n+1})$, we check its intersection with the exceptional divisors $\bar{F}_1, \ldots \bar{F}_8$. For example, to check intersections with $\bar{F}_1$ and $\bar{F}_5$, we substitute $\bar{x} = \bar{u}_1\bar{v}_1 + k$ and $\bar{y} = \bar{v}_1$ into the equation of the curve (4.29), which gives the equation of the total transform in the chart $(\bar{u}_1, \bar{v}_1)$ as

$$\bar{v}_1 \left(k(k\bar{v}_1 - 1)^2\bar{u}_1 + (k^4 - 1)\bar{v}_1 - 2k(k^2 - 1) \right) = 0. \tag{4.39}$$

The factor $\bar{v}_1$ appearing here with exponent one indicates that the proper transform of the curve intersects $\bar{F}_1$ with multiplicity one, so $(\psi_n)_*(\mathcal{F}_5) \cdot \bar{\mathcal{F}}_1 = 1$. Further, the proper transform of the curve (4.29) is given in the $(\bar{u}_1, \bar{v}_1)$-chart by

$$k(k\bar{v}_1 - 1)^2\bar{u}_1 + (k^4 - 1)\bar{v}_1 - 2k(k^2 - 1) = 0. \tag{4.40}$$

The coordinates of the point $\bar{q}_5$ do not satisfy this equation, so we deduce that

$$(\psi_n)_*(\mathcal{F}_5) \cdot \bar{\mathcal{F}}_5 = 0, \tag{4.41}$$

so the coefficient of $\bar{\mathcal{F}}_5$ in $(\psi_n)_*(\mathcal{F}_5)$ is zero. Similar calculations in charts covering the rest of the exceptional lines, and the observation of the bi-degree of the polynomial defining the curve allow us to deduce the coefficients, and we arrive at

$$(\psi_n)_*(\mathcal{F}_5) = \bar{\mathcal{H}}_x + 2\bar{\mathcal{H}}_y - \bar{\mathcal{F}}_1 - \bar{\mathcal{F}}_3 - \bar{\mathcal{F}}_4 - \bar{\mathcal{F}}_7 - \bar{\mathcal{F}}_8. \tag{4.42}$$

By similar calculations we obtain more conditions on φ:

$$\begin{aligned}
(\psi_n)_*(\mathcal{F}_2 - \mathcal{F}_6) &= \bar{\mathcal{F}}_2 - \bar{\mathcal{F}}_6, \\
(\psi_n)_*(\mathcal{F}_3 - \mathcal{F}_7) &= \bar{\mathcal{F}}_3 - \bar{\mathcal{F}}_7, \\
(\psi_n)_*(\mathcal{F}_4 - \mathcal{F}_8) &= \bar{\mathcal{F}}_4 - \bar{\mathcal{F}}_8, \\
(\psi_n)_*(\mathcal{H}_y - \mathcal{F}_1) &= \bar{\mathcal{H}}_x + 3\bar{\mathcal{H}}_y - \bar{\mathcal{F}}_1 - \bar{\mathcal{F}}_2 - \bar{\mathcal{F}}_3 - \bar{\mathcal{F}}_4 - \bar{\mathcal{F}}_6 - \bar{\mathcal{F}}_7 - \bar{\mathcal{F}}_8, \\
(\psi_n)_*(\mathcal{H}_y - \mathcal{F}_2) &= \bar{\mathcal{H}}_x + 3\bar{\mathcal{H}}_y - \bar{\mathcal{F}}_1 - \bar{\mathcal{F}}_2 - \bar{\mathcal{F}}_3 - \bar{\mathcal{F}}_4 - \bar{\mathcal{F}}_5 - \bar{\mathcal{F}}_7 - \bar{\mathcal{F}}_8, \\
(\psi_n)_*(\mathcal{F}_6) &= \bar{\mathcal{H}}_x + 2\bar{\mathcal{H}}_y - \bar{\mathcal{F}}_2 - \bar{\mathcal{F}}_3 - \bar{\mathcal{F}}_4 - \bar{\mathcal{F}}_7 - \bar{\mathcal{F}}_8, \\
(\psi_n)_*(\mathcal{F}_7) &= \bar{\mathcal{H}}_y - \bar{\mathcal{F}}_3, \\
(\psi_n)_*(\mathcal{F}_8) &= \bar{\mathcal{H}}_y - \bar{\mathcal{F}}_4.
\end{aligned} \tag{4.43}$$

These are sufficient to deduce the pushforward $(\psi_n)_*$ on all generators of $\mathrm{Pic}(\mathcal{X}_{k,n})$, and the pullback is deduced directly as its inverse. □

In order to deduce the Cremona isometry induced by the pullbacks $(\psi_n)^*$, we recall how the identification of the Picard groups of a family of $\mathcal{R}$-surfaces works in practice for the family

$$\mathcal{X} = \{\mathcal{X}_{k,n} \mid k \in \mathbb{C}\backslash\{0, \pm 1\}, n \in \mathbb{Z}\}\,. \tag{4.44}$$

As before we have $\mathcal{H}_x, \mathcal{H}_y$ being the divisor classes in $\mathrm{Pic}(\mathcal{X}_{k,n})$ of total transforms of hyperplanes in $\mathbb{P}^1 \times \mathbb{P}^1$ of constant x, y respectively. We also have $\mathcal{F}_i$ being the class of the total transform of the exceptional divisor F_i arising from the blow-up of $q_i(k,n)$, where we have emphasised the dependence of the location of these points on k and n. In $\mathrm{Pic}(\mathcal{X}_{k,n+1})$, where $\mathcal{X}_{k,n+1}$ is obtained from $\mathbb{P}^1 \times \mathbb{P}^1$ extended from $\mathbb{C}^2$ with coordinates $(\bar{x}, \bar{y})$, we have $\bar{\mathcal{H}}_x, \bar{\mathcal{H}}_y$ similarly being classes of total transforms of hyperplanes of constant $\bar{x}, \bar{y}$ respectively. The generators $\bar{\mathcal{F}}_i$ correspond to classes of total transforms of exceptional divisors $\bar{F}_i$ arising from the blow-ups of $q_i(k, n+1)$. The identification is of $\mathcal{H}_x$ with $\bar{\mathcal{H}}_x$, $\mathcal{H}_y$ with $\bar{\mathcal{H}}_y$ and $\mathcal{F}_i$ with $\bar{\mathcal{F}}_i$, and we denote the resulting $\mathbb{Z}$-module by $\mathrm{Pic}(\mathcal{X})$, of which $(\psi_n)^*$ induces a $\mathbb{Z}$-module automorphism, denoted ψ, according to the following commutative diagram, where the vertical arrows indicate this identification.

$$\begin{array}{ccc} \mathrm{Pic}(\mathcal{X}_{k,n+1}) & \xrightarrow{(\psi_n)^*} & \mathrm{Pic}(\mathcal{X}_{k,n}) \\ \downarrow \wr & & \downarrow \wr \\ \mathrm{Pic}(\mathcal{X}) & \xrightarrow{\psi} & \mathrm{Pic}(\mathcal{X}) \end{array} \tag{4.45}$$

According to Theorem 2.2.6, the Cremona isometries of a family of generic $D_4^{(1)}$-surfaces form the group

$$\widetilde{W}(D_4^{(1)}) = \left\langle r_0, r_1, r_2, r_3, r_4, \pi_{(01)}, \pi_{(34)}, \pi_{(14)} \right\rangle, \tag{4.46}$$

subject to the relations

$$r_i^2 = 1, \quad (r_i r_j)^{m_{ij}} \;\; (i \neq j), \quad r_{\sigma(i)}\pi_\sigma = \pi_\sigma r_i, \quad \pi_\sigma \pi_\tau = \pi_{\sigma\tau}, \tag{4.47}$$

where $i, j \in \mathbb{Z}/5\mathbb{Z}$, $(a_{ij})_{i,j=0}^4$ is the generalised Cartan matrix $D_4^{(1)}$, m_{ij} are as in Definition 2.1.2, and σ, τ are permutations of the indices $\{0, 1, 2, 3, 4\}$ of the simple roots. We remark here that r_i is the simple reflection associated to α_i from our basis of symmetry roots in Figure 4.2, which we recall gives a Cremona isometry

$$r_j(\lambda) = \lambda + (\alpha_j \cdot \lambda)\alpha_j, \tag{4.48}$$

for $\lambda \in \mathrm{Pic}(\mathcal{X})$, but we have chosen slightly different generators for $\mathrm{Aut}(D_4^{(1)})$ than we did in the standard model in Section 2.3 and used notation to emphasise the permutations of simple roots which they induce.

Proposition 4.2.4. *The mapping ψ is a Cremona isometry for the family $\mathcal{X}$ of $D_4^{(1)}$-surfaces and acts on the symmetry roots according to*

$$\psi : \begin{cases} \alpha_0 & \mapsto & \alpha_1 \\ \alpha_1 & \mapsto & \alpha_0 \\ \alpha_2 & \mapsto & \alpha_2 + \delta \\ \alpha_3 & \mapsto & \alpha_4 - \delta \\ \alpha_4 & \mapsto & \alpha_3 - \delta. \end{cases} \tag{4.49}$$

Here $\delta = -\mathcal{K}_{\mathcal{X}} = 2\mathcal{H}_x + 2\mathcal{H}_y - \mathcal{F}_1 - \cdots \mathcal{F}_8$. Further, ψ can be written in terms of generators of $\widetilde{W}(D_4^{(1)})$ as

$$\psi = r_2 r_0 r_1 r_2 r_3 r_4 = \pi_{(01)(34)} T_v, \tag{4.50}$$

where T_v is the Kac translation associated to the weight $v = \frac{1}{2}(\alpha_3 + \alpha_4) \in \mathring{P}(R^{\perp}) = P(D_4)$, and $\pi_{(01)(34)} = \pi_{(01)}\pi_{(34)}$ is the Dynkin diagram automorphism corresponding to the permutation $(01)(34)$ of indices of simple roots.

Proof. To verify that ψ is a Cremona isometry, we check directly from (4.36) that ψ fixes each of $\delta_0, \delta_1, \delta_2, \delta_3$ and δ_4 and therefore the canonical class in $\mathrm{Pic}(X)$, and that ψ preserves the intersection product. We also note that as ψ is induced by the pullbacks of isomorphisms it must preserve effectiveness of classes in $\mathrm{Pic}(\mathcal{X})$. The action of the element ψ on the symmetry root lattice $Q(R^{\perp})$ is found to be given by (4.49) by direct calculation. By standard techniques [Kac90, KNY17, DT18], we obtain the expression

$$\psi = r_2 r_0 r_1 r_2 r_3 r_4 = r_{201234}, \tag{4.51}$$

where for conciseness we have used the subscript notation to indicate the composition of a sequence of simple reflections. We note that ψ is not itself a translation, otherwise it would act on the simple roots by adding multiples of the null root δ. Consider the Dynkin diagram automorphism $\pi_{(01)(34)}$ which acts on the simple roots by permutation $(01)(34)$ of their indices, and is realised by the following action on $\mathrm{Pic}(\mathcal{X})$:

$$\pi_{(01)(34)}: \quad \mathcal{F}_1 \leftrightarrow \mathcal{F}_2, \quad \mathcal{F}_3 \leftrightarrow \mathcal{F}_4, \quad \mathcal{F}_5 \leftrightarrow \mathcal{F}_6, \quad \mathcal{F}_7 \leftrightarrow \mathcal{F}_8. \tag{4.52}$$

The composition of this with ψ acts on the symmetry root lattice according to

$$\pi_{(01)(34)}\psi \;:\; \langle \alpha_0, \alpha_1, \alpha_2, \alpha_3, \alpha_4 \rangle \mapsto \langle \alpha_0, \alpha_1, \alpha_2, \alpha_3, \alpha_4 \rangle + \langle 0, 0, 1, -1, -1 \rangle \, \delta, \tag{4.53}$$

which is translational, as we now demonstrate. To determine the weight vector $v \in P(\mathring{R}^{\perp}) = P(D_4)$ giving this action via the Kac translation T_v, we form an ansatz $v = \sum_{j=1}^{4} c_j \alpha_j$, and determine rational coefficients c_j such that

$$(v \cdot \alpha_0, v \cdot \alpha_1, v \cdot \alpha_2, v \cdot \alpha_3, v \cdot \alpha_4) = (0, 0, 1, -1, -1), \tag{4.54}$$

which ensures T_v gives the action (4.53) according to the Kac translation formula (2.19). By direct calculation in this case we obtain the unique solution $(c_1, c_2, c_3, c_4) = (0, 0, 1/2, 1/2)$, so we have the translation weight

$$v = \frac{1}{2} \left(\alpha_3 + \alpha_4 \right), \tag{4.55}$$

and the proof is complete. □

Remark 4.2.5. *The weight vector v has squared length $||v||^2 = -(v \cdot v) = 1$, which is minimal among all nonzero elements of $P(D_4)$, so we may think of v as a 'nearest-neighbour connecting vector' in the D_4 weight lattice, in the same sense as in the work of Ramani, Grammaticos and Ohta on inequivalent discrete Painlevé equations from non-conjugate translations* [ORG01]*, which was built on by Joshi and Nakazono* [JN17]. *Further, we have that*

$$\psi^2 = T_v^2 = T_{2v}, \tag{4.56}$$

so in particular the element $\psi = \pi_{(01)(34)} T_v$ is of infinite order in $\widetilde{W}(D_4^{(1)})$. Further, if we *are to regard* (4.3) *as a projective reduction of a discrete Painlevé equation, it is the one given by the translation* T_{2v}. *This contrasts with the projective reduction* (4.11) *introduced in the introduction, in the sense that the element* $R \in \widetilde{W}\left((A_2 + A_1)^{(1)}\right)$ *squared to give a translation by a nearest-neighbour connecting vector, which* T_{2v} *is not.*

4.3 Generic version of the equation

We have found that the system (4.3) is associated with a family of $D_4^{(1)}$-surfaces with less than the full number of parameters, and corresponds to a non-translation element of infinite order in $\widetilde{W}(D_4^{(1)})$. In this section, we demonstrate first how the equation may be recovered as a projective reduction using a birational representation of the symmetry group on a family of generic $D_4^{(1)}$-surfaces generalising that obtained above. Unlike previous studies of projective reductions, we proceed to show that although the action of the element of the symmetry group is not translational on the full parameter space, it still defines a discrete equation with the full number of parameters, which we construct explicitly from the Cremona action on the generic family of surfaces.

4.3.1 Family of $D_4^{(1)}$-surfaces and Cremona action

The first step in our construction of a full-parameter version of the system (4.3) is to define a family of generic $D_4^{(1)}$-surfaces through a point configuration generalising that which gave $X_{k,n}$ in Subsection 4.2.1. We introduce extra parameters controlling basepoint locations first in a naive way, and give a birational representation of $\widetilde{W}(D_4^{(1)})$ on this family, with the system (4.3) recovered as a projective reduction. We then obtain the root variable parametrisation in Subsection 4.3.2, which allows our full-parameter version to be constructed explicitly.

Proposition 4.3.1. *Consider the surface* $\mathcal{X}_{\mathbf{b}} = \mathcal{X}_{(k,b_1,b_2,b_3,b_4)}$ *obtained from* $\mathbb{P}^1 \times \mathbb{P}^1$ *by blowing up points* $q_1, \ldots, q_8$ *given in coordinates by*

$$\begin{aligned}
q_1 &: (x,y) = (k,0), & q_5 &: (u_1,v_1) = \left(\frac{x-k}{y}, y\right) = (b_1, 0)\,, \\
q_2 &: (X,Y) = (k,0), & q_6 &: (u_2,v_2) = \left(\frac{X-k}{Y}, Y\right) = (b_2, 0)\,, \\
q_3 &: (x,y) = (0,k), & q_7 &: (u_3,v_3) = \left(\frac{x}{y-k}, y-k\right) = (b_3, 0)\,, \\
q_4 &: (X,Y) = (0,k), & q_8 &: (u_4,v_4) = \left(\frac{X}{Y-k}, Y-k\right) = (b_4, 0)\,.
\end{aligned} \tag{4.57}$$

Then $\mathcal{X}_{\mathbf{b}}$ form a family of generic $D_4^{(1)}$-surfaces, with surface and symmetry root bases in $\mathrm{Pic}(\mathcal{X})$ *given as in Figure 4.2. Further, we have a Cremona action of the symmetry group* $\widetilde{W}(D_4^{(1)})$*, with generators as in* (4.46)*. We give this as in Subsection 2.2.4, namely as maps*

$$\begin{aligned} \phi_w :\ \mathcal{X}_{\mathbf{b}} &\to \mathcal{X}_{w\cdot\mathbf{b}}, \\ (x,y) &\mapsto (w\cdot x, w\cdot y), \end{aligned} \tag{4.58}$$

such that $\phi_w^* : \mathrm{Pic}(\mathcal{X}_{w\cdot\mathbf{b}}) \to \mathrm{Pic}(\mathcal{X}_{\mathbf{b}})$ *induces the Cremona isometry* $w \in \widetilde{W}(D_4^{(1)})$*. We specify the action below in the following format:*

$$w : \begin{pmatrix} w\cdot b_1 & w\cdot b_2 & \multirow{2}{*}{$w\cdot k$} & \multirow{2}{*}{;} & w\cdot x \\ w\cdot b_3 & w\cdot b_4 & & & w\cdot y \end{pmatrix} \tag{4.59}$$

For the simple reflections we have the following:

$$r_0 : \begin{pmatrix} k^2-1-b_1 & \frac{(k^2-1)^2-b_1b_2}{k^2-1-b_1} & k & ; & \frac{(b_1+1)xy-kx-ky+k^2}{kxy-x+(b_1-k^2)y+k} \\ \frac{1-b_1b_3}{k^2-1-b_1} & \frac{1-b_1b_4}{k^2-1-b_1} & & & y \end{pmatrix}$$

$$r_1 : \begin{pmatrix} \frac{(k^2-1)^2-b_1b_2}{k^2-1-b_2} & k^2-1-b_2 & k & ; & \frac{kxy+(b_2-k^2)x-ky+k}{k^2xy-kx-ky+(b_2+1)} \\ \frac{1-b_2b_3}{k^2-1-b_2} & \frac{1-b_2b_4}{k^2-1-b_2} & & & y \end{pmatrix}$$

$$r_2 : \begin{pmatrix} \frac{(k^2-1)^2}{b_1} & \frac{(k^2-1)^2}{b_2} & k & ; & \frac{y-k}{ky-1} \\ \frac{1}{b_3(k^2-1)^2} & \frac{1}{b_4(k^2-1)^2} & & & \frac{x-k}{kx-1} \end{pmatrix}$$

$$r_3 : \begin{pmatrix} \frac{(k^2-1)(b_1b_3-1)}{(k^2-1)b_3-1} & \frac{(k^2-1)(b_2b_3-1)}{(k^2-1)b_3-1} & k & ; & \frac{x(k-y)\big((k^2-1)b_3-1\big)}{x(ky-1)-b_3(k^2-1)(y-k)} \\ (k^2-1)^{-1}-b_3 & \frac{(k^2-1)^2b_3b_4-1}{(k^2-1)^2b_3-k^2+1} & & & y \end{pmatrix}$$

$$r_4 : \begin{pmatrix} \frac{(k^2-1)^2(1-b_1b_4)}{(k^2-1)b_4-1} & \frac{(k^2-1)^2(1-b_2b_4)}{(k^2-1)b_4-1} & k & ; & \frac{b_4(k^2-1)x(ky-1)-y+k}{(ky-1)(b_4(k^2-1)-1)} \\ \frac{(k^2-1)^2b_3b_4-1}{1-k^2-b_4(k^2-1)^2} & (k^2-1)^{-1}-b_4 & & & y \end{pmatrix}$$

For our chosen generators of $\mathrm{Aut}(D_4^{(1)})$ *we have the following:*

$$\pi_{(10)}: \begin{pmatrix} -b_2/k^2 & -b_1/k^2 & \multirow{2}{*}{k} & ; & x \\ -k^2 b_3 & -k^2 b_4 & & & \frac{1}{y} \end{pmatrix}$$

$$\pi_{(34)}: \begin{pmatrix} -b_1/k^2 & -b_2/k^2 & \multirow{2}{*}{\frac{1}{k}} & ; & \frac{1}{x} \\ -k^2 b_4 & -k^2 b_3 & & & y \end{pmatrix}$$

$$\pi_{(14)}: \begin{pmatrix} b_1/(k^2-1)^2 & b_4 & \multirow{2}{*}{\frac{k}{(k^2-1)^2}} & ; & \frac{x(k^2-1)^{1/2}}{kx-1} \\ (k^2-1)^2 b_3 & b_2 & & & \frac{y(k^2-1)^{1/2}}{ky-1} \end{pmatrix}$$

Proof. We first note that the point configuration given in (4.57) generalises the one leading to $\mathcal{X}_{k,n}$, and clearly leads to a unique anticanonical divisor with the same $D_4^{(1)}$ intersection configuration of irreducible components. The fact that this configuration leads to a family of generic $D_4^{(1)}$-surfaces will be established when we compute the root variables for $\mathcal{X}_{\mathbf{b}}$ in Subsection 4.3.2. The birational mapping defined by the action of each generator may be verified to give an isomorphism with required pullback by the same methods as used throughout the thesis to lift mappings to isomorphisms and deduce their pullbacks. The methods for constructing the Cremona action are the same as those used in Subsection 3.2.8 and Subsection 3.3.2 to obtain isomorphisms of Sakai surfaces from a required action on the level of Picard lattices. For more examples of this kind of calculation we refer the reader to, for example, one of [Sak01, MSY03, DT18, JNS1608, KNY17]. □

Before we construct the generic version of the system (4.3), we illustrate how to recover it from the Cremona action action of ψ. To reconstruct the equation, we compute the action of the element $\psi = r_{201234}$ on the variables and parameters. Using the formulae given in Proposition 4.3.1, we compute $\psi \cdot f$ and $\psi \cdot g$, which are complicated rational functions of the variables and parameters, which we omit for the moment for conciseness.

We also find that $\psi \cdot \mathbf{b} = (\psi \cdot k, \psi \cdot b_1, \psi \cdot b_2, \psi \cdot b_3, \psi \cdot b_4)$ is given by

$$\psi \cdot k = k, \tag{4.60a}$$
$$\psi \cdot b_1 = b_2 + \frac{b_2 b_3 - 1}{b_3 + t} + \frac{b_2 b_4 - 1}{b_4 + t} + \frac{b_1 - b_2}{1 + b_1 t}, \tag{4.60b}$$
$$\psi \cdot b_2 = b_1 + \frac{b_1 b_3 - 1}{b_3 + t} + \frac{b_1 b_4 - 1}{b_4 + t} + \frac{b_2 - b_1}{1 + b_2 t}, \tag{4.60c}$$
$$\psi \cdot b_3 = \frac{(1 + b_1 t)(1 + b_2 t)(b_3 + t) b_4}{(b_4 + t)\left(2 b_1 b_2 b_3 t + b_1 b_2 t^2 + (b_1 + b_2) b_3 - 1\right)}, \tag{4.60d}$$
$$\psi \cdot b_4 = \frac{(1 + b_1 t)(1 + b_2 t)(b_4 + t) b_3}{(b_3 + t)\left(2 b_1 b_2 b_4 t + b_1 b_2 t^2 + (b_1 + b_2) b_4 - 1\right)}, \tag{4.60e}$$

where we have denoted $t = 1/(1 - k^2)$. We note that this is not a translational motion in the parameter space, but if we restrict to the case when $\mathbf{b} = (k, b_1, b_1, 0, 0)$, then ψ acts on this parameter subspace by translation, with $\psi \cdot (k, b_1, b_1, 0, 0) = (k, b_1 - 2/t, b_1 - 2/t, 0, 0)$. Therefore the result of iterating the action on parameters n times is given by

$$\begin{aligned} \psi^n \cdot (k, b_1, b_1, 0, 0) &= (k, b_1 - 2n/t, b_1 - 2n/t, 0, 0) \\ &= (k, b_1 - 2n(1 - k^2), b_1 - 2n(1 - k^2), 0, 0). \end{aligned} \tag{4.61}$$

With this restriction of parameters the rational functions giving the action of ψ on x and y simplify considerably, and letting $x_n = \psi^n \cdot x, y_n = \psi^n \cdot y$ we obtain the following system of difference equations.:

$$\bar{x} = \frac{(\bar{y} - k)^2}{x(k\bar{y} - 1)^2}, \tag{4.62a}$$
$$\bar{y} = \frac{(x - k)}{(kx - 1)} \frac{k(1 - k^2)xy + (b_1 + 2n(k^2 - 1))x + (k^2 - 1)y - k(b_1 + 2n(k^2 - 1))}{(k(b_1 + 2n(k^2 - 1))xy + (1 - k^2)x - (b_1 + 2n(k^2 - 1))y + k(k^2 - 1)}, \tag{4.62b}$$

where $(x, y) = (x_n, y_n), (\bar{x}, \bar{y}) = (x_{n+1}, y_{n+1})$. Setting the initial value of the parameter to be $b_1 = k^2 - 1 = -1/t$, we recover (4.3), as well as the family of surfaces $\mathcal{X}_{k,n}$ constructed in Subsection 4.2.1.

Remark 4.3.2. *We note that the process by which we recovered the system* (4.3) *from the birational representation is a projective reduction as described in Section 4.1. However, with the root variable parametrisation, the action of ψ becomes translational on a larger parameter subspace than the one on which $\mathbf{b} = (k, b_1, b_1, 0, 0)$. This involves four free parameters, and is given by $a_1 = a_2, a_3 = a_4$ in the root variable parametrisation to be ob-*

tained in the next subsection. Thus the system (4.3) *differs from the example from* [KNT11] *described in the introduction, in which the projection was onto the maximal parameter subspace on which the element $R \in \widetilde{W}((A_2 + A_1)^{(1)})$ gave translational motion. The way in which* (4.3) *was obtained from ψ above corresponds to restricting to the parameter subspace defined in terms of root variables by $a_1 = a_2, a_3 = a_4$, so in this sense equation* (4.3) *is not the most general projective reduction associated with the Cremona isometry ψ. At the end of Subsection 4.3.3 we will explain how to recover the most general projective reduction arising from ψ from our full-parameter generalisation.*

4.3.2 Root variables and transformation to the standard model

To write down an equation from the Cremona action of ψ on the full family of generic $D_4^{(1)}$-surfaces, we let $(x_n, y_n) = \psi^n \cdot (x, y)$ be the result of acting by ψ on the variables n times, and seek an explicit form of $\psi^n \cdot \mathbf{b}$ as a function of n. Obtaining this expression amounts to solving the system of difference equations (4.60), which are nonlinear in their present form. However, if we change our parametrisation of the family of surfaces to that given by root variables, the transformation of parameters will linearise the system (4.60) and it will be explicitly solvable by elementary methods. This will be the case for the action of any element of infinite order on the root variables, so difference equations can always be explicitly constructed from these elements, as we will demonstrate.

Rather than obtaining the root variable parametrisation from the period map by directly computing integrals as in Subsection 2.3.2 and Subsection 3.2.7, we will obtain it via a transformation to the standard model of $D_4^{(1)}$ surfaces from Section 2.3, which also reveals (4.3) as a Bäcklund transformation for a special case of $\mathrm{P_{VI}}$. The method will be similar to that in Subsection 3.2.8, though here it is not used to identify some equation with a standard example, but rather to provide a shortcut for obtaining the root variables.

We denote the family of surfaces from the standard model again by $\mathcal{X}^{\mathrm{KNY}}$, but denote the individual surfaces by $\mathcal{X}_{\mathbf{a}}^{\mathrm{KNY}}$ with parameters given by root variables $\mathbf{a} = (t, a_0, a_1, a_2, a_3, a_4)$, to distinguish them from our surfaces $\mathcal{X}_{\mathbf{b}}$. Again we begin with an identification on the level of Picard lattices, then find an isomorphism of the surfaces realising this.

Proposition 4.3.3. *The identification of* $\mathrm{Pic}(\mathcal{X})$ *and* $\mathrm{Pic}(\mathcal{X}^{\mathrm{KNY}})$ *given by*

$$\begin{aligned} \mathcal{H}_x &= \mathcal{H}_f + \mathcal{H}_g - \mathcal{E}_1 - \mathcal{E}_5, & \mathcal{H}_y &= \mathcal{H}_f, \\ \mathcal{F}_1 &= \mathcal{E}_3, & \mathcal{F}_5 &= \mathcal{E}_4, \\ \mathcal{F}_2 &= \mathcal{H}_f - \mathcal{E}_1, & \mathcal{F}_6 &= \mathcal{E}_2, \\ \mathcal{F}_3 &= \mathcal{E}_7, & \mathcal{F}_7 &= \mathcal{E}_8, \\ \mathcal{F}_4 &= \mathcal{H}_f - \mathcal{E}_5, & \mathcal{F}_8 &= \mathcal{E}_6. \end{aligned} \tag{4.63}$$

preserves the intersection product and identifies the surface and symmetry root bases from the standard model with those in Figure 4.2 for our family of surfaces.

Proposition 4.3.4. *We have an isomorphism inducing the identification above, defined by*

$$\begin{aligned} \eta \,:\, \mathcal{X}_{\mathbf{b}} &\to \mathcal{X}_{\mathbf{a}}^{\mathrm{KNY}}, \\ (x,y) &\mapsto (f(x,y), g(x,y)) \end{aligned} \tag{4.64}$$

where

$$f = \frac{ky-1}{k^2-1}, \qquad g = \frac{a_2}{k}\frac{(1-kx)(ky-1)}{k(kxy-x-y+k)}, \tag{4.65}$$

and the parameters $\mathbf{a}$ *and* $\mathbf{b}$ *are related according to*

$$\begin{aligned} &b_1 = -\frac{a_0+a_2}{ta_0}, \qquad b_2 = -\frac{a_1+a_2}{ta_1}, \qquad b_3 = -\frac{t(a_2+a_3)}{a_3}, \\ &b_4 = -\frac{t(a_2+a_4)}{a_4}, \qquad t = \frac{1}{1-k^2}. \end{aligned} \tag{4.66}$$

Proof. This is once again a standard computation, but we will give some details to complement those given for the similar calculation in Subsection 3.2.8. Again we begin with an ansatz for the map in coordinates. As our identification requires $\eta^*(\mathcal{H}_f) = \mathcal{H}_y$, we take

$$f = \frac{\lambda_1 y + \lambda_2}{\lambda_3 y + \lambda_4}, \tag{4.67}$$

with $\lambda_1, \ldots, \lambda_4$ to be determined. Similarly we require $\eta^*(\mathcal{H}_g) = \mathcal{H}_x + \mathcal{H}_y - \mathcal{F}_2 - \mathcal{F}_4$, so a generic line of constant g should correspond to a $(1,1)$-curve in (x,y) coordinates passing through q_2 and q_4, each with multiplicity one, and we take

$$g = \frac{\mu_1 xy + \mu_2 x + \mu_3 y + \mu_4}{\mu_5 xy + \mu_6 x + \mu_7 y + \mu_8}, \tag{4.68}$$

where $\mu_1, \ldots, \mu_8$ are also to be determined. Indeed, letting $c \in \mathbb{C}$ be arbitrary and setting $y = c$ in (4.68) we obtain a $(1,1)$-curve, which we rewrite in the chart (X, Y), in which q_2, q_4 are visible, as

$$c\left(\mu_5 + \mu_6 Y + \mu_7 X + \mu_8 XY\right) = \mu_1 + \mu_2 Y + \mu_3 X + \mu_4 XY. \tag{4.69}$$

If $q_2 : (X, Y) = (k, 0)$ lies on this curve, we must have

$$c(\mu_5 + k\mu_7) = \mu_1 + k\mu_3. \tag{4.70}$$

This must be true independent of the value of the constant c, so that g is a coordinate on a pencil of curves with q_2 as a basepoint, so we require

$$\mu_1 = -k\mu_3, \qquad \mu_5 = -k\mu_7. \tag{4.71}$$

Similarly, the requirement that $q_4 : (X, Y) = (0, k)$ is also a basepoint of the pencil leads to the conditions

$$\mu_6 = \mu_7, \qquad \mu_3 = \mu_2, \tag{4.72}$$

after which our ansatz reads

$$g = \frac{\mu_4(kxy - x - y) + k\mu_1}{k(kxy - x - y + k)}. \tag{4.73}$$

Before finding the coefficients μ_1, μ_4, it will be convenient to first determine the fractional linear transformation (4.67) relating f and y. It is convenient to consider hyperplanes of certain constant values of f and y, whose proper transforms give unique representatives of their divisor classes. For example, we require $\eta_*(\mathcal{H}_y - \mathcal{F}_3) = \mathcal{H}_f - \mathcal{E}_7$, so setting $y = k$ in (4.67) should lead to $f = 1$ and we obtain

$$\lambda_4 = k(\lambda_1 - \lambda_3) + \lambda_2. \tag{4.74}$$

Similarly, $\eta_*(\mathcal{H}_y - \mathcal{F}_1) = \mathcal{H}_f - \mathcal{E}_3$ so when $y = k$ we should have $f = t$, which gives λ_2 in terms of the other coefficients and parameters, and our ansatz is refined:

$$f = \frac{\lambda_1(t-1)y + kt(\lambda_3 - \lambda_1)}{\lambda_3(t-1)y + k(\lambda_1 - \lambda_3)}. \tag{4.75}$$

A third condition may be deduced from the requirement that $\eta_*(\mathcal{H}_y - \mathcal{F}_2) = \mathcal{E}_1$, so the proper transform of the line $Y = 0$ should be mapped to the exceptional divisor E_1, and in particular rewriting (4.75) in terms of $Y = 1/y$ and setting $Y = 0$ should recover the f-coordinate of p_1. Direct calculation yields $\lambda_3 = 0$, and therefore

$$f = \frac{(1-t)y + kt}{k}. \tag{4.76}$$

The parameters k and t each correspond to the 'extra parameter' playing the role of the independent variable of $\mathrm{P_{VI}}$ in their respective families of $D_4^{(1)}$-surfaces, and their relationship can be deduced as follows. We have already found the unknown coefficients in the relation between y and f, by considering (-1)-curves given by proper transforms of lines of constant y passing through basepoints q_1, q_2, q_3. However, there is one more such exceptional class which we have not considered, and we must verify that (4.76) is consistent with the required image of the corresponding divisor class under η_*. To be precise, we should have $\eta_*(\mathcal{H}_y - \mathcal{F}_4) = \mathcal{E}_5$, so setting $Y = k$ in (4.76) should recover the f-coordinate of p_5, namely $f = 0$. This condition is computed to be equivalent to

$$t = \frac{1}{1-k^2}, \tag{4.77}$$

so we have obtained a necessary correspondence between the parameters k and t such that η realises the identification.

We now return to our expression (4.73) for g, and use similar calculations to determine the remaining unknown coefficients. For instance, in order to satisfy the condition $\eta_*(\mathcal{H}_y - \mathcal{F}_2) = \mathcal{E}_1$, we require that setting $Y = 0$ with $X \neq k$ in (4.73) and (4.76) gives the (x, y)-coordinates of p_1. We have already imposed this condition on the expression for x, so substitute in to (4.73) to obtain

$$\mu_4 = -k a_2. \tag{4.78}$$

A similar calculation based on $\eta_*(\mathcal{H}_y - \mathcal{F}_4) = \mathcal{E}_5$ leads to the condition

$$\mu_1 = -(a_1 + a_2)/k, \tag{4.79}$$

and we have determined all unknown coefficients and obtained the birational map $(x, y) \mapsto (f, g)$ as in (4.65).

We now demonstrate how to obtain the correspondences between the remaining parameters. We require that $\eta_*(\mathcal{F}_5) = \mathcal{E}_4$, so the basepoint q_5 on the exceptional line F_1 in $\mathcal{X}_{\mathbf{b}}$ should be mapped under η to somewhere over p_4 on the line E_3. To compute this condition, we will use the same notation for the chart (u_1, v_1) in the neighbourhood of the exceptional line F_1 on $\mathcal{X}_{\mathbf{b}}$, but relabel the one defined in Section 2.3 covering an affine part of E_3 from (u_3, v_3) to $(\tilde{u}_3, \tilde{v}_3)$ to distinguish between the surfaces $\mathcal{X}_{\mathbf{b}}$ and $\mathcal{X}_{\mathbf{a}}^{\mathrm{KNY}}$. We recall that this chart is given by

$$\tilde{u}_3 = \frac{f-t}{G}, \qquad \tilde{v}_3 = G. \tag{4.80}$$

Substituting these coordinates in our expressions (4.65) for f, g in terms of x, y, we obtain

$$\tilde{u}_3 = \frac{a_2(kv_1-1)(1-k^2-ku_1v_1)}{(k^2-1)(k^2-1-u_1+ku_1v_1)}, \qquad \tilde{v}_3 = \frac{kv_1(k^2-1-u_1+ku_1v_1)}{a_2(kv_1-1)(1-k^2-ku_1v_1)}, \tag{4.81}$$

in which setting $v_1 = 0$ leads to

$$\tilde{u}_3 = \frac{a_2}{k^2-1-u_1}, \qquad \tilde{v}_3 = 0, \tag{4.82}$$

which demonstrates that η indeed gives a one-to-one correspondence between the exceptional lines F_1 and E_3. Requiring that $q_5 : (u_1, v_1) = (b_1, 0)$ is mapped to $p_4 : (\tilde{u}_3, \tilde{v}_3) = (ta_0, 0)$, we obtain the condition

$$b_1 = -\frac{a_0+a_2}{ta_0}. \tag{4.83}$$

Similar calculations based on the requirements $\eta_*(\mathcal{F}_7) = \mathcal{E}_8,\ \eta_*(\mathcal{F}_6) = \mathcal{E}_2,\ \eta_*(\mathcal{F}_8) = \mathcal{E}_6$ yield the rest of the correspondences (4.66). The proof is completed by checking, using the same calculation methods as throughout the thesis, that the birational map $(x, y) \mapsto (f, g)$ we have obtained does indeed induce the required identification when parameters are related according to (4.66). $\square$

We note that this transformation, and in particular the parameter correspondence, recovers the root variables for the surface $\mathcal{X}_{\mathbf{b}}$ for with the symmetry roots given in Figure 4.2. This is for the same reason, as was given in Subsection 2.2.4, for the correspondence between the Cremona isometry induced by a discrete Painlevé equation and the evolution of the root variables. Because the isomorphism η has been chosen such that it identifies the surface and symmetry roots, in choosing the rational 2-form defining the period mapping on $\mathcal{X}_{\mathbf{b}}$ we can choose the normalisation such that it coincides with the pullback $\eta^*\omega$ of the one on $\mathcal{X}_{\mathbf{a}}^{\mathrm{KNY}}$. As in Lemma 2.3.1, take the (normalised) rational 2-form ω on $\mathcal{X}_{\mathbf{a}}^{\mathrm{KNY}}$ and use it to define the period mapping χ, so the root variables associated with $\alpha_i \in \mathrm{Pic}(\mathcal{X}_{\mathbf{a}})$ are

$$a_i = \chi(\alpha_i). \tag{4.84}$$

To find the root variables for $\mathcal{X}_{\mathbf{b}}$ we take the symmetry roots for $\mathcal{X}_{\mathbf{b}}$ from Figure 4.2, which we now write as $\bar{\alpha}_i = \eta^*(\alpha_i)$ to make the identification via η explicit. Using the 2-form $\eta^*\omega$ we define the period mapping $\bar{\chi}$ on $\mathcal{X}_{\mathbf{b}}$, so the root variables are $\bar{\chi}(\bar{\alpha}_i)$.
As in the computation of root variables in Subsection 2.3.2, write each symmetry root as the difference of two classes of curves

$$\bar{\alpha}_i = [\bar{C}_i^1] - [\bar{C}_i^0] = \eta^*[C_i^1] - \eta^*[C_i^0], \tag{4.85}$$

where we have used the fact that η is an isomorphism to pull back $\bar{C}_i^1, \bar{C}_i^0$. We then have a unique component D_k of the anticanonical divisor of $\mathcal{X}_{\mathbf{b}}$ such that

$$D_k \cdot C_i^1 = D_k \cdot C_i^0 = \eta_*(D_k) \cdot \eta_*(C_i^1) = \eta_*(D_k) \cdot \eta_*(C_i^0) = 1, \tag{4.86}$$

and we have the points of intersection $P_i, Q_i \in \mathcal{X}_{\mathbf{b}}$, $\bar{P}_i, \bar{Q}_i \in \mathcal{X}_{\mathbf{a}}^{\mathrm{KNY}}$ given by:

$$\begin{aligned} P_i &= D_k \cap C_i^0, & \bar{P}_i &= \eta_*(D_k) \cap \eta_*(C_i^0), \\ Q_i &= D_k \cap C_i^1, & \bar{Q}_i &= \eta_*(D_k) \cap \eta_*(C_i^1). \end{aligned} \tag{4.87}$$

We can then compute the root variables, with the isomorphism η essentially giving a change of variables in the integral::

$$\begin{aligned} \bar{\chi}(\bar{\alpha}_i) &= \bar{\chi}\left([\bar{C}_i^1] - [\bar{C}_i^0]\right) = \bar{\chi}\left(\eta^*[C_i^1] - \eta^*[C_i^0]\right) \\ &= \int_{\bar{P}_i}^{\bar{Q}_i} \frac{1}{2\pi \mathrm{i}} \oint_{\eta_*(D_k)} \eta^*\omega = \int_{P_i}^{Q_i} \frac{1}{2\pi \mathrm{i}} \oint_{D_k} \omega = \chi(\alpha_i) = a_i. \end{aligned} \tag{4.88}$$

Remark 4.3.5. *The process of constructing the isomorphism η has given us the root variable parametrisation of the family $\mathcal{X}_{\mathbf{b}}$. Solving the system* (4.66) *for the root variables $a_0, \ldots, a_4$, we see that they are given by rational functions of degree three in the parameters $b_1, \ldots, b_4$, which suggests that if we were to compute them directly using the period* *mapping it would have involved evaluating complicated integrals, which this transformation has allowed us to avoid.*

4.3.3 Full-parameter generalisation of Hoffmann's discrete $\mathbf{P}_{\mathrm{III}}$

We are now in a position to construct the full-parameter version of (4.3) using our Cremona action of $\widetilde{W}(D_4^{(1)})$ on the family of generic $D_4^{(1)}$-surfaces. We begin by taking the parametrisation of this family by root variables, so the surface $\mathcal{X}_{\mathbf{b}}$ is now written as $\mathcal{X}_{\mathbf{a}}$, where $\mathbf{a} = (t, a_0, a_1, a_2, a_3, a_4)$ are the root variables as computed in the previous section. We emphasise again that the key to writing down an explicit form of the discrete system defined by the Cremona action of an element of the symmetry group is to obtain the parameter evolution as a function of n. In our case, we are able to do this as the system (4.60) giving the action of the element $\psi = r_{201234}$ on the parameters is linearised by the transformation to root variables, and we now have

$$\psi \cdot (t, a_0, a_1, a_2, a_3, a_4) = (t, a_1, a_0, a_2 + 1, a_4 - 1, a_3 - 1). \tag{4.89}$$

This leads to a linear difference equation for $\psi^n \cdot \mathbf{a}$, which we may solve explicitly by elementary methods to arrive at the following formulae:

$$\psi^n \cdot t = t, \qquad \psi^n \cdot k = k, \tag{4.90a}$$

$$\psi^n \cdot a_0 = \frac{1}{2}\left((1 + (-1)^n)a_0 + (1 - (-1)^n)a_1\right) = \begin{cases} a_0 & \text{for } n \text{ even}, \\ a_1 & \text{for } n \text{ odd}, \end{cases} \tag{4.90b}$$

$$\psi^n \cdot a_1 = \frac{1}{2}\left((1 - (-1)^n)a_0 + (1 + (-1)^n)a_1\right) = \begin{cases} a_1 & \text{for } n \text{ even}, \\ a_0 & \text{for } n \text{ odd}, \end{cases} \tag{4.90c}$$

$$\psi^n \cdot a_2 = a_2 + n, \tag{4.90d}$$

$$\psi^n \cdot a_3 = \frac{1}{2}\left((1 + (-1)^n)a_3 + (1 - (-1)^n)a_4 - 2n\right) = \begin{cases} a_3 - n & \text{for } n \text{ even}, \\ a_4 - n & \text{for } n \text{ odd}, \end{cases} \tag{4.90e}$$

$$\psi^n \cdot a_4 = \frac{1}{2}\left((1 - (-1)^n)a_3 + (1 + (-1)^n)a_4 - 2n\right) = \begin{cases} a_4 - n & \text{for } n \text{ even}, \\ a_3 - n & \text{for } n \text{ odd}. \end{cases} \tag{4.90f}$$

Therefore by setting $x_n = \psi^n \cdot x$ and $y_n = \psi^n \cdot y$ with the Cremona action of ψ, we obtain the explicit form of our full-parameter version of equation (4.3), which we write with $(x, y) = (x_n, y_n)$ and $(\bar{x}, \bar{y}) = (x_{n+1}, y_{n+1})$ as follows, where a_i are now parameters and we have written the n-dependence explicitly:

$$\bar{x} = \frac{(\bar{y} - k)}{(k\bar{y} - 1)} \frac{\Big((a_2 + a_{34}^{(n+1)})x(k\bar{y} - 1) + (\bar{y} - k)(a_{34}^{(n)} - n - 1)\Big)}{\Big((a_2 + a_{34}^{(n)})(\bar{y} - k) + x(k\bar{y} - 1)(a_{34}^{(n+1)} - n - 1)\Big)}, \tag{4.91a}$$

$$\bar{y} = \frac{(x - k)}{(kx - 1)} \frac{\Big((x - k)(a_2 + n) - a_{01}^{(n+1)}(kxy - x - y + k)\Big)}{\Big(y(kx - 1)(a_2 + n) + a_{01}^{(n)}(kxy - x - y + k)\Big)}, \tag{4.91b}$$

$$\text{where} \qquad a_{01}^{(n)} = \begin{cases} a_0 & \text{for } n \text{ even}, \\ a_1 & \text{for } n \text{ odd}, \end{cases} \qquad a_{34}^{(n)} = \begin{cases} a_3 & \text{for } n \text{ even}, \\ a_4 & \text{for } n \text{ odd}, \end{cases}$$

and $a_0 + a_1 + 2a_2 + a_3 + a_4 = 1$. The parameter specialisation $(b_1, b_2, b_3, b_4) = (k^2 - 1, k^2 - 1, 0, 0)$ by which we recovered (4.3) in subsection 4.1 is given in terms of the parameters in (4.91) as $(a_0, a_1, a_2, a_3, a_4) = (1/2, 1/2, 0, 0, 0)$, substitution of which again recovers the original system (4.3).

More generally, the root variable parametrisation of a generic family of $\mathcal{R}$-surfaces ensures that the parameter evolution associated with any Cremona isometry leads to a system of linear equations. For multiplicative surface types this will be a linear system for the logarithms of the root variables, and for the elliptic surface type this will be a system of linear difference equations for the arguments of elliptic functions appearing in the coefficients. In any case this can be solved so write the system explicitly with the independent variable n appearing the coefficients, as we illustrate in the following section.

4.4 Integrability and other full-parameter systems from non-translation symmetries

We now discuss the integrability of the full-parameter system (4.91), and give more systems obtained explicitly from the Cremona action of non-translation symmetries of families of $\mathcal{R}$-surfaces without the need for parameter restrictions.

4.4.1 Algebraic entropy

Firstly, we note that system (4.91) in integrable in the sense of vanishing algebraic entropy, which follows from the same result of Takenawa [Tak01a] guaranteeing this property for the discrete Painlevé equations defined by Sakai in terms of translations. To study the degree growth of the system (4.91), we first compute the degrees of the iterates as rational functions of initial conditions as in Subsection 1.2.4. That is, we consider the iteration mappings of (4.91) purely as birational maps of $\mathbb{P}^1 \times \mathbb{P}^1$ defined by

$$\Psi_n : (x_n, y_n) \mapsto (x_{n+1}, y_{n+1}), \tag{4.92}$$

and compute the degrees of the maps

$$\begin{aligned} \Psi^{(n)} = \Psi_{m+n-1} \circ \cdots \circ \Psi_{m+1} \circ \Psi_m \ : \ \mathbb{P}^1 \times \mathbb{P}^1 \to \mathbb{P}^1 \times \mathbb{P}^1, \\ (x_m, y_m) \mapsto (P_n(x_m, y_m), Q_n(x_m, y_m)), \end{aligned} \tag{4.93}$$

as rational functions of initial conditions (x_m, y_m) at some generic iteration step m. Computing the first few iterates of the system (4.91) in this way, we obtain the following:

$$\begin{aligned} \deg P_n(x_m, y_m) = 1, 7, 21, 43, 73, \ldots \\ \deg Q_n(x_m, y_m) = 1, 3, 13, 31, 57, \ldots \end{aligned} \tag{4.94}$$

This appears to be quadratic, and certainly not exponential, which we may confirm by computing explicit expressions for $\deg P_n$ and $\deg Q_n$ using the following method of Takenawa [Tak01a], which is applicable to any second-order discrete system with birational iteration mappings on $\mathbb{P}^1 \times \mathbb{P}^1$ which lift to isomorphisms.

Consider a discrete system given by the Cremona action of some element $w \in \mathrm{Cr}(\mathcal{X}(\mathcal{R}))$ on a family of $\mathcal{R}$-surfaces, where we write the family of isomorphisms lifted from the iteration mappings as

$$\begin{aligned} \phi_n : \ \mathcal{X}_{w^n \cdot \mathbf{a}} \to \mathcal{X}_{w^{n+1} \cdot \mathbf{a}}, \\ (x_n, y_n) = (x, y) \mapsto (w \cdot x, w \cdot y) = (x_{n+1}, y_{n+1}). \end{aligned} \tag{4.95}$$

We then denote the system considered as a birational mapping of $\mathbb{P}^1 \times \mathbb{P}^1$ by

$$\begin{aligned} \Phi_n : \ \mathbb{P}^1 \times \mathbb{P}^1 \to \mathbb{P}^1 \times \mathbb{P}^1, \\ (x_n, y_n) \mapsto (x_{n+1}, y_{n+1}), \end{aligned} \tag{4.96}$$

and the following diagram commutes, where the vertical arrows indicate blow-up projections :

$$\begin{array}{ccc} \mathcal{X}_{w^n\cdot\mathbf{a}} & \xrightarrow{\phi_n} & \mathcal{X}_{w^{n+1}\cdot\mathbf{a}} \\ \downarrow & & \downarrow \\ \mathbb{P}^1\times\mathbb{P}^1 & \xrightarrow{\Phi_n} & \mathbb{P}^1\times\mathbb{P}^1 \end{array} \tag{4.97}$$

In terms of the Cremona isometry w induced by the maps ψ_n via their pullbacks, we have the following formulae due to Takenawa [Tak01a]:

$$\begin{aligned} \deg P_n &= w^{-n}(\mathcal{H}_x+\mathcal{H}_y)\cdot\mathcal{H}_x = w^n(\mathcal{H}_x)\cdot(\mathcal{H}_x+\mathcal{H}_y), \\ \deg Q_n &= w^{-n}(\mathcal{H}_x+\mathcal{H}_y)\cdot\mathcal{H}_y = w^n(\mathcal{H}_y)\cdot(\mathcal{H}_x+\mathcal{H}_y). \end{aligned} \tag{4.98}$$

To apply this to the Cremona isometry ψ corresponding to the system (4.91), we obtain an expression for $w^{-n}(\mathcal{H}_x+\mathcal{H}_y)$ in terms of $\mathcal{H}_f, \mathcal{H}_g, \mathcal{E}_1, \dots, \mathcal{E}_8$. Letting this be

$$w^{-n}(\mathcal{H}_x+\mathcal{H}_y) = a_x(n)\mathcal{H}_x + a_y(n)\mathcal{H}_y + \sum_{i=1}^{8} b_i(n)\mathcal{F}_i, \tag{4.99}$$

we use the expression for w in Proposition 4.2.3 to obtain a system of recurrences with respect to n for the functions $a_x(n), a_y(n), b_i(n)$, which is guaranteed to be linear as w is a $\mathbb{Z}$-module automorphism. We solve this using elementary elements subject to the initial conditions $a_x(0) = a_y(0) = 1, b_i(0) = 0$ for $i = 1, \dots, 8$ and obtain

$$\begin{aligned} a_x(n) &= 4n^2 - 2n - 1, \\ a_y(n) &= 4n^2 + 2n + 1, \\ b_1(n) &= -\frac{n}{2}(2n-1), \\ b_2(n) &= b_5(n) = b_6(n) = -n(2n-1), \\ b_3(n) &= b_4(n) = b_7(n) = b_8(n) = -n(2n+1). \end{aligned} \tag{4.100}$$

We can then compute intersection numbers to obtain the degrees exactly as

$$\deg P_n(f,g) = 4n^2 + 2n + 1, \qquad \deg Q_n(f,g) = 4n^2 - 2n + 1. \tag{4.101}$$

These formulae recover the observations of the first few degrees in (4.94) and we have proven that the degree growth is quadratic and the algebraic entropy of the system (4.91) is zero. Takenawa's proof [Tak01a] that the discrete Painlevé equations defined by Sakai have at most quadratic degree growth also applies to any system obtained as the Cremona action of an element of the symmetry group of a family of $\mathcal{R}$-surfaces, so full-parameter systems from non-translational Cremona isometries are guaranteed to be integrable in this sense too.

4.4.2 More examples

We have seen that with the root variable parametrisation, we can always obtain discrete equations explicitly from the Cremona action of non-translation elements of the symmetry group of a generic family of Sakai surfaces of a given type. We will now demonstrate this in the case of the Cremona action of $\widetilde{W}((A_2+A_1)^{(1)})$ on a family of generic $A_5^{(1)}$-surfaces, related to the example of projective reduction in Section 4.1.

Consider again the element $R = \pi^2 s_1$, which we recall acts on the root variables according to

$$R \cdot (a_0, a_1, a_2, c) = (a_2 a_0, q^{-1} a_2 a_1, q a_2^{-1}, c). \tag{4.102}$$

Without imposing the parameter constraint $a_1 = q^{1/2}$ which led to equation (4.11), this gives a linear system of equations, this time of multiplicative type, for $R^n \cdot (a_0, a_1, a_2, c)$, which we may solve explicitly to obtain

$$R^n \cdot a_0 = q^{\frac{1}{4}(3+(-1)^n+2n)} a_1^{-1} a_2^{-\frac{1}{2}(1+(-1)^n)} = \begin{cases} a_0 q^{n/2} & \text{for } n \text{ even}, \\ a_1 q^{1/2+n/2} & \text{for } n \text{ odd} \end{cases},$$

$$R^n \cdot a_1 = q^{\frac{1}{4}(-1+(-1)^n-2n)} a_1 a_2^{\frac{1}{2}(1+(-1)^n)} = \begin{cases} a_1 q^{-n/2} & \text{for } n \text{ even}, \\ a_1 a_2 q^{-1/2-n/2} & \text{for } n \text{ odd}, \end{cases}$$

$$R^n \cdot a_2 = q^{\frac{1}{2}(1+(-1)^{n+1})} a_2^{(-1)^n} = \begin{cases} a_2 & \text{for } n \text{ even}, \\ q a_2^{-1} & \text{for } n \text{ odd}, \end{cases}$$

$$R^n \cdot c = c.$$

With this, we can write down an explicit form of the discrete system induced by the action of R on the variables by setting $F_n = R^n.f_0$, and therefore obtain the following generic version of (4.11):

$$F_{n+1}F_{n-1} = \frac{qc^2\left(a_0^{\frac{1}{2}((-1)^n-1)} + a_0 q^{\frac{n}{2}} q^{\frac{1}{4}((-1)^n-1)} F_n\right)}{F_n\left(a_0 q^{\frac{n}{2}} q^{\frac{1}{4}((-1)^n-1)} + a_0^{\frac{1}{2}((-1)^n-1)} F_n\right)}. \tag{4.103}$$

Computing the first few iterates of this system directly as rational functions of initial data, we see this degree growth identical to that of the projective reduction (4.11), which is to be expected given that they correspond to the same Cremona isometry. We now consider an element of $\widetilde{W}((A_2 + A_1)^{(1)})$ which may be regarded as a 'twisted translation' similarly to the element of $\widetilde{W}(D_4^{(1)})$ associated with the systems (4.3) and (4.91), and construct another integrable full-parameter system from its Cremona action. Keeping the notation of [KNT11], we consider the translation $T_4 = rw_0$, whose action on the parameters is given by

$$T_4 \cdot (a_0, a_1, a_2, c) = (a_0, a_1, a_2, qc). \tag{4.104}$$

It can be shown that the Dynkin diagram automorphism π preserves the weight in $P(A_2 + A_1)$ corresponding to T_4, and the element $\tilde{T}_4 = \pi T_4$ is of infinite order, and satisfies $\tilde{T}_4^3 = T_4^3$. Its action on the parameters is given by

$$\tilde{T}_4 \cdot (a_0, a_1, a_2, c) = (a_1, a_2, a_0, qc), \tag{4.105}$$

from which we may deduce, by solving a linear system of difference equations as above, that the result of acting on the parameters n times has the explicit form

$$\tilde{T}_4^n \cdot c = q^n c, \qquad \tilde{T}_4^n \cdot (a_0, a_1, a_2) = \begin{cases} (a_0, a_1, a_2) & \text{for } n \equiv 0 \mod 3, \\ (a_1, a_2, a_0) & \text{for } n \equiv 1 \mod 3, \\ (a_2, a_0, a_1) & \text{for } n \equiv 2 \mod 3. \end{cases} \tag{4.106}$$

From this, take the action of $\tilde{T}_4$ on the variables f_0, f_1, f_2 subject to $f_0 f_1 f_2 = a_0 a_1 a_2 c^2$ as in Section 4.1, letting $(F_n, G_n, H_n) = \tilde{T}_4^n.(f_0, f_1, f_2)$ to obtain the following second-order system:

$$F_{n+1} = a_{(n+1)}a_{(n-1)}H_n \frac{1 + a_{(n)}F_n(1 + a_{(n+1)}G_n)}{1 + a_{(n+1)}G_n(1 + a_{(n-1)}H_n)}, \tag{4.107a}$$

$$G_{n+1} = a_{(n-1)}a_{(n)}F_n \frac{1 + a_{(n+1)}G_n(1 + a_{(n-1)}H_n)}{1 + a_{(n-1)}H_n(1 + a_{(n)}F_n)}, \tag{4.107b}$$

$$H_{n+1} = a_{(n)}a_{(n+1)}G_n \frac{1 + a_{(n-1)}H_n(1 + a_{(n)}F_n)}{1 + a_{(n)}F_n(1 + a_{(n+1)}G_n)}, \tag{4.107c}$$

where

$$F_n G_n H_n = q^{2n+1}c^2, \qquad a_{(m)} = \begin{cases} a_0 & \text{for } m \equiv 0 \mod 3, \\ a_1 & \text{for } m \equiv 1 \mod 3, \\ a_2 & \text{for } m \equiv 2 \mod 3. \end{cases}$$

We emphasise again that the method we have outlined for obtaining full-parameter systems from elements of infinite order works for any of the surface types in Sakai's list which admit non-translation elements of infinite order in their symmetry groups. The equations (4.103), (4.107), and more generally any system given by the Cremona action on a family of generic $\mathcal{R}$-surfaces of a non-translation element will contain the maximum number of free parameters for their surface type. Moreover, they will be integrable in the sense of vanishing algebraic entropy for the same reason that Sakai's discrete Painlevé equations are.

We conclude this chapter with a remark on how such full-parameter non-translation systems may play a role in understanding recent developments in the theory of discrete Painlevé equations made independently of the geometric framework. There exist systems proposed to be of discrete Painlevé type, obtained via deautonomisation by singularity confinement of QRT mappings, in which the independent variable enters in a similar way to our full-parameter non-translation equations. These include the so-called strongly asymmetric discrete Painlevé equations [GRT$^+$14, GRT$^+$16], as well as those obtained recently by Grammaticos, Ramani and collaborators [RG17, GRWS20] which are claimed to include fifty new classes of discrete Painlevé equations. It is natural to ask whether they correspond to the Cremona actions of non-translation symmetries on families of generic $\mathcal{R}$-surfaces, and if so whether this perspective allows us to better understand their relation to Sakai's discrete Painlevé equations and how many of them are truly inequivalent.

Chapter 5

Singularity confinement in delay-differential Painlevé equations

We now present work developing the geometric framework beyond the classes of second-order discrete and differential Painlevé equations, namely to that of delay-differential equations, which involve shifts and derivatives with respect to a single independent variable. Similarly to the discrete case, these have been studied from the point of view of a kind of singularity confinement property, and tests based on this have been used to isolate integrability candidates and obtain delay-differential analogues of the Painlevé equations [GRM93, RGT93]. These so-called delay Painlevé equations possess analogues of many integrability properties of their discrete and differential counterparts, and it is natural to ask whether a geometric theory may be developed for them.

Though the examples we consider have been shown to exhibit singularity confinement-type behaviour associated with certain simple singularities, compared to the discrete case the situation is significantly complicated by the fact that a given delay-differential equation may admit infinitely many different singularity patterns. In this chapter, we propose a geometric definition of singularity confinement for three-point birational delay-differential equations in terms of iteration mappings between jet spaces, and prove it for three delay Painlevé equations by studying infinite families of singularity patterns.

5.1 Introduction

Compared to the discrete case, the understanding of singularity confinement in delay-differential equations is limited for the following reasons. Firstly, the possible singularity structures are significantly more complicated than for second-order discrete systems given by birational mappings. For these discrete systems, there are only a finite number of singularities to check, which correspond to curves that are blown down under the iteration mapping. For delay-differential equations, however, the presence of derivatives means that there may be infinitely many different singularity behaviours corresponding to solutions taking singular values with different multiplicities. Secondly, we do not have available to us the geometric picture of singularity confinement for second-order discrete systems, namely its relation with the iteration maps of the system lifting to isomorphisms between rational surfaces.

For the purpose of isolating integrability candidates in the class of delay-differential equations, it has so far been sufficient to require only that the simplest singularities are confined, but if singularity confinement is to lead to a geometric theory in this case, a more detailed analysis is required. Taking the first steps in this direction is the aim of this chapter.

We consider the following three examples of delay-differential analogues of the Painlevé equations

$$u(\bar{u} - \underline{u}) = au - bu', \tag{5.1}$$

$$v^2(\bar{v} - \underline{v}) = pv + qv', \tag{5.2}$$

$$\bar{w}w = \underline{w}\left(\lambda z w + \alpha w'\right) \tag{5.3}$$

where u, v and w are functions of the complex independent variable z, we take p, q, a, b, λ to be complex parameters independent of z, and we denote up- and down-shifts by $\bar{u}(z) = u(z+1), \underline{u}(z) = u(z-1)$ etc. The equation (5.1) was obtained by Quispel, Capel and Sahadevan [QCS92] as a similarity reduction of the Kac-van Moerbeke differential-difference equation, also known as the Manakov equation or Volterra lattice. They also showed that it has a continuum limit to $\mathrm{P_I}$ and that it exhibits some singularity confinement-type behaviour, which will be recalled in Section 5.2. The equation (5.2) is a symmetry reduction of a known integrable differential-difference modified Korteweg-de Vries equation, and extensions of it have been studied by Halburd and Korhonen from the point of view of Nevanlinna theory [HK17]. Further, it has a continuum limit to $\mathrm{P_I}$ and may be obtained from Bäcklund transformations of $\mathrm{P_{III}}$ [Ber17], or using singularity confinement tests adapted from those in [TRGO99]. The third equation (5.3) was isolated as an integrability candidate by Ramani, Grammaticos and Moreira [GRM93] using a kind of singularity confinement test (which also recovered equation (5.1)), and also has a continuum limit to $\mathrm{P_I}$. We also note that other integrability properties analogous to those of differential and discrete Painlevé equations have been studied in equations (5.1 - 5.3), for example the fact that they may be rewritten in bilinear forms [Car11] and that degenerate cases admit elliptic function solutions [Ber17], in parallel with the discrete case where autonomous degenerations of discrete Painlevé equations are Quispel-Roberts-Thompson (QRT) mappings [QRT88, QRT89], solved by elliptic functions.

We remark that we are considering examples of so-called three-point delay differential equations, which are of the form

$$\bar{u} = \frac{f_1(u, u', ...) + f_2(u, u', ...)\underline{u}}{f_3(u, u', ...) + f_4(u, u', ...)\underline{u}}, \tag{5.4}$$

where f_i are polynomials in u and its derivatives. There are known integrable delay-differential equations of other forms, for example the so-called bi-Riccati equations [GRM93, Ber17, Ber18], but studies of singularity confinement in these more closely resembles classical Painlevé analysis than birational geometry, and will not be discussed here. The class of three-point equations is the one considered by Halburd and Korhonen through the Nevanlinna theoretic approach [HK17], and fits into the family for which Viallet defined algebraic entropy in the delay-differential setting [Via14].

There are known transformations between the equations we consider, which will be useful later in the chapter. Firstly, we have the following relation between equation (5.1) and equation (5.2), which may be easily detected given the well-known transformation between the differential-difference systems that give these equations as similarity reductions, and is proved by direct calculation:

Lemma 5.1.1. *If v solves* (5.2) *with parameters p, q, then $v = \underline{u}u$ solves* (5.1) *with parameters $a = 2p, b = -q$.*

Secondly, we have a transformation between equation (5.1) and equation (5.3), which was pointed out in [GRM93]:

Lemma 5.1.2. *If w solves* (5.3) *with parameters λ, α, then $u = \bar{w}/\underline{w}$ solves* (5.1) *with parameters $a = 2\lambda, b = -\alpha$.*

5.1.1 Outline of the chapter

We will begin our analysis working on the level of equations, without invoking geometric language. In Section 5.2 we recall previous observations of singularity confinement behaviour in the three equations, and extend them to include infinite families of confined singularity patterns in each case. The proofs of these are deferred to Section 5.5. In Section 5.3 we shift to the geometric setting, first recasting our equations as mappings between jet spaces and defining 'blow-down type' singularities, and propose a notion of confinement for them. Rephrased in these geometric terms, we use the results of Section 5.2 to show that in the three examples, all such singularities are, in the sense of our definition, confined. We conclude with a discussion of how the geometric framework and the techniques developed for proving the singularity confinement property may be utilised and built upon in the study of other examples, as well as some open questions that arise from our work.

5.2 Singularity analysis of delay-differential equations

We begin by recalling previous observations of singularity confinement phenomena in the three examples we consider. Beginning with equation (5.2), the forward iteration, which gives $\bar{v}$ in terms of v, v' and $\underline{v}$, is given by

$$\bar{v} = \underline{v} + p\frac{1}{v} + q\frac{v'}{v^2}, \tag{5.5}$$

so if we take, as initial data, a pair of Laurent series expansions of $v, \underline{v}$ about $z = z_0$, then (5.5) and its upshifts determine all subsequent iterates $\bar{v}, \bar{\bar{v}}, \ldots$ as Laurent series about z_0. If we only wish to iterate a finite number of steps forward from generic initial data, we need only finitely many coefficients. For example, we could begin by giving initial $\underline{v}, v$ as Taylor expansions in $\zeta = z - z_0$ about some $z = z_0$:

$$\underline{v} = \underline{a}_0 + \underline{a}_1\zeta + \underline{a}_2\zeta^2 + \ldots, \tag{5.6a}$$

$$v = a_0 + a_1\zeta + a_2\zeta^2 + \ldots. \tag{5.6b}$$

If we assume that the iterates $\bar{v}(z) = v(z+1), \bar{\bar{v}}(z) = v(z+2), \ldots, v^{(k)}(z) = v(z+k)$ are all regular and nonzero at z_0, it is clear from the form of the equation (5.5) that the value $v(z_0 + k)$ depends only on the following coefficients from the expansions (5.6a-5.6b):

$$\begin{pmatrix} \underline{a}_0 & \underline{a}_1 & \cdots & \underline{a}_{k-1} & \\ a_0 & a_1 & \cdots & a_{k-1} & a_k \end{pmatrix}. \tag{5.7}$$

We will be iterating systems arbitrarily many times forward, so we will use this kind of notation for the iterates, i.e. $v^{(k)}(z) = v(z+k)$, throughout the chapter. Further, the form of the right-hand side of the forward iteration (5.5) ensures that if we start from $\underline{v}, v$ given by Taylor series, the only way that a pole may develop is through some iterate having a zero first. If while iterating, some iterate v develops a zero of order one, say at $\zeta = z - z_0 = 0$, with

$$\underline{v} = \underline{a}_0 + \underline{a}_1\zeta + \dots, \tag{5.8a}$$

$$v = a_1\zeta + a_2\zeta^2 + \dots, \tag{5.8b}$$

where $a_1 \neq 0$, then we have by direct calculation that

$$\bar{v} = \frac{q}{a_1}\zeta^{-2} + \mathcal{O}(\zeta^{-1}), \tag{5.9a}$$

$$\bar{\bar{v}} = -a_1\zeta^1 + \mathcal{O}(\zeta^2), \tag{5.9b}$$

$$\bar{\bar{\bar{v}}} = \left(5\underline{a}_0 + \frac{7p^2}{qa_1} + \frac{2pa_2}{a_1^2} - \frac{4qa_2^2}{a_1^3} + \frac{6qa_3}{a_1^2}\right) + \mathcal{O}(\zeta). \tag{5.9c}$$

We summarise the observations above by saying that the equation (5.2) admits the singularity pattern

$$\left(\mathrm{rg}, 0^1, \infty^2, 0^1, \mathrm{rg}\right),$$

where rg indicates a regular iterate with generic coefficients. We note here that this behaviour is exceptional for the following reason. In the computation of $\bar{\bar{v}}$ here, it is natural to expect a zero of order one, as this is what happens generically when v and $\bar{v}$ are of order ζ, ζ^{-2} respectively. However, while $\bar{v}, \bar{\bar{v}}$ having orders ζ^{-2}, ζ^1 respectively would generically lead to $\bar{\bar{\bar{v}}}$ having another pole of order 2, in this singularity pattern we note that two terms have vanished as $\bar{\bar{\bar{v}}}$ regains regularity. In the language of previous studies of singularity confinement behaviour, the information lost when entering the singularity is recovered in the iterate $\bar{\bar{\bar{v}}}$, in the form of the coefficient $\underline{a}_0$ from the initial data. Though this behaviour has not, to our knowledge, been reported explicitly, we note that the equation (5.2) may be obtained by singularity confinement tests along the lines of [GRM93, TRGO99].

We next consider equation (5.1), which was first observed in [QCS92] to exhibit the following singularity confinement behaviour. The forward iteration is given by

$$\bar{u} = \underline{u} + a - b\frac{u'}{u}, \tag{5.10}$$

so again it is clear that the only way that a pole may develop while iterating from formal Taylor series is following a zero. Suppose that while iterating, the solution u develops a zero of order one at $\zeta = z - z_0 = 0$, so

$$\underline{u} = \underline{c}_0 + \underline{c}_1\zeta + \dots, \tag{5.11a}$$

$$u = c_1\zeta + c_2\zeta^2 + \dots, \tag{5.11b}$$

where $c_1 \neq 0$. Then direct calculation shows that

$$u^{(1)} = -\frac{b}{\zeta} + \left(a + \underline{c}_0 - b\frac{c_2}{c_1}\right) + \mathcal{O}(\zeta), \tag{5.12a}$$

$$u^{(2)} = \frac{b}{\zeta} + \left(2a + \underline{c}_0 - b\frac{c_2}{c_1}\right) + \mathcal{O}(\zeta), \tag{5.12b}$$

$$u^{(3)} = \left(\frac{2a^2}{b} - \frac{\underline{c}_0^2}{b} + \frac{2c_2\underline{c}_0}{c_1} - 3\underline{c}_1 + \frac{2b\left(3c_1c_3 - 2c_2^2\right)}{c_1^2} - 2c_1\right)\zeta + \mathcal{O}(\zeta^2), \tag{5.12c}$$

$$u^{(4)} = F(\underline{c}_0, \underline{c}_1, \underline{c}_2, c_1, c_2, c_3, c_4) + \mathcal{O}(\zeta), \tag{5.12d}$$

where F is a known rational function of the generic initial data, which we omit for conciseness. Again, this behaviour is exceptional as $u^{(1)}, u^{(2)}$ both having simple poles would generically lead to $u^{(3)}$ also having a simple pole, but here two terms have vanished as $u^{(3)}$ instead has a zero of order one, so equation (5.1) admits the singularity pattern

$$\left(\mathrm{rg}, 0^1, \infty^1, \infty^1, 0^1, \mathrm{rg}\right).$$

We next turn to equation (5.3), which was obtained in [GRM93] by singularity confinement methods, though details were not given explicitly. The forward iteration mapping is given by

$$\bar{w} = \underline{w}\left(\lambda z + \alpha\frac{w'}{w}\right). \tag{5.13}$$

Say, while iterating, we arrive at a pair $\underline{\underline{w}}, \underline{w}$ given by expansions in $\zeta = z - z_0$ by

$$\underline{\underline{w}} = \underline{\underline{c}}_0 + \underline{\underline{c}}_1 \zeta + \underline{\underline{c}}_2 \zeta^2 + \dots, \tag{5.14a}$$

$$\underline{w} = \underline{c}_0 + \underline{c}_1 \zeta + \underline{c}_2 \zeta^2 + \dots, \tag{5.14b}$$

with

$$\alpha \underline{c}_1 + \lambda(z_0 - 1)\underline{c}_0 = 0, \quad 2\alpha \underline{c}_2 + \lambda \underline{c}_1 (z_0 - 1) \neq 0, \quad \underline{c}_1 \neq 0, \quad \underline{\underline{c}}_0 \neq 0. \tag{5.15}$$

This means that w will have a simple zero at $z = z_0$, and by direct calculation we find the following:

$$w = \frac{\lambda \underline{\underline{c}}_0 (1 - z_0) \left(2\alpha \underline{c}_2 + \lambda \underline{c}_1 (z_0 - 1)\right)}{\alpha \underline{c}_1} \zeta + \mathcal{O}(\zeta^2), \tag{5.16a}$$

$$\bar{w} = \frac{\alpha^2 \underline{c}_1}{\lambda(1 - z_0)} \zeta^{-1} + \mathcal{O}(\zeta^0) \tag{5.16b}$$

$$\bar{\bar{w}} = \frac{\lambda \underline{\underline{c}}_0 (z_0 - 1) \left(2\alpha \underline{c}_2 + \lambda \underline{c}_1 (z_0 - 1)\right)}{\underline{c}_1} + \mathcal{O}(\zeta^1), \tag{5.16c}$$

$$\bar{\bar{\bar{w}}} = \frac{G(\underline{\underline{c}}_0, \underline{\underline{c}}_1, \underline{\underline{c}}_2, \underline{c}_1, \underline{c}_2, \underline{c}_3)}{\underline{\underline{c}}_0^2 \left(2\alpha \underline{c}_2 + \lambda \underline{c}_1 (z_0 - 1)\right)^2} + \mathcal{O}(\zeta^1), \tag{5.16d}$$

where G is a polynomial function of the generic initial data as well as z_0. Again, this behaviour is exceptional as a simple pole of $\bar{w}$ with $\bar{\bar{w}}$ regular and nonzero would generically lead to $\bar{\bar{\bar{w}}}$ having another simple pole, whereas in this case a term has vanished and the iterate $\bar{\bar{\bar{w}}}$ is regular. Again, we summarise this observation by saying that the equation (5.3) admits the singularity pattern

$$\left(\mathrm{rg}, \underline{\zeta}_0^1, 0^1, \infty^1, \bar{\bar{\zeta}}_0^1, \mathrm{rg}\right),$$

where $\underline{\zeta}_0^{(1)}$ indicates that the iterate $\underline{w}$ satisfies the condition for w to develop a simple zero, namely $\alpha \underline{c}_1 + \lambda(z_0 - 1)\underline{c}_0 = 0, \quad 2\alpha \underline{c}_2 + \lambda \underline{c}_1 (z_0 - 1) \neq 0$, and $\bar{\bar{\zeta}}_0^1$ indicates the iterate $\bar{\bar{w}} = \bar{\bar{c}}_0 + \bar{\bar{c}}_1 \zeta + \bar{\bar{c}}_2 \zeta^2 + \dots$ satisfies $\alpha \bar{\bar{c}}_1 + \lambda(z_0 + 2)\bar{\bar{c}}_0 = 0$.

5.2.1 Infinite families of singularity patterns

In the previous section, we outlined certain singularity patterns admitted by the equations (5.1), (5.2) and (5.3) which involved zeroes of order one developing while iterating the systems. We now extend these observations to higher order zeroes, and show that each of the equations admits an infinite family of singularity patterns with similar confinement behaviour.

For equation (5.2), we have observed the singularity pattern $\left(\mathrm{rg}, 0^1, \infty^{-2}, 0^1, \mathrm{rg}\right)$, which corresponds to $\underline{v}$ being regular and v having a zero of order one at $z = z_0$. Similarly, if v has a zero of order two, then we pass through the following sequence of orders, which is generic until three terms vanish as $v^{(5)}$ becomes regular instead of a pole (with leading coefficient depending on data from $\underline{v}$):

$$\underline{v} = \mathcal{O}(\zeta^0),\;\; v \sim \zeta^2,\;\; v^{(1)} \sim \zeta^{-3},\;\; v^{(2)} \sim \zeta^2,\;\; v^{(3)} \sim \zeta^{-3},\;\; v^{(4)} \sim \zeta^2,\;\; v^{(5)} = \mathcal{O}(\zeta^0).$$

From above, we see that equation (5.2) admits the singularity pattern

$$\left(\mathrm{rg}, 0^2, \infty^3, 0^2, \infty^3, 0^2, \mathrm{rg}\right),$$

and because of the return to regularity and the iterate $v^{(5)}$ depending on the generic initial data from $\underline{v}$, the singularity is confined in a similar sense to that which we observed in the case of a zero of order one. More generally, if v has a zero of order $m > 1$, and $\underline{v}$ is regular, say $v = c_m\zeta^m + \mathcal{O}(\zeta^{m+1})$, with $c_m \neq 0$, and $\underline{v} = \mathcal{O}(1)$, then it can be seen from the equation (5.2) that

$$v^{(1)} = -\frac{mq}{c_m}\zeta^{-m-1} + \mathcal{O}(\zeta^{-m}), \tag{5.17a}$$

$$v^{(2)} = -\frac{c_m}{m}\zeta^m + \mathcal{O}(\zeta^{m+1}), \tag{5.17b}$$

$$v^{(3)} = \frac{m(m-1)q}{c_m}\zeta^{-m-1} + \mathcal{O}(\zeta^{-m}), \tag{5.17c}$$

and more generally, it can be shown by induction that for $k \leq m$,

$$v^{(2k)} = \frac{(-1)^k k!}{\prod_{i=0}^{k-1}(m-i)}c_m\zeta^m + \mathcal{O}(\zeta^{m+1}), \tag{5.18a}$$

$$v^{(2k+1)} = \frac{(-1)^k \prod_{i=0}^{k}(m-i)}{k!}\frac{q}{c_m}\zeta^{-m-1} + \mathcal{O}(\zeta^{-m}). \tag{5.18b}$$

What we deduce from this is that a singularity sequence beginning with $\underline{v}$ regular and v with a zero order m will contain $m+1$ zeroes of order m alternating with m poles of order $m+1$. We know that the coefficient of ζ^{-m-1} in the iterate $v^{(2m+1)}$ will vanish according to the formulae (5.18), but it turns out that the entire singular part of the expansion vanishes, so regularity is regained at the iterate $v^{(2m+1)}$.

Theorem 5.2.1. *For each integer $m > 0$, equation* (5.2) *admits the singularity pattern*

$$\left(\text{rg}, 0^m, \infty^{m+1}, 0^m, \infty^{m+1}, \dots, \infty^{m+1}, 0^m, \infty^{m+1}, 0^m, \text{rg}\right),$$

which includes $m+1$ zeroes of order m alternating with m poles of order $m+1$.

The proof of this theorem is provided in Section 5.5, along with those of similar results for the equations (5.1) and (5.3):

Theorem 5.2.2. *For each integer $m > 0$, equation* (5.1) *admits the singularity pattern*

$$\left(\text{rg}, 0^m, \infty^1_{-m}, \infty^1_1, \infty^1_{1-m}, \dots, \infty^1_k, \infty^1_{k-m}, \dots, \infty^1_{-1}, \infty^1_m, 0^m, \text{rg}\right),$$

which includes $2m$ simple poles with residues alternating between positive and negative multiples of β, which we denote

$$\infty^1_j = \frac{j\beta}{z - z_0} + O(1).$$

Theorem 5.2.3. *Equation* (5.3) *admits the singularity pattern*

$$\left(\text{rg}, \zeta_0(-1)^m, 0^m, \infty^1, 0^{m-1}, \dots, \infty^j, 0^{m-j}, \dots, \infty^{m-1}, 0^1, \infty^m, \zeta_0(2m)^m, \text{rg}\right),$$

where $\zeta_0(-1)^m$ indicates that the iterate $\underline{w} = w^{(-1)}$ satisfies $\frac{d^k}{dz^k}\left(\lambda z \underline{w} + \alpha \underline{w}'\right) = 0$ at $z = z_0$ for $k = 0, ..., m-1$, and $\zeta_0(2m)^m$ indicates that the iterate $w^{(2m)}$ satisfies

$$\frac{d^k}{dz^k}\left(\lambda(z+m)w^{(2m)} + \alpha w^{(2m)'}\right) = 0,$$

at $z = z_0$ for $k = 0, ..., m-1$.

5.3 Geometric description of singularity confinement

We now rephrase the results of the previous section geometrically, and propose a characterisation of singularity confinement in the delay-differential setting in terms of the birational geometry of jet spaces. Our guiding principle in developing the theory in parallel with the discrete setting will be that of generic information loss, in particular the ways in which iterating a delay-differential equation may result in a departure from this, and in what sense it is recovered. To explain the motivations for this analogy, we first note that a birational mapping between smooth projective algebraic surfaces is an isomorphism between Zariski open subsets given by the complement of subvarieties that are blown down by either the mapping or its inverse. Almost all curves are mapped bijectively to curves, and in this sense no information loss occurs generically while iterating the corresponding discrete system. Singularities of a second-order discrete system occuring when curves are blown down to points may be interpreted as more information loss occurring than normal. The system having the singularity confinement property means that, in such a case when iterating the system results in more than the generic amount of information loss, we may compose the mapping a finite number of times to recover the generic behaviour: an isomorphism from a curve to a curve.

We will formulate a concept of generic information loss for our delay-differential equations. In terms of this we will define singularity confinement as being able to, in the case when iterating the system results in more than generic levels of information loss, compose the iteration mapping of the system a finite number of times to recover the generic amount. This concept of generic information loss has two elements: first is the amount of initial data required generically to iterate the system forward a given number of times, which we will phrase in Subsection 5.3.1 in terms of the orders of jet spaces on which the systems give well-defined mappings. Second is the behaviour of subspaces under the these mappings in terms of their codimension, which will be used to describe phenomena analogous to degrees of freedom being lost, which we define as 'blow-down type' singularities in Subsection 5.3.2. We then outline what it means for such a singularity to be confined, and finally verify that this geometric description fits with our analysis of the three examples, and that they confine all singularities in this sense.

5.3.1 Delay-differential equations as mapping between jet spaces

Similarly to how second-order discrete systems are described by birational mappings between algebraic surfaces, we will recast our delay-differential equations as mappings between jet spaces. We consider jets associated with the trivial bundle over $\mathbb{C}$ with fibre $\mathbb{P}^1 \times \mathbb{P}^1$. We use the same coordinate charts for $\mathbb{P}^1 \times \mathbb{P}^1$ as in the discrete case, namely $(x, y), (X, y), (x, Y), (X, Y)$ where $X = 1/x, Y = 1/y$. The space $J^r_{z_0}$ of r-jets about z_0 is the set of equivalence classes of local holomorphic sections about some $z_0 \in \mathbb{C}$ under the following equivalence relation. The sections σ_1, σ_2 define the same r-jet if, when written in coordinates, their derivatives at z_0 coincide up to and including order r.

We will be always considering jets at z_0, so we omit the subscript. We will use coordinates for J^r induced by writing sections as expansions in our coordinates for $\mathbb{P}^1 \times \mathbb{P}^1$. For example, if a section about z_0 is visible in the (x, y)-chart, it may be written in coordinates as

$$\begin{pmatrix} x(z) \\ y(z) \end{pmatrix} = \begin{pmatrix} x_0 + x_1\zeta + x_2\zeta^2 + \dots \\ y_0 + y_1\zeta + y_2\zeta^2 + \dots \end{pmatrix}, \tag{5.19}$$

where $\zeta = z - z_0$ as before, so we have one part of J^r covered by the chart with coordinates

$$\begin{pmatrix} x_0 & x_1 & x_2 & \dots & x_r \\ y_0 & y_1 & y_2 & \dots & y_r \end{pmatrix}, \tag{5.20}$$

and J^r can be thought of as four copies of $\mathbb{C}^{2r+2}$ with coordinates being coefficients from expansions of sections in the four charts for $\mathbb{P}^1 \times \mathbb{P}^1$, with gluing determined by that of $\mathbb{P}^1 \times \mathbb{P}^1$ itself, namely $X = 1/x, Y = 1/y$.

Consider a three-point delay-differential equation of the form (5.4), with l being the highest order of derivative that appears. Similarly to how the scalar difference equation (1.17) is recast as a QRT mapping on $\mathbb{P}^1 \times \mathbb{P}^1$, we let $(x, y) = (u, \underline{u})$ and $(\bar{x}, \bar{y}) = (\bar{u}, u)$ given by series expansions about z_0, so we have a mapping on sections near z_0, which in the (x, y)-charts for both domain and target copies of $\mathbb{P}^1 \times \mathbb{P}^1$ is written as:

$$\begin{gathered} \begin{pmatrix} x(z) \\ y(z) \end{pmatrix} \mapsto \begin{pmatrix} \bar{x}(z) \\ \bar{y}(z) \end{pmatrix}, \\ \bar{x} = \frac{f_1(x, x', \dots, \partial^l x/\partial z^l) + f_2(x, x', \dots, \partial^l x/\partial z^l)y}{f_3(x, x', \dots, \partial^l x/\partial z^l) + f_4(x, x', \dots, \partial^l x/\partial z^l)y}, \qquad \bar{y} = x. \end{gathered} \tag{5.21}$$

We now introduce a space of jets on which we consider this, corresponding to generic initial data. Consider a section written as a series expansion in one of the four coordinate charts for $\mathbb{P}^1 \times \mathbb{P}^1$, for example (5.19) in the (x, y)-chart. Denote the numerator and denominator of the function giving $\bar{x}(z)$ in this chart by $P(z), Q(z)$, so for example in the (x, y)-chart we use (5.21) and consider

$$\begin{aligned} P &= f_1(x, x', \dots, \partial^l x/\partial z^l) + f_2(x, x', \dots, \partial^l x/\partial z^l)y, \\ Q &= f_3(x, x', \dots, \partial^l x/\partial z^l) + f_4(x, x', \dots, \partial^l x/\partial z^l)y. \end{aligned} \tag{5.22}$$

Substitute expansions giving $(x(z), y(z))$ into these, to obtain formal expansions of $P(z), Q(z)$ about z_0, which we denote

$$P(z) = P_0 + P_1\zeta + P_2\zeta^2 + \dots, \qquad Q(z) = Q_0 + Q_1\zeta + Q_2\zeta^2 + \dots, \tag{5.23}$$

where P_0, Q_0 are polynomials in $x_0, \dots, x_l, y_0$ because of the highest order derivative appearing in the equation (or the equivalent for an expansion of a section in another coordinate chart). Consider the rational function P_0/Q_0 on J^{r+l}, using the transition functions between x_i, X_i etc. being defined by the $\mathbb{P}^1 \times \mathbb{P}^1$ gluing as before, and denote its indeterminacy locus (where the numerator and denominator simultaneously vanish) by I_1. We then have a well-defined map

$$\varphi_r : J^{r+l} \backslash I_1 \to J^r. \tag{5.24}$$

The reason we do not have to worry about indeterminacies of rational functions giving later coefficients in the expansion of P/Q to obtain a well-defined map is the following: all of the rational functions giving expansions of P/Q have denominator being a power of Q_0. Similarly, all rational functions giving coefficients in the expansion of Q/P are powers of P_0. Thus if $Q_0 = 0$ but $P_0 \neq 0$, we get a well-defined expansion of Q/P, in which none of the coefficients have indeterminacies (their denominators cannot vanish as $P_0 \neq 0$) so we have a well-defined a section visible in the $(\bar{X}, \bar{y})$-chart. Similarly, if $P_0 = 0$ but $Q_0 \neq 0$, we get a well-defined expansion of Q/P, in which none of the coefficients have indeterminacies (their denominators cannot vanish, as $P_0 \neq 0$).

Example 5.3.1. *If we consider the mapping induced by equation* (5.1) *applied to a section visible in the* (x, y)*-chart, written as an expansion* (5.19)*, direct substitution yields*

$$\begin{aligned} \bar{x}_0 &= \frac{ax_0 - bx_1 + x_0y_0}{x_0}, & \bar{x}_1 &= \frac{bx_1^2 - 2x_0x_2 + x_0^2y_1}{x_0^2}, & &\dots \\ \bar{y}_0 &= x_0, & \bar{y}_1 &= x_1, & &\dots \end{aligned} \tag{5.25}$$

so when $x_0 \neq 0$ *we have a section visible in the* $(\bar{x}, \bar{y})$*-chart for the target bundle. Similarly, if we have a section written in the* (x, y)*-chart as an expansion with coefficients* X_i, Y_i*, we* *may use the chart* $(\bar{x}, \bar{Y})$ *and calculate*

$$\begin{aligned} \bar{x}_0 &= \frac{aX_0Y_0 + bX_1Y_0 + X_0}{X_0Y_0}, & \bar{x}_1 &= \frac{2bX_2X_0Y_0^2 - bX_1^2Y_0^2 - X_0^2Y_1}{X_0^2Y_0^2}, & \dots \\ \bar{Y}_0 &= X_0, & \bar{Y}_1 &= X_1, & \dots \end{aligned} \tag{5.26}$$

so when $X_0Y_0 \neq 0$ *we have a section visible in the* $(\bar{x}, \bar{Y})$*-chart for the target bundle. Calculating in the other charts, we find the subset* $I_1 \subset J^{r+1}$ *is defined by*

$$\begin{aligned} I_1 = &\{(x_0, x_1) = (0,0)\} \cup \{(X_0, X_1) = (0,0)\} \\ &\cup \{(x_0, Y_0) = (0,0)\} \cup \{(X_0, Y_0) = (0,0)\}. \end{aligned} \tag{5.27}$$

So we have, for each $r \geq 0$, *a map*

$$\varphi_r : J^{r+1} \backslash I_1 \to J^r. \tag{5.28}$$

We note that the domain J^{r+1} *corresponds to the lowest order of jets to which the equation* (5.1) *gives a well-defined map from* $J^{r+1} \backslash I_1$ *to* J^r.

Returning to the general case, we also have, for each $r \geq 0$, a map

$$\varphi_r^{(k)} = \varphi_r \circ \varphi_{r+1} \cdots \circ \varphi_{r+k-1} \quad : \quad J^{r+kl} \backslash I_k \to J^r, \tag{5.29}$$

defined on the Zariski open subset of $J^{(r+kl)}$ where the numerators and denominators of the rational functions giving leading coefficients of successive iterates do not simultaneously vanish.

Example 5.3.2. *To illustrate this in the case of equation* (5.1) *being iterated twice, we obtain in the* (x, y)*-chart rational functions giving* $(\bar{\bar{x}}_0, \bar{\bar{y}}_0)$ *as*

$$\begin{aligned} \bar{\bar{x}}_0 &= \frac{a^2x_0^2 - abx_1x_0 + ax_0^2y_0 + ax_0^3 + 2b^2x_2x_0 - b^2x_1^2 - bx_0^2y_1 - bx_1x_0^2 + x_0^3y_0}{x_0\left(ax_0 - bx_1 + x_0y_0\right)}, \\ \bar{\bar{y}}_0 &= \frac{ax_0 - bx_1 + x_0y_0}{x_0}. \end{aligned} \tag{5.30}$$

Computing the indeterminacy loci of these rational functions in all charts and taking its *union with I_1, we obtain*

$$\begin{aligned} I_2 = &\{(x_0, x_1) = (0,0)\} \cup \{(X_0, X_1) = (0,0)\} \\ &\cup \{(x_0, Y_0) = (0,0)\} \cup \{(X_0, Y_0) = (0,0)\} \\ &\cup \left\{ax_0 - bx_1 + x_0y_0 = bx_1^2 - 2bx_0x_2 + x_0^2y_1 = 0\right\} \\ &\cup \{X_0 = 0, X_1 = -1/b\} \cup \{Y_0 = Y_1 = 0\}, \end{aligned} \tag{5.31}$$

and we have a well-defined map

$$\varphi_r^{(2)} = \varphi_r \circ \varphi_{r+1} \ : \ J^{r+2} \backslash I_2 \to J^r. \tag{5.32}$$

We interpret this map $\varphi_r^{(k)}$ in (5.29) on the set specified above as the generic behaviour of the system, and in particular the initial data that is required to iterate the system k times in almost all cases. We now consider the parts of the jet spaces where the rational functions we have considered above have indeterminacies. For example, if we consider a jet in the charts coming from (X,Y), $(\bar{X},\bar{Y})$, if $(X_0,Y_0) = (0,0)$ then we have

$$\begin{aligned} &\bar{X}_0 = 0, \quad \bar{X}_1 = \frac{Y_1}{1+bY_1}, \quad \bar{X}_2 = \frac{X_1\left(Y_2 - aY_1^2\right) - bX_2Y_1^2}{X_1\left(1+bY_1\right)^2}, \quad \dots \\ &\bar{Y}_0 = 0, \quad \bar{Y}_1 = X_1, \quad \bar{Y}_2 = X_2, \quad \dots \end{aligned} \tag{5.33}$$

and so on. By direct calculation using formal series expansions, it can be seen that as long as $X_1 \neq 0, 1+bY_1 \neq 0$, the jet in $(\bar{X},\bar{Y})$ coordinates is determined up to the same order as the one in (X,Y) coordinates. Thus, on the part of $J^r (r \geq 1)$ where $(X_0,Y_0) = (0,0)$ but $X_1 \neq 0, 1+bY_1 \neq 0$, the system induces a mapping $J^r \to J^r$ and we have less information loss than in the generic case. Comparing this to the discrete case, we see a parallel to the fact that indeterminacies of the iteration mappings are blown up to curves.

5.3.2 Blow-down type singularities

After considering a concept of generic information loss in terms of the amount of initial data generically required to iterate k times, we turn to parts of jet spaces on which the system induces maps with more information loss. We will refer to these as blow-down type singularities, in parallel with the discrete case where information loss corresponds to curves being blown down under iteration mappings.

Consider the mapping $\varphi_r : J^{r+1} \backslash I_1 \to J^r$ induced by equation (5.1) derived above. We will be interested in the behaviour under this mapping of subvarieties defined locally by a finite number of algebraic constraints. For most codimension m subsets of this part of J^{r+1} (where r is chosen large enough such that it includes all the variables appearing in the constraints defining the subset), the image under φ_r will be of codimension $\leq m$ in J^r. For example, we can see a variety of behaviours of subspaces as follows. The subspace defined in the (x_i, y_i)-chart by the single algebraic constraint $y_i = c$, where $i \leq r+1$ and $c \neq 0$ is some constant, is of codimension one, and its image under φ_r is of codimension zero. Another subspace defined by $x_i = c$, for some $i \leq r$ and c again a nonzero constant, will have image under φ_r of codimension one. The codimension two subspace where $(X_0, Y_0) = (0, 0)$ with the rest of the coefficients X_i, Y_i generic can be quickly seen from (5.33) to have image again of codimension two.

Definition 5.3.3. *A blow-down type singularity of a delay differential equation of the form* (5.4) *is a codimension m subvariety of J^{r+l} , for some $r \geq 0$, (locally defined as the vanishing locus of a number of polynomials in coordinates introduced above) whose image under the induced map φ_r is of codimension greater than m.*

We emphasise again that this is in analogy with the discrete setting, where singularities are defined in the sense of an increase in codimension, namely where curves are blown down to points under the iteration mappings. Again we note that in the following examples, r is taken large enough such that J^{r+1} includes all variables appearing in the algebraic constraints defining the blow-down singularities, and all other variables are generic.

Example 5.3.4. *The equation* (5.1) *has a blow-down singularity in $J^{r+1} \backslash I_1$ given in coordinates by $x_0 = 0$ which is of codimension one (with all other x_i, y_i generic) but has image of codimension three in J^r, given in coordinates as follows:*

$$\begin{aligned} \{x_0 = 0\} \quad &\to \quad \left\{\bar{X}_0 = 0, \quad \bar{X}_1 = -1/b, \quad \bar{y}_0 = 0\right\} \\ \text{codim}\, 1 \quad &\to \quad \text{codim}\, 3 \end{aligned}$$

Similarly, we see that the development of double and triple zeroes correspond to the follow-

ing blow-down singularities:

$$\{x_0 = 0, \quad x_1 = 0\} \quad \to \quad \left\{ \begin{matrix} \bar{X}_0 = 0, \quad \bar{X}_1 = -1/2b, \\ \bar{y}_0 = 0, \quad \bar{y}_1 = 0 \end{matrix} \right\}$$

$$\text{codim}\, 2 \quad \to \quad \text{codim}\, 4$$

$$\{x_0 = 0, \quad x_1 = 0, \quad x_2 = 0\} \quad \to \quad \left\{ \begin{matrix} \bar{X}_0 = 0, \quad \bar{X}_1 = -1/3b, \\ \bar{y}_0 = 0, \quad \bar{y}_1 = 0, \quad \bar{y}_2 = 0 \end{matrix} \right\}$$

$$\text{codim}\, 3 \quad \to \quad \text{codim}\, 5$$

and more generally the development of a zero of order m corresponds to the following blow-down singularity:

$$\{x_i = 0, \ \forall i = 0, \ldots, m-1\} \quad \to \quad \left\{ \begin{matrix} \bar{X}_0 = 0, \quad \bar{X}_1 = -1/mb, \\ \bar{y}_i = 0, \ \forall i = 0, \ldots, m-1 \end{matrix} \right\}$$

$$\text{codim}\, m \quad \to \quad \text{codim}\ (m+2)$$

Example 5.3.5. *The equation* (5.2) *has a blow-down singularity given in coordinates by $x_0 = 0$ which is of codimension one (with all other x_i, y_i generic) but has image of codimension five given in coordinates as follows:*

$$\{x_0 = 0\} \quad \to \quad \{\bar{X}_0 = 0, \quad \bar{X}_1 = 0, \quad \bar{y}_0 = 0, \quad \bar{y}_1 = q\bar{X}_2, \quad p\bar{y}_1 = -q^2\bar{X}_3\}$$

$$\text{codim}\, 1 \quad \to \quad \text{codim}\, 5$$

We also have a blow-down singularity corresponding to the development of a double zero

$$\{x_0 = 0, \quad x_1 = 0\} \quad \to \quad \left\{ \begin{matrix} \bar{X}_0 = 0, \quad \bar{X}_1 = 0, \quad \bar{X}_2 = 0, \quad \bar{y}_0 = 0, \quad \bar{y}_1 = 0 \\ \bar{y}_2 - 2q\bar{X}_3 = 0, \quad \bar{y}_3 - 2p\bar{X}_3 - 4q\bar{X}_4 = 0, \\ p^2\bar{X}_3^2 + 2pq\bar{X}_3\bar{X}_4 + 2q^2\bar{X}_4^2 - 2q^2\bar{X}_3\bar{X}_5 = 0 \end{matrix} \right\}$$

$$\text{codim}\, 2 \quad \to \quad \text{codim}\, 8$$

and more generally the development of a zero of order m corresponds to the following *blow-down singularity:*

$$\{x_i = 0,\ \forall i = 0, \dots, m-1\} \quad \rightarrow \quad \left\{ \begin{array}{c} \bar{X}_i = 0\ \ \forall i = 0, \dots, m, \\ \bar{y}_i = 0,\ \ \forall i = 0, \dots, m-1 \\ F_i(\bar{X}_{m+1}, \bar{X}_{m+2}, \dots, \bar{y}_m, \bar{y}_{m+1}, \dots) = 0 \\ \forall i = m+1, \dots, 2m+1 \end{array} \right\}$$

$$\text{codim}\, m \quad \rightarrow \quad \text{codim}\ (3m+2)$$

Here F_i are polynomial in their variables that give $m+1$ independent algebraic constraints, which may be identified by substituting series expansions for $x(z), y(z)$ and noting that $\bar{X}_{2m+2}$ is the first coefficient in which any y_i appears.

Example 5.3.6. *The equation* (5.3) *has a blow-down singularity in ($\underline{x}_i, \underline{y}_j$ coordinates) corresponding to $x(z)$ developing a zero of order one. This is given by*

$$\{(z_0 - 1)\lambda \underline{x}_0 + \alpha \underline{x}_1 = 0\} \quad \rightarrow \quad \{x_0 = 0, \quad (z_0 - 1)\lambda y_0 + \alpha y_1 = 0\}$$

$$\text{codim}\, 1 \quad \rightarrow \quad \text{codim}\, 2$$

and more generally the development of a zero of order m corresponds to the following blow-down singularity, which for conciseness we write in terms of derivatives of the sections, as opposed to explicitly in terms of coefficients:

$$\left\{ \begin{array}{c} \frac{d^i}{dz^i}\left(\lambda z \underline{x}(z) + \alpha \underline{x}'(z)\right)|_{z=z_0} = 0 \\ \forall i = 0, \dots, m-1 \end{array} \right\} \quad \rightarrow \quad \left\{ \begin{array}{c} x_i = 0 \quad \forall i = 0, \dots, m-1 \\ \frac{d^i}{dz^i}|_{z=z_0}\left(\lambda z y(z) + \alpha y'(z)\right) = 0 \\ \forall i = 0, \dots, m-1 \end{array} \right\}$$

$$\text{codim}\, m \quad \rightarrow \quad \text{codim}\ 2m$$

5.3.3 Singularity confinement in equations (1.1-1.3)

We now formulate a geometric description of the confinement type behaviour we observed in our three examples. Again, the analogy with the discrete case is that if, when iterating the system, we arrive at a blow-down type singularity we only need to iterate a finite number of times further to recover the generic level of information loss, both in terms of orders of jet spaces between which the system induces maps, and the behaviour of the singularity under these in terms of codimension.

Definition 5.3.7. *Consider a three-point delay differential equation of the form* (5.4) *with iteration mappings φ_r, which has a blow-down type singularity B_m of codimension m. We say the singularity B_m is confined if there exists some $k > 0$ such that iterating the system k times induces a map from $B_m \subset J^{r+kl}$ whose image is of codimension $\leq m$ in J^r.*

We note that this definition captures both the recovery from the increase in codimension of B_m as well as the amount of initial data required to iterate k times generically. Take B_m as a subset of the same order jet space J^{r+kl} as for the generic behaviour $\varphi_r^{(k)} : J^{r+kl} \backslash I_k \to J^r$. We consider accessible blow-down singularities: those that may arise when iterating the system from regular nonzero initial data. For the three equations we consider, we first describe the set of all such singularities and then use our results concerning infinite families of singularity patterns to deduce that they are all confined in the above sense.

5.3.3.1 Equation (5.1)

Lemma 5.3.8. *The only accessible blow-down type singularities of equation* (5.1) *are*

$$B_m = \{x_i = 0 \ \ \forall i = 0, \ldots, m-1\},$$

with all other coefficients generic, so in particular we assume $x_m \neq 0$ in B_m.

Proof. We will first show that the only blow-down singularities visible in the x_i, y_j chart are contained in $\{x_0 = 0\}$. Suppose $B \subset J^{r+1}$ is of codimension m, so dimension $d = 2(r+1) - m$, defined locally by $F_1 = \cdots = F_l = 0$, where F_i are polynomial in $x_0, \ldots, x_m, y_0, \ldots, y_m$, and that $x_0 \neq 0$ on B. Then near $p \in B$ (at which B is nonsingular) given in coordinates by $p : (x_i, y_j) = (x_i^*, y_j^*)$, we have a parametrisation of B by d free parameters. That is, there exist $i_1, \ldots, i_p$, $j_1, \ldots j_{d-p} \subset \{0, \ldots, r+1\}$ such that we have a parametrisation

$$\begin{pmatrix} s_1 \\ \vdots \\ s_p \\ t_1 \\ \vdots \\ t_{d-p} \end{pmatrix} \mapsto \begin{matrix} x_{i_1} = x_{i_1}^* + s_1 \\ \vdots \\ x_{i_p} = x_{i_p}^* + s_p \\ y_{j_1} = y_{j_1}^* + t_1 \\ \vdots \\ y_{j_{d-p}} = y_{j_{d-p}}^* + t_{d-p} \end{matrix} \tag{5.34}$$

with the rest of the variables x_i, y_j given by analytic functions of $s_1, \dots, s_p, t_1, \dots, t_{d-p}$:

$$\begin{aligned} x_i &= x_i^* + F_i(s_1, \dots, s_p, t_1, \dots, t_{d-p}), \\ y_j &= y_j^* + G_j(s_1, \dots, s_p, t_1, \dots, t_{d-p}), \end{aligned} \tag{5.35}$$

for $i \notin \{i_1, \dots, i_p\}$, $j \notin \{j_1, \dots, j_{d-p}\}$, with F_i, G_j analytic and zero when all s_i, t_j are zero, and the Jacobian of this parametrisation at p is of rank d. We now show, using this parametrisation, that the image of B in J^r under φ_r is of dimension $\geq 2r - m$ as long as $x_0 \neq 0$ on B. In coordinates, the mapping is of the form

$$\bar{y}_n = x_n, \qquad \bar{x}_n = y_n - \frac{P_n(x_0, \dots, x_{n+1})}{x_0^{n+1}}. \tag{5.36}$$

Here P_n is a homogeneous polynomial of degree $n+1$, which follows from the repeated application of the quotient rule in computing expressions for derivatives of $\bar{x} = y + \frac{ax - bx'}{x}$. We obtain a local parametrisation of the image of B:

$$\begin{aligned} \bar{y}_{i_1} &= x_{i_1}^* + s_1 & \bar{x}_{j_1} &= y_{j_1}^* + t_1 + H_1 \\ &\vdots & &\vdots \\ \bar{y}_{i_p} &= x_{i_p}^* + s_p & \bar{x}_{j_{d-p}} &= y_{j_{d-p}}^* + t_{d-p} + H_{d-p} \end{aligned} \tag{5.37}$$

where $H_1, \dots H_{d-p}$ are analytic in $s_1, \dots, s_p$ (as $x_0 \neq 0$ on B), with the rest of the coordinates $\bar{y}_i, \bar{x}_j$ being analytic functions of the parameters. The Jacobian of this parametrisation can be seen to have rank at least $d-2$, with linearly independent columns corresponding to partial derivatives with respect to $s_1, \dots s_p, t_1, \dots, t_{d-p-1}$ (t_{d-p} will not contribute to the rank if $d - p = r + 1$, i.e. if y_{r+1} is one of the free variables in the parametrisation of B). The possibility that the image is of codimension less than m has already been illustrated at the start of subsection 3.2, where constraints on y_j may not induce constraints on the image.

Similarly, if we consider a subvariety of codimension m in the chart (X, y) away from $\{X_0 = 0\}$, we see that its image under φ_r must be again of codimension $\leq m$. This is done in exactly the same way as above, noting that the mapping in charts is of the form

$$\bar{Y}_n = X_n, \qquad \bar{x}_n = y_n - \frac{P_n(X_0, \dots, X_{n+1})}{X_0^{n+1}}, \tag{5.38}$$

where again P_n is a homogeneous polynomial of degree $n+1$. Regarding the part of the jet space with $X_0 = 0$, we remark that $X_0 = 0$ with $y_0 \neq 0$ is not an accessible singularity, as for a pole to develop while iterating, it must follow a zero. Further, the only parts of $\{X_0 = 0, y_0 = 0\}$ accessible from regular and nonzero initial data are those coming from one of the blow-down singularities B_m. Similar calculations in the charts (x, Y) and (X, Y) show that it suffices to consider blow-down singularities visible in the (x, y)-chart where at least $x_0 = 0$. If we take $x(z) = x_m\zeta^m + x_{m+1}\zeta^{m+1} + \ldots$ for $m > 0$ and $y = y_0 + y_1\zeta + \ldots$, then direct calculation shows that we have

$$\bar{X}_0 = 0, \quad \bar{X}_1 = -\frac{1}{bm}, \quad \bar{X}_2 = \frac{bx_{m+1} - ax_m}{b^2m^2x_m} - \frac{y_0}{b^2m^2}, \quad \ldots \tag{5.39}$$

and more generally that

$$\begin{aligned} \bar{X}_n &= \frac{P_n(x_m, \ldots, x_{m+n}, y_0, \ldots, y_{n-1})}{b^n m^n x_m^{n-1}} - \frac{y_{n-2}}{b^2m^2}, \\ \bar{y}_n &= 0 \text{ for } n < m, \quad \bar{y}_n = x_m \text{ for } n \geq m, \end{aligned} \tag{5.40}$$

where P_n is polynomial in its arguments. By again considering parametrisations and their Jacobians, it is straightforward to show that we cannot have blow-down singularities away from $x_m = 0$. Applying this argument inductively completes the proof that the only accessible blow-down singularities are as claimed. □

We now show how the singularity patterns pointed out in Subsection 5.2.1 correspond to confinement of blow-down singularities for equation (5.1).

Example 5.3.9. *The singularity B_1, which corresponds to the beginning of the singularity pattern*

$$(\mathrm{rg}, 0^1, \infty^1, \infty^1, 0^1, \mathrm{rg}),$$

is confined after five iterations. We calculate as we did in Section 5.2 but keep track of orders of jets and codimensions to find that composing the iteration on sections gives maps *as follows:*

$$\begin{array}{lll} B_1 \subset J^{r+5} & \mathrm{codim}(B_1) = 1 & (x^{(0)}, y^{(0)}) = (0^1, \mathrm{rg}) \\ \varphi^{(1)} : B_1 \to J^{r+5} & \mathrm{codim}(\varphi^{(1)}(B_1)) = 3 & (x^{(1)}, y^{(1)}) = (\infty^1, 0^1) \\ \varphi^{(2)} : B_1 \to J^{r+5} & \mathrm{codim}(\varphi^{(2)}(B_1)) = 5 & (x^{(2)}, y^{(2)}) = (\infty^1, \infty^1) \\ \varphi^{(3)} : B_1 \to J^{r+3} & \mathrm{codim}(\varphi^{(3)}(B_1)) = 3 & (x^{(3)}, y^{(3)}) = (0^1, \infty^1) \\ \varphi^{(4)} : B_1 \to J^{r+1} & \mathrm{codim}(\varphi^{(4)}(B_1)) = 1 & (x^{(4)}, y^{(4)}) = (\mathrm{rg}, 0^1) \\ \varphi^{(5)} : B_1 \to J^{r} & \mathrm{codim}(\varphi^{(5)}(B_1)) = 0 & (x^{(5)}, y^{(5)}) = (\mathrm{rg}, \mathrm{rg}) \end{array}$$

For each iteration, we have indicated the order of jet space to which we have well-defined mappings from B_1, as well as codimensions of the images of B_1 and the corresponding parts of the singularity pattern. We note that the exceptional behaviour we observed in the singularity pattern, namely that when computing $x^{(3)}$, three terms vanished as it developed a zero rather than a pole, is reflected in the codimension falling from 5 *to* 3*.*

More generally, if we take the blow-down singularities B_m as in Lemma 5.3.8 as subsets of J^{2m+3+r} with the rest of the coefficients generic, from Theorem 5.2.2 we see that iterating the system (5.1) induces a map $\varphi^{(2m+3)} : B_m \to J^r$, where the image of B_m is a jet visible in the (x, y)-chart. To see that this image is of codimension zero, we must make some observations of how the initial data from the section $(x^{(0)}, y^{(0)})$ enters into the subsequent iterates, and in particular how it is recovered in $(x^{(2m+3)}, y^{(2m+3)})$. This will require detailed but straightforward analysis of the mapping on jets in three cases, corresponding to different parts of the singularity pattern. These are firstly when the first pole develops and how the coefficients from $(x^{(0)}, y^{(0)})$ enter into $X^{(1)}, X^{(2)}$, secondly, how the initial data is propagated through the sequence of simple poles $X^{(1)}, \ldots, X^{(2m)}$, then how it reenters $x^{(2m+2)}, x^{(2m+3)}$ after the zero develops at $x^{(2m+1)}$. The key technique for our analysis here is essentially identifying and counting free variables, which we illustrate in detail in this example.

We first consider the map from $(x^{(0)}, y^{(0)})$ to $(X^{(1)}, y^{(1)})$ corresponding to the development of the first simple pole in the sequence. Here we omit the superscripts for conciseness, working with the mapping in the charts (x, y) and $(\bar{X}, \bar{y})$. Beginning with initial data corresponding to B_m, namely sections in the (x, y)-chart with $x_0 = x_1 = \ldots x_{m-1} = 0$, with the rest of the coefficients x_i, y_j generic, by direct calculation we have

$$\bar{X}_0 = 0, \ \ \bar{X}_1 = -\frac{1}{mb}, \qquad \bar{X}_n = -\frac{y_{n-2}}{m^2 b^2} + \frac{P_n(x_m, \dots, x_{m+n-1}, y_0, \dots, y_{n-3})}{x_m^{n-1}}, \quad \text{for } n \geq 2$$

$$\bar{y}_0 = \cdots = \bar{y}_{m-1} = 0, \qquad \bar{y}_n = x_n, \quad \text{for } n \geq m,$$

where P_n is polynomial in its arguments. From this, we see that the coefficients $\bar{X}_{i\geq 2}, \bar{y}_{j\geq m}$ are algebraically independent functions of the initial data, which follows from the way in which the free variable y_{n-2} ($n \geq 2$) appears linearly in $\bar{X}_n$ but not at all in $\bar{X}_{n-1}$ and so on. In particular we have the image of B_m under a single iteration being of codimension $m+2$, as noted in Example 5.3.4. Similarly, we see that the next iterate is obtained from $\bar{X}_i, \bar{y}_j$ above as

$$\begin{aligned}
\bar{\bar{X}}_0 = 0, \ \ \bar{\bar{X}}_1 = \frac{1}{b}, \quad \bar{\bar{X}}_j &= P_j(\bar{X}_0, \dots, \bar{X}_j), && \text{for } 2 \leq j \leq m+1, \\
\bar{\bar{X}}_n &= -\frac{\bar{y}_{n-2}}{b^2} + Q_n(\bar{X}_0, \dots, \bar{X}_n, \bar{y}_m \dots \bar{y}_{n-3}), && \text{for } n \geq m+2, \\
\bar{\bar{Y}}_0 = 0, \quad \bar{\bar{Y}}_1 = -\frac{1}{mb}, \quad \bar{\bar{Y}}_n &= \bar{X}_n, && \text{for } n \geq 2.
\end{aligned}$$

Here P_j is again polynomial (linear in $\bar{X}_j$) and Q_n is polynomial in its arguments. From this, we see that the image of B_m is of codimension $m+4$, with $\bar{\bar{X}}_i, \bar{\bar{Y}}_j$ having the following dependence on the initial data x_i, y_j:

$$\begin{aligned}
\bar{\bar{X}}_0 = 0, \ \ \bar{\bar{X}}_1 = \frac{1}{b}, \qquad \bar{\bar{X}}_n &= F_n(y_0, \dots, y_{n-2}, x_m, \dots, x_{m+n-1}) && \text{for } n \geq m+2, \\
\bar{\bar{Y}}_0 = 0, \ \ \bar{\bar{Y}}_1 = -\frac{1}{mb}, \quad \bar{\bar{Y}}_n &= G_n(y_0, \dots, y_{n-2}, x_m, \dots, x_{m+n-1}) && \text{for } n \geq m+2,
\end{aligned}$$

where, importantly, F_n is linear in y_{n-2} with constant coefficient, and also linear in x_{m+n-1} with coefficient being a constant multiple of $1/x_m$.

We now consider the iterates $X^{(3)}, \dots, X^{(2m)}$, which correspond to simple poles, and show that we have the same kind of dependence of coefficients on the initial data. Building on our calculation (5.33) in the charts $(X, Y), (\bar{X}, \bar{Y})$, we see that sections with $(X_0, Y_0) = (0, 0)$

have images under the iteration mapping given by

$$\begin{aligned}
&\bar{X}_0 = 0, \quad \bar{X}_1 = \frac{Y_1}{1+bY_1}, \\
&\bar{X}_n = \frac{Y_n}{(1+bY_1)^2} + \frac{P_n(X_1,\dots,X_n,Y_1,\dots Y_{n-1})}{X_1^{n-1}(1+bY_1)^n}, \\
&\bar{Y}_0 = 0, \quad \bar{Y}_1 = X_1, \\
&\bar{Y}_n = X_n, \qquad \text{for } n \geq 2,
\end{aligned} \tag{5.41}$$

where P_n is polynomial in its arguments, and we note that these expansions are valid for determining all iterates $(X^{(2)},Y^{(2)}),\dots,(X^{(2m)},Y^{(2m)})$, as we have $X_1^{(k)} \neq 0, 1+bY_1^{(k)} \neq 0$, for $k=0,\dots,2m-1$, which we know from our explicit expressions of the residues of the simple poles in the singularity pattern, given in Theorem 5.2.2 . Iterating through this sequence of simple poles, we have well-defined maps $J^{2m+3+r} \backslash \{X_1(1+bY_1)=0\} \to J^{2m+3+r}$, and a simple calculation using the Jacobian as in the proof of Lemma 5.3.8 shows that the image of B_m cannot change codimension in J^{2m+3+r} under this sequence of maps, so we have the images of B_m under $\varphi^{(2)},\dots,\varphi^{(2m)}$ are all of codimension $m+4$.
Further, from (5.41) and our observations of $(\bar{\bar{X}},\bar{\bar{Y}})$ we see that for $k=2,\dots,2m$, the coefficients $X_n^{(k)},Y_n^{(k)}$ have the same kind of dependence on the initial data, and in particular the last iterate before the zero develops is of the form

$$\begin{aligned}
&X_0^{(2m)} = 0, \;\; X_1^{(2m)} = \frac{1}{mb}, \\
&X_n^{(2m)} = F_n^{(2m)}(y_0,\dots,y_{n-2},x_m,\dots,x_{m+n-1}) \quad \text{for } n \geq m+2, \\
&Y_0^{(2m)} = 0, \;\; Y_1^{(2m)} = -\frac{1}{b}, \\
&Y_n^{(2m)} = G_n^{(2m)}(y_0,\dots,y_{n-2},x_m,\dots,x_{m+n-1}) \quad \text{for } n \geq m+2,
\end{aligned} \tag{5.42}$$

where again $F_n^{(2m)},G_n^{(2m)}$ are linear in y_{n-2} with constant coefficient, and also linear in x_{m+n-1} with coefficient being a constant multiple of $1/x_m$.
We now consider the final step, when the map $(X^{(2m)},Y^{(2m)}) \mapsto (x^{(2m+1)},Y^{(2m+1)})$ shows a drop in codimension of the image of B_m, with the development of a zero of order m. Omiting the superscripts for conciseness and writing

$$(X^{(2m)},Y^{(2m)}) = (X_0+X_1\zeta+\dots,Y_0+Y_1\zeta+\dots), \tag{5.43}$$

we know that the coefficients for the image of B_m under the iterations up to this point in the singularity pattern must satisfy at least

$$Y_0 = 0, \quad Y_1 = -b^{-1}, \quad X_0 = 0, \quad X_1 = (mb)^{-1}. \tag{5.44}$$

Similarly writing $(x^{(2m+1)}, Y^{(2m+1)}) = (\bar{x}_0 + \bar{x}_1\zeta + \dots, \bar{Y}_0 + \bar{Y}_1\zeta + \dots)$, we see the mapping on coefficients from jets satisfying (5.44) gives

$$\begin{aligned} &\bar{x}_0 = 0, \quad \bar{x}_1 = a + b^2 m X_2 - b^2 Y_2, \\ &\bar{x}_2 = -b^2\left(bm^2X_2^2 + bY_2^2 - 2mX_3 + Y_3\right), \\ &\bar{x}_n = b^2(nmX_{n+1} - Y_{n+1}) + P_n(X_2, \dots, X_n, Y_2, \dots, Y_n), \quad \text{for } n \geq 1, \\ &\bar{Y}_0 = 0, \quad \bar{Y}_1 = \frac{1}{mb}, \quad \bar{Y}_j = X_j, \quad \text{for } j \geq 2, \end{aligned} \tag{5.45}$$

where we have again used P_n to denote a polynomial in its arguments. We know from Theorem 5.2.2 that if $(X^{(2m)}, Y^{(2m)})$ are obtained by iterating from B_m, then the coefficients X_i, Y_j must satisfy the algebraic conditions for $\bar{x}_0, \dots, \bar{x}_{m-1}$ given by (5.45) to all vanish, and we know exactly what relations must exist between the coefficients $(X_i^{(2m)}, Y_j^{(2m)})$, which have evolved through the singularity pattern from those defining B_m. Further, from the dependence of $X_i^{(2m)}, Y_j^{(2m)}$ on the initial data, and the way in which $X_i^{(2m)}, Y_j^{(2m)}$ enter into $x_i^{(2m+1)}, Y_j^{(2m+1)}$ according to (5.45), we see that the image of B_m under $\varphi^{(2m+1)}$ is of codimension $m+3$ in the jet space corresponding to $(x^{(2m+1)}, Y^{(2m+1)})$. Finally, another calculation on the exact same lines shows that after one more step, we have the image of B_m under $\varphi^{(2m+2)}$ being of codimension zero.

5.3.3.2 Equation (1.2)

The analysis in this case proceeds in exactly the same way as the previous one, so we omit details for conciseness. In particular, the following may be proved using the same techniques and approach as for Lemma 5.3.8:

Lemma 5.3.10. *The only accessible blow-down type singularities of equation* (5.1) *are*

$$B_m = \{x_i = 0 \ \forall i = 0, \dots, m-1\},$$

with all other coefficients generic.

We may also use the same techniques to examine the behaviour of blow-down singularities in terms of codimension, beginning with that associated with a simple zero:

Example 5.3.11. *The singularity* B_1 *of equation* (5.2)*, which corresponds to the start of the singularity pattern*

$$(\mathrm{rg}, 0^1, \infty^2, 0^1, \mathrm{rg}),$$

is confined after four iterations, with the following behaviour under compositions of the iteration maps:

$$\begin{array}{lll} B_1 \subset J^{r+4} & \mathrm{codim}(B_1) = 1 & (x^{(0)}, y^{(0)}) = (0^1, \mathrm{rg}) \\ \varphi^{(1)} : B_1 \to J^{r+4} & \mathrm{codim}(\varphi^{(1)}(B_1)) = 5 & (x^{(1)}, y^{(1)}) = (\infty^2, 0^1) \\ \varphi^{(2)} : B_1 \to J^{r+4} & \mathrm{codim}(\varphi^{(2)}(B_1)) = 5 & (x^{(2)}, y^{(2)}) = (0^1, \infty^2) \\ \varphi^{(3)} : B_1 \to J^{r+1} & \mathrm{codim}(\varphi^{(3)}(B_1)) = 1 & (x^{(3)}, y^{(3)}) = (\mathrm{rg}, 0^1) \\ \varphi^{(4)} : B_1 \to J^{r} & \mathrm{codim}(\varphi^{(4)}(B_1)) = 0 & (x^{(4)}, y^{(4)}) = (\mathrm{rg}, \mathrm{rg}) \end{array}$$

We note here again that the drop in codimension occurs when two terms vanish in the expansion for $x^{(3)}$ *as it regains regularity as opposed to having a double pole.*

Again, considering the blow-down singularities B_m from Lemma 5.3.10 as subsets of J^{2m+2+r}, Theorem 5.2.1 and tracing the dependence on initial data of the iterates through the sequence using exactly the same techniques as in the previous example, we see that we have $\varphi^{(2m+2)} : B_m \to J^r$ under which the image of B_m is of codimension zero, so all accessible blow-down singularities of equation (5.2) are confined.

5.3.3.3 Equation (1.3)

In this case we begin with an example, as the blow-down singularities for equation (5.3) occur not after x develops a zero at z_0, but under the mapping applied to the jets in $\underline{x}, \underline{y}$ coordinates satisfying the condition for a zero to develop.

Example 5.3.12. *The condition on* $(\underline{x}, \underline{y})$ *for a simple zero to develop while iterating equation* (5.3)*, namely*

$$B_1 = \{\alpha \underline{x}_1 + \lambda(z_0 - 1)\underline{x}_0 = 0\},$$

with the rest of the coefficients generic, corresponds to the start of the singularity pattern which we denoted in Section 5.2 by

$$\left(\mathrm{rg}, \underline{\zeta}_0^1, 0^1, \infty^1, \bar{\bar{\zeta}}_0^1, \mathrm{rg}\right).$$

We observe a jump in codimension not from $(x^{(0)}, y^{(0)})$ *to* $(x^{(1)}, y^{(1)})$*, but one step earlier, and we observe the following behaviour under compositions of the iteration maps:*

$$
\begin{array}{rll}
B_1 \subset J^{r+5} & \operatorname{codim}(B_1) = 1 & (x^{(-1)}, y^{(-1)}) = (\underline{\zeta}_0^1, \mathrm{rg}) \\
\varphi^{(1)} : B_1 \to J^{r+4} & \operatorname{codim}(\varphi^{(1)}(B_1)) = 2 & (x^{(0)}, y^{(0)}) = (0^1, \underline{\zeta}_0^1) \\
\varphi^{(2)} : B_1 \to J^{r+4} & \operatorname{codim}(\varphi^{(2)}(B_1)) = 2 & (x^{(1)}, y^{(1)}) = (\infty^1, 0^1) \\
\varphi^{(3)} : B_1 \to J^{r+3} & \operatorname{codim}(\varphi^{(3)}(B_1)) = 2 & (x^{(2)}, y^{(2)}) = (\bar{\bar{\zeta}}_0^1, \infty^1) \\
\varphi^{(4)} : B_1 \to J^{r+1} & \operatorname{codim}(\varphi^{(4)}(B_1)) = 1 & (x^{(3)}, y^{(3)}) = (\mathrm{rg}, \bar{\bar{\zeta}}_0^1) \\
\varphi^{(5)} : B_1 \to J^{r} & \operatorname{codim}(\varphi^{(5)}(B_1)) = 0 & (x^{(4)}, y^{(4)}) = (\mathrm{rg}, \mathrm{rg})
\end{array}
$$

We note here again that a drop in codimension occurs when $x^{(3)}$ *regains regularity as opposed to a simple zero.*

Again by the same approach, the following may be proved by local calculations in charts:

Lemma 5.3.13. *The only accessible blow-down type singularities of equation* (5.3) *are*

$$B_m = \left\{ \frac{d^i}{dz^i} \left(\lambda z \underline{x}(z) + \alpha \underline{x}'(z) \right)\Big|_{z=z_0} = 0, \quad \forall i = 0, \dots, m-1 \right\},$$

with all other coefficients generic.

In the same way as the other two examples, we see from Theorem 5.2.3 that for regarding B_m as a subset of $J^{(2m+2)}$, iterating the system gives a map $\varphi^{(2m+3)} : J^{(2m+3+r)} \to J^{(r)}$, under which the image of B_m is of codimension zero.

5.4 Conclusions

We now summarise our work in this chapter and discuss questions that follow it naturally, again organised into two parts: firstly singularity analysis on the level of equations and secondly its geometric interpretation. On this first level, we have significantly extended previous studies of delay Painlevé equations and discovered new confinement type behaviour, which we believe is interesting in its own right. In the process we have developed techniques for the analysis of singularity patterns of arbitrary length and proving confinement, which we hope will be useful in tackling one of the main difficulties in the singularity analysis of delay-differential equations. It would be interesting to adapt our methods to other integrable delay-differential equations, for example extensions of the examples considered in this paper such as the families generalising equation (5.2) isolated by Halburd and Korhonen by imposing Nevanlinna-theoretic integrability criteria [HK17]. Though preliminary calculations show that these equations admit some of the same confined singularity patterns as equation (5.2) (namely those associated with single, double and triple zeroes) it is a natural next step to determine whether these admit the same infinite families and whether this behaviour fits into our geometric framework. Further, the complete description of singularity patterns associated with zeroes has the potential to allow methods developed by Halburd [Hal17] for computing degree growth in systems from singularity analysis to be adapted for application to our three examples.

Another question that arises from our work on the level of equations relates to the use of singularity analysis techniques to isolate integrability candidates. The fact that each of these three examples may be obtained by requiring confinement of only the simplest singularity in the family associated with zeroes of different orders prompts the question of whether and how this could ensure confinement of all singularities in the family. Further, there may be applications of our results to the search for elliptic function solutions of degenerate cases of delay Painlevé equations. For example, the $a = 0$ and $p = 0$ cases of equations (5.1) and (5.2) respectively are known to admit elliptic function solutions [Ber17]. Degree 2 elliptic function solutions were identified with the help of singularity analysis, and in particular that these degenerate cases admit the singularity patterns associated with simple zeroes outlined in Section 5.2. These patterns are compatible with elliptic function solutions in the sense that the numbers of poles and zeroes in a pattern are equal (counted with multiplicity), and also that the residues of poles in the sequence sum to zero. We note that our proofs of the infinite families of singularity patterns are also valid for the degenerate cases, and we observe the same kind of compatibility with elliptic function solutions in all of them, so it would be interesting to determine whether they may be used to isolate higher degree elliptic function solutions.

The other aim of this work was to initiate the geometric study of delay Painlevé equations. The possibility of a geometric framework for Painlevé equations in the delay-differential class is an exciting prospect not only for the general theory of Painlevé equations, but for widening the range of equations whose integrability can be exploited in applications. Delay-differential equations of the kind we consider arise in a range of fields of applied mathematics, most notably in mathematical biology, for example as equations for steady states of systems of partial differential equations with a spatial delay [FBM19]. We have put forward a geometric description of singularity confinement in these three examples, and we hope to have worked in convincing parallel with the discrete case, and in particular captured in our description the exceptional nature of these equations in terms of the recovery of initial data when a singularity is confined. By no means, however, is this geometric framework complete or definitive, and we hope that our ideas are refined and built upon through singularity analysis in more examples.

5.5 Proofs of infinite families of singularity patterns

We now give proofs of the results of Subsection 5.2.1 relating to infinite families of singularity patterns.

5.5.1 Proof of Theorem 2.2

For equation (5.1), our strategy is to consider a singularity pattern beginning with $(\mathrm{rg}, 0^m)$, then derive and analyse recurrences for the coefficients in the expansions of the next $(2m+1)$ iterates, to deduce that the singularity pattern is as claimed.

Because the equation (5.1) is autonomous we can take without loss of generality the zero of order m to be at the origin, and start with the formal expansions

$$\underline{u} = \sum_{j=0}^{\infty} \underline{u}_j z^j, \tag{5.46a}$$

$$u = \sum_{j=m}^{\infty} u_j z^j, \qquad u_m \neq 0. \tag{5.46b}$$

Inserting these into the equation, we immediately see that $\bar{u}$ has a simple pole:

$$\bar{u} = -\frac{m\beta}{z} + O(1). \tag{5.47}$$

The iterates of interest to us are $u = u^{(0)}, \bar{u} = u^{(1)}, u^{(2)}, \ldots, u^{(2m)}, u^{(2m+1)}$. By inspection of the terms on the right-hand side of the forward iteration (5.10), these will be either regular or poles of order at most one, so we introduce the notation

$$u^{(i)} = \sum_{n=-1}^{\infty} u_n^{(i)} z^n, \tag{5.48}$$

for $i = 0, \ldots, 2m+1$, where any number of the $u_n^{(i)}$ may be zero.

By deriving recurrences for the coefficients $u_n^{(i)}$, we will show firstly that $u_{-1}^{(i)} \neq 0$ for $i = 1, \ldots, 2m$, then that $u_{-1}^{(2m+1)} = u_0^{(2m+1)} = \cdots = u_{m-1}^{(2m+1)} = 0$, from which we will deduce that $u^{(2m+1)} = \mathcal{O}(z^m)$, and in particular has a zero of order m if the rest of the initial data is generic.

It will be helpful to introduce some notation to deal with the logarithmic derivative u'/u in the forward iteration map.

Lemma 5.5.1. *Let r be a nonzero integer. If $u = \sum_{j=r}^{\infty} u_j z^j$ with u_r nonzero, then*

$$\frac{u'}{u} = \sum_{n=-1}^{\infty} U_n z^n, \tag{5.49}$$

where the coefficients U_n are given by $U_{-1} = r$, $U_0 = u_{r+1}/u_r$, and so on according to the recurrence

$$U_n = \frac{1}{u_r}\left((n+1)u_{r+n+1} - \sum_{j=1}^{n} u_{r+j}U_{n-j}\right). \tag{5.50}$$

We first deduce from the recurrence that following the zero of order m, the next $2m$ iterates have simple poles:

Proposition 5.5.2. *The iterates $u^{(i)}$ have simple poles at $z = 0$ for all $i = 1, \ldots, 2m$, and we have*

$$u_{-1}^{(2k)} = k\beta, \qquad \textit{for } k = 1, \ldots, m, \tag{5.51a}$$

$$u_{-1}^{(2k+1)} = (k-m)\beta \qquad \textit{for } k = 0, \ldots, m. \tag{5.51b}$$

Proof. We already have that $u_{-1}^{(0)} = 0$ and $u_{-1}^{(1)} = -m\beta$. We then insert the expansions (5.48) for the iterates $u^{(i)}$ into the relevant upshifts of the equation, making use of Lemma 5.5.1 with $r = -1$, which gives

$$u_{-1}^{(i+1)} = u_{-1}^{(i-1)} + \beta, \tag{5.52}$$

for all i such that $u^{(i)}$ has a simple pole. Iterating this from $i = 1$ from the initial values for $u_{-1}^{(0)}, u_{-1}^{(1)}$, we see that $u^{(i)}$ have simple poles for all $i = 1, \ldots, 2m$, and we obtain the formulae (5.51). □

It will now be helpful to introduce the following notation for the iterates:

$$
\begin{aligned}
u^{(2k)} &= f^{(k)} = \sum_{n=-1}^{\infty} f_n^{(k)} z^n, \qquad f_n^{(k)} = u_n^{(2k)}, \\
u^{(2k+1)} &= g^{(k)} = \sum_{n=-1}^{\infty} g_n^{(k)} z^n, \qquad g_n^{(k)} = u_n^{(2k+1)},
\end{aligned}
\tag{5.53}
$$

for $k = 0, \ldots, m$. As we now know that $u^{(1)}, \ldots, u^{(2m)}$ have simple poles at $z = 0$, we use Lemma 5.5.1 to write the logarithmic derivatives of $f^{(k)}, g^{(k-1)}$, for $k = 1, \ldots m$ as

$$
\frac{f^{(k)\prime}}{f^{(k)}} = \sum_{n=-1}^{\infty} F_n^{(k)} z^n, \qquad \frac{g^{(k)\prime}}{g^{(k)}} = \sum_{n=-1}^{\infty} G_n^{(k)} z^n. \tag{5.54}
$$

Further, we have from (5.51) that for $k = 0, \ldots, m$ that $F_{-1}^{(k)} = k\beta,\ G_{-1}^{(k)} = (m-k)\beta$, so we have the following recursive formulae for $F_n^{(k)}, G_n^{(k)}$:

$$
F_n^{(k)} = \frac{1}{k\beta}\left((n+1)f_n^{(k)} - \sum_{j=1}^{n} f_{j-1}^{(k)} F_{n-j}^{(k)}\right), \tag{5.55a}
$$

$$
G_n^{(k)} = \frac{1}{(k-m)\beta}\left((n+1)g_n^{(k)} - \sum_{j=1}^{n} g_{j-1}^{(k)} G_{n-j}^{(k)}\right), \tag{5.55b}
$$

valid for all k such that $f^{(k)}, g^{(k)}$ have simple poles. Using this notation, the forward iteration then leads to the recurrences,

$$
f_0^{(k)} = f_0^{(k-1)} + \alpha - \beta G_0^{(k-1)}, \tag{5.56a}
$$

$$
g_0^{(k)} = g_0^{(k-1)} + \alpha - \beta F_0^{(k)}, \tag{5.56b}
$$

and

$$
f_n^{(k)} = f_n^{(k-1)} - \beta G_n^{(k-1)}, \tag{5.57a}
$$

$$
g_n^{(k)} = g_n^{(k-1)} - \beta F_n^{(k)}, \tag{5.57b}
$$

for $n \geq 1$, and $k = 1, \ldots, m$. Using (5.55) with $n = 0$, we see that the recurrences (5.56) are a linear system of difference equations for $f_0^{(k)}, g_0^{(k)}$:

$$f_0^{(k)} = f_0^{(k-1)} + \alpha - \frac{1}{(k-1-m)} g_0^{(k-1)}, \tag{5.58a}$$

$$g_0^{(k)} = g_0^{(k-1)} + \alpha - \frac{1}{k} f_0^{(k)}, \tag{5.58b}$$

subject to the initial conditions $f_0^{(0)} = 0$ and $g_0^{(0)} = u_0^{(1)} = \alpha + \underline{u}_0 - \beta u_1/u_0$ determined by the initial data $\underline{u}, u$. The unique solution of (5.58) subject to these initial conditions is given by

$$f_0^{(k)} = k(\alpha + C), \tag{5.59a}$$

$$g_0^{(k)} = (m-k)C, \tag{5.59b}$$

where $C = u_0^{(1)}/m$. Similarly, after using the formula (5.55), the recurrences (5.57) become

$$f_n^{(k)} = f_n^{(k-1)} - \frac{1}{(k-1-m)} \left((n+1) g_n^{(k-1)} - \sum_{j=1}^{n} g_{j-1}^{(k-1)} G_{n-j}^{(k-1)} \right), \tag{5.60a}$$

$$g_n^{(k)} = g_n^{(k-1)} - \frac{1}{k} \left((n+1) f_n^{(k)} - \sum_{j=1}^{n} f_{j-1}^{(k)} F_{n-j}^{(k)} \right), \tag{5.60b}$$

subject to the initial conditions $f_n^{(0)} = 0$ for $n = 0, \dots, m-1$, and $g_n^{(0)}$ fixed by the initial data $\underline{u}, u$. Given the solution (5.59), the $n = 1$ case is then a linear system of recurrences in k for $f_1^{(k)}, g_1^{(k)}$, which may be solved by elementary methods. With both $n = 0, 1$ solutions in hand the system for $f_2^{(k)}, g_2^{(k)}$ can be solved, and so on. Observations of these solutions lead us to the following proposition:

Proposition 5.5.3. *The unique solution to* (5.60) *subject to the initial conditions is given by* $(f_n^{(k)}, g_n^{(k)})$, $n = 0, \dots, m-1, k = 0, \dots, m$ *of the form*

$$f_n^{(k)} = k P_n^{(k)} \tag{5.61a}$$

$$g_n^{(k)} = (k-m) Q_n^{(k)}, \tag{5.61b}$$

where $P_n^{(k)}, Q_n^{(k)}$ *are polynomial in* k *of degree at most* n.

Proof. We have from formulae (5.59) that the statement is true for $n = 0$, so we proceed by induction. Suppose that $f_0^{(k)}, \ldots, f_{n-1}^{(k)}$ and $g_0^{(k)}, \ldots, g_{n-1}^{(k)}$ are of the form (5.61). The recursive formulae (5.55) then imply that $F_0^{(k}, \ldots, F_{n-1}^{(k)}$ and $G_0^{(k)}, \ldots, G_{n-1}^{(k)}$ are polynomial in k, of degree at most $n-1$. We then see that the following terms from (5.60) are polynomial in k of degree at most $n-1$:

$$\frac{1}{k}\sum_{j=1}^{n} f_{j-1}^{(k)} F_{n-j}^{(k)} = \sum_{j=1}^{n} P_{j-1}^{(k)} F_{n-j}^{(k)} = \sum_{j=0}^{n-1} \lambda_j k^j, \tag{5.62a}$$

$$\frac{1}{(k-m)}\sum_{j=1}^{n} g_{j-1}^{(k)} G_{n-j}^{(k)} = \sum_{j=1}^{n} Q_{j-1}^{(k)} G_{n-j}^{(k)} = \sum_{j=0}^{n-1} \mu_j k^j, \tag{5.62b}$$

so we have

$$f_n^{(k+1)} = f_n^{(k)} - \frac{n+1}{k-m} g_n^{(k)} + \sum_{j=0}^{n-1} \mu_j k^j, \tag{5.63a}$$

$$g_n^{(k+1)} = g_n^{(k)} - \frac{n+1}{k+1} f_n^{(k)} \sum_{j=0}^{n-1} \lambda_j k^j, \tag{5.63b}$$

We write our ansatz (5.61) for the solution to this equation as

$$f_n^{(k)} = k \sum_{j=0}^{n} a_j k^j \tag{5.64a}$$

$$g_n^{(k)} = (k-m) \sum_{j=0}^{n} b_j k^j. \tag{5.64b}$$

We note that one initial condition $u_n^{(0)} = 0$ is satisfied automatically, but imposing the other requires us to set

$$b_0 = -u_n^{(1)}/m. \tag{5.65}$$

We now insert the ansatz (5.64) into the equation (5.63) and equate coefficients of powers of k to obtain a linear system in $2n+1$ variables $a_0, \ldots, a_n, b_1, \ldots, b_n$:

$$0 = a_n + b_n, \tag{5.66a}$$

$$\lambda_i = (n+1)a_i + (i+1)b_i + \sum_{j=i+1}^{n} (-1)^{j-i} \left(\begin{pmatrix} j+1 \\ i \end{pmatrix} + m \begin{pmatrix} j \\ i \end{pmatrix} \right) b_j, \tag{5.66b}$$

$$\mu_i = \sum_{j=i}^{n} \begin{pmatrix} j \\ i \end{pmatrix} a_j + (n+1)b_i, \tag{5.66c}$$

$$\lambda_0 = (n+1)a_0 + (m+1)\sum_{j=1}^{n}(-1)^j b_j, \tag{5.66d}$$

$$\mu_0 = \sum_{j=0}^{n} a_j + (n+1)b_0, \tag{5.66e}$$

for $i = 1, \ldots, n-1$. We write this as $\mathcal{M}_n \mathbf{v} = \mathbf{c}$, where $\mathbf{v} = (a_0, \ldots, a_n, b_1, \ldots, b_n)^T$, $\mathbf{c} = (0, \lambda_0, \ldots, \lambda_n, \mu_0, \ldots, \mu_n)^T$ and $\mathcal{M}_n$ is the square matrix of size $2n+1$ giving the right-hand side of the system (5.66). A simple sequence of row and column operations yields an upper-triangular matrix and we obtain

$$\det \mathcal{M}_n = (n!)^2 (m-n)_n, \tag{5.67}$$

where $(a)_n = \prod_{i=0}^{n-1}(a+i)$ is the usual Pochammer symbol, so the matrix is nonsingular for $n \leq m-1$, showing that the unique solution of the recurrence (5.63) is of the form (5.64) and the inductive step is complete. □

Together with Proposition 5.5.2, this allows us deduce that $u_n^{(2m+1)} = 0$ for $m \geq n$, and thus that $u^{(2m+1)} = O(z^m)$.

5.5.2 Proof of Theorem 2.1

While we may proceed along the same lines as in Subsection 5.5.1, a shortcut is provided by the known transformation between equation (5.1) and equation (5.2) in Lemma 5.1.1. So, we consider a singularity pattern for equation (5.2) beginning with $(\underline{v}, v) = (\mathrm{rg}, 0^m)$, and we also assume that the zero has developed while iterating through regular and nonzero iterates, so $\underline{\underline{v}}$ is also regular. Then under the transformation to a solution of (5.1), we have

$$(\underline{u}, u) = (\underline{\underline{v}}\underline{v}, \underline{v}v) = (\mathrm{rg}, 0^m), \tag{5.68}$$

so the transformation gives us a singularity pattern for (5.1), which by Theorem 5.2.2 must be

$$\left(\mathrm{rg}, 0^m, \infty^1, \infty^1, \infty^1, \ldots, \infty^1, \infty^1, 0^m, \mathrm{rg}\right),$$

with $u^{(k)} \sim \zeta^{-1}$ for $k = 1, \ldots, 2m$, then $u^{(2m+1)} \sim \zeta^m$, and $u^{(2m+2)}$ regular. So this implies that the iterates $v^{(k)}$ in the singularity pattern must satisfy:

$$v^{(k-1)}v^{(k)} = u^{(k)} \sim \zeta^{-1} \quad \text{for } k = 1, \ldots, 2m, \tag{5.69a}$$

$$v^{(2m)}v^{(2m+1)} = u^{(2m+1)} \sim \zeta^m, \tag{5.69b}$$

$$v^{(2m+1)}v^{(2m+2)} = u^{(2m+2)} = \mathcal{O}(\zeta^0). \tag{5.69c}$$

Beginning with our assumption that $v^{(0)} \sim \zeta^m$, we see from the $k = 1$ case of equation (5.69a) that $v^{(1)} \sim \zeta^{-(m+1)}$, and then using the $k = 2, \ldots, 2m$ cases successively that

$$v^{(2k)} \sim \zeta^m, \text{ for } k = 0, \ldots, m, \qquad v^{(2k+1)} \sim \zeta^{-(m+1)} \text{ for } k = 0, \ldots, m-1. \tag{5.70}$$

Then using equations (5.69b) and (5.69c) we have that $v^{(2m+1)} \sim \zeta^0$ and $v^{(2m+2)} = \mathcal{O}(\zeta^0)$ and the proof is complete.

5.5.3 Proof of Theorem 2.3

Again, while the strategy and techniques from the proof of Theorem 5.2.2 are available for this case, a shortcut is provided by the transformation between equation (5.1) and equation (5.3) in Lemma 5.1.2 Similarly to in the proof above, we consider a singularity pattern for equation (5.3) beginning with $(\underline{w}, w)$, where $\frac{d^i}{dz^i}\left(\lambda z \underline{w}(z) + \alpha \underline{w}'(z)\right) = 0$ at $z = z_0$ for $i = 0, \ldots, m-1$ and $w \sim \zeta^m$. and we also assume that the zero has developed while iterating through regular and nonzero iterates, so $\underline{w}, \underline{\underline{w}}$ are also regular and nonzero. Then under the transformation to a solution of (5.1), we have

$$(\underline{\underline{u}}, \underline{u}) = \left(\underline{w}/\underline{\underline{w}}, w/\underline{w}\right) = (\mathrm{rg}, 0^m), \tag{5.71}$$

so the transformation gives us a singularity pattern for (5.1), which by Theorem 5.2.2 must be

$$\left(\mathrm{rg}, 0^m, \infty^1, \infty^1, \ldots, \infty^1, \infty^1, 0^m, \mathrm{rg}\right),$$

with $u^{(k)} \sim \zeta^{-1}$ for $k = 0, \dots, 2m-1$, then $u^{(2m)} \sim \zeta^m$, and $u^{(2m+2)}$ regular. So this implies that the iterates $w^{(k)}$ in the singularity pattern must satisfy:

$$\frac{w^{(k+1)}}{w^{(k-1)}} = u^{(k)} \sim \zeta^{-1} \quad \text{for } k = 0, \dots, 2m-1, \tag{5.72a}$$

$$\frac{w^{(2m+1)}}{w^{(2m-1)}} = u^{(2m)} \sim \zeta^m, \tag{5.72b}$$

$$\frac{w^{(2m+2)}}{w^{(2m)}} = u^{(2m+1)} = \mathcal{O}(\zeta^0). \tag{5.72c}$$

Beginning with our assumptions that $w^{(0)} \sim \zeta^m$ and $w^{(-1)}$ is regular, we see recursively from equation (5.72a) that

$$w^{(2k)} \sim \zeta^{m-k} \text{ for } k = 0, \dots m-1, \qquad w^{(2k+1)} \sim \zeta^{-k} \text{ for } k = 0, \dots, m. \tag{5.73}$$

Then using equations (5.72b) and (5.72c) we see that $w^{(2m+1)} \sim \zeta^0$ and $w^{(2m+2)} = \mathcal{O}(\zeta^0)$ and the proof is complete.

Bibliography

[AC91] M. J. Ablowitz and P. A. Clarkson, *Solitons, nonlinear evolution equations and inverse scattering*, London Mathematical Society Lecture Note Series, vol. 149, Cambridge University Press, Cambridge, 1991. MR1149378

[ARS80a] M. J. Ablowitz, A. Ramani, and H. Segur, *A connection between nonlinear evolution equations and ordinary differential equations of P-type. I*, J. Math. Phys. **21** (1980), no. 4, 715–721. MR565716

[ARS80b] ______, *A connection between nonlinear evolution equations and ordinary differential equations of P-type. II*, J. Math. Phys. **21** (1980), no. 5, 1006–1015. MR574872

[AS77] M. J. Ablowitz and H. Segur, *Exact linearization of a Painlevé transcendent*, Phys. Rev. Lett. **38** (1977), no. 20, 1103–1106. MR442981

[Adl93] V. E. Adler, *Recuttings of polygons*, Functional Analysis and Its Applications **27** (1993), no. 2, 141–143.

[Adl94] ______, *Nonlinear chains and Painlevé equations*, Phys. D **73** (1994), no. 4, 335–351. MR1280883

[Ams55] M.-H. Amsler, *Des surfaces à courbure négative constante dans l'espace à trois dimensions et de leurs singularités*, Math. Ann. **130** (1955), 234–256. MR0073225

[Arn90a] V. I. Arnol′d, *Dynamics of complexity of intersections*, Bol. Soc. Brasil. Mat. (N.S.) **21** (1990), no. 1, 1–10. MR1139553

[Arn90b] ______, *Dynamics of intersections*, Analysis, et cetera, 1990, pp. 77–84. MR1039340

[AHJN16] J. Atkinson, P. Howes, N. Joshi, and N. Nakazono, *Geometry of an elliptic difference equation related to Q4*, J. Lond. Math. Soc. (2) **93** (2016), no. 3, 763–784. MR3509963

[BCH96] A. P. Bassom, P. A. Clarkson, and A. C. Hicks, *On the application of solutions of the fourth Painlevé equation to various physically motivated nonlinear partial differential equations*, Adv. Differential Equations **1** (1996), no. 2, 175–198. MR1364000

[BV99] M. P. Bellon and C. M. Viallet, *Algebraic entropy*, Comm. Math. Phys. **204** (1999), no. 2, 425–437. MR1704282

[Ber17] B. K. Berntson, *Integrable delay-differential equations*, Ph.D. Thesis, 2017. (University College London).

[Ber18] ______, *Special solutions of bi-Riccati delay-differential equations*, SIGMA Symmetry Integrability Geom. Methods Appl. **14** (2018), Paper No. 020, 9. MR3772835

[Bia10] L. Bianchi, *Vorlesungen über Differentialgeometrie*, B.G. Teubner, 1910.

[BP96] A. Bobenko and U. Pinkall, *Discrete surfaces with constant negative Gaussian curvature and the Hirota equation*, J. Differential Geom. **43** (1996), no. 3, 527–611. MR1412677

[Bor03] A. Borodin, *Discrete gap probabilities and discrete Painlevé equations*, Duke Math. J. **117** (2003), no. 3, 489–542. MR1979052

[BG16] A. Borodin and V. Gorin, *Lectures on integrable probability*, Probability and statistical physics in St. Petersburg, 2016, pp. 155–214. MR3526828

[Car11] A. S. Carstea, *Bilinear approach to delay-Painlevé equations*, J. Phys. A **44** (2011), no. 10, 105202, 7. MR2773893

[CDT17] A. S. Carstea, A. Dzhamay, and T. Takenawa, *Fiber-dependent deautonomization of integrable 2D mappings and discrete Painlevé equations*, J. Phys. A **50** (2017), no. 40, 405202, 41. MR3708091

[CDH19] Y. Chen, A. Dzhamay, and J. Hu, *Gap probabilities in the Laguerre Unitary Ensemble and discrete Painlevé equations*, 2019. preprint, arXiv:2001.00494.

[Chi78] T. S. Chihara, *An introduction to orthogonal polynomials*, Gordon and Breach Science Publishers, New York-London-Paris, 1978. Mathematics and its Applications, Vol. 13. MR0481884

[Cla06] P. A. Clarkson, *Painlevé equations—nonlinear special functions*, Orthogonal polynomials and special functions, 2006, pp. 331–411. MR2243533 (2007g:33020)

[Cla10] ______, *Painlevé transcendents*, NIST handbook of mathematical functions, 2010, pp. 723–740. MR2655372

[Dol83] I. V. Dolgachev, *Weyl groups and Cremona transformations*, Singularities, Part 1 (Arcata, Calif., 1981), 1983, pp. 283–294. MR713067

[Dui10] J. J. Duistermaat, *Discrete integrable systems*, Springer Monographs in Mathematics, Springer, New York, 2010. QRT maps and elliptic surfaces. MR2683025

[DJ11] J. J. Duistermaat and N. Joshi, *Okamoto's space for the first Painlevé equation in Boutroux coordinates*, Arch. Ration. Mech. Anal. **202** (2011), no. 3, 707–785. MR2854669

[DFS19a] A. Dzhamay, G. Filipuk, and A. Stokes, *On differential systems related to generalized Meixner and deformed Laguerre orthogonal polynomials*, submitted, 2019.

[DFS19b] ______, *Recurrence coefficients for discrete orthogonal polynomials with hypergeometric weight and discrete painlevé equations*, 2019. preprint, arXiv:1910.10981.

[DK19] A. Dzhamay and A. Knizel, *q-Racah Ensemble and q-P*$\left(E_7^{(1)}/A_1^{(1)}\right)$ *Discrete Painlevé Equation*, Int. Math. Res. Not. IMRN (2019). rnz211.

[DST13] A. Dzhamay, H. Sakai, and T. Takenawa, *Discrete Schlesinger transformations, their Hamiltonian formulation, and difference Painlevé equations*, 2013. preprint, arXiv:1302.2972.

[DT18] A. Dzhamay and T. Takenawa, *On some applications of Sakai's geometric theory of discrete Painlevé equations*, SIGMA Symmetry Integrability Geom. Methods Appl. **14** (2018), Paper No. 075, 20. MR3830210

[FVA18] G. Filipuk and W. Van Assche, *Discrete orthogonal polynomials with hypergeometric weights and Painlevé VI*, SIGMA Symmetry Integrability Geom. Methods Appl. **14** (2018), Paper No. 088, 19. MR3846851

[FN80] H. Flaschka and A. C. Newell, *Monodromy- and spectrum-preserving deformations. I*, Comm. Math. Phys. **76** (1980), no. 1, 65–116. MR588248

[FIKN06] A. S. Fokas, A. R. Its, A. A. Kapaev, and V. Yu. Novokshenov, *Painlevé transcendents: The Riemann-Hilbert approach*, Mathematical Surveys and Monographs, vol. 128, American Mathematical Society, Providence, RI, 2006. The Riemann-Hilbert approach. MR2264522

[FBM19] H. Z. Ford, H. M. Byrne, and M. R. Myerscough, *A lipid-structured model for macrophage populations in atherosclerotic plaques*, J. Theoret. Biol. **479** (2019), 48–63. MR3983063

[Fri91] S. Friedland, *Entropy of polynomial and rational maps*, Ann. of Math. (2) **133** (1991), no. 2, 359–368. MR1097242

[Fri07] ———, *Entropy of holomorphic and rational maps: a survey*, Dynamics, ergodic theory, and geometry, 2007, pp. 113–128. MR2369444

[FM89] S. Friedland and J. Milnor, *Dynamical properties of plane polynomial automorphisms*, Ergodic Theory Dynam. Systems **9** (1989), no. 1, 67–99. MR991490

[Fuc07] R. Fuchs, *Über lineare homogene Differentialgleichungen zweiter Ordnung mit drei im Endlichen gelegenen wesentlich singulären Stellen*, Math. Ann. **63** (1907), no. 3, 301–321. MR1511408

[Fuc11] ———, *Über lineare homogene Differentialgleichungen zweiter Ordnung mit drei im Endlichen gelegenen wesentlich singulären Stellen*, Math. Ann. **70** (1911), no. 4, 525–549. MR1511634

[Gam10] B. Gambier, *Sur les équations différentielles du second ordre et du premier degré dont l'intégrale générale est a points critiques fixes*, Acta Math. **33** (1910), no. 1, 1–55. MR1555055

[GRM93] B. Grammaticos, A. Ramani, and I. d. C. Moreira, *Delay-differential equations and the Painlevé transcendents*, Phys. A **196** (1993), no. 4, 574–590. MR1226401

[GRP91] B. Grammaticos, A. Ramani, and V. G. Papageorgiou, *Do integrable mappings have the Painlevé property?*, Phys. Rev. Lett. **67** (1991), no. 14, 1825–1828. MR1125950

[GRT$^+$14] B. Grammaticos, A. Ramani, K. M. Tamizhmani, T. Tamizhmani, and J. Satsuma, *Strongly asymmetric discrete Painlevé equations: the additive case*, J. Math. Phys. **55** (2014), no. 5, 053503, 17. MR3390630

[GRT$^+$16] ———, *Strongly asymmetric discrete Painlevé equations: the multiplicative case*, J. Math. Phys. **57** (2016), no. 4, 043506, 30. MR3488852

[GRWS20] B. Grammaticos, A. Ramani, R. Willox, and J. Satsuma, *Discrete Painlevé equations from singularity patterns: The asymmetric trihomographic case*, J. Math. Phys. **61** (2020), no. 3, 033503, 20. MR4071232

[GLS02] V. I. Gromak, I. Laine, and S. Shimomura, *Painlevé differential equations in the complex plane*, de Gruyter Studies in Mathematics, vol. 28, Walter de Gruyter & Co., Berlin, 2002. MR1960811 (2003m:34210)

[Hal17] R. Halburd, *Elementary exact calculations of degree growth and entropy for discrete equations*, Proc. A. **473** (2017), no. 2201, 20160831, 13. MR3668125

[HK17] R. Halburd and R. Korhonen, *Growth of meromorphic solutions of delay differential equations*, Proc. Amer. Math. Soc. **145** (2017), no. 6, 2513–2526. MR3626508

[HHNS15] M. Hay, P. Howes, N. Nakazono, and Y. Shi, *A systematic approach to reductions of type-Q ABS equations*, J. Phys. A **48** (2015), no. 9, 095201, 24. MR3317164

[HV98] J. Hietarinta and C. M. Viallet, *Singularity confinement and chaos in discrete systems*, Phys. Rev. Lett. **81** (1998Jul), 325–328.

[Hir77] R. Hirota, *Nonlinear partial difference equations. III. Discrete sine-Gordon equation*, J. Phys. Soc. Japan **43** (1977), no. 6, 2079–2086. MR0460936

[Hof99] T. Hoffmann, *Discrete Amsler surfaces and a discrete Painlevé III equation*, Discrete integrable geometry and physics, 1999, pp. 83–96.

[HJ14] P. Howes and N. Joshi, *Global asymptotics of the second Painlevé equation in Okamoto's space*, Constr. Approx. **39** (2014), no. 1, 11–41. MR3144379

[HFC19] J. Hu, G. Filipuk, and Y. Chen, *Differential and difference equations for recurrence coefficients of orthogonal polynomials with hypergeometric weights and Bäcklund transformations of the sixth Painlevé equation*, submitted, 2019.

[Hum90] J. E. Humphreys, *Reflection groups and Coxeter groups*, Cambridge Studies in Advanced Mathematics, vol. 29, Cambridge University Press, Cambridge, 1990. MR1066460 (92h:20002)

[Ism05] M. E. H. Ismail, *Classical and quantum orthogonal polynomials in one variable*, Encyclopedia of Mathematics and its Applications, vol. 98, Cambridge University Press, Cambridge, 2005. With two chapters by Walter Van Assche, With a foreword by Richard A. Askey. MR2191786

[JM81a] M. Jimbo and T. Miwa, *Monodromy preserving deformation of linear ordinary differential equations with rational coefficients. II*, Phys. D **2** (1981), no. 3, 407–448. MR625446

[JM81b] ———, *Monodromy preserving deformation of linear ordinary differential equations with rational coefficients. III*, Phys. D **4** (1981/82), no. 1, 26–46. MR636469

[JMU81] M. Jimbo, T. Miwa, and K. Ueno, *Monodromy preserving deformation of linear ordinary differential equations with rational coefficients. I. General theory and τ-function*, Phys. D **2** (1981), no. 2, 306–352. MR630674

[JS96] M. Jimbo and H. Sakai, *A q-analog of the sixth Painlevé equation*, Lett. Math. Phys. **38** (1996), no. 2, 145–154. MR1403067

[JN17] N. Joshi and N. Nakazono, *Elliptic Painlevé equations from next-nearest-neighbor translations on the $E_8^{(1)}$ lattice*, J. Phys. A **50** (2017), no. 30, 305205, 17. MR3673467

[JNS1608] N. Joshi, N. Nakazono, and Y. Shi, *Reflection groups and discrete integrable systems*, Journal of Integrable Systems **1** (201608), no. 1. xyw006.

[JR18] N. Joshi and M. Radnović, *Asymptotic behaviour of the fifth Painlevé transcendents in the space of initial values*, Proc. Lond. Math. Soc. (3) **116** (2018), no. 6, 1329–1364. MR3816383

[JR19] ______, *Asymptotic behaviour of the third Painlevé transcendents in the space of initial values*, Trans. Amer. Math. Soc. **372** (2019), no. 9, 6507–6546. MR4024529

[Kac90] V. G. Kac, *Infinite-dimensional lie algebras*, 3rd ed., Cambridge University Press, 1990.

[KN15] K. Kajiwara and N. Nakazono, *Hypergeometric solutions to the symmetric q-Painlevé equations*, Int. Math. Res. Not. IMRN **4** (2015), 1101–1140. MR3340349

[KNT11] K. Kajiwara, N. Nakazono, and T. Tsuda, *Projective reduction of the discrete Painlevé system of type* $(A_2 + A_1)^{(1)}$, Int. Math. Res. Not. IMRN **4** (2011), 930–966. MR2773334

[KNY01] K. Kajiwara, M. Noumi, and Y. Yamada, *A study on the fourth q-Painlevé equation*, J. Phys. A **34** (2001), no. 41, 8563–8581. MR1876614

[KNY17] ______, *Geometric aspects of Painlevé equations*, J. Phys. A **50** (2017), no. 7, 073001, 164. MR3609039

[KTGR00] M. D. Kruskal, K. M. Tamizhmani, B. Grammaticos, and A. Ramani, *Asymmetric discrete Painlevé equations*, Regul. Chaotic Dyn. **5** (2000), no. 3, 273–280. MR1789477

[Loo81] E. Looijenga, *Rational surfaces with an anticanonical cycle*, Ann. of Math. (2) **114** (1981), no. 2, 267–322. MR632841

[Mas18] T. Mase, *Studies on spaces of initial conditions for non-autonomous mappings of the plane*, J. Integrable Syst. **3** (2018), no. 1, xyy010. MR3824765

[MMT99] T. Matano, A. Matumiya, and K. Takano, *On some Hamiltonian structures of Painlevé systems. II*, J. Math. Soc. Japan **51** (1999), no. 4, 843–866. MR1705251

[Mat97] A. Matumiya, *On some Hamiltonian structures of Painlevé systems. III*, Kumamoto J. Math. **10** (1997), 45–73. MR1446392

[MSY03] M. Murata, H. Sakai, and J. Yoneda, *Riccati solutions of discrete Painlevé equations with Weyl group symmetry of type* $E_8^{(1)}$, J. Math. Phys. **44** (2003), no. 3, 1396–1414. MR1958273

[NP91] F. W. Nijhoff and V. G. Papageorgiou, *Similarity reductions of integrable lattices and discrete analogues of the Painlevé* II *equation*, Phys. Lett. A **153** (1991), no. 6-7, 337–344. MR1098879

[Nou04] M. Noumi, *Painlevé equations through symmetry*, Translations of mathematical monographs, American Mathematical Society, 2004.

[NY98a] M. Noumi and Y. Yamada, *Affine Weyl groups, discrete dynamical systems and Painlevé equations*, Comm. Math. Phys. **199** (1998), no. 2, 281–295. MR1666847

[NY98b] ______, *Higher order Painlevé equations of type* $A_l^{(1)}$, Funkcial. Ekvac. **41** (1998), no. 3, 483–503. MR1676885

[ORG01] Y. Ohta, A. Ramani, and B. Grammaticos, *An affine Weyl group approach to the eight-parameter discrete Painlevé equation*, J. Phys. A **34** (2001), no. 48, 10523–10532. Symmetries and integrability of difference equations (Tokyo, 2000). MR1877472

[Oka79] K. Okamoto, *Sur les feuilletages associés aux équations du second ordre à points critiques fixes de P. Painlevé*, Japan. J. Math. (N.S.) **5** (1979), no. 1, 1–79. MR614694 (83m:58005)

[Pai02] P. Painlevé, *Sur les équations différentielles du second ordre et d'ordre supérieur dont l'intégrale générale est uniforme*, Acta Math. **25** (1902), no. 1, 1–85. MR1554937

[QCS92] G. R. W. Quispel, H. W. Capel, and R. Sahadevan, *Continuous symmetries of differential-difference equations: the Kac-van Moerbeke equation and Painlevé reduction*, Phys. Lett. A **170** (1992), no. 5, 379–383. MR1190898

[QRT88] G. R. W. Quispel, J. A. G. Roberts, and C. J. Thompson, *Integrable mappings and soliton equations*, Phys. Lett. A **126** (1988), no. 7, 419–421. MR924318

[QRT89] ______, *Integrable mappings and soliton equations. II*, Phys. D **34** (1989), no. 1-2, 183–192. MR982386

[Rai13] E. M. Rains, *Generalized Hitchin systems on rational surfaces*, 2013. preprint, arXiv:1307.4033.

[RG96] A. Ramani and B. Grammaticos, *Discrete Painlevé equations: coalescences, limits and degeneracies*, Phys. A **228** (1996), no. 1-4, 160–171. MR1399286

[RG09] ______, *The number of discrete Painlevé equations is infinite*, Phys. Lett. A **373** (2009), no. 34, 3028–3031. MR2559808

[RG17] ______, *Singularity analysis for difference Painlevé equations associated with the affine Weyl group E_8*, J. Phys. A **50** (2017), no. 5, 055204, 18. MR3600574

[RGH91] A. Ramani, B. Grammaticos, and J. Hietarinta, *Discrete versions of the Painlevé equations*, Phys. Rev. Lett. **67** (1991), no. 14, 1829–1832. MR1125951

[RGT93] A. Ramani, B. Grammaticos, and K. M. Tamizhmani, *Painlevé analysis and singularity confinement: the ultimate conjecture*, J. Phys. A **26** (1993), no. 2, L53–L58. MR1210713

[ST02] M.-H. Saito and T. Takebe, *Classification of Okamoto-Painlevé pairs*, Kobe J. Math. **19** (2002), no. 1-2, 21–50. MR1980990

[STT02] M.-H. Saito, T. Takebe, and H. Terajima, *Deformation of Okamoto-Painlevé pairs and Painlevé equations*, J. Algebraic Geom. **11** (2002), no. 2, 311–362. MR1874117

[Sak01] H. Sakai, *Rational surfaces associated with affine root systems and geometry of the Painlevé equations*, Comm. Math. Phys. **220** (2001), no. 1, 165–229. MR1882403 (2003c:14030)

[ST97] T. Shioda and K. Takano, *On some Hamiltonian structures of Painlevé systems. I*, Funkcial. Ekvac. **40** (1997), no. 2, 271–291. MR1480279

[Sho39] J. A. Shohat, *A differential equation for orthogonal polynomials*, Duke Math. J. **5** (1939), no. 2, 401–417. MR1546133

[Sto18] A. Stokes, *Full-parameter discrete Painlevé systems from non-translational Cremona isometries*, J. Phys. A **51** (2018), no. 49, 495206, 31. MR3884504

[Sze75] G. Szegő, *Orthogonal polynomials*, Fourth, American Mathematical Society, Providence, R.I., 1975. American Mathematical Society, Colloquium Publications, Vol. XXIII. MR0372517

[Tak01a] T. Takenawa, *Algebraic entropy and the space of initial values for discrete dynamical systems*, J. Phys. A **34** (2001), no. 48, 10533–10545. Symmetries and integrability of difference equations (Tokyo, 2000). MR1877473

[Tak01b] ———, *A geometric approach to singularity confinement and algebraic entropy*, J. Phys. A **34** (2001), no. 10, L95–L102. MR1828835

[Tak03] ———, *Weyl group symmetry of type $D_5^{(1)}$ in the q-Painlevé V equation*, Funkcial. Ekvac. **46** (2003), no. 1, 173–186. MR1996297

[TRGO99] K. M. Tamizhmani, A. Ramani, B. Grammaticos, and Y. Ohta, *Integrability criteria for differential-difference systems: a comparison of singularity confinement and low-growth requirements*, J. Phys. A **32** (1999), no. 38, 6679–6685. MR1733847

[Tsu04] T. Tsuda, *Integrable mappings via rational elliptic surfaces*, J. Phys. A **37** (2004), no. 7, 2721–2730. MR2047557

[VA18] W. Van Assche, *Orthogonal polynomials and Painlevé equations*, Australian Mathematical Society Lecture Series, vol. 27, Cambridge University Press, Cambridge, 2018. MR3729446

[Ves91] A. P. Veselov, *Integrable mappings*, Uspekhi Mat. Nauk **46** (1991), no. 5(281), 3–45, 190. MR1160332

[Ves92] ———, *Growth and integrability in the dynamics of mappings*, Comm. Math. Phys. **145** (1992), no. 1, 181–193. MR1155288

[VS93] A. P. Veselov and A. B. Shabat, *A dressing chain and the spectral theory of the Schrödinger operator*, Funktsional. Anal. i Prilozhen. **27** (1993), no. 2, 1–21, 96. MR1251164

[Via14] C. M. Viallet, *Algebraic entropy for differential-delay equations*, 2014. preprint, arXiv:1408.6161.

[Yam09] Y. Yamada, *A Lax formalism for the elliptic difference Painlevé equation*, SIGMA Symmetry Integrability Geom. Methods Appl. **5** (2009), Paper 042, 15. MR2506170

[Yam11] ———, *Lax formalism for q-Painlevé equations with affine Weyl group symmetry of type $E_n^{(1)}$*, Int. Math. Res. Not. IMRN **17** (2011), 3823–3838. MR2836394